U.PORTO

DOUTORAMENTO

BIOTECNOLOGIA MOLECULAR E CELULAR APLICADA ÀS CIÊNCIAS DA SAÚDE

Decellularized fetal nucleus pulposus extracellular matrix for intervertebral disc regeneration

Morena Francesca Fiordalisi

D

2023

U.PORTO

Morena Francesca Fiordalisi. Decellularized fetal nucleus pulposus extracellular matrix for intervertebral disc regeneration

Decellularized fetal nucleus pulposus extracellular matrix for intervertebral disc regeneration

Morena Francesca Fiordalisi

D.ICBAS 2023

SEDE ADMINISTRATIVA

INSTITUTO DE CIÊNCIAS BIOMÉDICAS ABEL SALAZAR

FACULDADE DE FARMÁCIA

U.PORTO

DOUTORAMENTO

BIOTECNOLOGIA MOLECULAR E CELULAR APLICADA ÀS CIÊNCIAS DA SAÚDE

Decellularized fetal nucleus pulposus extracellular matrix for intervertebral disc regeneration

Morena Francesca Fiordalisi

D

2023

MORENA FRANCESCA FIORDALISI

DECELLULARIZED FETAL NUCLEUS PULPOSUS EXTRACELLULAR MATRIX FOR INTERVERTEBRAL DISC REGENERATION

Tese de Candidatura ao grau de Doutor em Biotecnologia Molecular e Celular Aplicada às Ciências da Saúde, submetida ao Instituto de Ciências Biomédicas de Abel Salazar da Universidade do Porto.

Orientador – Professora Doutora Raquel Madeira Gonçalves

Categoria – Professora Auxiliar (ICBAS) e Investigadora Auxiliar do Grupo Microenvironments for New Therapies (i3S/INEB)

Afiliação – Instituto de Ciências Biomédicas de Abel Salazar, Universidade do Porto (ICBAS); Instituto de Investigação e Inovação em Saúde/Instituto Nacional Engenharia Biomédica, Universidade do Porto (i3S/INEB)

Co-orientador – Doutora Joana Caldeira Fernandes Frey Ramos

Categoria – Investigadora Júnior (i3S/INEB)

Afiliação – Instituto de Investigação e Inovação em Saúde/Instituto Nacional Engenharia Biomédica, Universidade do Porto (i3S/INEB)

Co-orientador – Professor Stephen Richardson

Categoria – Senior Lecturer

Afiliação – University of Manchester


INSTITUTO DE INVESTIGAÇÃO
E INOVAÇÃO EM SAÚDE
UNIVERSIDADE DO PORTO


INEB
30 years
Instituto de Engenharia Biomédica


U.PORTO
ICBAS
INSTITUTO DE CIÊNCIAS BIOMÉDICAS ABEL SALAZAR
SCHOOL OF MEDICINE AND
BIOMEDICAL SCIENCES


U.PORTO
FACULDADE DE FARMÁCIA
UNIVERSIDADE DO PORTO


BiotechHealth
International Doctoral Programme in Molecular
and Cellular Biotechnology Applied to Health Sciences


MANCHESTER
1824
The University of Manchester


U.PORTO
CEMUP
CENTRO DE MATERIAIS DA UNIVERSIDADE DO PORTO

A Zio Salvatore,

per aver sempre creduto in me.

FUNDING

The work included in this thesis was financially supported by:

- Fundação para a Ciência e a Tecnologia (FCT) through PhD Grant PD/BD/135544/2018, and FETBIO project: “Fetal-inspired hierarchical biomaterials for regeneration in a harsh microenvironment: the nucleus of the intervertebral disc" (FCT-2020-PTDC/BTM-MAT/0438/2020) and through BiotechHealth PhD Programme (Doctoral Programme on Cellular and Molecular Biotechnology Applied to Health Sciences).

- EUROSPINE/ON Foundation (20-165), (UIDB/04293/2020), EUROSPINE Task Force Research (TFR) through a grant (2018_15), FEedIT (EXPL/BTM-ORG/0880/2021), and QREN (Quadro de Referência Estratégica Nacional).

PUBLICATIONS

Under the terms of nº 2, alínea a) do artigo 31º do Decreto-Lei n.º 230/2009, the work presented in this doctoral thesis, is already published or in preparation for publication:

ARTICLE I

Original research article published

Fiordalisi, M. F., Ferreira, J. R., Pinto, M. L., Ribeiro-Machado, C., Teixeira Pinto, M., Oliveira, M. J., Barbosa, M. A., Madeira Gonçalves, R., & Caldeira, J. (**2022**). The impact of matrix age on intervertebral disc regeneration. *Biomaterials advances*, 143, 213192.

DOI: 10.1016/j.bioadv.2022.213192
URL: https://www.sciencedirect.com/science/article/pii/S2772950822004691?via%3Dihub

ARTICLE II

Original review manuscript published

Fiordalisi, M. F., Silva, A. J., Barbosa, M., Gonçalves, R. M., & Caldeira, J. (**2021**). Intervertebral disc decellularisation: progress and challenges. *European cells & materials*, 42, 196–219.

DOI: 10.22203/eCM.v042a15
URL: https://www.ecmjournal.org/papers/vol042/vol042a15.php

ARTICLE III

Original forum review published

Fiordalisi, M., Silva, A. J., Barbosa, M., Gonçalves, R., & Caldeira, J. (**2020**). Decellularized Scaffolds for Intervertebral Disc Regeneration. *Trends in biotechnology*, 38(9), 947–951.

DOI: 10.1016/j.tibtech.2020.05.002
URL: https://www.sciencedirect.com/science/article/pii/S0167779920301232?via%3Dihub

COMPLEMENTARY PUBLICATIONS IN THE FIELD:

Maria Molinos, **Morena F. Fiordalisi**, Joana Caldeira, Catarina R. Almeida, Mário A. Barbosa, Raquel M. Gonçalves (2023). Alterations of Bovine Nucleus Pulposus Cells with Ageing. *Aging Cell*. Accepted for publication.

ACKNOWLEDGMENTS

The end of this important step of my life has arrived and I feel extremely happy of my journey. I have learned so much towards these years and I have growth both at personal and professional levels. I confess it was a difficult journey, especially for being far from my family, friends and boyfriend for so many years. But, it was also full of amazing moments shared with great people, which I will never forget. Today, for the first time, I can say I am extremely proud of myself and of the scientist I became. I am proud for having faced the difficulties and overcome them, instead of taking the easiest decision and give up. But this was not possible without the extraordinary people around me, who were fundamental for my growth along these years.

First of all, I am extremely grateful to **Raquel Gonçalves**, who during this time was always by my side. Throughout these years, you were not only my supervisor, but more importantly a mentor and friend. Thank you for all your support and help, for our scientific discussion, for transmitting me your knowledges and passion for science and for taking in considerations always my opinion and ideas. With you, I have learned a lot both at professional and personal level. Thank you for your care in the difficult moments, for pushing me in giving my best and for always believing in my capacities. Without your precious help and support, I won't be here today with a PhD thesis in my hands. I admire you as a woman and scientist.

To **Joana Caldeira** (**Xu**), for always being present in these years, not only as a co-supervisor but more importantly as a friend. Thank you for accepting me in the Erasmus internship and for introducing me the amazing world of intervertebral disc and low back pain. With you, I dissected a bovine tail and decellularized the nucleus pulposus for the first time. You transmitted me the passion for this scientific field and for the work that I decided to pursue during my PhD. I am really grateful to you for this. Thank you for listening my ideas, for believing in me and always trust in my potential. The first time I arrived in Porto during my Erasmus, I did not know how to talk English and I felt lost. But you helped me trying to speak in Spanish, Portuguese and even Italian (ahah). Thank you for all your hugs, care, unicorn balloons and precious words of support, which helped me to arrive where I am now. I am sure our friendship is for life.

I am extremely grateful to **Professor Mario Barbosa** for accepting me in his group "Microenvironments for New Therapies". Thank you for all the support along these years

and for transmitting me knowledges, which were fundamental for my scientific growth. The scientific discussions we had were essential contributions for this PhD thesis.

To **Dr. Stephen Richardson**, for accepting to be my co-supervisor and for the help in the PhD project writing. Thank you for being part of my PAC and for sharing your ideas as well as suggestions, which extremely improved this work.

To **Professor Manuel Vilanova,** Director of the Biotech Health PhD Programme, for all the support and help. To the **Biotech Health PhD Programme** and **FCT** for giving me the possibility to conduct my PhD research work. Moreover, a special thanks to **Helena Martins**, from the Serviços Académicos – Pós-Graduação e Educação Contínua, for all the help during these years.

To all the **MiNTs**, who were with me during these years, both the formal and the actual ones, for immediately integrate me in this great group, for all the fun and help at the lab, for the patience and the kindness during the stressful period of thesis writing. To the **Stem Cell Bioengineering Team** for all your support and the exchange of ideas during our meetings.

Ana Luísa Castro (Luisinha), I don't have enough word to express all my thankfulness to you for being such an amazing friend and always by my side. Without your support and your presence, I would not be able to do all of this. I consider you as my sister, full of positive energy and with a special soul. Thank you for all your help, for always understanding me and never judging. You always have the right word to make me feel better in the bad moment. We celebrated together every single victory, but also overcome the bad moments. Thank you for reading all my emails before sending, for helping me in translating the abstract in Portuguese (my Portuguese skills are still not good), for the pictures at the confocal, for being near me during the "DAY OF THE ARRAY" (ahaha), for your letters in the computer, for sharing with me the love for the good food, for going to the supermarket during my COVID isolation and buying all the things I like most, for being patience with me in a bad day, for saying random things just to make me laugh, when I was sad or stressed. You are the sweetest and most altruist person I ever met in my life. Thank you for welcoming me in your family, that now I consider as my second family <3. I will never forget every single moment with you and I am sure our friendship will last forever. Wherever I will be, you can always count on me. To **Claudia Machado (Claudinha),** for all the moments together. You were with me since I started my Erasmus internship and with time we became friends. Thank you for our crazy nights at the lab, doing inventory, unfreezing -80°C or -20 °C, cleaning the cold room, putting the tissue processor, dissolving graphene (ahah) and alginate. Thanks for being with me until 4 am under the flow chamber, dissecting tails and chopping tissues and for all the dinner at Mac Donald as reward for our overnight work, as

well as for teaching me everything I know about histology and for your patience in answering to my 1000 questions and doubts. Thanks for being part of my life. To **Mafalda Gonçalves (Mufalda)**, for being so special and sweet friend. We were together since the beginning and shared unforgettable moments. Thank you for being such a crazy friend, for making me always laugh, for all the cute names you gave me (Murena, Mirena), for showing me your skills in imitating animal sounds (hiiiii), for making me the cutest photos at the microscope with my feet not touching the floor, for all your "delicate" caresses and hugs and for making work fun. Thank you for being near me in the difficult and happy moments. Together we are stronger. To **João Bras** (**daddy shark**), for being an amazing friend, but also my personal psychologist, for always listening me, for our scientific discussion on the results (which helped me a lot in thinking out of the box) and for always caring about my feelings. **José Henrique Teixeira** (Zezinho), you have a special place in my heart and you know it. Thank you for our special friendship, for being always on my side, for our long WhatsApp calls, which helped me to think differently and overcome the difficulties, for encouraging to believe in my potential, for celebrating together all our successes, for all the fun moments outside. Our friendship goes beyond the distance and I know I can always count on you. To **Ana João** for teaching me all the Brazilian songs and dance, for making funny video of me dancing Brazilian songs and for all the amazing moments together at work and outside. To **Catarina Pereira** (**Cati**), for all I have learned from you both at scientific and human levels. I am really grateful for all your support, our scientific discussion, for being present in all my seminars and for having always kinds words for me. To **Flavia Castro**, for all the support and kindness along these years, for our special friendship and help during the difficult moments. To **Andreia Silva**, **Bianca Lourenco, Daniela Vasconcelos**, **Estrela Neto**, **Ruben Pereira**, for all your help and all the fun together. To **Marco Araujo**, for making the work fun, for trying to speak Italian (with questionable results) and for always helping me. To **Carla Cunha**, **Cristina Ribeiro, Inês Almeida**, **Judite Barbosa**, **Susana Santos**, for all the constructive ideas and suggestions, as well as for your precious help. To **Ana Beatriz**, for being so kind and sweet with me, for all the support and the patience during the thesis writing and for our "creepy" smile. You are a special person, always ready to help the others. To **Joana Rita Ferreira**, for all the help in these years and for involving me in the amazing PhD dance. To **Sara Moura**, for taking care of my feelings, for your help and for all the moments together. To **Catarina Milheiro,** for all our laugh and fun at the lab. To **Beatriz Ribeiro** and **Inês Sousa**, for all the great moments together. To **Carlos Botelho**, for being such an enthusiastic guy and making me laugh even in a bad day. To **Barbara Adem, Margarida Dantas and Vanessa Nunes**, for sharing with me this experience and for all your precious help.

I am truly thankful to all the **technician of i3S**, who gave me an essential help in the experimental works, especially **Dalila Pedro**, **Manuela Bras**, **Maria Lazaro, Ricardo Vidal**. A special thanks to **all the people from INEB**, for all the help and support through these years. I am really proud to be part of this big family. To **Marta Teixeria Pinto**, for all your help at work with the CAM assay, but also at the personal level.

To **Ana Paula Filipe**, for your precious help when I arrived at i3s for the first time, for welcoming me into your family during Christmas, for bringing me food during the pandemic, for never leaving me alone, for all your warm hugs and for adopting me as daughter. I will never forget what you have done for me. To **Luis Castro**, for all the time we spent together and the delicious homemade food. To **Francisco Castro**, for all our time together, our dinners, our laugh, smile, and gossip about Luisa. À **Manuela** pelos abraços calorosos e por ser como uma avó para mim.

To **Anurag Singh (Anu)**, **Henrique Reis** and **Abhishek Chatterjee (Abi)**, for our precious friendship. When I arrived in the residence you immediately integrated me in your group and we had a lot of fun together. Thank you for all our dinners and lunch, for the fun in the kitchen, for showing me your cooking skills and let me taste new delicious food, for all the cakes in front of my room to celebrate my birthdays. The moments with you were special and I will never forget them. A special thanks to **Miguel Santos** (**Miguelito**) for all your kindness and care, for our talk, for distracting me from work, for our walk along the river, for listening my emotions and helping me in every single day. You are a special person with a wonderful soul.

Un grazie speciale a **Monica Scaranari** e **Rui Pereira** per tutto l'aiuto in laboratorio, per avermi fatto parlare Italiano anche a lavoro, per tutti i momenti insieme che sono stati preziosi per me.

A **Linachiara Demasi**, **Martina Commisso** (**Commi**) e **Martina Tassone** (**Ami**), le amiche di una vita che mi sono state sempre accanto con un amore incodizionato in tutte le tappe della mia vita. La nostra amicizia dura da 12 anni ed è il regalo più bello che la vita avesse potuto farmi. Grazie per essere parte della mia vita e avermi aiutato a rialzarmi nei momenti di difficoltà. Senza di voi mi sentirei persa. A **Martina Tassone (Ami)** per tutto quello che hai fatto per me, per avermi dato l'onore di essere la tua testimone in uno dei giorni più importanti della tua vita, per tutte le nostre risate, abbracci e pianti, per essermi stata sempre vicino in ogni momento della mia vita (sia bello che brutto), per non avermi mai abbandonato durante questo percorso difficile, per essere una seconda sorella e per i momenti indimenticabili trascorsi insieme. Sei la mia piccolina e una delle persone più importanti della mia vita. A **Martina Commisso (Commi)**, per essere la mia psicologa

personale, per ascoltare tutte le mie paranoie e consolarmi nei momenti di difficoltà, per essere più “rozza” di me, per avermi insegnato che c’è sempre qualcosa per sorridere anche quando sembra che tutto il mondo intorno stia crollando a pezzi. Sei una forza della natura e mi hai insegnato ad affrontare sempre le difficoltà con positività e a non lasciarsi mai andare alla tristezza. A **Linachiara Demasi**, la mia compagna di brutte figure in pubblico. Grazie per essermi stata vicina in questo periodo con un semplice messaggio, per avermi fatto sorridere nei brutti momenti, per aver compreso i miei problemi e le mie decisioni, per avermi aiutata a superare le difficoltà, per tutti i momenti indimenticabili trascorsi a Porto e le lunghe camminate che mi hanno distrutta. Sei un’amica speciale con un grande cuore.

A **Emanuele Milano** (**Scimmione**), per tutte le nostre pazzie, le nostre risate, le nostre telefonate e chiacchierate che sono riuscite a strapparmi un sorriso nei momenti tristi. A **Eleonora Calvosa (Nora**) per tutto il tuo supporto e per avermi accolta nella tua famiglia come una figlia. A **Francesca (Chicca), Federica (Fuffa) e Valeria (Vali) Lanza**, le mie cognate, che ormai considero come sorelle, grazie per tutto il vostro sostegno. A **Francesco Lanza** per avermi insegnato a lavorare nel laboratorio di analisi (e ad usare la centrifuga) e per tutti i suoi consigli. Ai miei nipoti, **Eleonora**, **Federico, Francesco**, per avermi donato la gioia di diventare zia e per tutto l’immenso affetto che mi trasmettete ogni giorno.

Il ringraziamento più importante va ai miei genitori, **Vincenzo Fiordalisi** e **Maria Antonietta Larocca**, i pilastri fondamentali della mia vita. Non penso di avere abbastanza parole per poter esprimere quanto io vi sia riconoscente. Grazie per ogni vostro sacrificio che mi ha permesso di continuare gli studi e raggiungere questo importante traguardo oggi. Grazie per aver appoggiato ogni mia decisione, inclusa la scelta di studiare in un altro Pese, nonostante la distanza che ci divide. Grazie per avermi sempre supportata in questi anni e avermi dimostrato di essere orgigliosi di me, per aver sempre creduto in me e aver celebrato insieme ogni singolo successo. Senza il vostro sostegno tutto questo non sarebbe stato possibile. Vi amo immensamente e non avrò mai abbastanze parole per esprimere tutta la mia gratitudine e l’amore che provo nei vostri confronti. A **Vincenzo Fiordalisi** (**il mio papi**), per essere un padre esemplare e il mio supereroe, per avermi trasmesso la forza e il coraggio per superare ogni difficoltà che la vita può riservare, per tutto l’amore che mi doni ogni giorno. Grazie per avermi sempre spinto a dare il massimo e aver creduto sempre in me. A **Maria Antonietta Larocca (la mia mamma),** per essere una mamma dolce e meravigliosa e per amarmi incondizionatamente, per essere una grande donna da cui ho sempre preso esempio, per essermi accanto in ogni momento della mia vita, per essere riuscita sempre a capirmi e avermi tenuto la mano nei momenti di difficoltà, per avermi sempre sostenuto ed essere stata paziente nei miei confronti, nonostante il mio carattere

impulsivo. A **Federica Fiordalisi**, la mia sorellina, che mi è sempre stata accanto in tutti i momenti della mia vita. Grazie per la tua pazienza, per avermi supportata e anche sopportata nei momenti difficili, per essere sempre al mio fianco nonostante i km di distanza, per aver gioito con me per le mie conquiste e avermi consolata nei momenti tristi. So che potrò sempre contare su di te e io ci sarò sempre per te. Siamo unite da un legame indissolubile che mai nessuno potrà scalfire. Grazie per tutto l'amore che mi doni ogni giorno e spero che tu possa essere orgogliosa di me oggi.

A **nonno Saverio**, per aver sempre dimostrato tutto il suo orgoglio nei miei confronti ed aver creduto in me, supportandomi in ogni mia scelta, per avermi trasmesso insegnamenti importanti di vita e avermi donato amore incondizionato. Ai miei nonni che non sono più tra noi (**Nonna Teresa, Nonna Rita, Nonno Peppe**), per avermi sempre protetto in questi anni ed essermi sempre stati accanto. Ovunque vi troviate, spero di avervi reso orgogliosi oggi. Ai miei zii, **Zia Filomena (Zia Mena)**, **Zia Raffaella, Zia Francesca (Checca) e Federico, Zia Franca e Giorgio, Zio Silvestro e Zia Cenzina, Zia Pina,** per il vostro supporto durante questi anni. A **zio Carmelo,** per essere constantamente presente nella mia vita con lo spirito e per avermi aiutata in ogni singolo momento. Un grazie speciale a mio **Zio Salvatore**, che considero come un secondo padre. Grazie per essere sempre stato il mio primo sostenitore, per aver sempre creduto in me, per avermi trasmesso la passione per la scienza. La tua forza e il tuo coraggio sono stati degli esempi e mi hanno aiutata a crescere in questi anni. Grazie per tutto l'amore che mi hai donato e spero che oggi, ovunque tu sia, tu possa essere orgoglioso di me. Questa tesi la dedico a te. A mio cugino **Saverio Fiordalisi**, per tutto il suo sostegno in questi anni e per avermi sempre dato saggi consigli. Al mio cuginetto **Michele Fiordalisi**, per aver sempre creduto nelle mie capacità e avermi spronato a continuare in questo percorso. Grazie per le nostre lunghe chiacchierate al telefono, per la forza che mi trasmetti ogni giorno, per i tuoi consigli nei momenti di difficoltà e per essere sempre stato orgoglioso dei miei traguardi.

Per ultimo, ma non per importanza, ringrazio immensamente **Michele Lanza** (**Amo**), l'amore della mia vita. Questi anni vissuti a distanza sono stati difficili per la nostra relazione, ma nonostante ciò siamo ancora insieme, dopo 14 anni. Non avrò mai abbastanza parole per poterti ringraziare per tutto ciò che hai fatto per me, per aver appoggiato tutte le mie scelte, per aver accettato di vivere a distanza per quasi 6 anni, per avermi lasciato libera di inseguire i miei sogni, nonostante sono consapevole sia stata dura per te. Grazie per essere sempre stato il mio più grande fan e aver cercato di spiegare con orgoglio a tutti i tuoi amici e colleghi il mio lavoro di ricerca sul disco intervertebrale, il mal di schiena e la decellularizzazione. Ma soprattutto grazie per amarmi incondizionatamente, per avermi supportata e anche sopportata in ogni istante, per avermi incorraggiata a non mollare mai,

per avermi consolata al telefono nei momenti tristi, per avermi spronato a continuare in questo percorso e avermi fatto credere di essere forte. Senza di te tutto questo non sarebbe stato possibile. Sono certa che il futuro ci riserverà momenti indimenticabili e felici insieme e recupereremo tutto il tempo vissuto lontani, più forti di prima. Tu sei il mio universo <3.

Thanks to all of you for being part of my life and for making these years unforgettable and wonderful (forgive me if I forgot someone). **I will keep in my heart every single moment together. This is not only my PhD thesis, but it is also yours.**

GRAZIE A TUTTI DI CUORE! <3

INDEX OF CONTENTS

ABSTRACT

Intervertebral discs (IVD) show age-associated hallmarks at morphological, cellular and biochemical levels. While ageing, the IVD degenerates leading to low back pain (LBP), which is one of the leading conditions of disability worldwide. Current LBP treatments do not restore/reestablishes the aged/degenerated IVD. Also, the scarce capacity of adult IVD to self-repair render problematic tissue regeneration. Recently, matrix-engineering strategies, particularly the use of decellularized extracellular matrix (ECM)-based biomaterials, started to be explored for IVD repair, knowing their capacity to induce tissue regeneration by recapitulating essential cues of native tissue microenvironment. Our group has demonstrated the presence of specific pro-regenerative proteins (Collagen [COL] 12 and COL14), exclusively in the matrisome profiling of fetal bovine nucleus pulposus (NP). Therefore, the main hypothesis of this thesis was that fetal decellularized NP ECM could have a superior potential for IVD regeneration.

To address this question, we have firstly developed acellular scaffolds from bovine NP of different donor ages (fetus, young and old), by using an optimal sodium dodecyl sulfate (SDS)-based protocol with reduced concentration and time exposure (0.1 %, 1 h). This method showed to be effective in maintaining structural, biochemical and biomechanical features of native tissues, while efficiently removing DNA and cells. Knowing that IVD cells are characterized by a limited capacity to proliferate and synthesize ECM proteins, we afterwards repopulated decellularized matrices from different donor ages with adult bovine NP cells, to uncover the potential of fetal decellularized ECM in rejuvenating IVD endogenous cellular and biochemical signals. After 7 days of *ex vivo* culture, cells seeded on younger decellularized matrices showed the highest cellular viability and increased capacity to produce ECM proteins, namely aggrecan (ACAN). Since healthy IVDs are characterized by absence of vasculature, we explored the anti-angiogenic potential of decellularized matrices from different donor ages, by performing the chick embryo chorioallontoic membrane (CAM) *in vivo* assay. Results showed reduced neo-vascularization in fetal matrices, although with a higher inflammatory score.

Then, we have explored the different mechanisms responsible for the increased pro-regenerative potential of fetal decellularized matrices. To unravel the mechanism behind the higher ECM production after repopulation, an attempt to neutralize CD44 in bovine NP

cells prior to cell seeding in fetal NPs was performed. However, no significant differences were detected in term of ACAN production, most probably due to insufficient CD44 blocking. After, we analyzed bovine cytokine released from decellularized ECM using a protein array. Results did not show significant changes of inflammatory neither pro-angiogenic cytokines in all the aged donors. Finally, an *in vivo* proof-of-concept of decellularized matrices of different donor ages with human IVD cells was conducted. For that, matrices with immortalized NP (iNP) cells were inoculated in CAM assay. As results, fetal matrices showed a decreased angiogenic response in the presence of iNP cells, when compared to young and old ones.

Overall, we have demonstrated that fetal decellularized matrices are ideal substrates for the re-activation of cellular and biochemical cues of native cells, which lead to IVD reconstruction through matrix remodeling by ECM *de novo* synthesis and low angiogenic activity. In parallel, this work also opens the horizons for the use of decellularized matrices from old bovines as suitable 3D models to explore pathological features of IVD degeneration, as well as to screen the efficacy of novel drugs for LBP treatment.

Thus, this thesis uncovered the importance of tissue donor age for the development of suitable biomaterials for IVD regeneration. Moreover, this work also opens new avenues for the development of fetal ECM-based hydrogels as minimally invasive therapeutic strategies to halt IVD degeneration, ultimately reducing LBP.

RESUMO

Os discos intervertebrais (IVD) mostram marcas associadas à idade em níveis morfológicos, celulares e bioquímicos. Com o envelhecimento, o IVD degenera levando à dor lombar (LBP), que é uma das principais fontes de incapacidade em todo o mundo. Os tratamentos atuais para lombalgia não restauram/restabelecem o IVD envelhecido/degenerado. A escassa capacidade de auto-reparação do IVD num adulto contribui para uma regeneração tecidual problemática. Recentemente, estratégias de engenharia de matriz, particularmente o uso de biomateriais baseados em matriz extracelular (ECM) descelularizada, têm vindo a ser exploradas para a reparação do IVD, graças sua capacidade de induzir a regeneração tecidual recapitulando sinais essenciais do microambiente do tecido nativo. O nosso grupo demonstrou a presença de proteínas pró-regenerativas específicas (Colagénio [COL] 12 e COL14), exclusivamente no perfil matrissómico de núcleo pulposo (NP) fetais bovinos. Assim, a principal hipótese desta tese propõe que a ECM fetal descelularizada possa ter um potencial superior para a regeneração do IVD.

Para responder a esta questão, começamos por desenvolver scaffolds acelulares de NP bovino de doadores de diferentes idades (feto, jovem e velho), usando um protocolo baseado em sodium dodecyl sulfate (SDS) com concentração e tempo de exposição reduzidos (0.1 %, 1 h). Este método mostrou-se eficaz na preservação das características estruturais, bioquímicas e biomecânicas dos tecidos nativos, tendo ao mesmo tempo removido o DNA e as células de forma eficiente. Sabendo que as células do IVD são caracterizadas por uma capacidade limitada de proliferação e de síntese de proteínas da ECM, posteriormente repovoamos as matrizes descelularizadas de diferentes idades com células NP bovinas adultas, para descobrir o potencial da ECM fetal descelularizada no rejuvenescimento de sinais celulares e bioquímicos endógenos do IVD. Após 7 dias de cultura *ex vivo*, as células cultivadas em matrizes descelularizadas mais jovens apresentaram a maior viabilidade celular e maior capacidade de produzir proteínas da ECM, nomeadamente o agrecano (ACAN). Uma vez que IVDs saudáveis são caracterizados pela ausência de vasculatura, exploramos o potencial anti-angiogénico de matrizes descelularizadas de doadores de diferentes idades, realizando o ensaio *in vivo* da membrana corioalontóica (CAM) de embriões de galinha. Os resultados mostraram redução da neovascularização em matrizes fetais, embora com maior índice inflamatório.

Em seguida, exploramos os diferentes mecanismos responsáveis pelo aumento do potencial pró-regenerativo de matrizes fetais descelularizadas. Para desvendar o mecanismo por trás da maior produção de ECM após o repovoamento, foi realizada uma tentativa de neutralizar CD44 em células NP bovinas antes da cultura celular em NPs fetais. Não foram detetadas diferenças significativas em termos de produção de ACAN, provavelmente devido ao bloqueio insuficiente de CD44. Em seguida, analisamos citocinas bovinas liberadas da ECM descelularizada usando um array de proteínas. Os resultados não mostraram alterações significativas de citocinas inflamatórias nem pró-angiogênicas em todos os doadores idosos. Finalmente, foi realizada uma prova de conceito *in vivo* de matrizes descelularizadas de diferentes idades de doadores com células IVD humanas. Para isso, matrizes com células NP imortalizadas (iNP) foram inoculadas no ensaio CAM. Como resultados, as matrizes fetais apresentaram uma resposta angiogênica diminuída na presença de células iNP, quando comparadas às jovens e velhas.

No geral, demonstramos que as matrizes fetais descelularizadas são substratos ideais para a reativação de sinais celulares e bioquímicos de células nativas, que levam à reconstrução do IVD por meio da remodelação da matriz pela síntese *de novo* da ECM e baixa atividade angiogênica. Paralelamente, este trabalho também abre horizontes para o uso de matrizes descelularizadas de bovinos velhos como modelos 3D adequados para explorar as características patológicas da degeneração do IVD, bem como para rastrear a eficácia de novos medicamentos para o tratamento da lombalgia.

Assim, esta tese revelou a importância da idade do doador de tecido para o desenvolvimento de biomateriais adequados para a regeneração do IVD. Além disso, este trabalho também abre novos caminhos para o desenvolvimento de hidrogéis à base de ECM fetal como estratégias terapêuticas minimamente invasivas para interromper a degeneração do IVD, reduzindo a lombalgia.

LIST OF ABBREVIATIONS

ACAN	Aggrecan
ADAMTs	Disintegrin and metalloproteinase with thrombospondin motifs
ADSCs	Adipose-derived stem cells
AF	Annulus fibrosus
AMSCs	Amniotic stem cells
ANG-1	Angiopoietin-1
APC	Adenomatous polyposis coli gene product
APR	Aprotinin
Au/Pd	Gold/Palladium
bFGF	Basic fibroblast growth factor
$bFGF_2$	Basic fibroblast growth factor 2
BM-MSCs	Bone-marrow-derived mesenchymal stem cells
BMP	Bone morphogenic protein
BSA	Bovine serum albumin
Ca12	Carbonic anhydrase XII
CAM	Chick embryo chorioallantoic membrane
CCK8	Cell counting kit 8
CD	Cluster of differentiation
CD40L	CD40 ligand
CEMUP	Materials Centre of the University of Porto
CHAPS	3-[(3-cholamidopropyl)dimethylammonio]-1-propanesulfonate)
CILP	Cartilage intermediate layered protein

CK1	Casein kinase 1
CO_2	Carbon dioxide
COL	Collagen
COL1	Collagen type 1
COL10	Collagen type 10
COL12	Collagen type 12
COL14	Collagen type 14
COL2	Collagen type 2
COL2A1	Collagen type II alpha 1 chain
COL3	Collagen type 3
COL5A1	Collagen type V alpha 1 chain
Cq	Quantification cycle
Cryo-SEM	Cryo-scanning electron microscopy
Ctrl	Control
CXCL-10	C–X–C motif chemokine 10
DAB	3,3′-Diaminobenzidine
DAF-G	Decellularized AF-based hydrogel
DAPI	4′,6-diamidino-2-phenylindole
DMEM	Dulbecco’s modified Eagle medium
DMEM/F12	Dulbecco's Modified Eagle Medium/Nutrient Mixture F-12
DMMB	1,9-dimethylmethylene blue
DN	Definitive notochord
DNA	Deoxyribonucleic Acid
dNTP	Deoxynucleotide
dsDNA	Double-stranded DNA
DTT	Dithiothreitol

Dvl	Dishevelled
E	Embryonic day
ECM	Extracellular matrix
EDTA	Ethylenediaminetetraacetic acid
F	Fetus
FBLN1	Fibulin-1
FBS	Fetal bovine serum
FCT	Fundação para a Ciência e a Tecnologia
FDA	Food and Drug Administration
FGF-1	Fibroblast growth factor-1
Flh	Floating head
FN	Fibronectin
Foxa	Forkhead box A
Foxa2	Forkhead box A2
Foxf1	Forkhead box F1
Fz	Frizzled
G*	Complex shear modulus
GA	Gastrulation area
GAGs	Glycosaminoglycans
Gal	Galactose-a-1,3-galactose
GAPDH	Glyceraldehyde-3-phosphate dehydrogenase
GASP-1	Growth and differentiation factor-associated serum protein-1
GD2	Disialoganglioside 2
g-DAF-G	Genipin-crosslinked DAF-G
Gdf10	Growth differentiation factor 10
Gpc3	Glypican 3

GSK3	Glycogen synthase kinase 3
H	Hours
H&E	Hematoxylin & Eosin
H_2O	Water
HCl	Hydrochloric Acid
HEMS	Histology and Electron Microscopy
HYP	Hydroxyproline
Hz	Hertz
Ibsp	Integrin-binding sialoprotein
IF	Immunofluorescence
IFN	Interferons
IGF-1	Insulin-like growth factor-1
IgM	Immunoglobulin M
IHC	Immunohistochemistry
IL	Interleukins
iNP	Immortalized nucleus pulposus
IP-10	Interferon γ-induced protein-10 (IP-10)
IVD	Intervertebral disc
KCl	Potassium Chloride
Krt19	Keratin-19
LAP	Latency-associated polypeptide
LBP	Low back pain
LDH	Lactate dehydrogenase
LIF	Leukemia inhibitory factor
LRP	Low-density lipoprotein receptor-related protein
LTBP-2	Latent Transforming Growth Factor Beta Binding Protein 2

LVR	Linear viscoelastic region
MAC387	Macrophage monoclonal antibody clone 387
MAGP-1	Microfibril-associated glycoproteins-1
MAPK	Mitogen-activated protein kinase
MCP-1	Monocyte chemoattractant protein-1
MCT-1	Monocarboxylate transporter-1
$MgCl_2$	Magnesium chloride
MHC	Major histocompatibility complex
MIG	Monokine induced by gamma interferon
Min	Minutes
MMP	Matrix metalloproteinase
mRNA	Messenger RNA
MSCs	Mesenchymal stem/stromal cells
N_2	Nitrogen
NaCl	Sodium chloride
NC	Notochordal cells
NCAM-1	Neural cell adhesion molecule 1
NEEA	Non-essential amminoacid
Noto	Notochord homolog
NP	Nucleus pulposus
NPL	Notochordal plate
NPR	Notochordal process
O	Old
O_2	Oxygen
OCT	Cutting temperature compound
P/S	Penicillin/Streptomycin

PAGE	SDS-polyacrilamide gel electrophoresis
Pax-1	Paired box-1
PBS	Phosphate-buffered saline
PDK	Pyruvate dehydrogenase kinase
PEDF	Pigment Epithelium-derived factor
PEEK	Polyetheretherketone
PG	Proteoglycans
PI	Propidium iodide
PKH26	Paul Karl Horan 26
PMSF	Phenylmethylsulfonyl fluoride
PolyHEMA	2-hydroxyethyl methacrylate
PP	Prechordal plate
qRT-PCR	Real-time reverse transcription–polymerase chain reaction
RANTES	Regulated on activation, normal T cell expressed and secreted
Ref	References
RFU	Relative Fluorescence unit
RNA	Ribonucleic Acid
ROS	Reactive oxygen species
RT	Reverse Transcription
S	Seconds
SB	Sulphobetaine
SDC	Sodium deoxycholate
SDS	Sodium dodecyl sulphate
SEM	Standard Error of the Mean
sGAG	Sulfated GAGs
Shh	Sonic hedgehog

SMAD	Small mother against decapentaplegic
SOX9	SRY-box transcription factor 9
TCF/LEF	T cell factor/lymphoid enhancer factor
TGF	Transforming growth factor
TGF-βR	TGF-β receptor
Tie2	Angiopoeitin-1 receptor
TIMP	Tissue inhibitors of metalloproteinase
TNF	Transforming growth factor
TNMD	Tenomodulin
TSP	Thrombospondin
VEGF-A	Vascular endothelial growth factor - A
VEGF-R	Vascular endotelial growth factor - receptor
Y	Young
β-TrCP	β-transducin-repeat–containing protein

CHAPTER I

CHAPTER I – INTERVERTEBRAL DISC: FROM EMBRYONIC DEVELOPMENT TO AGEING

GENERAL INTRODUCTION

1. EMBRYONIC DEVELOPMENT OF THE IVD AND ITS REGULATION

1.1. THE ROLE OF THE NOTOCHORD IN IVD EMBRYONIC DEVELOPMENT

Human spine originates from the notochord and mesenchyme (Roughley, 2004) through a precise regulation mechanism, which involves several genes and signaling pathways. During the gastrulation process, the three germ layers of the embryo (ectoderm, endoderm and mesoderm) are formed and afterwards give rise to the tissues and organs of the human body. In particular, the epidermis and neurons derive from the ectoderm, the digestive and respiratory organs from the endoderm and the connective tissues, like cartilage and bones, originate from the mesoderm (Williams et al., 2019).

Concerning specifically the notochord structure, it develops from the invagination of epiblast cells at the Hensen's node and subsequent colonization of the mesoblastic zone during the gastrulation process (Colombier et al., 2014). Different theories on human notochord development are reported in the following schematic illustration [Figure 1, (de Bree et al., 2018)].

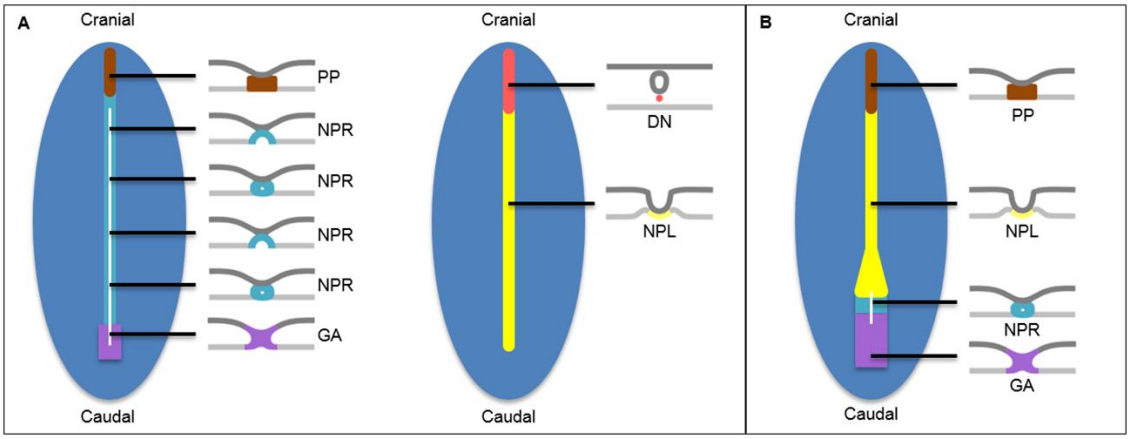

Figure 1. Schematic representation of different theories on human notochord development. This scheme reports the ventral view without endoderm. The level of transversal sections is indicated by the black lines (in the sections the epiblast/ectoderm is in the superior zone). **A.** The notochordal process (NPR) expands over almost all the embryo (left). Along the neurenteric canal, the NPR intercalates between the endoderm and the bottom of the NPR "breaks down". This is essential for the formation of the notochordal

plate (right), whose retraction between the mesenchyme allow the formation of the definitive notochord. **B.** This scheme summarizes the theory suggested by de Bree and colleagues (2018). They suggested the simultaneously presence of all notochord precursors and that the definitive notochord develop in the middle region of the embryo, and not cranially. This figure is from (de Bree et al., 2018). Definitive notochord (DN): red; endoderm: light grey (in sections); epiblast or ectoderm: dark blue, dark grey (in sections); gastrulation area (GA): purple; neurenteric canal: white; notochordal plate (NPL): yellow; notochordal process (NPR): cyan blue; prechordal plate (PP): brown.

The notochord is a rod-like mesoderm-derived structure, which plays a crucial role during embryogenic processes (*e.g*., development of central nervous system, embryonic and somite patterning, formation of blood vessel) (Harfe, 2021), and regulates several cellular functions during intervertebral disc (IVD) formation, including migration, differentiation and survival (Smith et al., 2011). It is composed by large and vacuolated notochordal cells (NCs), which are delimited by a basement membrane, rich in collagen (COL), laminin and proteoglycans (PG) (Bach et al., 2022). The notochord represents the core of early embryonic development and orchestrates the formation of several surrounding tissues (neural tube, sclerotome, pancreas, aorta) through the release of growth factors and morphogens (Hickman et al., 2022; McCann & Séguin, 2016).

In the context of the IVD, the notochord is involved in the direct formation of the nucleus pulposus (NP) and indirect stimulation of cell differentiation within the sclerotome (Smits & Lefebvre, 2003). As shown in Figure 2, sclerotome's cells migrate from the somites at day 30 of fetal gestation and condense around the notochord, forming a more condensed zone, which give rise to the annulus fibrosus (AF) and a less condensed zone, from where the vertebral bodies originate (Smith et al., 2011). Simultaneously, the notochord contracts through the vertebral bodies and expands within the other regions of the IVDs, giving rise to the NP (Smith et al., 2011). During this process, several genes and signaling pathways are involved, as described in detail in the next paragraph. Importantly, the notochord structure disappears after the development of the vertebral column, which in mammals occurs after birth.

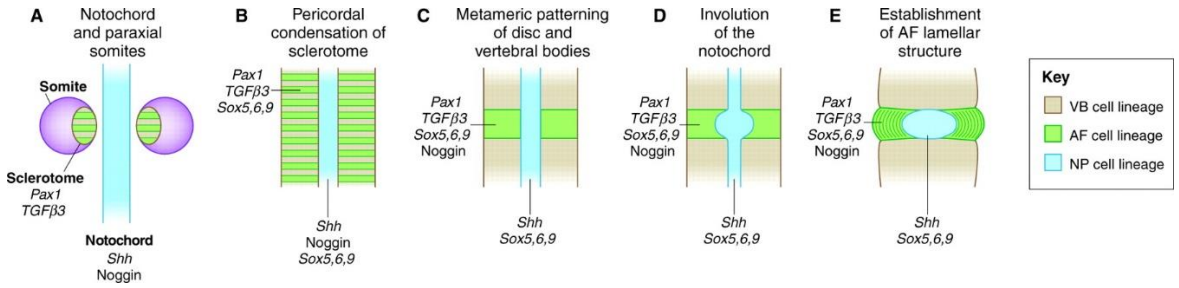

Figure 2. Overview of IVD embryonic development. A. Notochord and paraxial somites with associated signaling pathways (*Shh* and *Noggin* for notochord; *Pax1* and TGF-β3 for sclerotome). **B.** Condensation of sclerotome cells around the notochord. **C.** Development of IVD from more condensed zone (green) and vertebral bodies (brown) from less condensed zone. **D.** Involution of the notochord within the vertebral body and expansion through the disc to form the NP. **E.** Establishment of the AF lamellar structure to form the complete IVD. Adapted from (Smith et al., 2011).

1.2. MOLECULAR REGULATION DURING IVD FORMATION

In the last decades, several researchers started to investigate genes and signaling pathways involved in the regulation of IVD development. Most studies used mice models, since they are characterized by a short gestation period and can be easily manipulated at the genetic level (McCann & Séguin, 2016). As already reported, several genes, including *Brachyury, Forkhead box A2 (Foxa2) and Notochord homolog (Noto)* are involved in notochord development (Colombier et al., 2014; Hickman et al., 2022) and consequently in NP formation. Moreover, *Sonic hedgehog (Shh) factor and FoxA2* are also essential for NC survival and differentiation (Hickman et al., 2022). Shh gene expression and members of Transforming growth factor (TGF) family regulate the development of vertebrae, endplates and AF, while TGF-β is also involved in the differentiation of sclerotome in AF cells. (Colombier et al., 2014).

Brachyury is a transcription factor of the T-box gene family and is crucial for notochord and NP development. Dysregulation of its expression can lead to several spine alterations. For instance, Zhu and colleagues have shown spine defects (*e.g.*, loss of vertebrae, malformations) in a mice embryo model, where Brachyury was selectively depleted (Zhu et al., 2016), thus demonstrating that *Brachyury* gene expression in the

notochord is fundamental for the formation of a functional IVD (Harfe, 2021). *Brachyury* is lost with notochord disappearance before birth (Chen et al., 2020), as well as with replacement of NC with chondrocyte like-cells. However, contrasting hypotheses exists in the literature regarding the preservation of NC in adult NPs. Interestingly, Richardson and co-authors (2016) have shown the expression of NC markers, including *Brachyury*, in adult human NPs (independently of age and degeneration) (Richardson et al., 2017), demonstrating that, at least a subset of NP cells could still preserve a NC-like phenotype within the adult NPs. Interestingly, it has also been shown that *Brachyury* is essential for extracellular matrix (ECM) synthesis, by inducing aggrecan (ACAN) transcription (Wu Y. et al., 2022, preprints, The Lancet) and by being able to mitigate IVD degeneration, thus representing a valuable therapeutic target for IVD regeneration.

Foxa is a family of transcription factors which regulates embryonic development, differentiation and cell identity (Golson & Kaestner, 2016). *Foxa2* is essential to establish notochord identity together with *Brachyury* and *Noto* (Tessier & Risbud, 2021). *Foxa2* modifications can lead to several alterations during embryonic development and pathologies. Specifically, null embryos for *Foxa2* are characterized by node and notochord absence (Ang & Rossant, 1994; Tessier & Risbud, 2021). In 1994, Weinstein *et al.*, showed that mutations in *Foxa2* gene resulted in the lack of notochord formation and node alterations, while knockdown mice for this gene died at day 10 -11 (Weinstein et al., 1994).

Another gene involved in IVD development is *Noto*, which is a homeobox transcription factor expressed at E7.5-E12.5 (McCann et al., 2012), firstly in the axial mesoderm and endoderm and afterwards uniquely at the notochord level (Tessier & Risbud, 2021). Talbot *et al.* (1995) have discovered that Zebrafish with a mutation of *floating head (flh)*, which is a Noto ortholog, were characterized by notochord absence (Talbot et al., 1995; Tessier & Risbud, 2021), unveiling its importance along development. McCann and colleagues (2012), developed a mouse model which expresses *Cre* recombinase in the notochord and, by targeting *Noto* homeobox gene, were able to demonstrate that NP cells derive from the notochord (McCann et al., 2012).

Finally, *Shh* is another essential regulator along embryonic development and IVD preservation. Specifically, *Shh* is important for the determination of the anterior-posterior axis (Hickman et al., 2022) as well as for the preservation of IVD function after birth (Harfe, 2021). Interestingly, Choi *et al*. demonstrated that *Shh* signaling is fundamental for appropriate IVD development (Choi & Harfe Brian, 2011). When they removed *Shh* from all

the cells expressing this gene, mutant mice were characterized by smaller NPs, as compared to the controls. Moreover, AFs lost the surrounding lamellae, probably as a consequence of the aberrant NP formation. Since *Shh* is involved in the regulation of cell proliferation and survival in different tissues, the authors hypothesized that the smaller NPs could be due to a reduction of NC proliferation after signaling removal (Choi & Harfe Brian, 2011; Hickman et al., 2022). In another study, Choi and colleagues (2012) have shown that the development of IVDs and vertebral columns was normal after removing *Shh* from mice floor plate. However, when the signaling was depleted in the notochord, IVDs and vertebrae loss were detected, demonstrating that *Shh* expression is essential for IVDs patterning (Choi et al., 2012). *Shh* signaling is also involved in AF embryonic development, by driving sclerotome formation through regulation of *Pax1* expression. In this precise mechanism, *Shh* signaling is antagonized by Bone morphogenic protein (BMP), that in turn, is antagonized by *Noggin* and *Gremlin-1* (Séguin et al., 2018).

1.3. MAJOR SIGNALING PATHWAYS INVOLVED IN IVD DEVELOPMENT AND MAINTENANCE

The Wnt family has a central role in IVD development. It is constituted by secreted glycoproteins rich in cysteine, which act as ligands for different receptors and co-receptors (Krishnamurthy & Kurzrock, 2018) and are involved in several cellular processes during embryonic development, including cell proliferation, cell polarity and cell identity, as well as in tissue homeostasis (MacDonald et al., 2009). Wnt is responsible for the activation of different signaling pathways, which can be canonical (Wnt/β-catenin pathway) or non-canonical (beta-catenin independent pathway) (Krishnamurthy & Kurzrock, 2018; Wu et al., 2021).

The Wnt/β-catenin pathway is highly conserved during evolution (Moon Randall, 2005) and represents a key regulator of several processes, including embryonic development, metabolism, cell fate and epithelial-mesenchymal transition (Lecarpentier et al., 2019). Thus, Wnt signaling regulation is fundamental to preserve physiological homeostasis and avoid the onset of pathological disorders. Specifically, when Wnt ligand is not present, β-catenin binds to Axin, adenomatous polyposis coli gene product (APC), glycogen synthase kinase 3 (GSK3) and casein kinase 1 (CK1), and its amino terminal region is phosphorylated. As a consequence, β-catenin interacts with β-transducin-repeat–containing protein (β-TrCP), resulting in its degradation, which is mediated by the

proteasome. Following degradation, β-catenin is no longer able to enter the nucleus and Wnt-related genes are inhibited (Figure 3A) (MacDonald et al., 2009; Moon Randall, 2005). Wnt signaling pathway is activated by the binding of secreted Wnts to serpentine receptors Frizzled (Fz) and low-density lipoprotein receptor-related protein (LRP)-6 and to LRP-5 co-receptors (MacDonald et al., 2009; Moon Randall, 2005). The complex Wnt-Fz-LRP6 and the scaffolding protein Dishevelled (Dvl) phosphorylate and activate the LRP6 with the consequent recruitment of Axin complex. Afterwards, Axin-mediated β-catenin phosphorylation is inhibited and β-catenin translocates into the cell nuclei to form a complex with T cell factor/lymphoid enhancer factor (TCF/LEF) consequently activating the expression of specific genes (MacDonald et al., 2009), such as CYCLIN D1, cMYC, MCT1, PDK and fibronectin (FN), among others (Lecarpentier et al., 2019) (Figure 3B).

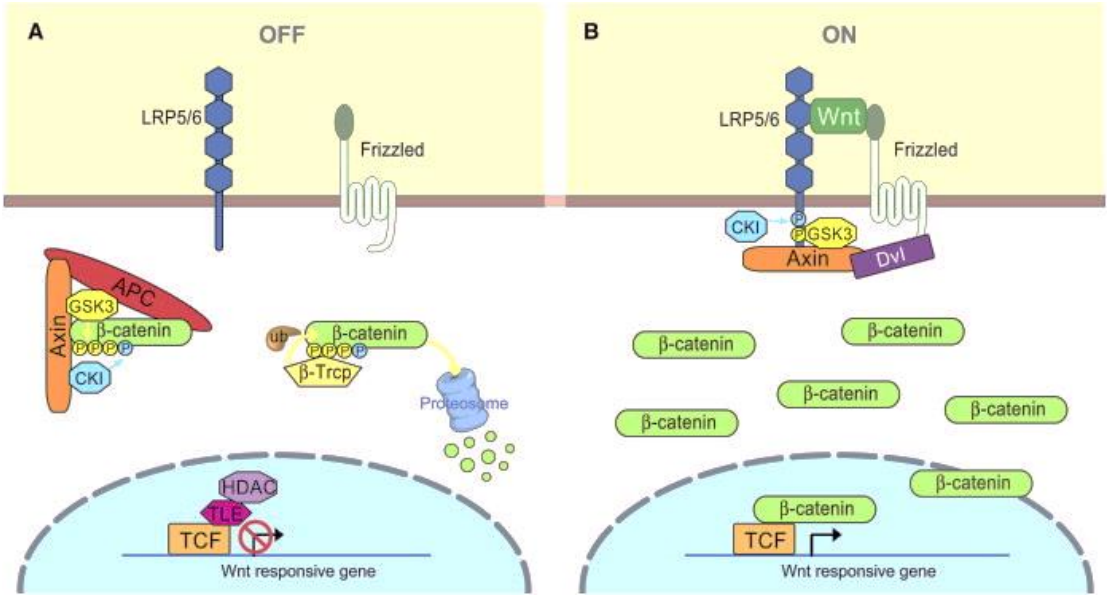

Figure 3. Wnt/β-catenin signaling pathway. (A) In the state OFF, β-catenin is phosphorylated by CK1 and GSK3 and consequently degraded through its binding with β-TrCP. **(B)** In the state ON, Wnt binds Fz receptors and LRP5/6 co-receptors, thus inhibiting β-catenin degradation through activation of Dvl and recruitment of Axin complex. Finally, β-catenin enters the cell nuclei and activates the expression of Wnt responsive genes, thanks to its binding to TCF. Adapted from (MacDonald et al., 2009).

The Wnt signaling pathway plays an essential role in IVD formation during embryonic development, particularly by inducing the differentiation of progenitor cells into

NCs and by promoting notochord extension (Wu et al., 2021). In 2011, Kondo and co-workers analyzed the distribution of Wnt/β-catenin signal by performing β-galactosidase staining on lumbar vertebral bodies isolated from mice reporter. Interestingly, they showed that at embryonic age 18.5 the signal was higher at the level of the growth plate, endplate and AF, while at 5 weeks, it increased in NP cells, thus demonstrating that Wnt/β-catenin is differently activated depending on embryonic and postnatal stages. Then, they analyzed how activation or depletion of Wnt/β-catenin signaling affected IVD tissue structure. When they excessively activate the signaling pathway, severe modifications in vertebral bodies growth plate were detected. Moreover, the AF became disorganized with increased cell proliferation, while the NPs were enlarged with few PGs. In turn, when they depleted Wnt signaling, the endplates were affected. The authors were able to demonstrate the critical role of Wnt/β-catenin on the preservation of IVD tissue structure, especially for the AF and endplates (Kondo et al., 2011).

Other studies have shown the role of Wnt/β-catenin pathway in IVD degenerative cascade (Chen et al., 2017; Holguin & Silva, 2018; Wang et al., 2012; Wang et al., 2018), although information is still controversial. In 2012, Wang *et al.* observed by immunohistochemistry (IHC), the upregulation of β-catenin in human degenerated IVD tissues, when compared to normal ones. Moreover, they created inducible β-catenin conditional activation mice models (cAct mice), in order to investigate the role of β-catenin in IVD architecture and function. They discovered that β-catenin upregulation lead to alterations in IVD, both at the cellular and matrix level. Particularly, cAct mice (3 and 6 months old) were characterized by decreased spine length, as well as loss of growth plate cartilage and osteophyte development, which in turn caused IVD space narrowing and vertebrae fusion. Moreover, PG decrease was also detected at the matrix level, as well as alterations in NP and AF tissues (Wang et al., 2012).

TGF-β is another signaling pathway involved in embryonic development and tissue homeostasis, by controlling several cellular processes (*e.g*., proliferation, differentiation, stem cell renewal) (Wu et al., 2021). TGF-β family is composed by different members (TGF-β1, TGF-β2 and TGF-β3) with specific functions. Inactive TGF-β is expressed in a latent complex, consisting in latency-associated polypeptide (LAP) and a mature polypeptide. TGF-β signaling pathway is activated by binding of the mature polypeptide, which is converted in a 25 kD dimer, to the TGF-β receptor (TGF-βR), located at the cell surface. Initially, the ligand binds the receptor subunit TGF-βRII with consequent trans-

phosphorylation of the receptor subunit TGF-βRI. In the canonical pathway, TGF-βRI activates small mother against decapentaplegic (SMAD)-2, SMAD-3 and SMAD–4, which translocate into the cell nuclei to activate or inhibit the expression of specific genes. In the non-canonical pathway, TGF-β activates other signaling pathways, including mitogen-activated protein kinase (MAPK) (Chen et al., 2019) (Figure 4).

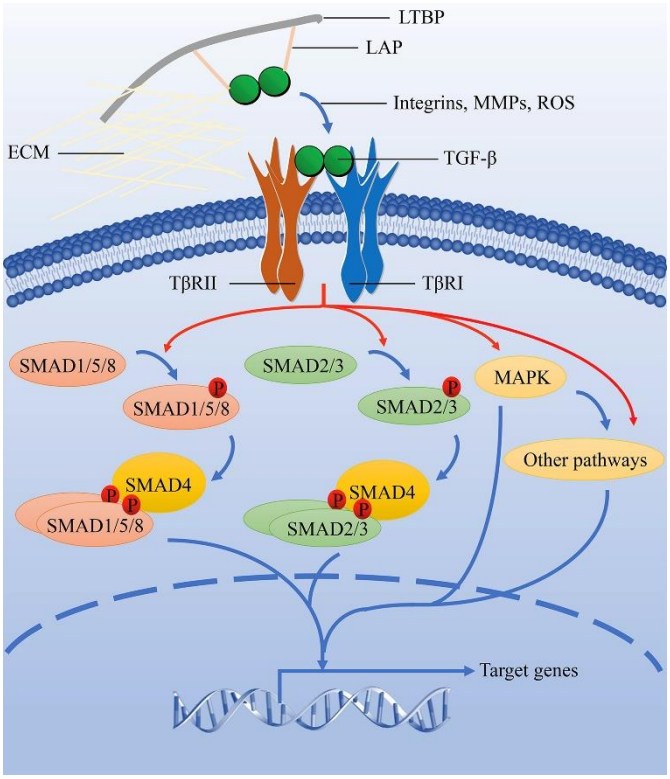

Figure 4. TGF-β signaling pathway in IVD. The latent form of TGF-β (LAP and mature polypeptide) is activated by integrin, MMPs or ROS and bind to TβRI and TβRII. Afterwards, TβRI is transphosphorylated by TβRII and induces the transcription of target genes through the activation of the associated pathways (SMADs or MAPK, among others). Image adapted from (Chen et al., 2019).

TGF- β signaling pathway plays an essential role in both cartilage and skeleton formation at embryonic stages, but it is also involved in IVD growth and preservation after birth (Hongting Jin et al., 2011). In 2011, Jin and co-authors investigated the role of this pathway in IVD tissue preservation, which was still poorly understood. By depleting TGF-

βR2 in inner AF cells and growth plate chondrocytes, they observed postnatal matrix and endplate cell loss in mutant mice, when compared to the wildtype. Moreover, 3-months old mutant mice were characterized by alterations of growth plate chondrocytes, being disorganized and reduced in number. Thus, the authors demonstrate that TGF-β pathway is important for IVD tissue development, specifically for growth plate and endplate formation. They hypothesize that its inhibition may have a role in the observed tissue modifications, through metalloproteinase (MMP)-13 activation (H. Jin et al., 2011). In another work, Risbud and colleagues have shown over-expression of ECM genes, increased incorporation of ^{35}S in PG and decreased ACAN turnover, when rat IVDs were cultured in the presence of TGF-β3, when compared to TGF-β1 culture (Risbud et al., 2006).

Finally, TGF-β and Wnt/β-catenin signaling pathways can also interact to guarantee mesoderm development or to induce tumorigenesis in different tissues. In the context of IVD, these two pathways can cross-talk during degeneration. For instance, the Wnt/β-catenin can activate TFG-β expression in NP cells (Wu et al., 2021). Hiyama *et al.* have demonstrated that expression of both TGF-β and MMPs in rat NP cells, stimulated by Wnt/β-catenin signaling, could be responsible for matrix degradation leading to IVD degeneration (Hiyama et al., 2010).

1.4. EXTRACELLULAR MATRIX COMPONENTS PRESENT IN THE IVD DURING EARLY DEVELOPMENTAL STAGES

In addition to genes and associated signaling pathways, ECM content is also essential for guiding IVD development. The ECM of fetal IVDs represents a unique network and is very different from adult ECM. However, the comprehension of its composition and how this influences IVD development is still poor understood. Specifically, there are few studies in the literature that have tried to dissect developmental-associated changes in matrix microenvironment between different ages, especially in humans.

Recently, Rajasekaran *et al*., have performed a proteomic and bioinformatic analysis in fetal *vs* adult human NPs, in order to unravel differences in the matrisome profiling at different aged stages. They have shown overexpression of several proteins involved in matrix assembly and growth in fetus NPs, including PGs, glycoproteins and COL. When comparing fetus *vs* adult tissues, fetal matrices showed a decrease of several PGs and over-expression of biglycan and fibromodulin. Moreover, different glycoproteins were also

down-regulated in fetal NPs, including FN, while others were up-regulated (*e.g.*, TGF-β1). Interestingly, also thrombospondin (TSP) showed to be higher in fetus NPs, when compared to adult ones, despite no statistical significance. Finally, they have revealed the presence of proteins in fetal NPs (matrillin-2 and COL triple helix repeat containing 1), with a role in tissue development and regeneration (Rajasekaran et al., 2020). Some of these proteins were also found in the matrisome profiling of fetal bovine NPs (Caldeira et al., 2017), thus demonstrating that several ECM features are highly conserved between species.

Rutges and colleagues have previously demonstrated the presence of MMP-1, MMP-2, MMP-3 and MMP-14 in fetal human IVDs (gestation age 15.5 – 40.3 weeks) and non-fetal human IVDs (age 3.3–21.8 years), particularly in NP and NC cells. Specifically, MMP-1 and MMP-14 were shown to significantly increase in fetal IVDs, when compared to non-fetal ones. Moreover, they have found higher MMP-2 activity between 15 and 22 weeks of gestation in fetal tissue, which decreased with gestational weeks as well as in postnatal and young IVDs (Rutges et al., 2010). Despite MMPs expression being mainly associated with matrix degradation along IVD degeneration and ageing, they also may have a key role during skeletal development.

In another study, human fetal AF, specifically the outer tissue, were characterized by the presence of several elastic fiber-associated proteins (fibrillin-1, Latent Transforming Growth Factor Beta Binding Protein 2 [LTBP-2] and microfibril-associated glycoproteins [MAGP-1]). Moreover, fibrillin-1, MAGP-1 and versican showed immunolocalization with elastin, thus the authors hypothesized that these proteins could have a role in the stabilization and integration of AF fibers, as well as in the formation of the tissue through generation of tensional forces (Hayes et al., 2011).

Despite several efforts to understand the fascinating area of IVD embryonic development, there is still a lack of knowledge on the fetal ECM composition, which is of utmost importance for guiding IVD formation. Understanding specific cues necessary and sufficient during early stages of development would be beneficial for the creation of more appropriate therapeutic strategies, which recapitulate a pro-regenerative microenvironment, thus triggering IVD matrix reconstruction in a degenerative context.

2. INTERVERTEBRAL DISC AGEING AND ASSOCIATED ALTERATIONS

2.1. HALLMARKS OF IVD AGEING

Ageing is caused by an increase of molecular alterations at the cellular and matrix level, which lead to modifications of physiological environment (Hartman et al., 2018). The IVD undergoes ageing, as many other tissues and organs of the human body, by showing typical age-associated hallmarks (Vo et al., 2016): genetic factors (Feng et al., 2016) (*e.g.*, TSP, COL, ACAN, MMPs, among others) (Munir et al., 2018), shortening of telomere length (Le Maitre et al., 2007; Wang et al., 2016), epigenetic modifications (Ikuno et al., 2019; Tajerian et al., 2011), matrisome profiling changes (Qiu et al., 2020; Sarath Babu et al., 2016; Ye et al., 2015; Yee et al., 2016), deregulation of nutrient-sensing (Vo et al., 2016), mitochondrial dysfunction (Li et al., 2020; Nasto et al., 2013), cellular senescence (Le Maitre et al., 2007; Patil et al., 2018; Wang et al., 2016), stem cell exhaustion (Sakai et al., 2012) and abnormal intercellular communication (Dahia et al., 2009) (López-Otín et al., 2013; Vo et al., 2016).

However, the ageing cascade starts earlier in the IVD as a consequence of numerous degenerative changes at the morphological, biochemical and cellular level. Thus, degeneration and ageing are linked. As it is well known, the IVD is characterized by a harsh microenvironment, being avascular, hypoxic, hyperosmotic, acidic and with low nutrient accessibility (Dou et al., 2021), which renders problematic cell survival. Moreover, its scarce capacity to regenerate and self-repair affects tissue structure and function. The age–associated changes occurring in the IVD, consist in an increased number and size of tissue fissures, accumulation of debris, as well as neovascularization inside the AF (Vo et al., 2016). With ageing, the NP becomes more fibrotic due to the decline of PGs and water content, leading to a loss of osmotic pressure within the NP and a consequent decrease of overall IVD height (Vo et al., 2016). The disc turns yellowish in elder individuals, as a consequence of oxidized matrix proteins' accumulation. Furthermore, the ossification of the endplates and the reduction of vascular nutrient supply within the tissue contribute to an increased accumulation of metabolites and a harsher acidic microenvironment (Vo et al., 2016), which cause alterations at cellular and ECM levels, ultimately affecting disc function. Previously, we have shown macroscopic changes of bovine IVDs along ageing. In particular, elder IVD tissues were more fibrotic, drier and yellowish when compared to young

and fetal ones, which were characterized by a hydrogel-like NP surrounded by well-distinguished concentric AF lamellae (Caldeira et al., 2017). Thus, some of the age-related changes occurring in human tissue are also common to IVDs from other species.

2.2. AGE-ASSOCIATED CELL ALTERATIONS IN THE IVD

Cellular changes in the IVD, particularly in the NP, can be readily observed after birth with a gradual decrease of NCs, until their complete disappearance (Smith et al., 2011), being replaced by chondrocyte–like cells (also known as NP cells). NCs are large vacuolated cells, reminiscent of the notochord, which are involved in NP preservation. On the contrary, NP cells are smaller and without vacuoles, being unable to induce NP homeostasis and repair. Interestingly, animals that have a persisting presence of NCs into adulthood (*e.g*., mice, rats, rabbits, and pigs) (Daly et al., 2016), are not affected by severe IVD degeneration unlike humans. This suggests a possible correlation between NC loss and the onset of age-associated IVD degeneration (McCann & Séguin, 2016).

As it is known, NP cells constitute an heterogenous population within the IVD, rendering problematic the understanding of their origin. Thus, the information in the literature remains controversial. Several studies have hypothesized that NP cells directly derive from the embryonic notochord (Risbud et al., 2010), while others have proposed their recruitment from adjacent tissues (*e.g*., endplates) (Kim et al., 2003) (Smith et al., 2011). Thus, the mechanism that guides the transition from NCs to NP cells is still poorly understood. One factor that may trigger cellular changes in the NP is the alteration of the nutritional and mechanical microenvironment experienced during ageing (Smith et al., 2011). Indeed, cells are sensitive to their surrounding environment and are able to respond and adapt to any change in order to preserve tissue function. Specifically, the IVD is subjected to an increase in mechanical strength after birth, which could induce NC differentiation into NP cells or NC apoptosis (Smith et al., 2011). It is known that after birth the IVD environment becomes harsh due to the decrease of oxygen and nutrient supply, rendering cell survival problematic. The environmental changes may induce the appearance of NP cells, which are able to survive under low nutrient and oxygen supply when compared to NCs (Smith et al., 2011). Moreover, as referred before, cell density starts to dramatically decrease during childhood (Galbusera et al., 2014). By using IVD specimens isolated from autopsies of individuals ranging from 0 to 86 years old, Boos' group showed that cell density

starts to decline in the NP, AF and endplate between 0 and 16 years old. From 0 to 3 years old, NP and AF were affected by major changes, while afterwards no significant alterations were observed (Liebscher et al., 2011).

Previous work from our group have dissected age-associated phenotypical changes in primary human IVD cells, isolated from degenerated tissues, by using flow cytometry. Specifically, Molinos *et al*. (2018) were able to identify three sub-populations of IVD cells with different diameter (small, large and super large), as well as a negative correlation between donor age and cell yield. With ageing, IVD cells showed increased diameter due to an enlargement of the pericellular matrix. By analyzing several markers for progenitor and inflammatory cells, the authors have shown decreased CD90+ and CD73+ cells with ageing. Interestingly, CD146+ cells were also found in IVD degenerated tissues, thus suggesting that a small portion of progenitor cells could still persist in the aged IVDs (Molinos et al., 2018). More recently, the same authors have also investigated age-associated changes of NP cells, isolated from young (1 year old) and old (10-16 years old) bovine IVDs, by adopting a high-throughput analysis (flow cytometry). They have shown a decreased percentage of CD29+, CD44+, Tie2+ cells with ageing, while GD2+ cells increased. Moreover, the expression of CD146 was preserved along ageing. Interestingly, the existence of four NP cells sub-population, with different size, was also uncovered both in young and old donors, contrarily to the three population previously identified in human IVD cells (Molinos et al., 2018). With ageing, the cell population with smallest size increased, being the most prevalent present (Molinos et al., 2023, under review). These discoveries highlighted the importance of investigating cellular changes in IVD occurring with ageing in order to unravel specific targets, which will be essential for the development of targeted therapies for IVD degeneration.

Since cells are responsible for producing the major components of the ECM, their changes in number and phenotype lead to several matrix modifications, which ultimately affect tissue homeostasis and function. A more detailed description of the age-associated IVD ECM alterations is reported in the next paragraph.

2.3. ECM CHANGES DURING AGEING

With ageing, the most dramatic changes in matrix composition occur in the NP. As a consequence of cell decline, the production of PG and COL decreases in the NP (Galbusera et al., 2014; Roughley, 2004). As it is well known, both PG and COL are essential for maintaining appropriate tissue hydration by providing swelling pressure and resistance to it, respectively (Roughley, 2004). Thus, the reduction of both proteins leads to a decrease of water within the NP, which becomes drier. With the progression of age, COL2, which is the most prevalent COL in the NP, is replaced by COL1. Moreover, COL10 was also detected in the adult NP and inner AF, while in younger tissues this protein is only present at the endplates level (Roughley, 2004). COL10 has also been found at high levels in patients affected by osteoarthritis and associated to inflammation and tissue degradation at least in cartilage (He et al., 2014). In addition, increased COL damage in the NP and outer AF can also be observed due to a higher collagenase activity, which causes a reduction of mechanical IVD strength and ultimately leads to tissue loss (Roughley, 2004).

Another protein that is altered in aged IVDs is FN, which is involved in the cross-talk between cells and the ECM in physiological conditions. However, FN is overexpressed during IVD ageing and is associated with pathological progression and the grade of tissue degeneration. Interestingly, Yee and colleagues analyzed the protein composition of normal and degenerated IVDs (specifically AFs and NPs) by liquid chromatography combined with tandem mass spectrometry. They found several proteins upregulated during ageing and degeneration, including FN (Yee et al., 2016). More recently, Castro *et al*. (2022), have shown an increase of both FN and COL2 in human AFs with severe herniation (Castro et al., 2022). Prolargin, which is important for anchoring the basement membrane to the connective tissue (Caldeira et al., 2017), was also found at higher levels in old bovine NPs together with FN. As a consequence, COL fibers resulted to be disrupted within the tissue (Caldeira et al., 2017).

As it is well known, alterations in inflammatory cytokines (*e.g.*, interleukins [IL]-1, IL-6), and MMPs, as well as in a disintegrin and metalloproteinase with thrombospondin motifs (ADAMTs) and TGF-β signaling pathway, are also involved in the IVD ageing cascade (Ohnishi et al., 2020). Specifically, the high level of ECM degradation and the reduction of ACAN content may be correlated with an increase of degrading enzymes, including ADAMTS - 4 and 5, aggrecanases, MMP-1, MMP-2, MMP-3 and MMP-13, among others (Yee et al., 2016). Given that MMPs and ADAMTs are not only responsible for the

degradation of COL but also for that of PGs, their increase leads to tissue dehydration as well as tearing and cracking formation (Colombier et al., 2014). Thus, it is essential that a constant balance between matrix degradation and *de novo* ECM synthesis is maintained in order to preserve IVD physiological structure and function. However, with ageing and associated tissue degeneration, this specific mechanism is impaired, ultimately leading to fibrosis.

Recently, differences in the fetal and geriatric lumbar NPs were revealed, by liquid chromatography-tandem mass spectrometry. The authors have demonstrated an upregulation of several proteins involved in inflammatory response in geriatric tissues, particularly LTA and IL-11, which are involved in the IVD degenerative cascade. Moreover, vascular endothelial growth factor-A (VEGF-A) was also overexpressed in geriatric NPs compared to fetal ones, thus showing an increased vasculogenesis along ageing and degeneration (Qiu et al., 2020).

The described biochemical imbalance of the IVD is responsible for the inhibition of matrix turnover with associated tissue modifications. At the end, the IVD function is dramatically affected with consequent reduction of disc height and altered biological function (Caldeira et al., 2017). Indeed, the NP has scarce capacity to self-repair and the accumulation of age-associated alterations leads to a painful pathological onset, as is the case of disc herniation. Although ageing is inevitable in the disc, a more comprehensive study on the pathological cascade and on the factors involved is needed in order to develop specific solutions that could arrest the degenerative scenario at earlier stages.

3. REFERENCES

Ang, S.-L., & Rossant, J. (1994). HNF-3β is essential for node and notochord formation in mouse development. *Cell*, *78*(4), 561-574. https://doi.org/https://doi.org/10.1016/0092-8674(94)90522-3

Bach, F. C., Poramba-Liyanage, D. W., Riemers, F. M., Guicheux, J., Camus, A., Iatridis, J. C., Chan, D., Ito, K., Le Maitre, C. L., & Tryfonidou, M. A. (2022). Notochordal Cell-Based Treatment Strategies and Their Potential in Intervertebral Disc Regeneration [Review]. *Frontiers in Cell and Developmental Biology*, *9*. https://doi.org/10.3389/fcell.2021.780749

Caldeira, J., Santa, C., Osório, H., Molinos, M., Manadas, B., Gonçalves, R., & Barbosa, M. (2017). Matrisome Profiling During Intervertebral Disc Development And Ageing. *Scientific Reports*, *7*(1), 11629-11629. https://doi.org/10.1038/s41598-017-11960-0

Castro, A. L., Ribeiro-Machado, C., Oliveira, C. M., Teixeira, G. Q., Neidlinger-Wilke, C., Pereira, P., Vaz, R., Barbosa, M. A., & Gonçalves, R. M. (2022). Fibrotic alterations in human annulus fibrosus correlate with progression of intervertebral disc herniation. *Arthritis Research & Therapy*, *24*(1), 25. https://doi.org/10.1186/s13075-021-02690-w

Chen, J., Jia, Y.-S., Liu, G.-Z., Sun, Q., Zhang, F., Ma, S., & Wang, Y.-J. (2017). Role of LncRNA TUG1 in intervertebral disc degeneration and nucleus pulposus cells via regulating Wnt/β-catenin signaling pathway. *Biochemical and Biophysical Research Communications*, *491*(3), 668-674. https://doi.org/https://doi.org/10.1016/j.bbrc.2017.07.146

Chen, M., Wu, Y., Zhang, H., Li, S., Zhou, J., & Shen, J. (2020). The Roles of Embryonic Transcription Factor BRACHYURY in Tumorigenesis and Progression [Review]. *Frontiers in Oncology*, *10*. https://doi.org/10.3389/fonc.2020.00961

Chen, S., Liu, S., Ma, K., Zhao, L., Lin, H., & Shao, Z. (2019). TGF-β signaling in intervertebral disc health and disease. *Osteoarthritis Cartilage*, *27*(8), 1109-1117. https://doi.org/10.1016/j.joca.2019.05.005

Choi, K.-S., & Harfe Brian, D. (2011). Hedgehog signaling is required for formation of the notochord sheath and patterning of nuclei pulposi within the intervertebral discs. *Proceedings of the National Academy of Sciences*, *108*(23), 9484-9489. https://doi.org/10.1073/pnas.1007566108

Choi, K.-S., Lee, C., & Harfe, B. D. (2012). Sonic hedgehog in the notochord is sufficient for patterning of the intervertebral discs. *Mechanisms of Development*, *129*(9), 255-262. https://doi.org/https://doi.org/10.1016/j.mod.2012.07.003

Colombier, P., Clouet, J., Hamel, O., Lescaudron, L., & Guicheux, J. (2014). The lumbar intervertebral disc: from embryonic development to degeneration. *Joint Bone Spine*, *81*(2), 125-129. https://doi.org/10.1016/j.jbspin.2013.07.012

Dahia, C. L., Mahoney, E. J., Durrani, A. A., & Wylie, C. (2009). Intercellular signaling pathways active during intervertebral disc growth, differentiation, and aging. *Spine (Phila Pa 1976)*, *34*(5), 456-462. https://doi.org/10.1097/BRS.0b013e3181913e98

Daly, C., Ghosh, P., Jenkin, G., Oehme, D., & Goldschlager, T. (2016). A Review of Animal Models of Intervertebral Disc Degeneration: Pathophysiology, Regeneration, and Translation to the Clinic. *BioMed Research International*, *2016*, 5952165. https://doi.org/10.1155/2016/5952165

de Bree, K., de Bakker, B. S., & Oostra, R.-J. (2018). The development of the human notochord. *PLOS ONE*, *13*(10), e0205752. https://doi.org/10.1371/journal.pone.0205752

Dou, Y., Sun, X., Ma, X., Zhao, X., & Yang, Q. (2021). Intervertebral Disk Degeneration: The Microenvironment and Tissue Engineering Strategies. *Frontiers in bioengineering and biotechnology*, *9*, 592118-592118. https://doi.org/10.3389/fbioe.2021.592118

Feng, Y., Egan, B., & Wang, J. (2016). Genetic Factors in Intervertebral Disc Degeneration. *Genes & diseases*, *3*(3), 178-185. https://doi.org/10.1016/j.gendis.2016.04.005

Galbusera, F., van Rijsbergen, M., Ito, K., Huyghe, J. M., Brayda-Bruno, M., & Wilke, H. J. (2014). Ageing and degenerative changes of the intervertebral disc and their impact on spinal flexibility. *Eur Spine J*, *23 Suppl 3*, S324-332. https://doi.org/10.1007/s00586-014-3203-4

Golson, M. L., & Kaestner, K. H. (2016). Fox transcription factors: from development to disease. *Development (Cambridge, England)*, *143*(24), 4558-4570. https://doi.org/10.1242/dev.112672

Harfe, B. D. (2021). Intervertebral disc repair and regeneration: Insights from the notochord. *Seminars in Cell & Developmental Biology*. https://doi.org/https://doi.org/10.1016/j.semcdb.2021.11.012

Hartman, R., Patil, P., Tisherman, R., St Croix, C., Niedernhofer, L. J., Robbins, P. D., Ambrosio, F., Van Houten, B., Sowa, G., & Vo, N. (2018). Age-dependent changes in intervertebral disc cell mitochondria and bioenergetics. *Eur Cell Mater*, *36*, 171-183. https://doi.org/10.22203/eCM.v036a13

Hayes, A. J., Smith, S. M., Gibson, M. A., & Melrose, J. (2011). Comparative Immunolocalization of the Elastin Fiber–Associated Proteins Fibrillin-1, LTBP-2, and MAGP-1 With Components of the Collagenous and Proteoglycan Matrix of the Fetal Human Intervertebral Disc. *Spine*, *36*(21). https://journals.lww.com/spinejournal/Fulltext/2011/10010/Comparative_Immunolocalization_of_the_Elastin.19.aspx

He, Y., Siebuhr, A. S., Brandt-Hansen, N. U., Wang, J., Su, D., Zheng, Q., Simonsen, O., Petersen, K. K., Arendt-Nielsen, L., Eskehave, T., Hoeck, H. C., Karsdal, M. A., & Bay-Jensen, A. C. (2014). Type X collagen levels are elevated in serum from human osteoarthritis patients and associated with biomarkers of cartilage degradation and inflammation. *BMC Musculoskeletal Disorders*, *15*(1), 309. https://doi.org/10.1186/1471-2474-15-309

Hickman, T. T., Rathan-Kumar, S., & Peck, S. H. (2022). Development, Pathogenesis, and Regeneration of the Intervertebral Disc: Current and Future Insights Spanning Traditional to Omics Methods. *Frontiers in Cell and Developmental Biology*, *10*, 841831-841831. https://doi.org/10.3389/fcell.2022.841831

Hiyama, A., Sakai, D., Risbud, M. V., Tanaka, M., Arai, F., Abe, K., & Mochida, J. (2010). Enhancement of intervertebral disc cell senescence by WNT/β-catenin signaling–induced matrix metalloproteinase expression [https://doi.org/10.1002/art.27599]. *Arthritis & Rheumatism*, *62*(10), 3036-3047. https://doi.org/https://doi.org/10.1002/art.27599

Holguin, N., & Silva, M. J. (2018). In-Vivo Nucleus Pulposus-Specific Regulation of Adult Murine Intervertebral Disc Degeneration via Wnt/Beta-Catenin Signaling. *Scientific Reports*, *8*(1), 11191. https://doi.org/10.1038/s41598-018-29352-3

Ikuno, A., Akeda, K., Takebayashi, S.-I., Shimaoka, M., Okumura, K., & Sudo, A. (2019). Genome-wide analysis of DNA methylation profile identifies differentially methylated loci associated with human intervertebral disc degeneration. *PLOS ONE*, *14*(9), e0222188-e0222188. https://doi.org/10.1371/journal.pone.0222188

Jin, H., Shen, J., Wang, B., Wang, M., Shu, B., & Chen, D. (2011). TGF-β signaling plays an essential role in the growth and maintenance of intervertebral disc tissue. *FEBS Letters*, *585*(8), 1209-1215. https://doi.org/https://doi.org/10.1016/j.febslet.2011.03.034

Jin, H., Shen, J., Wang, B., Wang, M., Shu, B., & Chen, D. (2011). TGF-β signaling plays an essential role in the growth and maintenance of intervertebral disc tissue. *FEBS Lett*, *585*(8), 1209-1215. https://doi.org/10.1016/j.febslet.2011.03.034

Kim, K. W., Lim, T. H., Kim, J. G., Jeong, S. T., Masuda, K., & An, H. S. (2003). The origin of chondrocytes in the nucleus pulposus and histologic findings associated with the transition of a notochordal nucleus pulposus to a fibrocartilaginous nucleus pulposus in intact rabbit intervertebral discs. *Spine (Phila Pa 1976)*, *28*(10), 982-990. https://doi.org/10.1097/01.Brs.0000061986.03886.4f

Kondo, N., Yuasa, T., Shimono, K., Tung, W., Okabe, T., Yasuhara, R., Pacifici, M., Zhang, Y., Iwamoto, M., & Enomoto-Iwamoto, M. (2011). Intervertebral disc development is regulated by Wnt/β-catenin signaling. *Spine*, *36*(8), E513-E518. https://doi.org/10.1097/BRS.0b013e3181f52cb5

Krishnamurthy, N., & Kurzrock, R. (2018). Targeting the Wnt/beta-catenin pathway in cancer: Update on effectors and inhibitors. *Cancer Treatment Reviews*, *62*, 50-60. https://doi.org/https://doi.org/10.1016/j.ctrv.2017.11.002

Le Maitre, C. L., Freemont, A. J., & Hoyland, J. A. (2007). Accelerated cellular senescence in degenerate intervertebral discs: a possible role in the pathogenesis of intervertebral disc degeneration. *Arthritis Res Ther*, *9*(3), R45. https://doi.org/10.1186/ar2198

Lecarpentier, Y., Schussler, O., Hébert, J.-L., & Vallée, A. (2019). Multiple Targets of the Canonical WNT/β-Catenin Signaling in Cancers [Review]. *Frontiers in Oncology*, *9*. https://doi.org/10.3389/fonc.2019.01248

Li, D., Tao, F., & Jin, L. (2020). Mitochondrial Dysfunction in Intervertebral Disc Degeneration: From Pathogenesis to Therapeutic Target. *Oxidative Medicine and Cellular Longevity*, *2020*, 8880320. https://doi.org/10.1155/2020/8880320

Liebscher, T., Haefeli, M., Wuertz, K., Nerlich, A. G., & Boos, N. (2011). Age-Related Variation in Cell Density of Human Lumbar Intervertebral Disc. *Spine*, *36*(2). https://journals.lww.com/spinejournal/Fulltext/2011/01150/Age_Related_Variation_in_Cell_Density_of_Human.9.aspx

López-Otín, C., Blasco, M. A., Partridge, L., Serrano, M., & Kroemer, G. (2013). The hallmarks of aging. *Cell*, *153*(6), 1194-1217. https://doi.org/10.1016/j.cell.2013.05.039

MacDonald, B. T., Tamai, K., & He, X. (2009). Wnt/β-Catenin Signaling: Components, Mechanisms, and Diseases. *Developmental Cell*, *17*(1), 9-26. https://doi.org/https://doi.org/10.1016/j.devcel.2009.06.016

McCann, M. R., & Séguin, C. A. (2016). Notochord Cells in Intervertebral Disc Development and Degeneration. *J Dev Biol*, *4*(1). https://doi.org/10.3390/jdb4010003

McCann, M. R., Tamplin, O. J., Rossant, J., & Séguin, C. A. (2012). Tracing notochord-derived cells using a Noto-cre mouse: implications for intervertebral disc development. *Disease Models & Mechanisms*, *5*(1), 73-82. https://doi.org/10.1242/dmm.008128

Molinos, M., Cunha, C., Almeida, C. R., Gonçalves, R. M., Pereira, P., Silva, P. S., Vaz, R., & Barbosa, M. A. (2018). Age-Correlated Phenotypic Alterations in Cells Isolated From Human Degenerated Intervertebral Discs With Contained Hernias. *Spine (Phila Pa 1976)*, *43*(5), E274-e284. https://doi.org/10.1097/brs.0000000000002311

Moon Randall, T. (2005). Wnt/β-Catenin Pathway. *Science's STKE*, *2005*(271), cm1-cm1. https://doi.org/10.1126/stke.2712005cm1

Munir, S., Rade, M., Määttä, J. H., Freidin, M. B., & Williams, F. M. K. (2018). Intervertebral Disc Biology: Genetic Basis of Disc Degeneration. *Current Molecular Biology Reports*, *4*(4), 143-150. https://doi.org/10.1007/s40610-018-0101-2

Nasto, L. A., Robinson, A. R., Ngo, K., Clauson, C. L., Dong, Q., St. Croix, C., Sowa, G., Pola, E., Robbins, P. D., Kang, J., Niedernhofer, L. J., Wipf, P., & Vo, N. V. (2013). Mitochondrial-derived reactive oxygen species (ROS) play a causal role in aging-related intervertebral disc degeneration [https://doi.org/10.1002/jor.22320]. *Journal of Orthopaedic Research*, *31*(7), 1150-1157. https://doi.org/https://doi.org/10.1002/jor.22320

Ohnishi, T., Novais, E. J., & Risbud, M. V. (2020). Alterations in ECM signature underscore multiple sub-phenotypes of intervertebral disc degeneration. *Matrix Biology Plus*, *6-7*, 100036. https://doi.org/https://doi.org/10.1016/j.mbplus.2020.100036

Patil, P., Niedernhofer, L. J., Robbins, P. D., Lee, J., Sowa, G., & Vo, N. (2018). Cellular Senescence in Intervertebral Disc Aging and Degeneration. *Current Molecular Biology Reports*, *4*(4), 180-190. https://doi.org/10.1007/s40610-018-0108-8

Qiu, C., Wu, X., Bian, J., Ma, X., Zhang, G., Guo, Z., Wang, Y., Ci, Y., Wang, Q., Xiang, H., & Chen, B. (2020). Differential proteomic analysis of fetal and geriatric lumbar nucleus pulposus: immunoinflammation and age-related intervertebral disc degeneration. *BMC Musculoskeletal Disorders*, *21*(1), 339. https://doi.org/10.1186/s12891-020-03329-8

Rajasekaran, S., Tangavel, C., Djuric, N., Raveendran, M., Soundararajan, D. C. R., Nayagam, S. M., Matchado, M. S., & Anand, K. S. S. V. (2020). Part 1: profiling extra cellular matrix core proteome of human fetal nucleus pulposus in search for regenerative targets. *Scientific Reports*, *10*(1), 15684. https://doi.org/10.1038/s41598-020-72859-x

Richardson, S. M., Ludwinski, F. E., Gnanalingham, K. K., Atkinson, R. A., Freemont, A. J., & Hoyland, J. A. (2017). Notochordal and nucleus pulposus marker expression is maintained by sub-populations of adult human nucleus pulposus cells through aging and degeneration. *Sci Rep*, *7*(1), 1501. https://doi.org/10.1038/s41598-017-01567-w

Risbud, M. V., Di Martino, A., Guttapalli, A., Seghatoleslami, R., Denaro, V., Vaccaro, A. R., Albert, T. J., & Shapiro, I. M. (2006). Toward an Optimum System for Intervertebral Disc Organ Culture: TGF-β3 Enhances Nucleus Pulposus and Anulus Fibrosus Survival and Function Through Modulation of TGF-β-R Expression and ERK Signaling. *Spine*, *31*(8). https://journals.lww.com/spinejournal/Fulltext/2006/04150/Toward_an_Optimum_System_for_Intervertebral_Disc.8.aspx

Risbud, M. V., Schaer, T. P., & Shapiro, I. M. (2010). Toward an understanding of the role of notochordal cells in the adult intervertebral disc: from discord to accord. *Dev Dyn*, *239*(8), 2141-2148. https://doi.org/10.1002/dvdy.22350

Roughley, P. J. (2004). Biology of intervertebral disc aging and degeneration: involvement of the extracellular matrix. *Spine (Phila Pa 1976)*, *29*(23), 2691-2699. https://doi.org/10.1097/01.brs.0000146101.53784.b1

Rutges, J. P. H. J., Nikkels, P. G. J., Oner, F. C., Ottink, K. D., Verbout, A. J., Castelein, R. J. M., Creemers, L. B., & Dhert, W. J. A. (2010). The presence of extracellular matrix degrading metalloproteinases during fetal development of the intervertebral disc. *European Spine Journal*, *19*(8), 1340-1346. https://doi.org/10.1007/s00586-010-1378-x

Sakai, D., Nakamura, Y., Nakai, T., Mishima, T., Kato, S., Grad, S., Alini, M., Risbud, M. V., Chan, D., Cheah, K. S. E., Yamamura, K.-i., Masuda, K., Okano, H., Ando, K., & Mochida, J. (2012). Exhaustion of nucleus pulposus progenitor cells with ageing and degeneration of the intervertebral disc. *Nature Communications*, *3*(1), 1264. https://doi.org/10.1038/ncomms2226

Sarath Babu, N., Krishnan, S., Brahmendra Swamy, C. V., Venkata Subbaiah, G. P., Gurava Reddy, A. V., & Idris, M. M. (2016). Quantitative proteomic analysis of normal and degenerated human intervertebral disc. *The Spine Journal*, *16*(8), 989-1000. https://doi.org/https://doi.org/10.1016/j.spinee.2016.03.051

Séguin, C. A., Chan, D., Dahia, C. L., & Gazit, Z. (2018). Latest advances in intervertebral disc development and progenitor cells. *JOR SPINE*, *1*(3), e1030. https://doi.org/10.1002/jsp2.1030

Smith, L. J., Nerurkar, N. L., Choi, K. S., Harfe, B. D., & Elliott, D. M. (2011). Degeneration and regeneration of the intervertebral disc: lessons from development. *Dis Model Mech*, *4*(1), 31-41. https://doi.org/10.1242/dmm.006403

Smits, P., & Lefebvre, V. (2003). Sox5 and Sox6 are required for notochord extracellular matrix sheath formation, notochord cell survival and development of the nucleus pulposus of intervertebral discs. *Development*, *130*(6), 1135-1148. https://doi.org/10.1242/dev.00331

Tajerian, M., Alvarado, S., Millecamps, M., Dashwood, T., Anderson, K. M., Haglund, L., Ouellet, J., Szyf, M., & Stone, L. S. (2011). DNA methylation of SPARC and chronic low back pain. *Molecular pain*, *7*, 65-65. https://doi.org/10.1186/1744-8069-7-65

Talbot, W. S., Trevarrow, B., Halpern, M. E., Melby, A. E., Farr, G., Postlethwait, J. H., Jowett, T., Kimmel, C. B., & Kimelman, D. (1995). A homeobox gene essential for zebrafish notochord development. *Nature*, *378*(6553), 150-157. https://doi.org/10.1038/378150a0

Tessier, S., & Risbud, M. V. (2021). Understanding embryonic development for cell-based therapies of intervertebral disc degeneration: Toward an effort to treat disc degeneration subphenotypes. *Dev Dyn*, *250*(3), 302-317. https://doi.org/10.1002/dvdy.217

Vo, N. V., Hartman, R. A., Patil, P. R., Risbud, M. V., Kletsas, D., Iatridis, J. C., Hoyland, J. A., Le Maitre, C. L., Sowa, G. A., & Kang, J. D. (2016). Molecular mechanisms of biological aging in intervertebral discs. *J Orthop Res*, *34*(8), 1289-1306. https://doi.org/10.1002/jor.23195

Wang, F., Cai, F., Shi, R., Wang, X. H., & Wu, X. T. (2016). Aging and age related stresses: a senescence mechanism of intervertebral disc degeneration. *Osteoarthritis and Cartilage*, *24*(3), 398-408. https://doi.org/https://doi.org/10.1016/j.joca.2015.09.019

Wang, M., Tang, D., Shu, B., Wang, B., Jin, H., Hao, S., Dresser, K. A., Shen, J., Im, H.-J., Sampson, E. R., Rubery, P. T., Zuscik, M. J., Schwarz, E. M., O'Keefe, R. J., Wang, Y., & Chen, D. (2012). Conditional activation of β-catenin signaling in mice leads to severe defects in intervertebral disc tissue. *Arthritis and rheumatism*, *64*(8), 2611-2623. https://doi.org/10.1002/art.34469

Wang, X., Zou, M., Li, J., Wang, B., Zhang, Q., Liu, F., & Lü, G. (2018). LncRNA H19 targets miR-22 to modulate H2O2-induced deregulation in nucleus pulposus cell senescence, proliferation, and ECM synthesis through Wnt signaling [https://doi.org/10.1002/jcb.26738]. *Journal of Cellular Biochemistry*, *119*(6), 4990-5002. https://doi.org/https://doi.org/10.1002/jcb.26738

Weinstein, D. C., Ruiz i Altaba, A., Chen, W. S., Hoodless, P., Prezioso, V. R., Jessell, T. M., & Darnell, J. E., Jr. (1994). The winged-helix transcription factor HNF-3 beta is required for notochord development in the mouse embryo. *Cell*, *78*(4), 575-588. https://doi.org/10.1016/0092-8674(94)90523-1

Williams, S., Alkhatib, B., & Serra, R. (2019). Development of the axial skeleton and intervertebral disc. *Curr Top Dev Biol*, *133*, 49-90. https://doi.org/10.1016/bs.ctdb.2018.11.018

Wu, Z. L., Xie, Q. Q., Liu, T. C., Yang, X., Zhang, G. Z., & Zhang, H. H. (2021). Role of the Wnt pathway in the formation, development, and degeneration of intervertebral discs. *Pathol Res Pract*, *220*, 153366. https://doi.org/10.1016/j.prp.2021.153366

Ye, D., Liang, W., Dai, L., Zhou, L., Yao, Y., Zhong, X., Chen, H., & Xu, J. (2015). Comparative and quantitative proteomic analysis of normal and degenerated human annulus fibrosus cells. *Clin Exp Pharmacol Physiol*, *42*(5), 530-536. https://doi.org/10.1111/1440-1681.12386

Yee, A., Lam, M. P. Y., Tam, V., Chan, W. C. W., Chu, I. K., Cheah, K. S. E., Cheung, K. M. C., & Chan, D. (2016). Fibrotic-like changes in degenerate human intervertebral discs revealed by quantitative proteomic analysis. *Osteoarthritis and Cartilage*, *24*(3), 503-513. https://doi.org/https://doi.org/10.1016/j.joca.2015.09.020

Zhu, J., Kwan, K. M., & Mackem, S. (2016). Putative oncogene Brachyury (T) is essential to specify cell fate but dispensable for notochord progenitor proliferation and EMT. *Proc Natl Acad Sci U S A*, *113*(14), 3820-3825. https://doi.org/10.1073/pnas.1601252113

CHAPTER II

CHAPTER II – ARTICLE I AND II

INTERVERTEBRAL DISC DECELLULARIZATION: A PROMISE FOR INTERVERTEBRAL DISC REGENERATION

The content of this chapter is adapted from two review manuscripts.

Published in European Cells and Materials (eCM) | doi: 10.22203/eCM.v042a15

Published in Trends in Biotechnology | doi: 10.1016/j.tibtech.2020.05.002

Intervertebral disc decellularisation: progress and challenges

Morena Francesca Fiordalisi[1,2,3], Ana João Silva[1,2], Mário Adolfo Barbosa[1,2,3], Raquel Madeira Gonçalves[1,2,3] and Joana Caldeira[1,2]

[1]i3S - Instituto de Investigação e Inovação em Saúde, Universidade do Porto, Porto, Portugal.

[2]INEB - Instituto de Engenharia Biomédica, Universidade do Porto, Porto, Portugal

[3]ICBAS - Instituto de Ciências Biomédicas Abel Salazar, Universidade do Porto, Porto, Portugal

Decellularized Scaffolds for Intervertebral Disc Regeneration

Morena Fiordalisi[1,2,3] Ana João Silva[1,2], Mário Barbosa[1,2,3], Raquel Gonçalves[1,2,3], Joana Caldeira[1,2]

[1]i3S – Instituto de Investigação e Inovação em Saúde, Universidade do Porto, Porto, Portugal

[2]INEB – Instituto de Engenharia Biomédica, Universidade do Porto, Porto, Portugal

[3]ICBAS – Instituto de Ciências Biomédicas Abel Salazar, Universidade do Porto, Porto, Portugal

ABSTRACT

Intervertebral disc (IVD) degeneration and the consequent low-back pain (LBP) affect over 80 % of people in western societies, constituting a tremendous socio-economic burden worldwide and largely impairing patients' life quality. Extracellular matrix (ECM)-based scaffolds, derived from decellularized tissues, are being increasingly explored in regenerative medicine for tissue repair. Decellularization plays an essential role for host cells and antigen removal, while maintaining native microenvironmental signals, including ECM structure, composition and mechanical properties, which are essential for driving tissue regeneration.

With the lack of clinical solutions for IVD repair/regeneration, implantation of decellularized IVD tissues has been explored to halt and/or revert the degenerative cascade and the associated LBP symptoms. Over the last few years, several researchers have focused on the optimization of IVD decellularization methods, combining physical, chemical and enzymatic treatments, in order to successfully develop a cell-free matrix. Recellularization of IVD-based scaffolds with different cell types has been attempted and numerous methods have been explored to address proper IVD regeneration.

Herein, the advances in IVD decellularization methods, sterilization procedures, repopulation and biocompatibility tests are reviewed. Additionally, the importance of the donor profile for therapeutic success is also addressed. Finally, the perspectives and major hurdles for clinical use of the decellularized ECM-based biomaterials for IVD are discussed. The studies reviewed support the notion that tissue-engineering-based strategies resorting to decellularized IVD may represent a major advancement in the treatment of disc degeneration and consequent LBP.

Graphical abstract

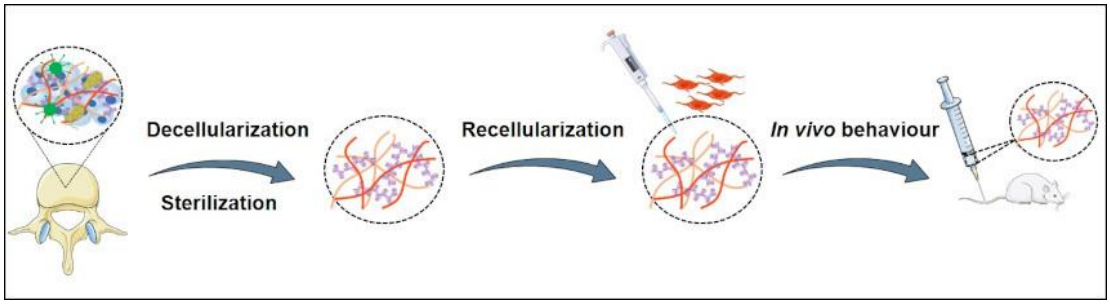

Keywords: Decellularization, recellularization, intervertebral disc, tissue engineering.

1. IVD DEGENERATION AND LBP

The human spine contains 24 intervertebral discs (IVDs) localized between the vertebrae (Anderson & Tannoury, 2005) providing flexion, extension and rotation during daily activities (Tomaszewski et al., 2015). The IVD is composed of an external region, called annulus fibrosus (AF), an internal region, named nucleus pulposus (NP), and the endplates that enclose the disc (Figure 1) (Tomaszewski et al., 2015). The AF, formed by 15-25 concentric lamellae that resist tensile stress (Colombier et al., 2014), is constituted mostly by collagen type 1 (Col1) (Oegema, 1993). In turn, the hydrogel-like NP is mainly composed of water, proteoglycans (PG) (Galbusera et al., 2014; Iatridis et al., 2007), collagen type 2 (Col2) (Urban & Roberts, 2003; Whatley & Wen, 2012) and elastin (Galbusera et al., 2014; White & Panjabi, 1990).

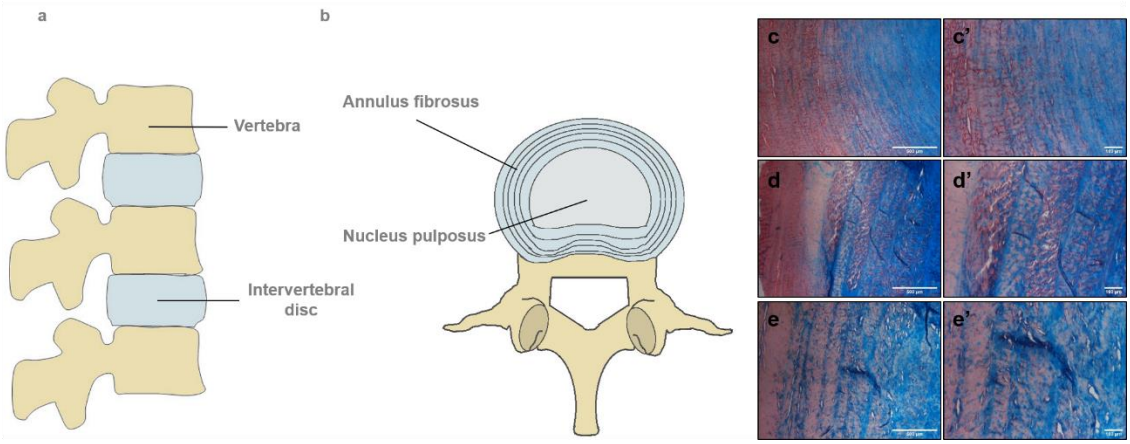

Figure 1. Gross anatomy of the IVD and histological comparison of different-age bovine IVDs. (a) Lateral view of the spine illustrating the IVD laying between adjacent vertebrae. **(b)** Upper view with the different disc regions – the AF formed by concentric rings organized around the central NP. Picrosirius red, alcian blue and H&E staining of (**c,c'**) fetus, (**d,d'**) young and (**e,e'**) old disc samples. Glycosaminoglycans (GAGs) are identified in blue, whereas collagens are coloured in red. For each image, the left region represents the outer AF and on the right is the NP. Note the smaller interlamellar space in fetal discs. In older IVDs, the layers present an irregular distribution with an increase in the interbundle spaces (optically empty spaces). Images were acquired at magnifications of 5× (c,d,e, scale bar 500 μm) and 10× (c',d',e' scale bar 100 μm).

Due to this composition, it supports the high compressive loads generated during daily activity (Mwale et al., 2004; Urban & Roberts, 2003; Whatley & Wen, 2012). Finally, the endplates, consist of hyaline cartilage (Raj, 2008; Tomaszewski et al., 2015) and control the diffusion of solutes and water (Tomaszewski et al., 2015). The disc extracellular matrix (ECM) comprises different molecules that are crucial for tissue function (cellular support, proliferation, survival, morphogenesis, differentiation and signal transduction, among others), as reviewed elsewhere (Molinos et al., 2015; Newell et al., 2017).

Degeneration of the IVD is one of the most frequent causes of low back pain (LBP) (Vos et al., 2012; Waddell, 1996) and occurs with ageing. Disc degeneration is characterized by morphological modifications (*e.g.* collapse of intervertebral space, loss of hydration, sclerosis of endplate and osteophyte formation) that affect disc biomechanics, particularly spine flexibility (Galbusera et al., 2014). As a result of degeneration, the IVD can start to bulge leading to disc herniation, with associated radiculopathy and discogenic pain (Martin et al., 2002). Moreover, cellular and biochemical changes occur as a consequence of cell density decline and altered matrix turnover (Galbusera et al., 2014). In the context of ECM composition, important age-associated alterations in the NP matrisome have been recently observed. The amount of fibronectin and prolargin increase with age, whereas collagen type XII and XIV are almost exclusively expressed in bovine fetal NPs (Caldeira et al., 2017). Others have also described a decrease in PG content, which results in water loss, increased expression of proteases as well as changes in collagen crosslinking and synthesis patterns (Adams & Roughley, 2006; Colombier et al., 2014; Cs-Szabo et al., 2002; Duance et al., 1998; Takaishi et al., 1997). As a result of such a homeostatic imbalance, the NP becomes much more fibrous and cartilaginous, affecting cell phenotype and ECM synthesis, in a degradative cascade that triggers LBP (Adams & Roughley, 2006).

Current therapies for LBP and IVD degeneration are mostly conservative, being addressed to control inflammation and relieve pain (Bydon et al., 2014). However, they do not eliminate the underlying pathology and, hence, cannot be considered long-term clinical solutions. Surgical treatment, namely discectomy, arthroplasty and lumbar fusion, is usually considered when the other options fail (Bydon et al., 2014). Nevertheless, these invasive treatments have limitations (Nasser et al., 2010; Onesti, 2004; Swann et al., 2016). Subsequent disc degeneration and recurrent herniation are major problems following surgery (Swartz & Trost, 2003). Spinal fusion, for instance, has been associated with long-term adverse consequences, such as dehydration, disc space narrowing, osteophyte

formation and progressive degeneration of the adjacent segment (Schizas et al., 2010). Although polyetheretherketone (PEEK) cages have been introduced as an alternative to metallic implants (Novotna et al., 2015), due to them presenting a more adequate load transfer and increased fusion success rate (Schimmel et al., 2016), their hydrophobic surface does not allow for protein absorption or cell adhesion, thus requiring further modifications to enhance cell attachment and biocompatibility (Novotna et al., 2015). IVD total replacement by a non-biological prosthesis represents an alternative but long-term results are limited due to prosthesis wear, often requiring revision surgery. With the lack of effective long-term solutions, there is an urgent need to develop novel therapeutic strategies that target IVD functional regeneration, improving LBP patients' lives.

IVD regeneration has been attempted using different strategies including protein injection (Masuda et al., 2006; Walsh et al., 2004), gene transfer (Leckie et al., 2012; Yue et al., 2016) and cell implantation (Okuma et al., 2000; Sakai et al., 2005). Still, only few treatment options have been effectively translated into the clinic (Veruva et al., 2014). Cell-based therapies, namely with mesenchymal stem/stromal cells (MSCs), have been used in clinical trials, decreasing pain but without signs of tissue regeneration (Orozco et al., 2011). Obstacles remain to cell transplantation, including cell leakage, which potentially causes undesired extra-discal bone formation (Vadalà et al., 2012) and poor cell survival in the harsh IVD microenvironment (acidic pH, low oxygen and limited access of nutrients). Several biomaterials have also been developed but much work is still needed to obtain clinically successful alternatives. Natural hydrogels (*e.g.* alginate, chitosan, agarose, collagen, chondroitin sulphate) are close to the NP matrix composition but do not meet its mechanical requirements (van Uden et al., 2017). In turn, synthetic materials (*e.g.* polyethylene glycol and polyvinyl alcohol) provide better biomechanical properties but have poor biocompatibility.

Decellularized ECM-based scaffolds, have received significant attention and started to be widely used in different tissues (cardiac valves, vascular grafts, cornea, *etc*.) (Mercuri et al., 2011). Decellularization is the technique used to remove host cells from tissues or organs (Londono & Badylak, 2015). Decellularized scaffolds should provide the same or similar microenvironment for seeded cells as native ECM (Xu et al., 2014). Given their pro-regenerative potential, they are currently being commercialized for many different therapeutic applications and could be a promising alternative for IVD regeneration (Gilbert et al., 2006). Recently, the combination of decellularized ECM and bioprinting has started

to be explored for IVD and cartilage. Although this strategy is still at an early stage, the use of this novel technique may improve the design of IVD-based scaffolds (Vernengo et al., 2020). The present review summarizes recent advances in IVD decellularization and discusses the need for novel therapeutic solutions for disc regeneration.

2. EVOLUTION OF IVD DECELLULARIZATION

In the last decade, several groups have started to improve IVD decellularization for tissue regenerative purposes (Figure 2).

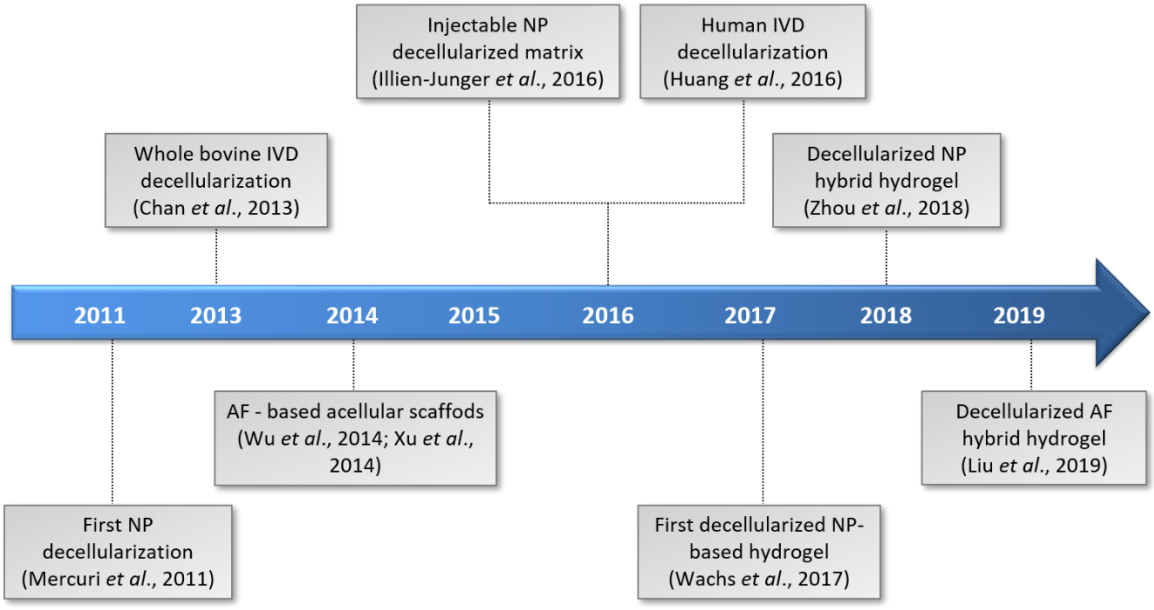

NP: nucleus pulposus; IVD: intervertebral disc; AF: annulus fibrosus.

Figure 2. Brief timeline of major scientific achievements in IVD decellularization.

Mercuri and coworkers were the first to achieve NP decellularization, using a combination of detergents (Triton and deoxycholic acid), ultrasonication (which greatly improved decellularization), and nucleases, to create an acellular porcine NP scaffold (Mercuri et al., 2011). Despite its efficacy, matrix disruption was observed as well as a reduction in collagen and glycosaminoglycan (GAG) content, still present at physiologically relevant levels. Although matrix disruption, and consequent increased porosity, may

facilitate cell infiltration, it can also affect scaffold biomechanical properties. In 2013, Chan and colleagues succeeded in whole disc decellularization with a protocol based on several freeze–thaw cycles and different sodium dodecyl sulfate (SDS) washing temperatures, adapted to bovine samples (Chan et al., 2013). This study opened new avenues for whole organ decellularization of human IVDs, which can be attractive for the development of more accurate models to study IVD development and associated pathologies that recapitulate unique features and functions of native tissue. Nevertheless, whole disc decellularization remains a challenge due to the dense nature of the tissue, which can constitute an obstacle for treatment efficiency (Illien-Junger et al., 2016). The only laboratory that proposed human IVD decellularization was that of Schulze-Tanzil. The authors combined freeze–thawing, trypsin digestion, SDS, and Triton treatments to decellularize human discs (Huang et al., 2016).

Two teams achieved porcine AF decellularization using different protocols (Wu et al., 2014; Xu et al., 2014). Liu and colleagues developed a hybrid hydrogel from decellularized AF and chitosan, using genipin as a crosslinker (Liu et al., 2019).

The focus has recently shifted to the development of injectable biomaterials for minimally invasive applications. Iatridis' laboratory identified a shorter sodium deoxycholate (SDC)-based method for bovine NP decellularization using lyophilized ground fragments, which improved decellularization and implantation (Illien-Junger et al., 2016). In 2017, Wachs and coworkers went a step further and obtained a hydrogel from decellularized porcine IVD tissue by digesting dried scaffolds in an acidic solution further neutralized with sodium hydroxide (Wachs et al., 2017). Despite being highly biocompatible, easy to produce, and attractive for minimally invasive applications, hydrogels show lower viscoelastic properties. Zhou and colleagues upgraded the acellular biomaterial by combining porcine fragments with chondroitin sulphate, which halted IVD degeneration *in vivo* (Zhou et al., 2018). This strategy is ideal to supplement the matrix with components lost with decellularization (*e.g.*, GAGs), which have a crucial role for tissue function and, at the same time, improve scaffold biomechanics.

2.1. IVD DECELLULARIZATION METHODS

Several decellularization procedures and agents have been investigated to overcome matrix disruption and preserve its composition. However, most decellularization

methods affect ECM properties at least to some extent. Optimal decellularization methods vary from different tissues or organs, depending on specific features: tissue size, thickness, shape, cell and matrix density (Vernengo et al., 2020; White et al., 2017). Following decellularization, the efficiency of the process can be evaluated considering several aspects, including the presence of DNA and cell removal. As such, acellular scaffolds should have less than 50 ng double – stranded DNA (dsDNA)/mg ECM dry weight, less than 200 bp DNA fragment and no visible cell nuclei (Gilpin & Yang, 2017). Also, matrix proteins content (collagen, laminin, fibronectin, GAGs, growth factors) as well as mechanical properties should be analyzed and maintained as close to native tissue as possible (Gilpin & Yang, 2017). In the end, even if cell residues such as DNA, RNA, cell membrane and debris remain, the decellularized scaffold needs to be biocompatible to avoid immune or inflammatory reactions (Crapo et al., 2011). Cell removal should be maximized while minimizing adverse effects on ECM composition, biological activity, integrity and biomechanical properties (Hoshiba et al., 2010). An overview of the most commonly used decellularization methods (physical, chemical and enzymatic) is shown in Figure 3 (for further details see Table 1).

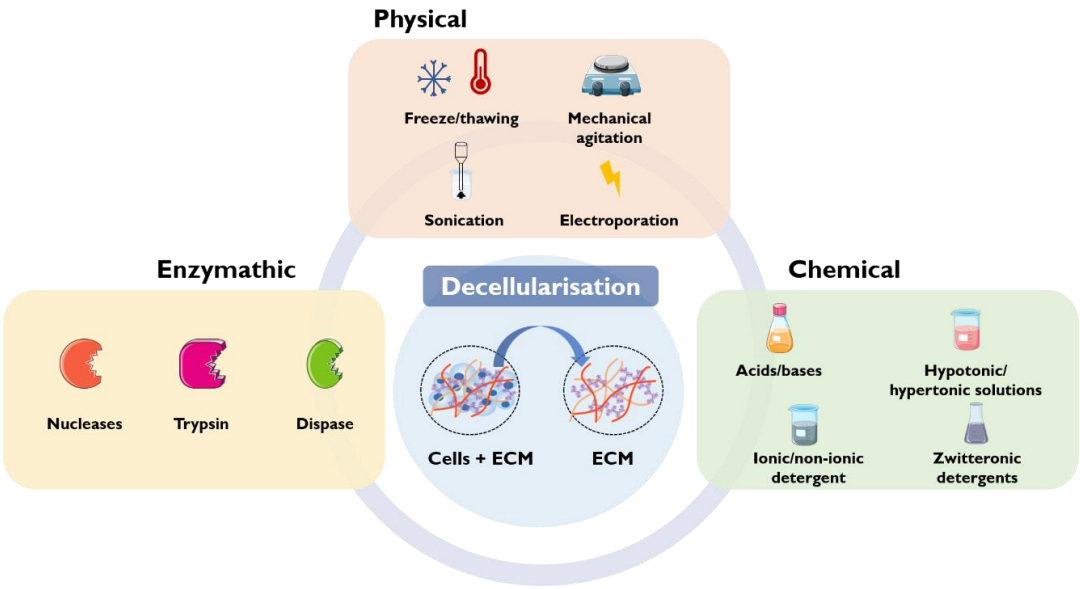

Figure 3. Overview of decellularization strategies. Tissue decellularization can be performed by using physical (freeze-thawing, mechanical agitation, sonication, electroporation), chemical (acids or bases, hypotonic or hypertonic solutions, ionic or non-ionic detergents and zwitteronic detergents) and enzymatic (nuclease, trypsin, dispase) methods. For details, see Table 1.

Table 1. **Overview of agents and methods commonly used for decellularization.**

Agent/Methods	Mechanism of action	ECM effect	References
Physical methods			
Freeze-thawing	Induces cell lysis by ice crystal formation	Preserves ECM proteins and mechanical properties. ECM can be disrupted with rapid freezing	(Crapo et al., 2011) (Gilbert et al., 2006) (Gilpin & Yang, 2017)
Mechanical agitation	Promotes diffusion of solutions into the tissue and removal of cellular debris	ECM structure damage with aggressive agitation or sonication	(Gilbert, 2012) (Gilbert et al., 2006)
Electroporation	Disrupts cell membranes by electrical pulse	Disrupts ECM structure	(Crapo et al., 2011)
Chemical agents			
Acids and bases	Denature proteins, solubilize cytoplasmatic elements and disrupt nucleic acids	Damage ECM components, particularly collagen, GAGs and growth factors	(Crapo et al., 2011) (Fu et al., 2014)
Hypotonic and hypertonic solutions	Provoke cell lysis by osmotic shock and disruption of cell membranes	Enable cell debris washout from the tissue	(Gilbert et al., 2006) (akbari zahmati et al., 2017)
Ionic detergents: sodium dodecyl sulphate	Solubilizes membrane proteins	Successfully removes cells from dense tissues and organs Perturbs tissue structure resulting in loss of GAGs and collagen integrity	(Boccafoschi et al., 2017) (Crapo et al., 2011) (Fu et al., 2014) (Seddon et al., 2004)
Ionic detergents: sodium deoxycholate	Solubilizes cells and nucleic membranes	Denatures ECM proteins, resulting in GAGs and collagen loss	(Cheng et al., 2009) (Seddon et al., 2004) (White et al., 2017)
Non-ionic detergent: Triton X-100	Disrupts lipid-lipid and lipid-proteins interactions and, to a lesser degree, protein-protein interaction	Less effective in DNA removal Disrupts ECM structure with GAGs loss	(Boccafoschi et al., 2017) (Crapo et al., 2011)
Non-ionic detergent: zwitterionic detergent	Mixed properties of non-ionic and ionic detergents	Removes cells from tissue with minimum disruption More efficient in thin (*e.g.*, lung) rather than tick tissues	(Crapo et al., 2011)

Table 1. **Overview of agents and methods commonly used for decellularization.**

Agent/Methods	Mechanism of action	ECM effect	References
Biological enzymes			
Nucleases	Hydrolyse ribonucleotide and deoxyribonucleotide chains	Remove DNA from tissues Enzyme residuals can provoke an immune response	(Crapo et al., 2011) (Keane et al., 2015) (Vernengo et al., 2020)
Trypsin	Cleaves peptide bonds on the carboxyl side of arginine or lysine	Effective as a decellularization adjuvant; however, long exposure can disrupt tissue structure and remove ECM proteins	(Crapo et al., 2011) (Keane et al., 2015)
Dispase	Cleaves fibronectin and collagen IV	Used for several tissues (*e.g.*, porcine skin and corneas), however needs to be combined with additional agents to perform efficient decellularization It can damage ECM structure and remove fibronectin and collagen IV with long exposure	(Crapo et al., 2011) (Keane et al., 2015)

In recent years, decellularization is being widely investigated as a novel strategy to develop functional substitutes for allogenic transplantation and resolve the major problems encountered in the clinic, such as donor shortage and immunosuppression (Tapias & Ott, 2014). Although several decellularized ECM scaffolds have already been approved by the Food and Drug Administration (FDA) and are being commercialized for clinical applications (Alloderm®, SurgiSIS®, Restore®, ACell, Synergraft®) (Gilbert et al., 2006), many challenges remain. Several attempts have been made to develop an ideal IVD decellularization protocol through the combination of numerous enzymatic, physical and chemical methods (Table 2) but a satisfactory method is still to be defined. GAGs loss after decellularization is one of the major issues to be solved. Large amounts of GAGs could improve IVD biomechanical properties after decellularization, namely by increasing ECM compressive properties. Recent research is focusing on the development of more efficient and milder protocols that could preserve GAGs in IVD-based scaffolds (Vernengo et al., 2020).

Table 2. Summary of the different strategies used for IVD decellularization and key outcomes reported for the optimal procedures.

	Physical		Treatment time*	Chemical						Enzymatic		Others	Results	Key outcomes		References
Animal	Sonication	Freeze-thaw		EDTA	Triton X-100	Triton X-200	SDC	NaN3	SDS	Dnase	Rnase					
NP tissue decellularization																
Porcine	-	-	19 h, 39 h, 72 h	0.10 %	0.15 %	-	0.25 %	0.02 %	-	720 mU/mL	720 mU/mL	EtOH	-	**ECM retention**	**DNA removal**	Mercuri *et al.* (2011)
					0.10 %		0.15 %							GAGs**:** 49 % loss Collagen: 75.24 µg/mg (decellularized); 36.20 µg/mg (native)	98.44 %	
					0.05 %		0.05 %									
					0.60 %		1 %									
	3^X; 10 min		72 h		0.15 %		0.25 %									
					0.60 %		1 %						**Optimal**			
Porcine	3^X; 10 min	-	72 h	0.10 %	0.60 %	-	1 %	0.02 %	-	720 mU/mL	720 mU/mL	Peracetic acid (0.1 %)	**Optimal**	Not determined		Mercuri *et al.* (2013)
Bovine	6^X	-	72 h	0.20 %	0.64 %	-	1 %	0.02 %	-	720 mU/mL	720 mU/mL	-	-	**ECM retention**	**DNA removal**	Fernandez *et al.* (2016)
	12^X				0.6 %									GAGs: 69.68 % loss Collagen: 13.87 µg /mg (decellularized); 8.63 µg /mg (native)	92.77 %	
	6^X		6 d													
	12^X															
	6^X		72 h							1440 mU/mL	1440 mU/mL					
	3^X			0.40 %	1.20 %		2 %	0.04 %		720 mU/mL	720 mU/mL					
				0.20 %	0.60 %		1 %	0.02 %				EtOH 30 min				
												EtOH 60 min				
												EtOH 45 min				
							-					-				
				2.21 mmol/L	-		-	-	0.40%							
				0.40 %	1.20 %		-	0.02 %	-				**Optimal**			

Table 2. Summary of the different strategies used for IVD decellularization and key outcomes reported for the optimal procedures.

	Physical		Treatment time*	Chemical						Enzymatic		Others	Results	Key outcomes		References
Animal	Sonication	Freeze-thaw		EDTA	Triton X-100	Triton X-200	SDC	NaN3	SDS	Dnase	Rnase					
NP cell-derived matrix decellularization																
Rabbit	-	-	1 h	-	2 %	-	-	-	-	-	-	-	-	**ECM retention**	**DNA removal**	Yuan *et al.* (2013)
			-		3 %									GAGs: ~0.1 µg (decellularized) Collagen: ~10 µg (decellularized)	~ 100 %	
			-									SDC 0.5 %				
			1 h									SDC 1 %				
			-									SDC 2 %				
			1 h 30 min			0.14 %	-					50 mmol/L SB-10 + 0.6 mmol/L SB-16	**Optimal**			
			1 h 30 min									125 mmol/L SB-10 + 0.6 mmol/L SB-16	-			

Table 2. Summary of the different strategies used for IVD decellularization and key outcomes reported for the optimal procedures.

Animal	Physical		Treatment Time*	Chemical						Enzymatic		Others	Results	Key outcomes		References
	Sonication	Freeze-thaw		EDTA	Triton X-100	Triton X-200	SDC	NaN3	SDS	Dnase	Rnase					
AF decellularization																
Porcine	-	5^X (22 h -80 °C; 2 h 37 °C)	48 h	-	-	-	-	-	0.10 %	50 U/mL	1 U/mL	APR (10 KIU/mL)	**Optimal**	**ECM retention** GAGs: 15.9% loss Collagen: 96.72 µg/mg (decellularized) and 98.65 µg/mg (native)	**DNA removal** 86 %	Wu *et al.* (2014)
Porcine	-	-	72 h	0.10 %	3 %	-	-	-	-	0.2 mg/mL	0.2 µg/mL	APR (10 KIU/mL)	**Optimal**	**ECM retention** GAGs: ~40 µg/mg (decellularized); ~50 µg/mg (native) Collagen: not significant differences	**DNA removal** No presence (qualitative analysis)	Xu *et al.* (2014)
		3^X (3 h -80 °C; 4 h RT)			-				0.50 %				-			
		-		0.20 %					-		20 µg/mL	Trypsin (0.50 %)				
Porcine	-	22 h -80 °C; 2 h 37 °C	24 h	0.10 %	-	-	-	-	0.10 %	50 U/mL	1 U/mL	APR (10 KIU/mL)	-	**ECM retention** GAGs: 114.77 µg/mg (decellularized) and 121.63 µg/mg (native) Collagen: 151.73 µg/mg (decellularized) and 153.63 µg/mg (native)	**DNA removal** 85.7 %	Wu *et al.* (2017)
		22 h liquid nitrogen; 2 h 37 °C	48 h		1 %				-				**Optimal**			
			72 h		-				0.10 %				-			
Rabbit	-	-	24 h	-	1 %	-	-	-	-	50 U/mL	1 U/mL	Trypsin (0.25 %)	**Optimal**	Not determined		Liu *et al.* (2019)

Table 2. Summary of the different strategies used for IVD decellularization and key outcomes reported for the optimal procedure.

	Physical		Treatment time*	Chemical						Enzymatic		Others	Results	Key outcomes		References
Animal	**Sonication**	**Freeze-thaw**		**EDTA**	**Triton X-100**	**Triton X-200**	**SDC**	**NaN3**	**SDS**	**Dnase**	**Rnase**					
Whole disc decellularization																
Bovine	-	6^{X} (1 h 37 °C; 1 h liquid nitrogen)	6 h 24 h 48 h	1^{X}	-	-	-	-	0.10 %	-	-	-	- **Optimal**	**ECM retention** GAGs: 557.46 µg/mg (decellularized NPs); 574.74 µg/mg (fresh NPs); 233.42 µg/mg (decellularized AFs); 277.54 µg/mg (native AFs) Collagen: qualitative	**DNA removal** 71 % of NP cells and 76 % of AF cells removal	Chan *et al.* (2013)
Bovine	3^{X}; 10 min	3^{X} (2 h - 80 °C; 22 h RT)	72 h	0.20 %	1.20 %	-	-	0.02 %	-	720 mU/mL	720 mU/mL	Distilled water, EtOH (30 min), peracetic acid (0.1 %)	**Optimal**	**ECM retention** GAGs: AF: 56.84% loss NP: 45% loss Collagen: qualitative	**DNA removal** AF: 73 % NP: 84 %	Hensley *et al.* (2018)
Human IVD decellularization																
Human	-	6^{X} (4 h - 20 °C; 30 min 37 °C)	72 h	0.04 %	3 %	-	-	-	2%	-	-	Trypsin (0.25 %), EtOH (20 min)	**Optimal**	**ECM retention** GAGs: ~500 µg/ml (decellularized); ~1000 µg/ml (native) Collagen: No significant differences	**DNA removal** No significant decrease	Huang *et al.* (2016)

Note: *Treatment time for detergent solutions. RT: room temperature.

2.2. NP TISSUE DECELLULARIZATION

Simionescu's group was the first to establish a decellularization protocol for the IVD (Mercuri et al., 2011). They were able to create a porcine decellularized NP-based scaffold by using a combination of Triton X-100 and deoxycholic acid detergents, ultrasonication and nucleases (DNAse and RNAse). Although the protocol was efficient in removing cells from the NP, it also affected tissue ultrastructure as well as ECM composition, leading to a 49 % GAGs loss. Decellularized scaffolds contained nearly twice as much collagen as fresh tissues (decellularized NPs: 75.24 µg/mg; fresh NPs: 36.20 µg/mg). This apparent increase corresponds to a decrease in other tissue components (Mercuri et al., 2011). After optimizing decellularization conditions, they showed higher Col2 expression in porcine explants seeded with human adipose-derived stem cells (ADSCs), when cultured in a differentiation medium as compared to normal Dulbecco's modified Eagle medium (DMEM) at days 7 and 14 (9-fold *vs*. 2-fold increase, respectively). Expression of *PAX-1*, *SOX9, COL3* and *TIMP-1* was also upregulated. Additionally, GAG content of seeded scaffolds cultured in differentiation medium was significantly higher than for non-seeded ones, after 7 days (non-seeded NPs: 18.3 µg/mg; repopulated NPs: 34.74 µg/mg) and 14 days (non-seeded NPs: 20.6 µg/mg; repopulated NPs: 46.28 µg/mg) (Mercuri et al., 2013). Recently, the same group performed a screening of different conditions to decellularize bovine NPs. The authors increased treatment time as well as amount of detergents and concentration of DNAse used. They found that 1.2 % of Triton X-100 treatment for 72 h combined with ultrasonication was the optimal procedure for bovine samples. An ethanol wash prior to decellularization was used to guarantee total detergent absorption. This protocol removed 93 % of DNA, while retaining around 30 % of GAGs and high collagen levels (decellularized NP: 13.87 µg hydroxyproline [HYP]/mg sample dry weight; native NPs: 8.63 µg HYP/mg sample dry weight). Mechanical features resembled those of native NPs. It is still necessary to discover whether a similar protocol without sonication would be less disruptive to the ECM structure (Fernandez et al., 2016). Indeed, ECM architecture of bovine NP was disrupted following decellularization, when ultrasonication was applied (unpublished data).

2.3. NP-CELL-DERIVED MATRIX DECELLULARIZATION

Yuan *et al.* (2013) focused on the decellularization of *in-vitro*-derived rabbit NP matrices (deposited onto collagen microsphere templates), which were used to instruct

human MSC differentiation towards NP-like lineages. A combinatorial protocol of Triton X-200 with sulphobetaine (SB)-10 and SB-16 avoided fast transitions of detergents to water, causing less structural damage than using them separately. Zwitterionic and anionic detergents removed most cell components while retaining around 0.1 µg/100 µL of solubilized GAGs from 30 microspheres and 10 µg of collagen per 100 µL of sample digest, by generating smaller surfactant micelles that were able to easily penetrate into the tissue. Higher detergent concentrations might have had reduced decellularization effectiveness since emulsifying micelles were too large to penetrate into the collagen microspheres (Yuan et al., 2013). The obtained scaffolds were further characterized by proteomics, demonstrating partial preservation of the ECM microenvironment (Yuan et al., 2018).

2.4. AF DECELLULARIZATION

Concerning the development of acellular AFs, Huang's lab used a combination of repeated freeze-thawing followed by incubation in 0.1 % SDS for 48 h to decellularize porcine tissue (Wu et al., 2014). A reduction of 86 % in DNA content and 16 % in GAGs was achieved in decellularized AF-based scaffolds when compared to fresh ones. No significant differences were seen in collagen content (fresh AF: 98.65 µg/mg; decellularized AF: 96.72 µg/mg). Although stiffness and Young's modulus have exhibited a tendency to decrease after decellularization, these differences were not statistically significant (Wu *et al.*, 2014). In contrast, Xu *et al.* (2014) compared different AF decellularization protocols and demonstrated that 3 % Triton X-100 treatment for 72 h was better than a freeze-thawing combination with a 0.5 % SDS treatment or even a trypsin-based enzymatic method. In this study, the Triton X-100-based protocol enabled the maintenance of biomechanical properties without affecting tissue structure and, also, retained the highest GAG content (~ 40 µg GAG/mg dry weight) (Xu et al., 2014). 3 years later, Huang's group validated the previous results but reducing the treatment time to 24 h, given that extension of the decellularization time had a greater effect on collagen (fresh AF: 120.94 µg/mg; decellularized AF for 24 h: 109.72 µg/mg; decellularized AF for 48 h: 94.18 µg/mg; decellularized AF for 72 h: 89.80 µg/mg) and GAGs (fresh AF: 96.09 µg/mg; decellularized AF for 24 h: 82.77 µg/mg; decellularized AF for 48 h: 47.49 µg/mg; decellularized AF for 72 h: 14.44 µg/mg) content (Wu et al., 2017). Finally, Liu *et al*. (2019) created a hydrogel by combining rabbit decellularized AF, chitosan and genipin as crosslinker. The tissue was decellularized using a similar protocol to that of Huang's group after tissue digestion with

trypsin. Basic fibroblast growth factor (bFGF) incorporation promoted expression of ECM genes and corresponding proteins in the supernatants of seeded rabbit AF stem cells (Liu et al., 2019).

2.5. WHOLE DISC DECELLULARIZATION

Chan *et al.* (2013) reported, for the first time, decellularization of an entire bovine IVD (including the endplates). They tried different SDS washing temperatures and freeze-thawing cycles to preserve GAG and collagen content. With 6 freeze-thaw cycles followed by 48 h washing with SDS 0.1 % at 4 °C, the authors succeeded in removing over 70 % of the cells in both the AF and NP. The protocol was improved by increasing the number of freeze-thaw cycles, which completely abolished metabolic activity of the remaining cells. After decellularization, both NP and AF maintained a GAG content similar to native tissue (fresh NP: 574.74 µg/mg; decellularized NP: 557.46 µg/mg; fresh AF: 277.54 µg/mg; decellularized AF: 233.42 µg/mg). Mechanical properties were also preserved. This enabled NP cell penetration after 7 days in culture (Chan et al., 2013).

5 years later, Mercuri's group also tried to decellularize a complete disc xenograft. To obtain large (C1-C4) acellular bovine scaffolds, they used a longer Triton-based protocol [adapted from the one for NP (Fernandez et al., 2016)]. However, unlike (Chan et al., 2013), they did not include the cartilaginous endplates. No significant differences were observed in swelling pressure or in toe-region modulus between decellularized and native tissues. However, decellularized IVDs showed a decrease of linear-region moduli, peak stress and equilibrium moduli (Hensley et al., 2018).

2.6. HUMAN IVD DECELLULARIZATION

In 2016, Schulze-Tanzil's lab was able to decellularize human IVDs from elder individuals undergoing spinal fusion or disc replacement. They adopted a protocol based on the combination of freeze-thawing, trypsin digestion and chemical detergents (2 % SDS and 3 % Triton X-100). Although decellularized IVDs contained almost half the GAGs content, as compared to native tissues, matrix architecture was maintained within the decellularized IVD cylindrical punches. Although cell removal was gauged by lack of nuclear and H&E staining, no significant differences were observed in total DNA content by the

CyQuant Assay. In addition, despite the larger numbers of human IVD cells found in repopulated scaffolds, only differentiated MSCs were capable of increasing collagen and GAG content (Huang et al., 2016).

3. INJECTABLE STRATEGIES FOR DECELLULARIZED MATRIX ADMINISTRATION

In recent years, the use of ECM-based scaffolds has advanced with the development of injectable and biocompatible hydrogels (Hussey et al., 2018).

Hydrogels are defined as highly hydrated polymer materials that are able to preserve their structural integrity by physical and chemical crosslinks between chains (Saldin et al., 2017). The development of hydrogels from decellularized tissue is guided by the presence of biochemical factors and proteins of decellularized tissue through a collagen-based self-assembly process (Saldin et al., 2017). Injectable ECM-based hydrogels can be formed mainly using two different methods. The first approach consists of grinding or milling the ECM into a fine powder, followed by resuspension in a solvent prior to injection. The second method consist of digesting enzymatically the ECM in an acidic solution and subsequently neutralizing the pH and salt concentration to mimic *in vivo* physiological conditions. After digestion, the ECM can form a hydrogel by thermal crosslinking (Spang & Christman, 2018). Pepsin is the most used enzyme for tissue solubilization, since it digests most protein structures (Hulmes, 2008) and hydrolyses collagen (León-López et al., 2019). However, dispase can be an alternative for soft tissues (Saldin et al., 2017).

In the disc field, hydrogels provide biochemical and biological signals to drive NP repair and regeneration and constitute a promising cell delivery system for minimally invasive strategies to treat IVD degeneration.

Illien-Junger *et al*. (2016) were able to develop decellularized injectable bovine NP fragments by using a protocol based on SDC. Prior to treatment, all samples went through a process of freeze-thawing, lyophilization and grinding to increase surface area, facilitating fragment suspension. To test its injectability, the hydrated ECM suspension was transferred into a dual-barrel syringe and injected through a 25-G needle into an injured IVD. Apart from the optimal protocol using 2 % deoxycholate and DNAse, other treatments tested included additional decellularization steps with 2 % SDS and 0.1 % Triton X-100. These alternatives

produced looser scaffolds with thicker fibers and resulted in increased DNA levels with minimal GAG and collagen content. Interestingly, several cell-seeded constructs were immersed in low-melting-point agarose to create a protective shell that avoided swelling and dissociation. No cytotoxicity was observed, neither with human NP cells nor MSCs, after 21 days in culture (Illien-Junger et al., 2016).

Lin *et al.* (2016) were also able to develop ECM microparticles from decellularized rabbit IVD by grinding the tissues. Following homogenization, the obtained microparticles were passed through a sieve and their size was confined to smaller than 200 µm. Acellular IVD derived-microparticles injected using a 27-G needle prevented disc degeneration in a rabbit model, by increasing water level and disc height as well as ECM integrity and content (Lin et al., 2016).

Lin and co-workers optimized porcine NP decellularization using an SDS-based method that could remove up to 95.1 % of DNA and still maintain tissue microstructure and ECM components, particularly collagen (decellularized NP: 174.8 µg/g; native NP: 90.3 µg/g). However, GAGs decreased after decellularization (decellularized NP: 19.33 µg/mg; native NP: 22.84 µg/mg). Moreover, mass spectrometry revealed the presence of important signalling molecules (*e.g.* lactadherin, metallopeptidase inhibitor 1 and alpha-1-antitrypsin) in NP-ECM scaffolds, which are involved in several cell activities. Particularly, transforming growth factor beta – 1 (TGF-β1), a protein associated with NP cells differentiation, was also detected. After repopulation with MSCs, NP-related genes (*COL2A1, ACAN* and *SOX9*) were upregulated in the NP-ECM scaffolds when compared to the controls as well as TGF-β receptor 2 (*TGF-βR2)* at an early culture stage (3 days). Finally, immunofluorescence (IF) showed higher synthesis of NP-cell-related proteins (ACAN and SOX9) in the repopulated scaffolds. These results suggested that NP-ECM scaffolds were able to induce MSC differentiation towards NP-like cells through the activation of TFG-β1 signalling pathway (Xu et al., 2019). After reseeding, decellularized NPs were cut into small pieces to allow the passage through a 25-G needle. Following resuspension, ECM fragments were injected into a rabbit model of disc degeneration. Following 4 and 8 weeks of injection, NP structure and IVD disc height were preserved, when compared to a degenerated IVD group. Although PG were partially lost, as shown by a reduction of safranin O staining, the typical ECM network structure was still maintained at 8 weeks upon injection. Overall, reseeded scaffolds were able to delay disc degeneration *in vivo* (Xu et al., 2019).

Wachs *et al*. (2017) developed, for the first time, a NP-based hydrogel from porcine tissue. The protocol was based on the combination of SB-10, Triton X-200 and SB-16 detergents and similar to that used by Yuan *et al.* (2013) for *in-vitro*-derived matrices. Instead of injecting a resuspension of lyophilized particles as in Illien-Junger *et al.* (2016), dried scaffolds were digested in an acidic solution and then neutralized with sodium hydroxide. The newly formed hydrogel retained native tissue architecture and was used to culture human NP cells that were able to acquire an elongated morphology and increased their GAG content over time, specifically from around 100 ng/mg on day 7 to 250 ng/mg on day 21 (Wachs et al., 2017).

Yu and colleagues created an injectable and thermosensitive decellularized NP-based hydrogel from bovine tissue, suitable for minimally invasive applications. Following decellularization with a combination of freeze-drying and SDS 1 % treatments, tissues were lyophilized, ground to a powder and digested in an acidic solution, using a similar method to that of (Wachs et al., 2017). Afterwards, digested NPs were turned into hydrogels at 37 °C. The hydrogels were not cytotoxic and were well tolerated (Yu et al., 2020).

Zhou *et al.* (2018) decellularized porcine NPs using Wachs' protocol (Wachs et al., 2017). As Illien- Junger *et al.* (2016) and Lin *et al.* (2016) had done earlier, they fragmented the decellularized samples. Since decellularization treatments can affect ECM ultrastructure, with a decrease in protein content, particularly GAGs, Zhou and colleagues decided to supplement the acellular scaffold with chondroitin sulphate (20 mg/mL) to obtain a GAG/HYP ratio similar to that of the native tissue. Human or rabbit ADSCs were encapsulated and this gel crosslinked using 0.02 % genipin (higher genipin concentrations were cytotoxic). The hydrogel was able to induce NP-like differentiation *in vitro* and partially recover the degenerated NP *in vivo*, in a rabbit IVD degeneration model (Zhou et al., 2018). Finally, Peng and colleagues developed an injectable genipin-crosslinked decellularized AF hydrogel (g-DAF-G) from bovine tissue that was able to direct human bone marrow – derived mesenchymal stem cells (BM-MSCs) differentiation towards an AF-cell-like phenotype *in vitro*. AF decellularization was achieved by using a combination of freeze-drying cycles, Triton X-100 (2 %) and SDS (1 %) detergents and sterile water. After lyophilization, decellularized AF samples were digested in 0.01 mol/L HCl containing 1.5 mg/mL pepsin under moderate agitation for 48 h to create a decellularized AF-based hydrogel (DAF-Gs). Finally, hydrogels were crosslinked using genipin, forming g-DAF-G. The storage modulus (G') of g-DAF-G was superior to that of DAF-G and increased with

higher concentration of genipin (DAF-G: 465.51 Pa; 0.01 % genipin: 2.57 MPa; 0.02 % genipin: 3.29 MP; 0.04 % genipin: 4.34 MPa). Therefore, g-DAF-G showed improved biomechanical properties when compared to DAF-G (Peng et al., 2020).

Apart from being used for hydrogel formation, solubilized decellularized matrices can also be used as coating of 2D substrates by adsorbing ECM proteins onto a tissue culture surface, as has been performed for other tissues (Agmon & Christman, 2016; DeQuach et al., 2010; Lee et al., 2014). Despite that they no longer retain native tissue architecture, coated plates will provide biochemical signals that can be sensed by the seeded cells, which will change their behaviour accordingly.

4. STERILIZATION OF DECELLULARIZED IVD MATRICES

Considering that implant-associated infections are one of the major issues halting the widespread use of biomaterials in the clinics (Campoccia et al., 2006; Li & Webster, 2018), the optimization of the sterilization methods for ECM-based scaffolds is crucial before their clinical application.

Acidic solutions or solvents, heat treatment, ethylene oxide exposure, iodine and irradiation (gamma or electron beam), represent some of the methods available for scaffold sterilization. Freeze-drying and supercritical carbon dioxide are also currently being tested (Dai et al., 2016). A combination of different techniques can be required to achieve complete removal of viral or bacterial contaminants from biomaterials. Sterilization conditions should be tightly controlled and post-sterilization effects evaluated individually. Problems that might arise from matrices' sterilization include insufficient cell penetration upon repopulation, incomplete microorganism inactivation, cell toxicity and loss of integrity (Crapo et al., 2011; Dai et al., 2016). Therefore, sterilization can compromise efficiency of biomaterials. Several approved and standardized methods of sterilization (*e.g.* heat, pressure, irradiation, chemical agents, supercritical carbon dioxide and ionised gas plasma) can induce degradation of ECM components, thus modifying its physiological and biomechanical properties (Fidalgo et al., 2018).

One option that has been used for IVD scaffold culture in sterile conditions is the addition of antibiotics or antifungal solutions such as sodium azide or a combination of

penicillin and streptomycin (Lin et al., 2016; Mercuri et al., 2013; Yuan et al., 2013). Peracetic acid (0.1 % or 0.01 %) might also be used in combination with an antibiotic infusion (Mercuri et al., 2013; Zhou et al., 2018). 70 % ethanol is another alternative (Huang et al., 2016; McGuire et al., 2017; Mercuri et al., 2011) although the final objective of at least some of the authors does not seem to be sterilization but only tissue dehydration (Fernandez et al., 2016; Huang et al., 2016). In addition, it can denature proteins, dehydrate ECM and affect cell-ECM interactions (Poornejad et al., 2015).

Xu *et al.* (2019) used gamma irradiation to sterilize porcine NP scaffolds. Nevertheless, at least for porcine renal decellularized matrices, Poornejad *et al.* (2015) showed that 0.2 % peracetic acid in 1 mol/L NaCl solution presented the best results in terms of GAG content and ECM structure preservation, rather than gamma-irradiation, ethanol alone or even peracetic acid in 4 % of alcohol. In this study, gamma-irradiation was the most damaging sterilization method since it caused modification of tissue microstructure and considerable reduction of ECM components (collagen and GAGs) as well as increased tissue porosity and altered mechanical properties. Significant decrease of cell adhesion and proliferation after scaffold repopulation were also observed (Poornejad et al., 2015). Badylak's group demonstrated that a high dose of gamma-irradiation (30 kGy) prevented hydrogel formation from ECM of several tissues (porcine intestinal submucosa, liver and urinary bladder, bovine bone), when compared to the supercritical CO_2 method (White et al., 2018). Finally, Peng *et al.* (2020) adopted a combination of 95 % alcohol fumigation and ultraviolet irradiation to sterilize lyophilized decellularized AF tissues.

All in all, it is crucial to choose an adequate sterilization method to maximize the properties and *in vivo* performance of biomaterials (Destefani et al., 2017).

5. RECELLULARIZATION OF DECELLULARIZED IVD SCAFFOLDS

After decellularization, acellular scaffolds can be repopulated with specific cell sources to reconstitute a healthy ECM and enhance the regenerative process. Choosing the appropriate cell source for recellularization is a complex issue that needs to be extensively studied.

Native IVD cells are widely used to recellularize IVD-based scaffolds, since they already present a chondrocyte-like phenotype and have shown positive outcomes (Chan et al., 2013; Ganey et al., 2003; Gruber et al., 2002). However, other cell types and different repopulation methods have been widely investigated. As summarized in Table 3, successful recellularization of IVD scaffolds [either injectable (Illien-Junger et al., 2016; Lin et al., 2016; Peng et al., 2020; Wachs et al., 2017; Xu et al., 2019; Yu et al., 2020; Zhou et al., 2018) or not] has already been reported with bovine (Chan et al., 2013) and human (Illien-Junger et al., 2016; Wachs et al., 2017) NP cells as well as with rabbit (Liu et al., 2019) [either stem or not (Xu et al., 2014)] and human (Huang et al., 2016) AF cells.

At first glance, healthy human IVD cells seem to be the ideal cell source. Nevertheless, they represent only a small population in the disc and their isolation is a complex process due to ethical issues in using healthy young volunteers and a high risk of tissue disruption. Alternatively, IVD cells can be collected from patient's undergoing spinal surgeries. However, their degenerative phenotype can negatively impact the subsequent regenerative cascade in the context of a therapeutic approach. Nevertheless, IVD cells' behaviour will better mimic the response within a diseased microenvironment, being ideal for developing *in vitro* models of disc degeneration.

MSCs have started to be widely used because of their relatively ease of isolation and expansion, ability to differentiate into native disc-like cells, immunomodulatory properties and ability to produce their own ECM, inducing disc repair. MSCs are a more readily available option than IVD cells (Le Maitre et al., 2009; Lin et al., 2016; Wei et al., 2009; Zhou et al., 2018) and have started to be used in clinical trials to treat LBP (Kumar et al., 2017; Noriega et al., 2017). Moreover, MSCs have long-term self-renewal capability, are reservoirs of growth factors and cytokines and can contribute to the restoration of the disc matrix (Wang et al., 2015; Watanabe et al., 2010; Yang et al., 2008; Zhang et al., 2005). MSCs used for IVD regeneration studies are mainly bone-marrow-or adipose-tissue-derived as they can be obtained through minimally invasive procedures (Huang et al., 2016; Illien-Junger et al., 2016; Lin et al., 2016; Mercuri et al., 2011; Mercuri et al., 2013; Peng et al., 2020; Yu et al., 2020; Yuan et al., 2013; Zhou et al., 2018). However, stem cells from other sources such as amniotic fluid (Fernandez et al., 2016) or synovial tissue (Pei et al., 2012; Shoukry et al., 2012) also exhibit promising results. As previously discussed, it is important to choose the appropriate cell type for recellularization but the use of autologous, allogenic

or xenogenic cells must be carefully considered to reduce the chance of having scaffold rejection by the host.

Several methods have been investigated to achieve successful recellularization of ECM-based scaffolds (Figure 4).

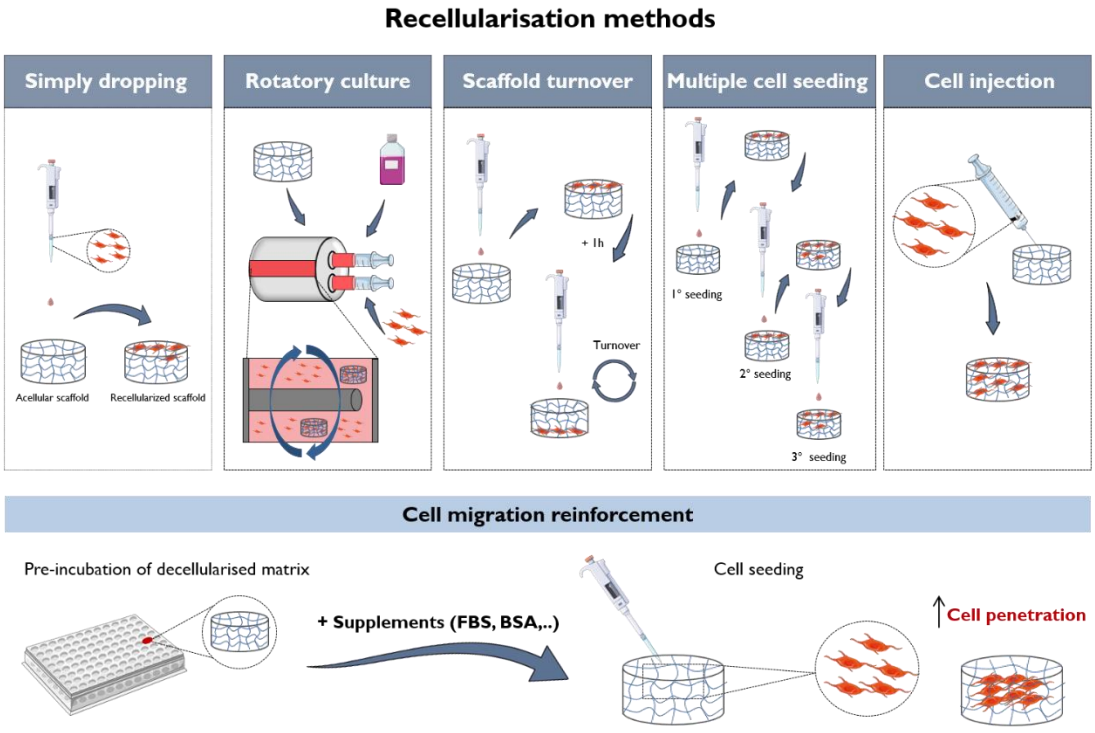

Figure 4. Scaffold repopulation strategies. IVD scaffold repopulation, either with IVD cells or MSCs from different origins can be performed by drop-wise addition onto the surface of the decellularized scaffold. To improve recellularization efficiency other strategies can be used such as mechanical agitation, scaffold turnover, multiple seedings or cell injection into the scaffold. To further promote cell penetration, decellularized matrices can be pre-incubated with protein-rich solutions such as fetal bovine serum (FBS) or bovine serum albumin (BSA).

Seeding cell suspension over the biomaterial by simple dropping is the most used approach. However, cells tend to form a monolayer on the surface of dense scaffolds, rendering problematic their penetration and migration (Chan et al., 2013; Fernandez et al.,

2016; Huang et al., 2016). Also, particular decellularization detergents, such as SDS, affect GAG content of the native tissue, which leads to decreased water retention and consequently reduced cell adhesion to the matrix (Gilbert et al., 2006; Huang et al., 2016). Several techniques can be adopted to improve cell penetration and migration into the scaffolds, such as: rotatory cultures (Huang et al., 2016), scaffold turnover (Xu et al., 2014), repetitive cell seedings with 1 h intervals (Lin et al., 2016), and cell injection (Fernandez et al., 2016). Finally, cell repopulation can be enhanced by pre-incubating acellular scaffolds with fetal bovine serum (FBS) or bovine serum albumin (BSA). These solutions can diminish the cytotoxicity caused by the decellularization reagents. Particularly, Mercuri *et al.* (2011) immersed the decellularized scaffold in culture medium with serum (50 %), 24 h prior to cell seeding and observed a relative 2.4-fold increase in cell number from ~ 2.5×10^4 cells on day 3 to ~ 6.1×10^4 cells on day 7 and cell migration into the scaffold after 7 days of culture. Nevertheless, with the same approach, Fernandez *et al.* (2016) did not observe cell migration within the scaffold. In another study, Schulze-Tanzil's group preconditioned the decellularized matrices in 5 % BSA for 24 h and FBS for additional 24 h. Although most of the seeded cells (either MSCs or IVD cells) survived, they only colonized the scaffold surface (Huang et al., 2016). It is important to consider that these differences may also reflect different cell sources or decellularization methods used, since each particular approach can have a different impact on the physicochemical properties of the ECM, affecting cell adhesion and migration. After choosing the recellularization method, it is also mandatory to determine the cell seeding density, which may depend on scaffold volume, cell type, culture duration and purpose of the experiment.

After reseeding, the success of the recellularization procedure should be estimated. In most studies, the authors evaluate cell number, proliferation, cell viability, DNA and water content, tissue organization, GAG and collagen composition. This information is also reviewed in Table 3. Overall, recellularized scaffolds are a valuable tool that can be optimized and refined to develop innovative therapies for IVD degeneration. In the future, high-throughput proteomics or single-cell transcriptomics could help to maximize the understanding of all the dynamic biological processes and different cell populations involved in the process of IVD regeneration.

Table 3. Current procedures for IVD recellularization.

IVD tissue origin	Cell source	Seeding method	Assays									Key outcomes	Ref.
			Cell number	Cell viability	DNA content	GAG content	Collagen content	Water content	Tissue organization	Gene expression	Others		
Bovine (NP)	Bovine NP cells	Seeding onto tissue surface	DAPI staining	Calcein/PKH26 staining	—	—	—	—	—	—	—	Day 7: cells viable and migration into the scaffolds with limited penetration	Chan *et al.* (2013)
	Human BM-MSCs, human NP cells	Cell seeded constructs	—	Calcein-AM/ethidium homodimer-1 assay	—	Alcian blue and toluidine blue	Picrosirius red staining	—	—	—	—	Day 21: cells viable. GAGs: decrease in scaffolds repopulated with hNP cells	Illien–Junjer *et al.* (2016)
	Human AMSCs	Drop-wise addition onto the tissue surface or cell injection	—	Calcein-AM/ethidium homodimer-3 assay	—	—	—	—	—	—	—	Cells viable for up to 14 days. No cell migration and penetration	Fernandez *et al.* (2016)
	Rat ADSCs	Seeding onto hydrogel	—	Live/Dead assay	—	—	—	—	—	*Acan, Sox9, Col2, Col1*	Cell proliferation (CCK8)	Day 5: cells viable. Higher expression of *Col2, Acan* and *Sox9*. No differences in *Col1*	Yu *et al.* (2020)

Table 3. Current procedures for IVD recellularization

IVD tissue origin	Cell source	Seeding method	Assays									Key outcomes	Ref.
			Cell number	Cell viability	DNA content	GAG content	Collagen content	Water content	Tissue organization	Gene expression	Others		
Rabbit (NP)	Rabbit BM-MSCs, human BM-MSCs	Dropping onto microspheres	Trypan Blue assay	Calcein-AM/ethidium homodimer-1 assay	Hoechst	DMMB assay, alcian blue staining	HYP assay	—	H&E	*Acan, Sox9, Col1, Col2, Gpc3, Krt19, Ca12, Pax1, Foxf1*	IHC (COLI, COLII, KRT19, TGFβ, TGFβR1)	Cells viable for 18 days in culture with migration into the microspheres. GAGs: more in scaffolds re-seeded with hMSCs. Increased *COL2* (>10 fold), *GPC3* (~6 fold) and *FOXF1* (~8 fold) expression in re-seeded microspheres with hMSCs.	Yuan *et al.* (2013)
	Human dermal fibroblasts	Dropping onto microspheres	DAPI staining	Live/Dead assay	—	Alcian blue staining	—	—	H&E	*Col1, Col2, Acan, Sox9, Krt19, Gpc3, Ca12, Foxf1, Pax1*	IHC (COLII, KRT19)	Day 18: cells viable with migration into the microspheres. Decreased *COL1* and increased *COL2* gene expression when cells were cultured in NPC-derived matrix	Yuan *et al.* (2018)

Table 3. Current procedures for IVD recellularization

IVD tissue origin	Cell source	Seeding method	Assays									Key outcomes	Ref.
			Cell number	Cell viability	DNA content	GAG content	Collagen content	Water content	Tissue organization	Gene expression	Others		
Porcine (NP)	Human ADSCs	Drop-wise	MTS proliferation assay	Calcein-AM/ethidium homodimer-1 assay kit	—	Alcian blue staining	—	—	—	—	—	Day 7: cells viable and increased cell migration and proliferation	Mercuri *et al.* (2011)
	Human ADSCs	Seeding onto hydrogel	—	Live/Dead assay	PicoGreen	DMMB assay, alcian blue staining	HYP assay	Wet-dry weight	H&E, Movat's pentachrome staining	*Acan, Sox9, Col2, Col3, Timp1, Pax1, Ibsp*	MMPs and TIMPs antibody arrays, dynamic mechanical analysis	Day 14: cells viable. Mixed cell phenotype between NP cell and chondrocyte. Higher *COL2* expression at day 7 and 14 (9-fold *vs*. 2-fold increase, respectively). GAGs: more synthesis at day 14 (non-seeded NPs: 20.6 µg/mg; repopulated NPs: 46.28 µg/mg)	Mercuri *et al.* (2013)

Table 3. Current procedures for IVD recellularization

IVD tissue origin	Cell source	Seeding method	Assays									Key outcomes	Ref.
			Cell number	Cell viability	DNA content	GAG content	Collagen content	Water content	Tissue organization	Gene expression	Others		
Porcine (NP)	Human NP cells	Cells mixed with NP gel	—	Calcein-AM/ethidium homodimer-1 assay	—	Blyscan assay	Soluble and insoluble collagen assays	—	—	—	—	Day 21: cells viable with a NP-like morphology and increased GAG content	Wachs *et al.* (2017)
	Human and rabbit ADSCs	Cells mixed with NP gel	DAPI staining	—	Hoechst	Alcian blue staining, blyscan assay	Picrosirius red staining, HYP assay	Wet-dry weight	—	*Acan, Sox9, Col1, Col2, Krt19, Pax1, Gdf10*	IHC (COLII), metabolic activity (CCK8), cytotoxicity (lactate dehydrogenase assay)	Day 14: higher cell proliferation and gene expression level (*Acan*, *Col2*, *Sox9*, *Krt19* and *Pax1*). Increase of GAGs and decrease of collagen	Zhou *et al.* (2018)
	Human MSCs	Dropping onto scaffold	DAPI staining	—	DNeasy	Alcian blue staining, blyscan assay	HYP assay	Wet-dry weight	H&E	*Col1, Col2, Acan, Sox9, Ncam1, Mmp13*	IHC (COLI, COLII), metabolic activity (CCK8), IF (ACAN, SOX9)	Day 14: higher cell proliferation. Upregulation of *COL2, ACAN, COL1A1, NCAM-1* and *SOX9* and downregulation of *MMP-13*. Day 14: higher ACAN and SOX9 production by reseeded cells.	Xu *et al.* (2019)

Table 3. Current procedures for IVD recellularization

IVD tissue origin	Cell source	Seeding method	Assays									Key outcomes	Ref.
			Cell number	Cell viability	DNA content	GAG content	Collagen content	Water content	Tissue organization	Gene expression	Others		
Rabbit (IVD)	Rabbit BM-MSCs, human IVD cells	Multiple seeding onto tissue surface	DAPI staining	Calcein-AM/ethidium homodimer-1 assay	DNeasy	Alcian blue staining	HYP assay	Wet-dry weight	H&E	*Col1, Col2, Sox9, Gpc3, Foxf1, Acan, Ca12, Timp1, Timp2, Tgfβ, Tgf-βr*	Metabolic activity (CCK8), IHC (COLI, COLII, ACAN, CD8, MAC387)	Day 21: cells viable and cell migration into the scaffolds. Increased *Col2* (more than 12-fold increase), *Sox9* (14 times greater), *Foxf1* (118-fold increase), *Ca12* (5-fold increase), *Acan* and *Gpc3* gene expression	Lin *et al.* (2016)
Human (IVD)	Human BM-MSCs, human IVD cells	Seeding onto tissue surface	—	Fluorescein diacetate/ ethidium bromide assay	CyQUANT	DMMB assay	HYP assay	—	—	—	—	Day 14: cells viable with limited migration. Higher DNA content in scaffolds seeded with hIVD cells. Increased GAG and collagen content in scaffolds seeded with hBM-MSC	Huang *et al.* (2016)

Table 3. Current procedures for IVD recellularization

IVD tissue origin	Cell source	Seeding method	Assays								Key outcomes	Ref.
			Cell number	Cell viability	DNA content	GAG content	Collagen content	Water content	Tissue organization	Gene expression	Others	
Bovine (AF)	Human BM-MSCs	Seeding onto hydrogel	—	Live/Dead assay	—	—	—	—	—	*Col1A1, Col5A1, Ibsp, Fbln1, Tnmd*	Cell compatibility (CCK8), cytotoxicity (lactate dehydrogenase assay)	Day 21: cells viable and higher gene expression level of *COL1A1, COL5A1, FBLN1, IBSP*, and *TNMD*	Peng *et al.* (2020)
Porcine (AF)	Rabbit AF cells	Drop-wise addition onto the tissue surface (with turnover)	—	Calcein-AM/ethidium homodimer-1 assay	—	—	—	—	H&E	—	—	Day 7: cell infiltration into the mid-horizontal plane of scaffolds. No dead cells observed	Xu *et al.* (2014)
Rabbit (AF)	Rabbit AF stem cells	Seeding onto hydrogel	DAPI staining	—	Hoechst	DMMB assay	COLI and COLII ELISA kit	—	—	*Col1, Col2, Acan*	Metabolic activity (CCK8)	Day 14: upregulation of *Col1, Col2* and *Acan*. GAGs: higher release in the hydrogel media with bFGF (4.43 µg/µg) than in those without (2.28 µg/µg), as well as col1 (with bFGF: 4.68 ng/µg; without bFGF: 3.56 ng/µg), col2 (with bFGF: 11.95 ng/µg; without bFGF: 10.42 ng/µg) and acan (with bFGF: 1022.23 pg/µg and without bFGF: 790.95 pg/µg)	Liu *et al.* (2019)

6. CONTROLLING THE IMMUNE RESPONSE AGAINST DECELLULARIZED IVD MATRICES

The main cause of implant failure is hyper immunoreactivity towards the graft or its degradation products. The most common antigens that trigger such an inflammatory response are DNA and galactose-a-1,3-galactose (Gal) (Badylak & Gilbert, 2008; Cheng et al., 2014). Their elimination can extend xenograft survival. Non-self-antigen (from transplants, bacteria or viruses) recognition initiates an immune response mediated by Major Histocompatibility Complex (MHC) class I and II (Boccafoschi et al., 2017; Chen et al., 2017; Warrington et al., 2011). Therefore, controlling non-self acute and chronic immune response (through adjusting both pro- and anti-inflammatory cues) is crucial for a successful implantation (Boccafoschi et al., 2017). Optimization of the decellularization process is key to avoid dampening the bioactivity of native ECM while minimizing residual immunological agents. This prevents disease transmission, reduces inflammation and immune response towards the scaffold, decreasing rejection after implantation (Badylak et al., 2011; Cheng et al., 2014). Given that ECM proteins are among the most conserved proteins in evolution, with high levels of sequence homology, decellularization should be enough for explants to be well tolerated (Hutter et al., 2000; Moroni & Mirabella, 2014; Ozbek et al., 2010; van der Rest & Garrone, 1991). In fact, due to being considered anti-immunogenic, decellularized matrices have been proposed not only for autografts (within the same individual) and allografts (from one individual to another of the same species with a different genotype) but also for xenografts (from another species) (Boccafoschi et al., 2017). Although dense matrices hinder complete cell removal, most commercially available decellularized materials do contain DNA traces without compromising their clinical efficacy (Cheng et al., 2014; Derwin et al., 2006; Gilbert et al., 2009; Zheng et al., 2005), thus, demonstrating that the DNA remnants may exist below a threshold that triggers a harsh immune response (Badylak & Gilbert, 2008; Cheng et al., 2014).

Gal epitopes are usually found in most species but not in humans. Because humans are constantly exposed to intestinal bacteria that carry Gal epitopes, they produce large amounts of anti-Gal antibodies (Badylak & Gilbert, 2008; Cheng et al., 2014). In that context, porcine bioprosthetic heart valves have shown to induce a xenograft-specific immune response with high levels of cytotoxic IgM antibodies against a-Gal and have failed in some patients (Cheng et al., 2014; Konakci et al., 2005). Although organs from Gal-knockout pigs have been rejected due to other antigens (Chen et al., 2005), graft treatment with a-

galactosidase has been able to remove Gal epitopes, minimizing an adverse host immune reaction (Cheng et al., 2014; Stone et al., 2007; Stone et al., 1998). Research is still limited and further studies are needed to improve the safety and efficacy of decellularized material (Cheng et al., 2014).

In the disc field, only two works describe a-Gal assessment after decellularization and in both cases there seems to be a removal (Mercuri et al., 2011) or at least a significant reduction of the a-Gal epitope in the decellularized scaffolds (native AFs: less than 10 ng/mL; decellularized AFs: less than 5 ng/mL) (Wu et al., 2017). Even if a residual amount remains, it evokes minimal to no immune response *in vivo* (Lin et al., 2016). Finally, it should be borne in mind that ECM fragments that result from degradation can also trigger inflammation (Molinos et al., 2015). This issue has not been given due consideration in most reports. Mechanisms responsible for macrophage switch from an M1 to an M2 profile should also be further studied *in vivo* to promote tissue remodelling and consequently improve scaffold biocompatibility (Moroni & Mirabella, 2014).

7. *IN VIVO* BEHAVIOR OF DECELLULARIZED ECMS

Biocompatibility of ECM-based scaffolds cannot be addressed only by using *in vitro* tests since they lack the complex biology and physiology of a whole organism. For that, *in vivo* assessments are needed to evaluate host responses to the scaffolds (Aamodt & Grainger, 2016). Mercuri *et al.* (2011) evaluated biocompatibility of the porcine-derived material in a rat model (subdermal pockets). Most non-crosslinked NP decellularized scaffolds were degraded completely after 4 weeks whereas crosslinking delayed degradation. In all the cases an inflammatory response was observed. Since DNA was removed in their previous work (Mercuri et al., 2011), the authors hypothesized that this reaction may be triggered by a delayed degradation of the crosslinked material and a possible interaction between GAGs, present in the scaffold, and pro-inflammatory cytokines (Mercuri et al., 2013).

Lin *et al.* (2016) assessed immunological response to decellularized rabbit IVD-based scaffolds *in vivo* in a rabbit model, in comparison to native tissue grafts. Subcutaneous decellularized implants presented minimal signs of inflammation 1 month post-implantation, while native scaffolds presented high levels of cell infiltration, namely of

neutrophils, blood vessel formation and additional signs of inflammation (Lin et al., 2016). A similar effect was observed when the same model was used with decellularized porcine xenografts seeded with MSCs (Xu et al., 2019).

Yu *et al*. (2020) evaluated the *in vivo* biocompatibility of a bovine NP hydrogel compared to a synthetic material (poly-ε-caprolactone) by subcutaneous implantation in a rat model. Following 2 and 4 weeks of NP hydrogel implantation, H&E staining showed a smaller neutrophil and giant cell number, evidencing mild inflammation and reduced foreign body reaction *in vivo* (Yu et al., 2020). Also, the immunocompatibility of porcine decellularized AF scaffolds has been under studied. Using Wistar rats (box incision in rat tail), the authors have shown cell infiltration and tissue remodelling in the implanted animals, as evidenced by an increase in collagen and GAG content (Wu et al., 2017). More recently, Peng and colleagues have explored the ability of bovine AF-derived hydrogels to repair AF defects *in vivo*. They injected AF pre-hydrogel solutions, crosslinked or not with genipin (g-DAF-G and DAF-G, respectively), that were able to form a hydrogel *in situ* and to fill in AF defects. Moreover, both hydrogels induced disc cell migration and ECM production, demonstrating their regenerative potential *in vivo* (Peng et al., 2020).

Although most works did not observe cytotoxicity *in vitro* (except as a response to material crosslinking) (Borem et al., 2017; Fernandez et al., 2016), *in vivo* cell recruitment and repopulation is required for biointegration of the decellularized matrix and should be given due consideration.

Experiments using human tissue will be the ultimate frontier before clinical trials. Human *ex vivo* organ cultures are already underway to serve other purposes (Gawri et al., 2011; Walter et al., 2014) and should be used not only to test the effect of decellularized tissue grafts but also to assess the host response, at least to some extent.

8. LIMITATIONS/PRECAUTIONS OF USING DECELLULARIZED MATRICES

8.1. DONOR PROFILE

The development of successful ECM-based scaffolds depends on a wide range of factors that need to be considered before their use in the clinics. The selection of tissue

donor profile, including animal source and age, for instance, can have a dramatic impact on the regenerative process. Concerning IVD source, on one hand, the use of human degenerated tissues can negatively influence tissue repair, leading to implantation failure. On the other hand, human cadaveric IVDs, although supposedly healthy, are scarce and difficult to obtain due to ethical restrictions. Therefore, animal tissues can be a good alternative to overcome this issue. Baboons would be ideal, as they are large and conduct forces through their spine similarly to humans to which they are closely related (Lauerman et al., 1992). However, they are also limited in number, raise ethical concerns and constitute a potential source of zoonoses (Mafuyai et al., 2013). Porcine tissues are also good candidates and are already available on the market, as replacement heart valves and for wound management solutions (Tsuchiya et al., 2014). Bovine discs are large, easily available, have a similar NP aspect ratio and an identical ECM composition (Alini et al., 2008; Demers et al., 2004; O'Connell et al., 2007; Oshima et al., 1993; Roberts et al., 2008).

The donor age can also affect biomechanical properties and composition of ECM-based scaffolds (Cramer & Badylak, 2019). With ageing, native ECM undergoes several biochemical and structural changes, which can influence cell response and tissue remodelling when using biomaterials derived from these tissues (Cramer & Badylak, 2019).

Neonatal-derived scaffolds have an enhanced pro-regenerative potential, as already reported in the heart, abdominal wall muscle and kidney (Nakayama et al., 2011; Sicari et al., 2012; Silva et al., 2016). In the disc field, pro-regenerative proteins (collagen type XII and XIV) are uniquely expressed in prenatal IVD microenvironments (Caldeira et al., 2017). Moreover, fetal discs are also characterized by a different topography, when compared to young and adult tissues (Caldeira et al., 2018). Other age-associated structural differences of bovine discs can be observed in Figure 1**.**

8.2. LEGISLATIVE ISSUES

Tissue engineering derivatives do not fall into the classification of drugs, transplants nor artificial tissues. As reviewed elsewhere (Boccafoschi et al., 2017), both the FDA and the European Commission proposed guidelines with a unified approach to regulate tissue-engineering products. Likewise, safety issues regarding xenotransplantation of cells and tissues should also be addressed. Characterization of animal source, facilities and maintenance as well as of xenotransplantation products, selection of adequate preclinical

models and recipient monitoring should be considered, as documented by the FDA and the European Union (Boccafoschi et al., 2017).

9. CONCLUSIONS AND FUTURE CHALLENGES

The present review summarized the latest advances in IVD decellularization. Recently, decellularized ECM-based scaffolds have gained significant attention for tissue remodelling with a regenerative purpose, given the success in cell removal and maintenance of most ECM properties with biological implications. Significant progress has been achieved in the last decade due to several exhaustive studies using a panoply of methods either alone or in combination, a wide range of reagents, several cell types and distinct animal sources. But there is still room for improvement, for instance by reducing treatment time and using milder detergents. Although recent progress is encouraging, several aspects need to be considered before commercialization and clinical application, such as the following.

- Absence of a standardized protocol for decellularization and for evaluating its efficacy, which renders the comparison of methods difficult. The ideal protocol should be scalable and effective, independent of donor species, age or pathological condition, and a final scaffold sterilization step must be contemplated.
- Lack of uniformity of the optimal cell type, cell seeding density and cell repopulation method required for effective recellularization. Appropriate selection of cell source will certainly determine the success of the therapy *in vivo*. Moreover, given the dense nature of the disc, cell infiltration into decellularized disc matrices can be hindered. The use of dynamic conditions could improve cell migration towards the inner scaffolds or, in alternative, decellularized matrix-based hydrogels (with increased porosity) or powders incorporated in different gels could be used to increase uniform cell distribution.
- Donor age (of the animals selected for tissue decellularization). Despite being an often-neglected aspect, IVD matrisome is profoundly affected by age (Caldeira et al., 2017; Caldeira et al., 2018). Therefore, novel solutions using fetal tissues that mimic a healthy pre-natal landscape should be pursued for IVD regeneration (Fiordalisi et al., 2020).

- Limited *in vivo* validation. To verify clinical potential, biocompatibility of decellularized IVD-based scaffolds should be pursued preferentially using chondrodystrophic dogs, given that small rodents maintain notochordal cells throughout adulthood and do not reproduce human-disc size nor loading (Daly et al., 2016; Novais et al., 2020).

In conclusion, decellularized ECM-based scaffolds have a great potential to be translated into clinical applications for IVD repair and regeneration. Still, many challenges need to be solved and clinical trials must be conducted before these scaffolds can be launched on the market. Natural biomaterials are already revolutionizing the tissue engineering field and their use for IVD could bring a new hope for LBP treatments.

10. ACKNOWLEDGMENTS

We would like to acknowledge Claúdia Ribeiro-Machado for all the technical support on histology troubleshooting. We would like to acknowledge support by The FCT funds FCT/DL 57/2016/CP1360/CT0005-JC, PhD grant (PD/BD/135544/2018-MF). This work was also financed by QREN (Quadro de Referência Estratégica Nacional). The project (20-165) was also supported by a grant from the ON Foundation, Switzerland.

11. REFERENCES

Aamodt, J. M., & Grainger, D. W. (2016). Extracellular matrix-based biomaterial scaffolds and the host response. *Biomaterials*, *86*, 68-82. https://doi.org/10.1016/j.biomaterials.2016.02.003

Adams, M. A., & Roughley, P. J. (2006). What is intervertebral disc degeneration, and what causes it? *Spine (Phila Pa 1976)*, *31*(18), 2151-2161. https://doi.org/10.1097/01.brs.0000231761.73859.2c

Agmon, G., & Christman, K. L. (2016). Controlling stem cell behavior with decellularized extracellular matrix scaffolds. *Current Opinion in Solid State and Materials Science*, *20*(4), 193-201. https://doi.org/https://doi.org/10.1016/j.cossms.2016.02.001

akbari zahmati, A., Alipoor, R., Rezaei Shahmirzadi, A., Khori, V., & Abolhasani, M. (2017). Chemical Decellularization Methods and Its Effects on Extracellular Matrix. *Internal Medicine And Medical Investigation Journal*, *2*. https://doi.org/10.24200/imminv.v2i3.63

Alini, M., Eisenstein, S. M., Ito, K., Little, C., Kettler, A. A., Masuda, K., Melrose, J., Ralphs, J., Stokes, I., & Wilke, H. J. (2008). Are animal models useful for studying human disc disorders/degeneration? *Eur Spine J*, *17*(1), 2-19. https://doi.org/10.1007/s00586-007-0414-y

Anderson, D. G., & Tannoury, C. (2005). Molecular pathogenic factors in symptomatic disc degeneration. *Spine J*, *5*(6 Suppl), 260S-266S. https://doi.org/10.1016/j.spinee.2005.02.010

Badylak, S. F., & Gilbert, T. W. (2008). Immune response to biologic scaffold materials. *Semin Immunol*, *20*(2), 109-116. https://doi.org/10.1016/j.smim.2007.11.003

Badylak, S. F., Taylor, D., & Uygun, K. (2011). Whole-organ tissue engineering: decellularization and recellularization of three-dimensional matrix scaffolds. *Annu Rev Biomed Eng*, *13*, 27-53. https://doi.org/10.1146/annurev-bioeng-071910-124743

Boccafoschi, F., Botta, M., Fusaro, L., Copes, F., Ramella, M., & Cannas, M. (2017). Decellularized biological matrices: an interesting approach for cardiovascular tissue repair and regeneration. *J Tissue Eng Regen Med*, *11*(5), 1648-1657. https://doi.org/10.1002/term.2103

Borem, R., Madeline, A., Walters, J., Mayo, H., Gill, S., & Mercuri, J. (2017). Angle-ply biomaterial scaffold for annulus fibrosus repair replicates native tissue mechanical properties, restores spinal kinematics, and supports cell viability. *Acta biomaterialia*, *58*, 254-268. https://doi.org/10.1016/j.actbio.2017.06.006

Bydon, M., De la Garza-Ramos, R., Macki, M., Baker, A., Gokaslan, A. K., & Bydon, A. (2014). Lumbar fusion versus nonoperative management for treatment of discogenic low back pain: a systematic review and meta-analysis of randomized controlled trials. *J Spinal Disord Tech*, *27*(5), 297-304. https://doi.org/10.1097/BSD.0000000000000072

Caldeira, J., Santa, C., Osorio, H., Molinos, M., Manadas, B., Goncalves, R., & Barbosa, M. (2017). Matrisome Profiling During Intervertebral Disc Development And Ageing. *Sci Rep*, *7*(1), 11629. https://doi.org/10.1038/s41598-017-11960-0

Caldeira, J., Sousa, A., Sousa, D., & Barros, D. (2018). Extracellular matrix constitution and function for tissue regeneration and repair. In M. A. Barbosa & M. C. L. Martins (Eds.), *Peptides and Proteins as Biomaterials for Tissue Regeneration and Repair* (pp. 29-72). Elsevier Woodhead Publishing Series. https://doi.org/10.1016/B978-0-08-100803-4.00002-4

Campoccia, D., Montanaro, L., & Arciola, C. R. (2006). The significance of infection related to orthopedic devices and issues of antibiotic resistance. *Biomaterials*, *27*(11), 2331-2339. https://doi.org/10.1016/j.biomaterials.2005.11.044

Chan, L. K., Leung, V. Y., Tam, V., Lu, W. W., Sze, K. Y., & Cheung, K. M. (2013). Decellularized bovine intervertebral disc as a natural scaffold for xenogenic cell studies. *Acta biomaterialia*, *9*(2), 5262-5272. https://doi.org/10.1016/j.actbio.2012.09.005

Chen, G., Qian, H., Starzl, T., Sun, H., Garcia, B., Wang, X., Wise, Y., Liu, Y., Xiang, Y., Copeman, L., Liu, W., Jevnikar, A., Wall, W., Cooper, D. K., Murase, N., Dai, Y., Wang, W., Xiong, Y., White, D. J., & Zhong, R. (2005). Acute rejection is associated with antibodies to non-Gal antigens in baboons using Gal-knockout pig kidneys. *Nat Med*, *11*(12), 1295-1298. https://doi.org/10.1038/nm1330

Chen, Y., Chen, J., Zhang, Z., Lou, K., Zhang, Q., Wang, S., Ni, J., Liu, W., Fan, S., & Lin, X. (2017). Current advances in the development of natural meniscus scaffolds: innovative approaches to decellularization and recellularization. *Cell Tissue Res*, *370*(1), 41-52. https://doi.org/10.1007/s00441-017-2605-0

Cheng, C. W., Solorio, L. D., & Alsberg, E. (2014). Decellularized tissue and cell-derived extracellular matrices as scaffolds for orthopaedic tissue engineering. *Biotechnol Adv*, *32*(2), 462-484. https://doi.org/10.1016/j.biotechadv.2013.12.012

Cheng, N. C., Estes, B. T., Awad, H. A., & Guilak, F. (2009). Chondrogenic differentiation of adipose-derived adult stem cells by a porous scaffold derived from native articular cartilage extracellular matrix. *Tissue engineering. Part A*, *15*(2), 231-241. https://doi.org/10.1089/ten.tea.2008.0253

Colombier, P., Clouet, J., Hamel, O., Lescaudron, L., & Guicheux, J. (2014). The lumbar intervertebral disc: from embryonic development to degeneration. *Joint Bone Spine*, *81*(2), 125-129. https://doi.org/10.1016/j.jbspin.2013.07.012

Cramer, M. C., & Badylak, S. F. (2019). Extracellular Matrix-Based Biomaterials and Their Influence Upon Cell Behavior. *Annals of Biomedical Engineering*. https://doi.org/10.1007/s10439-019-02408-9

Crapo, P. M., Gilbert, T. W., & Badylak, S. F. (2011). An overview of tissue and whole organ decellularization processes. *Biomaterials*, *32*(12), 3233-3243. https://doi.org/10.1016/j.biomaterials.2011.01.057

Cs-Szabo, G., Ragasa-San Juan, D., Turumella, V., Masuda, K., Thonar, E. J., & An, H. S. (2002). Changes in mRNA and protein levels of proteoglycans of the anulus fibrosus and nucleus pulposus during intervertebral disc degeneration. *Spine (Phila Pa 1976)*, *27*(20), 2212-2219. https://doi.org/10.1097/01.BRS.0000029249.02864.5B

Dai, Z., Ronholm, J., Tian, Y., Sethi, B., & Cao, X. (2016). Sterilization techniques for biodegradable scaffolds in tissue engineering applications. *Journal of tissue engineering*, *7*, 2041731416648810. https://doi.org/10.1177/2041731416648810

Daly, C., Ghosh, P., Jenkin, G., Oehme, D., & Goldschlager, T. (2016). A Review of Animal Models of Intervertebral Disc Degeneration: Pathophysiology, Regeneration, and Translation to the Clinic. *BioMed Research International*, *2016*, 5952165. https://doi.org/10.1155/2016/5952165

Demers, C. N., Antoniou, J., & Mwale, F. (2004). Value and limitations of using the bovine tail as a model for the human lumbar spine. *Spine (Phila Pa 1976)*, *29*(24), 2793-2799. http://www.ncbi.nlm.nih.gov/pubmed/15599281

DeQuach, J. A., Mezzano, V., Miglani, A., Lange, S., Keller, G. M., Sheikh, F., & Christman, K. L. (2010). Simple and High Yielding Method for Preparing Tissue Specific Extracellular Matrix Coatings for Cell Culture. *PLOS ONE*, *5*(9), e13039. https://doi.org/10.1371/journal.pone.0013039

Derwin, K. A., Baker, A. R., Spragg, R. K., Leigh, D. R., & Iannotti, J. P. (2006). Commercial extracellular matrix scaffolds for rotator cuff tendon repair. Biomechanical, biochemical, and cellular properties. *J Bone Joint Surg Am*, *88*(12), 2665-2672. https://doi.org/10.2106/JBJS.E.01307

Destefani, A. C., Sirtoli, G. M., & Nogueira, B. V. (2017). Advances in the Knowledge about Kidney Decellularization and Repopulation. *Front Bioeng Biotechnol*, *5*, 34. https://doi.org/10.3389/fbioe.2017.00034

Duance, V. C., Crean, J. K., Sims, T. J., Avery, N., Smith, S., Menage, J., Eisenstein, S. M., & Roberts, S. (1998). Changes in collagen cross-linking in degenerative disc disease and scoliosis. *Spine (Phila Pa 1976)*, *23*(23), 2545-2551. http://www.ncbi.nlm.nih.gov/pubmed/9854753

Fernandez, C., Marionneaux, A., Gill, S., & Mercuri, J. (2016). Biomimetic nucleus pulposus scaffold created from bovine caudal intervertebral disc tissue utilizing an optimal decellularization procedure. *J Biomed Mater Res A*, *104*(12), 3093-3106. https://doi.org/10.1002/jbm.a.35858

Fidalgo, C., Iop, L., Sciro, M., Harder, M., Mavrilas, D., Korossis, S., Bagno, A., Palù, G., Aguiari, P., & Gerosa, G. (2018). A sterilization method for decellularized xenogeneic cardiovascular scaffolds. *Acta biomaterialia*, *67*, 282-294. https://doi.org/https://doi.org/10.1016/j.actbio.2017.11.035

Fiordalisi, M., Silva, A. J., Barbosa, M., Gonçalves, R., & Caldeira, J. (2020). Decellularized Scaffolds for Intervertebral Disc Regeneration. *Trends in Biotechnology*. https://doi.org/https://doi.org/10.1016/j.tibtech.2020.05.002

Fu, R.-H., Wang, Y.-C., Liu, S.-P., Shih, T.-R., Lin, H.-L., Chen, Y.-M., Sung, J.-H., Lu, C.-H., Wei, J.-R., Wang, Z.-W., Huang, S.-J., Tsai, C.-H., Shyu, W.-C., & Lin, S.-Z. (2014). Decellularization and Recellularization Technologies in Tissue Engineering. *Cell Transplantation*, *23*(4-5), 621-630. https://doi.org/10.3727/096368914X678382

Galbusera, F., van Rijsbergen, M., Ito, K., Huyghe, J. M., Brayda-Bruno, M., & Wilke, H. J. (2014). Ageing and degenerative changes of the intervertebral disc and their impact on spinal flexibility. *Eur Spine J*, *23 Suppl 3*, S324-332. https://doi.org/10.1007/s00586-014-3203-4

Ganey, T., Libera, J., Moos, V., Alasevic, O., Fritsch, K. G., Meisel, H. J., & Hutton, W. C. (2003). Disc chondrocyte transplantation in a canine model: a treatment for degenerated or damaged intervertebral disc. *Spine (Phila Pa 1976)*, *28*(23), 2609-2620. https://doi.org/10.1097/01.Brs.0000097891.63063.78

Gawri, R., Mwale, F., Ouellet, J., Roughley, P. J., Steffen, T., Antoniou, J., & Haglund, L. (2011). Development of an organ culture system for long-term survival of the intact human intervertebral disc. *Spine (Phila Pa 1976)*, *36*(22), 1835-1842. https://doi.org/10.1097/BRS.0b013e3181f81314

Gilbert, T. W. (2012). Strategies for tissue and organ decellularization [https://doi.org/10.1002/jcb.24130]. *Journal of Cellular Biochemistry*, *113*(7), 2217-2222. https://doi.org/https://doi.org/10.1002/jcb.24130

Gilbert, T. W., Freund, J. M., & Badylak, S. F. (2009). Quantification of DNA in biologic scaffold materials. *J Surg Res*, *152*(1), 135-139. https://doi.org/10.1016/j.jss.2008.02.013

Gilbert, T. W., Sellaro, T. L., & Badylak, S. F. (2006). Decellularization of tissues and organs. *Biomaterials*, *27*(19), 3675-3683. https://doi.org/10.1016/j.biomaterials.2006.02.014

Gilpin, A., & Yang, Y. (2017). Decellularization Strategies for Regenerative Medicine: From Processing Techniques to Applications. *BioMed Research International*, *2017*, 9831534. https://doi.org/10.1155/2017/9831534

Gruber, H. E., Johnson, T. L., Leslie, K., Ingram, J. A., Martin, D., Hoelscher, G., Banks, D., Phieffer, L., Coldham, G., & Hanley, E. N., Jr. (2002). Autologous intervertebral disc cell implantation: a model using Psammomys obesus, the sand rat. *Spine (Phila Pa 1976)*, *27*(15), 1626-1633. https://doi.org/10.1097/00007632-200208010-00007

Hensley, A., Rames, J., Casler, V., Rood, C., Walters, J., Fernandez, C., Gill, S., & Mercuri, J. J. (2018). Decellularization and characterization of a whole intervertebral disk xenograft scaffold. *J Biomed Mater Res A*, *106*(9), 2412-2423. https://doi.org/10.1002/jbm.a.36434

Hoshiba, T., Lu, H., Kawazoe, N., & Chen, G. (2010). Decellularized matrices for tissue engineering. *Expert Opin Biol Ther*, *10*(12), 1717-1728. https://doi.org/10.1517/14712598.2010.534079

Huang, Z., Kohl, B., Kokozidou, M., Arens, S., & Schulze-Tanzil, G. (2016). Establishment of a Cytocompatible Cell-Free Intervertebral Disc Matrix for Chondrogenesis with Human Bone Marrow-Derived Mesenchymal Stromal Cells. *Cells Tissues Organs*, *201*(5), 354-365. https://doi.org/10.1159/000444521

Hulmes, D. J. S. (2008). Collagen Diversity, Synthesis and Assembly. In P. Fratzl (Ed.), *Collagen: Structure and Mechanics* (pp. 15-47). Springer US. https://doi.org/10.1007/978-0-387-73906-9_2

Hussey, G. S., Dziki, J. L., & Badylak, S. F. (2018). Extracellular matrix-based materials for regenerative medicine. *Nature Reviews Materials*, *3*(7), 159-173. https://doi.org/10.1038/s41578-018-0023-x

Hutter, H., Vogel, B. E., Plenefisch, J. D., Norris, C. R., Proenca, R. B., Spieth, J., Guo, C., Mastwal, S., Zhu, X., Scheel, J., & Hedgecock, E. M. (2000). Conservation and novelty in the evolution of cell adhesion and extracellular matrix genes. *Science*, *287*(5455), 989-994. http://www.ncbi.nlm.nih.gov/pubmed/10669422

Iatridis, J. C., MacLean, J. J., O'Brien, M., & Stokes, I. A. (2007). Measurements of proteoglycan and water content distribution in human lumbar intervertebral discs. *Spine (Phila Pa 1976)*, *32*(14), 1493-1497. https://doi.org/10.1097/BRS.0b013e318067dd3f

Illien-Junger, S., Sedaghatpour, D. D., Laudier, D. M., Hecht, A. C., Qureshi, S. A., & Iatridis, J. C. (2016). Development of a bovine decellularized extracellular matrix-biomaterial for nucleus pulposus regeneration. *J Orthop Res*, *34*(5), 876-888. https://doi.org/10.1002/jor.23088

Keane, T. J., Swinehart, I. T., & Badylak, S. F. (2015). Methods of tissue decellularization used for preparation of biologic scaffolds and in vivo relevance. *Methods*, *84*, 25-34. https://doi.org/https://doi.org/10.1016/j.ymeth.2015.03.005

Konakci, K. Z., Bohle, B., Blumer, R., Hoetzenecker, W., Roth, G., Moser, B., Boltz-Nitulescu, G., Gorlitzer, M., Klepetko, W., Wolner, E., & Ankersmit, H. J. (2005). Alpha-Gal on bioprostheses: xenograft immune response in cardiac surgery. *Eur J Clin Invest*, *35*(1), 17-23. https://doi.org/10.1111/j.1365-2362.2005.01441.x

Kumar, H., Ha, D. H., Lee, E. J., Park, J. H., Shim, J. H., Ahn, T. K., Kim, K. T., Ropper, A. E., Sohn, S., Kim, C. H., Thakor, D. K., Lee, S. H., & Han, I. B. (2017). Safety and tolerability of intradiscal implantation of combined autologous adipose-derived mesenchymal stem cells and hyaluronic acid in patients with chronic discogenic low back pain: 1-year follow-up of a phase I study. *Stem Cell Res Ther*, *8*(1), 262. https://doi.org/10.1186/s13287-017-0710-3

Lauerman, W. C., Platenberg, R. C., Cain, J. E., & Deeney, V. F. (1992). Age-related disk degeneration: preliminary report of a naturally occurring baboon model. *J Spinal Disord*, *5*(2), 170-174. http://www.ncbi.nlm.nih.gov/pubmed/1606375

Le Maitre, C. L., Baird, P., Freemont, A. J., & Hoyland, J. A. (2009). An in vitro study investigating the survival and phenotype of mesenchymal stem cells following injection into nucleus pulposus tissue. *Arthritis research & therapy*, *11*(1), R20-R20. https://doi.org/10.1186/ar2611

Leckie, S. K., Bechara, B. P., Hartman, R. A., Sowa, G. A., Woods, B. I., Coelho, J. P., Witt, W. T., Dong, Q. D., Bowman, B. W., Bell, K. M., Vo, N. V., Wang, B., & Kang, J. D. (2012). Injection of AAV2-BMP2 and AAV2-TIMP1 into the nucleus pulposus slows the course of intervertebral disc degeneration in an in vivo rabbit model. *Spine J*, *12*(1), 7-20. https://doi.org/10.1016/j.spinee.2011.09.011

Lee, J. S., Shin, J., Park, H. M., Kim, Y. G., Kim, B. G., Oh, J. W., & Cho, S. W. (2014). Liver extracellular matrix providing dual functions of two-dimensional substrate coating and three-dimensional injectable hydrogel platform for liver tissue engineering. *Biomacromolecules*, *15*(1), 206-218. https://doi.org/10.1021/bm4015039

León-López, A., Morales-Peñaloza, A., Martínez-Juárez, V. M., Vargas-Torres, A., Zeugolis, D. I., & Aguirre-Álvarez, G. (2019). Hydrolyzed Collagen-Sources and Applications. *Molecules (Basel, Switzerland)*, *24*(22), 4031. https://doi.org/10.3390/molecules24224031

Li, B., & Webster, T. J. (2018). Bacteria antibiotic resistance: New challenges and opportunities for implant-associated orthopedic infections. *J Orthop Res*, *36*(1), 22-32. https://doi.org/10.1002/jor.23656

Lin, X., Fang, X., Wang, Q., Hu, Z., Chen, K., Shan, Z., Chen, S., Wang, J., Mo, J., Ma, J., Xu, W., Qin, A., & Fan, S. (2016). Decellularized allogeneic intervertebral disc: natural biomaterials for regenerating disc degeneration. *Oncotarget*, *7*(11), 12121-12136. https://doi.org/10.18632/oncotarget.7735

Liu, C., Jin, Z., Ge, X., Zhang, Y., & Xu, H. (2019). Decellularized Annulus Fibrosus Matrix/Chitosan Hybrid Hydrogels with Basic Fibroblast Growth Factor for Annulus Fibrosus Tissue Engineering. *Tissue engineering. Part A*, *25*(23-24), 1605-1613. https://doi.org/10.1089/ten.TEA.2018.0297

Londono, R., & Badylak, S. F. (2015). Biologic scaffolds for regenerative medicine: mechanisms of in vivo remodeling. *Ann Biomed Eng*, *43*(3), 577-592. https://doi.org/10.1007/s10439-014-1103-8

Mafuyai, H. B., Barshep, Y., Audu, B. S., Kumbak, D., & Ojobe, T. O. (2013). Baboons as potential reservoirs of zoonotic gastrointestinal parasite infections at Yankari National Park, Nigeria. *Afr Health Sci*, *13*(2), 252-254. https://doi.org/10.4314/ahs.v13i2.7

Martin, M. D., Boxell, C. M., & Malone, D. G. (2002). Pathophysiology of lumbar disc degeneration: a review of the literature. *Neurosurg Focus*, *13*(2), E1. https://doi.org/10.3171/foc.2002.13.2.2

Masuda, K., Imai, Y., Okuma, M., Muehleman, C., Nakagawa, K., Akeda, K., Thonar, E., Andersson, G., & An, H. S. (2006). Osteogenic protein-1 injection into a degenerated disc induces the restoration of disc height and structural changes in the rabbit anular puncture model. *Spine (Phila Pa 1976)*, *31*(7), 742-754. https://doi.org/10.1097/01.brs.0000206358.66412.7b

McGuire, R., Borem, R., & Mercuri, J. (2017). The fabrication and characterization of a multi-laminate, angle-ply collagen patch for annulus fibrosus repair. *J Tissue Eng Regen Med*, *11*(12), 3488-3493. https://doi.org/10.1002/term.2250

Mercuri, J. J., Gill, S. S., & Simionescu, D. T. (2011). Novel tissue-derived biomimetic scaffold for regenerating the human nucleus pulposus. *J Biomed Mater Res A*, *96*(2), 422-435. https://doi.org/10.1002/jbm.a.33001

Mercuri, J. J., Patnaik, S., Dion, G., Gill, S. S., Liao, J., & Simionescu, D. T. (2013). Regenerative potential of decellularized porcine nucleus pulposus hydrogel scaffolds: stem cell differentiation, matrix remodeling, and biocompatibility studies. *Tissue engineering. Part A*, *19*(7-8), 952-966. https://doi.org/10.1089/ten.TEA.2012.0088

Molinos, M., Almeida, C. R., Caldeira, J., Cunha, C., Goncalves, R. M., & Barbosa, M. A. (2015). Inflammation in intervertebral disc degeneration and regeneration. *J R Soc Interface*, *12*(108), 20150429. https://doi.org/10.1098/rsif.2015.0429

Moroni, F., & Mirabella, T. (2014). Decellularized matrices for cardiovascular tissue engineering. *Am J Stem Cells*, *3*(1), 1-20. http://www.ncbi.nlm.nih.gov/pubmed/24660110

Mwale, F., Roughley, P., & Antoniou, J. (2004). Distinction between the extracellular matrix of the nucleus pulposus and hyaline cartilage: a requisite for tissue engineering of intervertebral disc. *Eur Cell Mater*, *8*, 58-63; discussion 63-54. http://www.ncbi.nlm.nih.gov/pubmed/15602703

Nakayama, K. H., Batchelder, C. A., Lee, C. I., & Tarantal, A. F. (2011). Renal tissue engineering with decellularized rhesus monkey kidneys: age-related differences. *Tissue engineering. Part A*, *17*(23-24), 2891-2901. https://doi.org/10.1089/ten.TEA.2010.0714

Nasser, R., Yadla, S., Maltenfort, M. G., Harrop, J. S., Anderson, D. G., Vaccaro, A. R., Sharan, A. D., & Ratliff, J. K. (2010). Complications in spine surgery. *J Neurosurg Spine*, *13*(2), 144-157. https://doi.org/10.3171/2010.3.SPINE09369

Newell, N., Little, J. P., Christou, A., Adams, M. A., Adam, C. J., & Masouros, S. D. (2017). Biomechanics of the human intervertebral disc: A review of testing techniques and results. *J Mech Behav Biomed Mater*, *69*, 420-434. https://doi.org/10.1016/j.jmbbm.2017.01.037

Noriega, D. C., Ardura, F., Hernández-Ramajo, R., Martín-Ferrero, M., Sánchez-Lite, I., Toribio, B., Alberca, M., García, V., Moraleda, J. M., Sánchez, A., & García-Sancho, J. (2017). Intervertebral Disc Repair by Allogeneic Mesenchymal Bone Marrow Cells: A Randomized Controlled Trial. *Transplantation*, *101*(8), 1945-1951. https://doi.org/10.1097/tp.0000000000001484

Novais, E. J., Tran, V. A., Miao, J., Slaver, K., Sinensky, A., Dyment, N. A., Addya, S., Szeri, F., van de Wetering, K., Shapiro, I. M., & Risbud, M. V. (2020). Comparison of inbred mouse strains shows diverse phenotypic outcomes of intervertebral disc aging. *Aging Cell*, *19*(5), e13148. https://doi.org/10.1111/acel.13148

Novotna, Z., Reznickova, A., Rimpelova, S., Vesely, M., Kolska, Z., & Svorcik, V. (2015). Tailoring of PEEK bioactivity for improved cell interaction: plasma treatment in action [10.1039/C5RA03861H]. *RSC Advances*, *5*(52), 41428-41436. https://doi.org/10.1039/C5RA03861H

O'Connell, G. D., Vresilovic, E. J., & Elliott, D. M. (2007). Comparison of animals used in disc research to human lumbar disc geometry. *Spine (Phila Pa 1976)*, *32*(3), 328-333. https://doi.org/10.1097/01.brs.0000253961.40910.c1

Oegema, T. R., Jr. (1993). Biochemistry of the intervertebral disc. *Clin Sports Med*, *12*(3), 419-439. http://www.ncbi.nlm.nih.gov/pubmed/8364983

Okuma, M., Mochida, J., Nishimura, K., Sakabe, K., & Seiki, K. (2000). Reinsertion of stimulated nucleus pulposus cells retards intervertebral disc degeneration: an in vitro and in vivo experimental study. *J Orthop Res*, *18*(6), 988-997. https://doi.org/10.1002/jor.1100180620

Onesti, S. T. (2004). Failed back syndrome. *Neurologist*, *10*(5), 259-264. http://www.ncbi.nlm.nih.gov/pubmed/15335443

Orozco, L., Soler, R., Morera, C., Alberca, M., Sánchez, A., & García-Sancho, J. (2011). Intervertebral disc repair by autologous mesenchymal bone marrow cells: a pilot study. *Transplantation*, *92*(7), 822-828. https://doi.org/10.1097/TP.0b013e3182298a15

Oshima, H., Ishihara, H., Urban, J. P., & Tsuji, H. (1993). The use of coccygeal discs to study intervertebral disc metabolism. *J Orthop Res*, *11*(3), 332-338. https://doi.org/10.1002/jor.1100110304

Ozbek, S., Balasubramanian, P. G., Chiquet-Ehrismann, R., Tucker, R. P., & Adams, J. C. (2010). The evolution of extracellular matrix. *Mol Biol Cell*, *21*(24), 4300-4305. https://doi.org/10.1091/mbc.E10-03-0251

Pei, M., Shoukry, M., Li, J., Daffner, S. D., France, J. C., & Emery, S. E. (2012). Modulation of in vitro microenvironment facilitates synovium-derived stem cell-based nucleus pulposus tissue regeneration. *Spine (Phila Pa 1976)*, *37*(18), 1538-1547. https://doi.org/10.1097/BRS.0b013e31825150bf

Peng, Y., Huang, D., Li, J., Liu, S., Qing, X., & Shao, Z. (2020). Genipin-crosslinked decellularized annulus fibrosus hydrogels induces tissue-specific differentiation of bone mesenchymal stem cells and intervertebral disc regeneration. *J Tissue Eng Regen Med*, *14*(3), 497-509. https://doi.org/10.1002/term.3014

Poornejad, N., Nielsen, J. J., Morris, R. J., Gassman, J. R., Reynolds, P. R., Roeder, B. L., & Cook, A. D. (2015). Comparison of four decontamination treatments on porcine renal decellularized extracellular matrix structure, composition, and support of renal tubular epithelium cells. *J Biomater Appl*, *30*(8), 1154-1167. https://doi.org/10.1177/0885328215615760

Raj, P. P. (2008). Intervertebral disc: anatomy-physiology-pathophysiology-treatment. *Pain Pract*, *8*(1), 18-44. https://doi.org/10.1111/j.1533-2500.2007.00171.x

Roberts, S., Menage, J., Sivan, S., & Urban, J. P. (2008). Bovine explant model of degeneration of the intervertebral disc. *BMC Musculoskelet Disord*, *9*, 24. https://doi.org/10.1186/1471-2474-9-24

Sakai, D., Mochida, J., Iwashina, T., Watanabe, T., Nakai, T., Ando, K., & Hotta, T. (2005). Differentiation of mesenchymal stem cells transplanted to a rabbit degenerative disc model: potential and limitations for stem cell therapy in disc regeneration. *Spine (Phila Pa 1976)*, *30*(21), 2379-2387. http://www.ncbi.nlm.nih.gov/pubmed/16261113

Saldin, L. T., Cramer, M. C., Velankar, S. S., White, L. J., & Badylak, S. F. (2017). Extracellular matrix hydrogels from decellularized tissues: Structure and function. *Acta biomaterialia*, *49*, 1-15. https://doi.org/10.1016/j.actbio.2016.11.068

Schimmel, J. J., Poeschmann, M. S., Horsting, P. P., Schönfeld, D. H., van Limbeek, J., & Pavlov, P. W. (2016). PEEK Cages in Lumbar Fusion: Mid-term Clinical Outcome and Radiologic Fusion. *Clin Spine Surg*, *29*(5), E252-258. https://doi.org/10.1097/BSD.0b013e31826eaf74

Schizas, C., Kulik, G., & Kosmopoulos, V. (2010). Disc degeneration: current surgical options. *Eur Cell Mater*, *20*, 306-315. https://doi.org/10.22203/ecm.v020a25

Seddon, A. M., Curnow, P., & Booth, P. J. (2004). Membrane proteins, lipids and detergents: not just a soap opera. *Biochim Biophys Acta*, *1666*(1-2), 105-117. https://doi.org/10.1016/j.bbamem.2004.04.011

Shoukry, M., Li, J., & Pei, M. (2012). Reconstruction of an In Vitro Niche for the Transition from Intervertebral Disc Development to Nucleus Pulposus Regeneration. *Stem Cells and Development*, *22*(8), 1162-1176. https://doi.org/10.1089/scd.2012.0597

Sicari, B. M., Johnson, S. A., Siu, B. F., Crapo, P. M., Daly, K. A., Jiang, H., Medberry, C. J., Tottey, S., Turner, N. J., & Badylak, S. F. (2012). The effect of source animal age upon the in vivo remodeling characteristics of an extracellular matrix scaffold. *Biomaterials*, *33*(22), 5524-5533. https://doi.org/10.1016/j.biomaterials.2012.04.017

Silva, A. C., Rodrigues, S. C., Caldeira, J., Nunes, A. M., Sampaio-Pinto, V., Resende, T. P., Oliveira, M. J., Barbosa, M. A., Thorsteinsdottir, S., Nascimento, D. S., & Pinto-do, O. P. (2016). Three-dimensional scaffolds of fetal decellularized hearts exhibit enhanced potential to support cardiac cells in comparison to the adult. *Biomaterials*, *104*, 52-64. https://doi.org/10.1016/j.biomaterials.2016.06.062

Spang, M. T., & Christman, K. L. (2018). Extracellular matrix hydrogel therapies: In vivo applications and development. *Acta biomaterialia*, *68*, 1-14. https://doi.org/10.1016/j.actbio.2017.12.019

Stone, K. R., Abdel-Motal, U. M., Walgenbach, A. W., Turek, T. J., & Galili, U. (2007). Replacement of human anterior cruciate ligaments with pig ligaments: a model for anti-non-gal antibody response in long-term xenotransplantation. *Transplantation*, *83*(2), 211-219. https://doi.org/10.1097/01.tp.0000250598.29377.13

Stone, K. R., Ayala, G., Goldstein, J., Hurst, R., Walgenbach, A., & Galili, U. (1998). Porcine cartilage transplants in the cynomolgus monkey. III. Transplantation of alpha-galactosidase-treated porcine cartilage. *Transplantation*, *65*(12), 1577-1583. http://www.ncbi.nlm.nih.gov/pubmed/9665073

Swann, M. C., Hoes, K. S., Aoun, S. G., & McDonagh, D. L. (2016). Postoperative complications of spine surgery. *Best Pract Res Clin Anaesthesiol*, *30*(1), 103-120. https://doi.org/10.1016/j.bpa.2016.01.002

Swartz, K. R., & Trost, G. R. (2003). Recurrent lumbar disc herniation. *Neurosurg Focus*, *15*(3), E10. http://www.ncbi.nlm.nih.gov/pubmed/15347228

Takaishi, H., Nemoto, O., Shiota, M., Kikuchi, T., Yamada, H., Yamagishi, M., & Yabe, Y. (1997). Type-II collagen gene expression is transiently upregulated in experimentally induced degeneration of rabbit intervertebral disc. *J Orthop Res*, *15*(4), 528-538. https://doi.org/10.1002/jor.1100150408

Tapias, L. F., & Ott, H. C. (2014). Decellularized scaffolds as a platform for bioengineered organs. *Current opinion in organ transplantation*, *19*(2), 145-152. https://doi.org/10.1097/mot.0000000000000051

Tomaszewski, K. A., Saganiak, K., Gladysz, T., & Walocha, J. A. (2015). The biology behind the human intervertebral disc and its endplates. *Folia Morphol (Warsz)*, *74*(2), 157-168. https://doi.org/10.5603/FM.2015.0026

Tsuchiya, T., Sivarapatna, A., Rocco, K., Nanashima, A., Nagayasu, T., & Niklason, L. E. (2014). Future prospects for tissue engineered lung transplantation: decellularization and recellularization-based whole lung regeneration. *Organogenesis*, *10*(2), 196-207. https://doi.org/10.4161/org.27846

Urban, J. P., & Roberts, S. (2003). Degeneration of the intervertebral disc. *Arthritis research & therapy*, *5*(3), 120-130. http://www.ncbi.nlm.nih.gov/pubmed/12723977

Vadalà, G., Sowa, G., Hubert, M., Gilbertson, L. G., Denaro, V., & Kang, J. D. (2012). Mesenchymal stem cells injection in degenerated intervertebral disc: cell leakage may induce osteophyte formation. *J Tissue Eng Regen Med*, *6*(5), 348-355. https://doi.org/10.1002/term.433

van der Rest, M., & Garrone, R. (1991). Collagen family of proteins. *FASEB J*, *5*(13), 2814-2823. http://www.ncbi.nlm.nih.gov/pubmed/1916105

van Uden, S., Silva-Correia, J., Oliveira, J. M., & Reis, R. L. (2017). Current strategies for treatment of intervertebral disc degeneration: substitution and regeneration possibilities. *Biomater Res*, *21*, 22. https://doi.org/10.1186/s40824-017-0106-6

Vernengo, A. J., Grad, S., Eglin, D., Alini, M., & Li, Z. (2020). Bioprinting Tissue Analogues with Decellularized Extracellular Matrix Bioink for Regeneration and Tissue Models of Cartilage and Intervertebral Discs [https://doi.org/10.1002/adfm.201909044]. *Advanced Functional Materials*, *30*(44), 1909044. https://doi.org/https://doi.org/10.1002/adfm.201909044

Veruva, S. Y., Steinbeck, M. J., Toth, J., Alexander, D. D., & Kurtz, S. M. (2014). Which design and biomaterial factors affect clinical wear performance of total disc replacements? A systematic review. *Clin Orthop Relat Res*, *472*(12), 3759-3769. https://doi.org/10.1007/s11999-014-3751-2

Vos, T., Flaxman, A. D., Naghavi, M., Lozano, R., Michaud, C., Ezzati, M., Shibuya, K., Salomon, J. A., Abdalla, S., Aboyans, V., Abraham, J., Ackerman, I., Aggarwal, R., Ahn, S. Y., Ali, M. K., Alvarado, M., Anderson, H. R., Anderson, L. M., Andrews, K. G., Atkinson, C., Baddour, L. M., Bahalim, A. N., Barker-Collo, S., Barrero, L. H., Bartels, D. H., Basanez, M. G., Baxter, A., Bell, M. L., Benjamin, E. J., Bennett, D., Bernabe, E., Bhalla, K., Bhandari, B., Bikbov, B., Bin Abdulhak, A., Birbeck, G., Black, J. A., Blencowe, H., Blore, J. D., Blyth, F., Bolliger, I., Bonaventure, A., Boufous, S., Bourne, R., Boussinesq, M., Braithwaite, T., Brayne, C., Bridgett, L., Brooker, S., Brooks, P., Brugha, T. S., Bryan-Hancock, C., Bucello, C., Buchbinder, R., Buckle, G., Budke, C. M., Burch, M., Burney, P., Burstein, R., Calabria, B., Campbell, B., Canter, C. E., Carabin, H., Carapetis, J., Carmona, L., Cella, C.,

Charlson, F., Chen, H., Cheng, A. T., Chou, D., Chugh, S. S., Coffeng, L. E., Colan, S. D., Colquhoun, S., Colson, K. E., Condon, J., Connor, M. D., Cooper, L. T., Corriere, M., Cortinovis, M., de Vaccaro, K. C., Couser, W., Cowie, B. C., Criqui, M. H., Cross, M., Dabhadkar, K. C., Dahiya, M., Dahodwala, N., Damsere-Derry, J., Danaei, G., Davis, A., De Leo, D., Degenhardt, L., Dellavalle, R., Delossantos, A., Denenberg, J., Derrett, S., Des Jarlais, D. C., Dharmaratne, S. D., Dherani, M., Diaz-Torne, C., Dolk, H., Dorsey, E. R., Driscoll, T., Duber, H., Ebel, B., Edmond, K., Elbaz, A., Ali, S. E., Erskine, H., Erwin, P. J., Espindola, P., Ewoigbokhan, S. E., Farzadfar, F., Feigin, V., Felson, D. T., Ferrari, A., Ferri, C. P., Fevre, E. M., Finucane, M. M., Flaxman, S., Flood, L., Foreman, K., Forouzanfar, M. H., Fowkes, F. G., Franklin, R., Fransen, M., Freeman, M. K., Gabbe, B. J., Gabriel, S. E., Gakidou, E., Ganatra, H. A., Garcia, B., Gaspari, F., Gillum, R. F., Gmel, G., Gosselin, R., Grainger, R., Groeger, J., Guillemin, F., Gunnell, D., Gupta, R., Haagsma, J., Hagan, H., Halasa, Y. A., Hall, W., Haring, D., Haro, J. M., Harrison, J. E., Havmoeller, R., Hay, R. J., Higashi, H., Hill, C., Hoen, B., Hoffman, H., Hotez, P. J., Hoy, D., Huang, J. J., Ibeanusi, S. E., Jacobsen, K. H., James, S. L., Jarvis, D., Jasrasaria, R., Jayaraman, S., Johns, N., Jonas, J. B., Karthikeyan, G., Kassebaum, N., Kawakami, N., Keren, A., Khoo, J. P., King, C. H., Knowlton, L. M., Kobusingye, O., Koranteng, A., Krishnamurthi, R., Lalloo, R., Laslett, L. L., Lathlean, T., Leasher, J. L., Lee, Y. Y., Leigh, J., Lim, S. S., Limb, E., Lin, J. K., Lipnick, M., Lipshultz, S. E., Liu, W., Loane, M., Ohno, S. L., Lyons, R., Ma, J., Mabweijano, J., MacIntyre, M. F., Malekzadeh, R., Mallinger, L., Manivannan, S., Marcenes, W., March, L., Margolis, D. J., Marks, G. B., Marks, R., Matsumori, A., Matzopoulos, R., Mayosi, B. M., McAnulty, J. H., McDermott, M. M., McGill, N., McGrath, J., Medina-Mora, M. E., Meltzer, M., Mensah, G. A., Merriman, T. R., Meyer, A. C., Miglioli, V., Miller, M., Miller, T. R., Mitchell, P. B., Mocumbi, A. O., Moffitt, T. E., Mokdad, A. A., Monasta, L., Montico, M., Moradi-Lakeh, M., Moran, A., Morawska, L., Mori, R., Murdoch, M. E., Mwaniki, M. K., Naidoo, K., Nair, M. N., Naldi, L., Narayan, K. M., Nelson, P. K., Nelson, R. G., Nevitt, M. C., Newton, C. R., Nolte, S., Norman, P., Norman, R., O'Donnell, M., O'Hanlon, S., Olives, C., Omer, S. B., Ortblad, K., Osborne, R., Ozgediz, D., Page, A., Pahari, B., Pandian, J. D., Rivero, A. P., Patten, S. B., Pearce, N., Padilla, R. P., Perez-Ruiz, F., Perico, N., Pesudovs, K., Phillips, D., Phillips, M. R., Pierce, K., Pion, S., Polanczyk, G. V., Polinder, S., Pope, C. A., 3rd, Popova, S., Porrini, E., Pourmalek, F., Prince, M., Pullan, R. L., Ramaiah, K.

D., Ranganathan, D., Razavi, H., Regan, M., Rehm, J. T., Rein, D. B., Remuzzi, G., Richardson, K., Rivara, F. P., Roberts, T., Robinson, C., De Leon, F. R., Ronfani, L., Room, R., Rosenfeld, L. C., Rushton, L., Sacco, R. L., Saha, S., Sampson, U., Sanchez-Riera, L., Sanman, E., Schwebel, D. C., Scott, J. G., Segui-Gomez, M., Shahraz, S., Shepard, D. S., Shin, H., Shivakoti, R., Singh, D., Singh, G. M., Singh, J. A., Singleton, J., Sleet, D. A., Sliwa, K., Smith, E., Smith, J. L., Stapelberg, N. J., Steer, A., Steiner, T., Stolk, W. A., Stovner, L. J., Sudfeld, C., Syed, S., Tamburlini, G., Tavakkoli, M., Taylor, H. R., Taylor, J. A., Taylor, W. J., Thomas, B., Thomson, W. M., Thurston, G. D., Tleyjeh, I. M., Tonelli, M., Towbin, J. A., Truelsen, T., Tsilimbaris, M. K., Ubeda, C., Undurraga, E. A., van der Werf, M. J., van Os, J., Vavilala, M. S., Venketasubramanian, N., Wang, M., Wang, W., Watt, K., Weatherall, D. J., Weinstock, M. A., Weintraub, R., Weisskopf, M. G., Weissman, M. M., White, R. A., Whiteford, H., Wiersma, S. T., Wilkinson, J. D., Williams, H. C., Williams, S. R., Witt, E., Wolfe, F., Woolf, A. D., Wulf, S., Yeh, P. H., Zaidi, A. K., Zheng, Z. J., Zonies, D., Lopez, A. D., Murray, C. J., AlMazroa, M. A., & Memish, Z. A. (2012). Years lived with disability (YLDs) for 1160 sequelae of 289 diseases and injuries 1990-2010: a systematic analysis for the Global Burden of Disease Study 2010. *Lancet*, *380*(9859), 2163-2196. https://doi.org/10.1016/S0140-6736(12)61729-2

Wachs, R. A., Hoogenboezem, E. N., Huda, H. I., Xin, S., Porvasnik, S. L., & Schmidt, C. E. (2017). Creation of an injectable in situ gelling native extracellular matrix for nucleus pulposus tissue engineering. *Spine J*, *17*(3), 435-444. https://doi.org/10.1016/j.spinee.2016.10.022

Waddell, G. (1996). Low back pain: a twentieth century health care enigma. *Spine (Phila Pa 1976)*, *21*(24), 2820-2825. http://www.ncbi.nlm.nih.gov/pubmed/9112705

Walsh, A. J., Bradford, D. S., & Lotz, J. C. (2004). In vivo growth factor treatment of degenerated intervertebral discs. *Spine (Phila Pa 1976)*, *29*(2), 156-163. https://doi.org/10.1097/01.BRS.0000107231.67854.9F

Walter, B. A., Illien-Junger, S., Nasser, P. R., Hecht, A. C., & Iatridis, J. C. (2014). Development and validation of a bioreactor system for dynamic loading and mechanical characterization of whole human intervertebral discs in organ culture. *J Biomech*, *47*(9), 2095-2101. https://doi.org/10.1016/j.jbiomech.2014.03.015

Wang, F., Shi, R., Cai, F., Wang, Y. T., & Wu, X. T. (2015). Stem Cell Approaches to Intervertebral Disc Regeneration: Obstacles from the Disc Microenvironment. *Stem Cells Dev*, *24*(21), 2479-2495. https://doi.org/10.1089/scd.2015.0158

Warrington, R., Watson, W., Kim, H. L., & Antonetti, F. R. (2011). An introduction to immunology and immunopathology. *Allergy Asthma Clin Immunol*, *7 Suppl 1*, S1. https://doi.org/10.1186/1710-1492-7-S1-S1

Watanabe, T., Sakai, D., Yamamoto, Y., Iwashina, T., Serigano, K., Tamura, F., & Mochida, J. (2010). Human nucleus pulposus cells significantly enhanced biological properties in a coculture system with direct cell-to-cell contact with autologous mesenchymal stem cells. *J Orthop Res*, *28*(5), 623-630. https://doi.org/10.1002/jor.21036

Wei, A., Chung, S. A., Tao, H., Brisby, H., Lin, Z., Shen, B., Ma, D. D., & Diwan, A. D. (2009). Differentiation of rodent bone marrow mesenchymal stem cells into intervertebral disc-like cells following coculture with rat disc tissue. *Tissue engineering. Part A*, *15*(9), 2581-2595. https://doi.org/10.1089/ten.TEA.2008.0458

Whatley, B., & Wen, X. (2012). Intervertebral disc (IVD): Structure, degeneration, repair and regeneration. *Mater Sci Eng C 32*, 61-77. https://doi.org/10.1016/j.msec.2011.10.011

White, A. A., & Panjabi, M. M. (1990). *Clinical biomechanics of the spine*. Lippincott Williams & Wilkins.

White, L. J., Keane, T. J., Smoulder, A., Zhang, L., Castleton, A. A., Reing, J. E., Turner, N. J., Dearth, C. L., & Badylak, S. F. (2018). The impact of sterilization upon extracellular matrix hydrogel structure and function. *Journal of Immunology and Regenerative Medicine*, *2*, 11-20. https://doi.org/https://doi.org/10.1016/j.regen.2018.04.001

White, L. J., Taylor, A. J., Faulk, D. M., Keane, T. J., Saldin, L. T., Reing, J. E., Swinehart, I. T., Turner, N. J., Ratner, B. D., & Badylak, S. F. (2017). The impact of detergents on the tissue decellularization process: A ToF-SIMS study. *Acta biomaterialia*, *50*, 207-219. https://doi.org/10.1016/j.actbio.2016.12.033

Wu, L. C., Chiang, C. J., Liu, Z. H., Tsuang, Y. H., Sun, J. S., & Huang, Y. Y. (2014). Fabrication and properties of acellular porcine anulus fibrosus for tissue engineering in spine surgery. *J Orthop Surg Res*, *9*, 118. https://doi.org/10.1186/s13018-014-0118-z

Wu, L. C., Kuo, Y. J., Sun, F. W., Chen, C. H., Chiang, C. J., Weng, P. W., Tsuang, Y. H., & Huang, Y. Y. (2017). Optimized decellularization protocol including alpha-Gal epitope reduction for fabrication of an acellular porcine annulus fibrosus scaffold. *Cell Tissue Bank*, *18*(3), 383-396. https://doi.org/10.1007/s10561-017-9619-4

Xu, H., Xu, B., Yang, Q., Li, X., Ma, X., Xia, Q., Zhang, Y., Zhang, C., Wu, Y., & Zhang, Y. (2014). Comparison of decellularization protocols for preparing a decellularized porcine annulus fibrosus scaffold. *PLOS ONE*, *9*(1), e86723. https://doi.org/10.1371/journal.pone.0086723

Xu, J., Liu, S., Wang, S., Qiu, P., Chen, P., Lin, X., & Fang, X. (2019). Decellularised nucleus pulposus as a potential biologic scaffold for disc tissue engineering. *Materials Science and Engineering: C*, *99*, 1213-1225. https://doi.org/https://doi.org/10.1016/j.msec.2019.02.045

Yang, S. H., Wu, C. C., Shih, T. T., Sun, Y. H., & Lin, F. H. (2008). In vitro study on interaction between human nucleus pulposus cells and mesenchymal stem cells through paracrine stimulation. *Spine (Phila Pa 1976)*, *33*(18), 1951-1957. https://doi.org/10.1097/BRS.0b013e31817e6974

Yu, L., Sun, Z. J., Tan, Q. C., Wang, S., Wang, W. H., Yang, X. Q., & Ye, X. J. (2020). Thermosensitive injectable decellularized nucleus pulposus hydrogel as an ideal biomaterial for nucleus pulposus regeneration. *J Biomater Appl*, *35*(2), 182-192. https://doi.org/10.1177/0885328220921328

Yuan, M., Pai, P.-J., Liu, X., Lam, H., & Chan, B. P. (2018). Proteomic Analysis of Nucleus Pulposus Cell-derived Extracellular Matrix Niche and Its Effect on Phenotypic Alteration of Dermal Fibroblasts. *Scientific Reports*, *8*(1), 1512. https://doi.org/10.1038/s41598-018-19931-9

Yuan, M., Yeung, C. W., Li, Y. Y., Diao, H., Cheung, K. M., Chan, D., Cheah, K., & Chan, P. B. (2013). Effects of nucleus pulposus cell-derived acellular matrix on the differentiation of mesenchymal stem cells. *Biomaterials*, *34*(16), 3948-3961. https://doi.org/10.1016/j.biomaterials.2013.02.004

Yue, B., Lin, Y., Ma, X., Xiang, H., Qiu, C., Zhang, J., Li, L., & Chen, B. (2016). Survivin-TGFB3-TIMP1 Gene Therapy Via Lentivirus Vector Slows the Course of Intervertebral Disc Degeneration in an In Vivo Rabbit Model. *Spine (Phila Pa 1976)*, *41*(11), 926-934. https://doi.org/10.1097/BRS.0000000000001474

Zhang, Y. G., Guo, X., Xu, P., Kang, L. L., & Li, J. (2005). Bone mesenchymal stem cells transplanted into rabbit intervertebral discs can increase proteoglycans. *Clin Orthop Relat Res*(430), 219-226. https://doi.org/10.1097/01.blo.0000146534.31120.cf

Zheng, M. H., Chen, J., Kirilak, Y., Willers, C., Xu, J., & Wood, D. (2005). Porcine small intestine submucosa (SIS) is not an acellular collagenous matrix and contains porcine DNA: possible implications in human implantation. *J Biomed Mater Res B Appl Biomater*, *73*(1), 61-67. https://doi.org/10.1002/jbm.b.30170

Zhou, X., Wang, J., Huang, X., Fang, W., Tao, Y., Zhao, T., Liang, C., Hua, J., Chen, Q., & Li, F. (2018). Injectable decellularized nucleus pulposus-based cell delivery system for differentiation of adipose-derived stem cells and nucleus pulposus regeneration. *Acta biomaterialia*. https://doi.org/10.1016/j.actbio.2018.09.044

CHAPTER III

CHAPTER III – AIM OF THE THESIS

AIM OF THE THESIS

The vision driving this work was that the recapitulation of a pro-regenerative microenvironment, by using fetal-derived biomaterials, will induce endogenous repair of intervertebral disc (IVD). So, the hypothesis behind this thesis was that fetal decellularized nucleus pulposus (NP) extracellular matrix (ECM) would have a superior potential for IVD regeneration.

This hypothesis was based on the advances from recent years, in which regenerative medicine and tissue engineering approaches, based on decellularized ECM, have been emerging. However, ECM donor age can have a dramatic impact in tissue repair/regeneration, as observed in rhesus monkey kidneys, rat abdominal wall muscle, rodent cardiac muscle, rat peripheral nerves and rabbit bladder submucosa, for which fetal and neonatal ECM have shown a superior pro-regenerative capacity, when compared to adult donors. In the disc field, our group has previously demonstrated that matrix signature of fetal bovine NP is dramatically different from adult and old ones, including the presence of two proteins, Collagen (COL) type 12 and COL14, exclusively in fetal NPs. These two proteins have been described to have a pro-regenerative role in other tissues.

Therefore, to address the hypothesis behind, the present work was divided into three main objectives:

1. Development of an optimal decellularization protocol to obtain acellular fetal bovine NPs. Bovine NPs from different donor ages (fetus, young and old) were decellularized by using an optimal protocol with reduced detergent concentration and decreased exposure time (SDS 0.1 %, 1 h). The efficiency of the process was evaluated in terms of cells and DNA removal, as well as, ECM preservation. NPs from different ages, decellularized with the optimal protocol, were further characterized at structural, biochemical and biomechanical levels.

2. Explore the regenerative potential of fetal decellularized ECM. NP cells were isolated from adult bovine IVDs and seeded on the top of decellularized matrices from different donor ages. After 7 days of *ex vivo* culture, NP cell behavior and scaffolds cytocompatibility were analyzed. Cell response to the different microenvironments was evaluated in terms of cell viability, metabolic activity and cytotoxicity. Moreover, ECM *de novo* synthesis and remodeling was also explored at molecular and protein levels. Finally,

the angiogenic potential of decellularized matrices was assessed through an *in vivo* chick embryo chorioallantoic membrane (CAM) assay by quantification of the new vessels growing towards the scaffolds' inoculation site.

Task 1 and 2 are addressed in the Chapter IV of this thesis.

3. Disclose the mechanism behind the enhanced IVD regenerative potential of fetal decellularized matrices. To dissect the mechanism behind ECM production in fetal decellularized NPs after repopulation, a CD44-blocking experiment was performed. Specifically, CD44 was neutralized in adult bovine NP cells, prior to cell seeding in fetal decellularized NPs, by using a specific blocking antibody. After 7 days of *ex vivo* culture, Hematoxylin&Eosin (H&E) staining, Sox9 and Aggrecan (ACAN) immunohistochemistry (IHC) were conducted. Next, angiogenic and inflammatory cytokines levels were explored in the conditioned media derived from decellularized NPs of different donor ages, to unravel the mechanism behind the pro-inflammatory and anti-angiogenic potential of fetal NPs, by using a semi-quantitative array kit. Finally, a first *in vivo* proof of concept of the anti-angiogenic capacity of fetal decellularized matrices repopulated with human immortalized NP (iNP) cells, was also delivered, by performing an *in vivo* CAM assay. Next, inflammatory and blood cells infiltration within the scaffolds was evaluated by H&E, while glycosaminoglycans (GAGs) production by seeded iNP cells, by Picro-Sirius Red/Alcian Blue staining.

Task 3 is addressed in the Chapter VI of this thesis.

Overall, this work uncovered the importance of donor age in tissue regeneration, opening new avenues for the development of appropriate therapeutic strategies for IVD degeneration and the consequent LBP, through the use of fetal pro-regenerative ECM based-scaffolds. Moreover, a first *in vivo* proof-of-concept of the superior potential of fetal matrices to decrease the angiogenic response of human cells was also addressed, thus demonstrating their capacity to mimic a healthy IVD microenvironment.

Finally, the work presented here opened new perspectives for the development of suitable 3D models to dissect age-associated features of disc degeneration, by using older decellularized matrices.

CHAPTER IV

CHAPTER IV – ARTICLE III

THE IMPACT OF MATRIX AGE ON INTERVERTEBRAL DISC REGENERATION

Published in Biomaterial Advances

doi: 10.1016/j.bioadv.2022.213192

The impact of matrix age on intervertebral disc regeneration

Morena Francesca Fiordalisi[a,b,c,], Joana Rita Ferreira[a,b,c], Marta Laranjeiro Pinto[d], Cláudia Ribeiro-Machado[a,b], Marta Teixeira Pinto[a,e], Maria José Oliveira[a,b,c,f], Mário Adolfo Barbosa[a,b,c], Raquel Madeira Gonçalves[a,b,c,1], Joana Caldeira[a,b,1]

[a]*i3S – Instituto de Investigação e Inovação em Saúde, Universidade do Porto, Porto 4200-135, Portugal*

[b]*INEB – Instituto de Engenharia Biomédica, Porto 4200-135, Portugal*

[c]*ICBAS - Instituto de Ciências Biomédicas Abel Salazar, Universidade do Porto, Porto 4050-313, Portugal*

[d]*CNC - Center for Neuroscience and Cell Biology, University of Coimbra, Coimbra 3004–504, Portugal*

[e]*IPATIMUP - Instituto de Patologia e Imunologia Molecular da Universidade do Porto, Porto 4200-135, Portugal*

[f]*Department of Pathology and Oncology, Faculty of Medicine, University of Porto, Porto 4200-319, Portugal*

[1]Equal contribution

ABSTRACT

With the lack of effective treatments for low back pain, the use of extracellular matrix (ECM)-based biomaterials have emerged with undeniable promise for intervertebral disc (IVD) regeneration. Decellularized scaffolds can recreate an ideal microenvironment inducing tissue remodeling and repair. In particular, fetal tissues have a superior regenerative capacity given their ECM composition. In line with this, we unraveled age-associated alterations of the nucleus pulposus (NP) matrisome. Thus, the aim of the present work was to evaluate the impact of ECM donor age on IVD de/regeneration.

Accordingly, we optimized an SDS (0.1 %, 1 h)-based decellularization protocol that preserves ECM cues in bovine NPs from different ages. After repopulation with adult NP cells, younger matrices showed the highest repopulation efficiency. Most importantly, cells seeded on younger scaffolds produced healthy ECM proteins suggesting an increased capacity to restore a functional IVD microenvironment. *In vivo*, only fetal matrices decreased neovessel formation, showing an anti-angiogenic potential.

Our findings demonstrate that ECM donor age has a strong influence on angiogenesis and ECM *de novo* synthesis, opening new avenues for novel therapeutic strategies for the IVD. Additionally, more appropriate 3D models to study age-associated IVD pathology were unveiled.

Keywords: IVD degeneration/regeneration, decellularization, ageing, tissue engineering, 3D models

1. INTRODUCTION

Low back pain (LBP) is the leader of musculoskeletal disorders in modern societies (Wu et al., 2020) affecting nearly 80% of the world population (Fatoye et al., 2019) and ranking first in terms of years lived with disability (Chen et al., 2022), in front of other conditions like lung cancer and road accidents, among others. Although many conditions (*e.g.*, genetic predisposition, obesity, smoking, physical workload) can contribute to the onset of LBP (Shiri et al., 2019; Urban & Fairbank, 2020), age-associated intervertebral disc (IVD) degeneration is the most prevalent cause.

IVDs are the largest avascular and aneural tissues in the human body (McCann & Séguin, 2016). They provide indispensable strength to support body weight and elasticity, allowing spine movements in different directions (flexion, extension and rotation) (Tomaszewski et al., 2015). With ageing, the IVD undergoes a physiological degenerative process (Dowdell et al., 2017), as a consequence of several alterations at the morphological, cellular and biochemical level (Fiordalisi et al., 2021). These modifications lead to structural and biomechanical tissue failure. Although disc degeneration is more frequent in adulthood, changes in the nucleus pulposus (NP), the inner part of IVD tissue, can be already observed after birth (Smith et al., 2011). Besides the changes in cellular composition of NP with age (Colombier et al., 2014), alterations in matrix composition can also be observed along ageing, with NP replacement of collagen type 2 (COL2) by collagen type 1 (COL1) (Colombier et al., 2014) and proteoglycan (PG) breakdown (Anderson & Tannoury, 2005). Extracellular matrix (ECM) disruption occurs as a consequence of matrix-degrading enzymes as metalloproteinases (MMPs) or desintegrin and MMP with thrombospondin motifs (ADAMTS) (Colombier et al., 2014; Vo et al., 2013).

Current treatments for IVD degeneration and the consequent LBP include palliative care (Woods et al., 2010) and invasive surgical procedures that carry several risks. In addition, none of these treatments is able to regenerate the IVD and restore native tissue function. Therefore, novel and effective strategies to treat LBP are needed.

In the last decades, tissue engineering-based solutions have been developed for IVD regeneration making use of several biomaterials including natural and synthetic hydrogels or scaffolds (Schutgens et al., 2015). Natural biomaterials provide a more appropriate microenvironment for cell crosstalk and tissue regeneration, being safer and more biocompatible than synthetic ones (Schutgens et al., 2015), despite failing to restore

disc mechanical and physical properties (van Uden et al., 2017). On the other hand, synthetic scaffolds can be chemically synthesized in large quantities and their properties modified for specific applications, but they have decreased biocompatibility (Schutgens et al., 2015).

Decellularized ECM-based biomaterials have recently emerged as therapeutic tools in many fields of study, including that of the IVD. Decellularization represents a promising method to obtain natural ECM-based scaffolds, by removing host cells and DNA, while maintaining structural, biochemical and biomechanical cues of native tissue (Gilpin & Yang, 2017). These naturally–derived biomaterials represent a promising strategy to mimic an healthy microenvironment (Gilpin & Yang, 2017). Moreover, cell removal by decellularization agents is enough to decrease the immunogenic potential of ECM-based scaffolds, thus reducing the probability of host rejection after implantation (Taylor et al., 2020). Due to the regenerative potential of such scaffolds, several researchers have optimized protocols specifically for the IVD. They consist in a combination of chemical, enzymatic and mechanical methods, ultimately creating a natural biomaterial suitable for clinical applications (Fiordalisi et al., 2020).

Despite the clear promise of this approach, tissue donor age can have a significant impact on scaffold biomechanics and composition (Cramer & Badylak, 2019). In particular, fetal and neonatal matrices have shown a superior regenerative potential when compared to adult tissues, as demonstrated in different organs (*e.g*. rhesus monkey kidneys (Nakayama et al., 2011), rat abdominal wall muscle (Sicari et al., 2012), rodent cardiac muscle (Silva et al., 2016), rat peripheral nerves (Ren et al., 2018) and rabbit bladder submucosa (Kajbafzadeh et al., 2018)). Our group has contributed to the field by dissecting the matrisome profile of bovine NP ECM from different aged donors (fetus, young and old IVDs), revealing alterations in ECM composition with development and ageing (Caldeira et al., 2017). In particular, we have demonstrated that fetal NP ECM is enriched in Collagen type 12 (COL12) and Collagen type 14 (COL14). These two molecules with a pro-regenerative role in other tissues (Marro et al., 2016; Nauroy et al., 2019; Schönborn et al., 2020; Wehner et al., 2017), are lost in adult and old IVDs (Caldeira et al., 2017). Given the importance of donor age for tissue regeneration, we hypothesized that the previously identified alterations associated with ECM ageing could strongly impact on IVD de/regeneration.

Herein, we optimized a decellularization protocol with reduced detergent amounts and short exposure time that can be effectively and transversally applied to bovine NPs

from different aged donors. To investigate the impact of ECM ageing on cell response and ultimately on IVD regenerative capacity, adult bovine NP cells were cultured on decellularized NP–based scaffolds from different aged donors and cell behavior was dissected. Moreover, an *in vivo* proof of concept of the anti-angiogenic potential of the above mentioned scaffolds was performed using the chick embryo chorioallantoic membrane (CAM) assay. The use of old-derived scaffolds to mimic disc degeneration was also explored to interrogate their capacity to model vessel ingrowth, cell death and ECM remodeling, prototypical of age-associated IVD degeneration.

The findings obtained provide new insights on the importance of ECM donor age and the associated microenvironmental cues on restoring an healthy and functional IVD, particularly focusing on the potential for ECM *de novo* synthesis and for angiogenesis suppression. In addition, the results will shed new light on the need for choosing wisely donor age when modeling age-associated disc degeneration. These discoveries, of utmost importance for the field of matrix engineering, developmental biology and biology of ageing, will certainly impact the development of next-generation materials for tissue regeneration.

2. MATERIALS AND METHODS

2.1. INTERVERTEBRAL DISC HARVEST

Fetal (~8 months of gestation), young (~1 year old) and old (~12 years old) bovine tails were obtained from local abattoirs (Carnes Landeiro, Barcelos, Portugal) within 2 h of animal sacrifice, under the approval of the Portuguese National Authority for Animal Health, and transported at the lab on ice. Bovine tails were disinfected with ethanol 70 % and dissected in sterile conditions, as previously described (Teixeira et al., 2016). Briefly, following skin, muscle and ligaments removal, caudal IVDs were isolated by dissecting as close as possible to the upper and lower cartilaginous endplates from each tail. After isolation, fresh IVDs were placed in plastic containers and covered with optimal cutting temperature compound (OCT, Kaltek srl), to protect the tissue from damage caused during the freezing process (tissue frozen dry at -80 °C resulted in sparser collagen network after unfreezing when compared to -80 °C in combination with OCT; Supplementary Figure 1), frozen in 2-methylbutane cooled with liquid nitrogen and stored at -80 °C until further analysis, as previously reported (Pinto et al., 2017; Silva et al., 2016).

2.2. OPTIMIZATION OF NUCLEUS PULPOSUS DECELLULARIZATION

Fetus, young and old IVDs were thawed at room temperature and washed in Phosphate-buffered saline (PBS), in order to remove the excess of OCT. NPs were isolated from the central zone of IVDs by the help of surgical punches of 4 mm (Kai medical). Samples were cut in similar height, weighted and placed in PBS. Fresh NPs from fetus, young and old bovine IVDs were used as native controls. NPs for decellularization were incubated in Hypotonic buffer A (10 mM Tris, 0.1 % EDTA, pH 7.8) for 18 h and washed three times in PBS (1 h/each). Afterwards, samples were placed in the detergent solutions, prepared in Hypotonic Buffer B (10 mM Tris, pH 7.8). Several detergents were tested at different time points and concentrations (sodium dodecyl sulphate [SDS] 0.1 % for 1 h, 3 h and 24 h; SDS 0.5 % for 24 h; Triton 0.6 % 24 h and Triton 1.2 % 24 h) in order to optimize the procedure. Following detergent treatments, NPs were washed three times in Hypotonic Buffer B (20 min/each) and incubate in DNAse solution (20 mM Tris and 2 mM $MgCl_2$, pH 7.8), supplemented with 50 U/mL DNAse I (WVR) for 3 h at 37 °C. Finally, samples were washed three times in PBS (20 min/each) to remove residual detergents and processed for

subsequent analysis (Benedetto et al., 2014; Pinto et al., 2017; Silva et al., 2016). Tissue decellularization was performed under constant agitation (165 rpm) and at room temperature (except for DNAse treatment). All solutions were supplemented with 1 % Penicillin/Streptomycin (P/S) (Invitrogen), 0.5 % Amphotericin B (Capricorn Scientific) and 0.1 % Gentamicin (Gibco) to avoid contaminations.

Native and decellularized samples were frozen dry at -80 °C to be used for DNA and glycosaminoglycans (GAGs) quantification, while samples for histological analysis were fixed in 10 % neutral buffered-formalin (Bio-Optica) overnight at 4 °C.

2.3. DNA QUANTIFICATION

DNA was isolated from decellularized and native NPs by using PureLink Genomic DNA mini kit (Invitrogen), following the manufacturer's instructions. Briefly, samples were cut in small pieces and digested in PureLink Genomic Digestion Buffer and Proteinase K for 4 h at 55 °C with occasional vortexing. After lysate preparation and RNA removal, DNA was purified through a spin column - based centrifugation protocol. Following extraction, DNA quantification was performed by adopting a Quant-iT™ PicoGreen® dsDNA kit (Invitrogen), according to the manufacturer's instructions. The fluorescence was measured at 480 nm of excitation and 520 nm of emission at Synergy™ Mx multi-mode microplate reader (BioTek). Samples were run in duplicate and a blank was included as a reference for the analysis. A high and low range standard curve was used to calculate DNA concentration of samples. Finally, DNA content was normalized by wet weight (mg) and data were expressed as ng DNA/mg wet weight.

2.4. GLYCOSAMINOGLYCAN QUANTIFICATION

Sulfated GAGs (sGAGs) content was quantified in decellularized and native NPs by Blyscan Sulfate GAGs Assay (biocolor). Briefly, tissues were cut in small pieces and placed in Papain Extraction Reagent (0.1 M sodium acetate, 0.01 M EDTA disodium salt, 0.005 M cysteine HCl), supplemented by papain crystallized suspension (Sigma-Aldrich) and incubated overnight at 65 °C, with occasionally vortexing. After digestion, sGAGs content was quantified by quantitative dye-binding method, following the manufacturer's instructions. The absorbance was measured at 656 nm at the Synergy™ Mx multi-mode microplate reader (BioTek). Deionized water was included as reference as well as a blank

sample. A standard curve was used to calculate sGAGs concentration of the samples. sGAGs content was normalized by wet weight (mg) and data were expressed as µg sGAGs/mg wet weight.

2.5. COLLAGEN QUANTIFICATION

Decellularized NPs were cut in small pieces and digested overnight at 4 °C, under mechanical digestion, in a solution of 0.5 M acetic acid supplemented with 0.1 mg/mL of Pepsin (Sigma-Aldrich). Afterwards, samples were centrifuged at 3000 g for 10 min in order to remove residual matrix. Supernatants were used for the quantification of soluble collagen (COL) by using Sircol Soluble Collagen Assay (biocolor), following the manufacturer's instructions. Absorbance was measured at 556 nm using the Synergy™ Mx multi-mode microplate reader (BioTek). Deionized water was included as reference as well as a blank sample. A standard curve was used to calculate COL concentration in the samples. COL content was normalized by wet weight (mg) and data were expressed as µg COL/mg wet weight.

2.6. HISTOLOGICAL EVALUATION

After fixation in 10 % neutral buffered-formalin (Bio-Optica) overnight, native and decellularized NPs were transferred to PBS and further processed for paraffin embedding. Sections of 5 µm were obtained and stained for Alcian Blue/Picro-Sirius Red. Briefly, sections were dewaxed and stained with Gill's Hematoxylin (Thermo Fisher Scientific) for 3 min, stained with Alcian Blue for 30 min, followed by an incubation in Picro-Sirius Red solution for 1 h and washed with Acidified water (0.01 N HCl). Finally, sections were dehydrated and mounted with Entellan (Merck).

2.7. CRYO-SCANNING ELECTRON MICROSCOPY

Cryo-scanning electron microscopy (Cryo-SEM) analysis of native and decellularized NPs was performed at Materials Centre of the University of Porto (CEMUP) by a high-resolution Scanning Electron Microscope with X-Ray Microanalysis and Cryo-SEM facilities (JEOL JSM 6301F/ Oxford INCA Energy 350/ Gatan Alto 2500). Briefly, NPs were rapidly cooled with liquid nitrogen and placed to the cold stage of the preparation

chamber under vacuum. Afterwards, samples were fractured, sublimated for 120 s at 90 °C and sputtered-coated with Au/Pd for 40 s. The samples were transferred to the scanning electron microscopy chamber and analyzed at -150 °C at 1000x and 5000x magnification. Number of pores and mean pore area parameter were quantified by DiameterJ, a plug in of ImageJ/Fiji software (Caldeira et al., 2017).

2.8. WESTERN BLOT ANALYSIS

Native and decellularized NPs were cut in small pieces and digested in Guanidine Extraction Buffer (4 M Guanidine HCl, 10 mM EDTA, 50 mM Sodium acetate), supplemented with Dithiothreitol (DTT), 1 mM PMSF and Proteases Inhibitor (Roche Diagnostic GmbH) overnight at 4 °C with agitation. Young and fetus native NPs were used as negative and positive controls, respectively. After centrifugation at 13.200 rpm, 4 °C for 20 min to remove any remaining ECM, supernatants were recovered and precipitated in absolute ethanol for 2 h at -20 °C. Finally, protein pellet was resuspended in sample buffer (7 M Ureia, 2 M Tioureia, 2 % CHAPS 3-[(3-cholamidopropyl)dimethylammonio]-1-propanesulfonate) and stored at -20 °C until protein quantification by using 2D Quant Kit (GE Healthcare), following the manufacturer's instructions.

Protein samples were denaturated for 10 min at 65 °C and separated by SDS-polyacrilamide gel electrophoresis (PAGE), by using 9 % polyacrylamide gels. Afterwards, samples were transferred to nitrocellulose membranes (GE Healthcare), and stained with Ponceau to confirm successful transfer. Following membranes blocking with a solution of 5 % milk in PBS with 5 % Tween for 1 h, incubation with optimal diluted antibodies for COL12 (anti-COL12 primary antibody was offered by Dr. Nick Morris; dilution:1:9) and COL14 (anti-COL14 primary antibody was offered by Dr. Nick Morris; dilution: 1:3) was performed overnight at 4 °C under agitation, as previously optimized (Caldeira et al., 2017). Finally, membranes were incubated with a secondary antibody (1:1000) for 1 hour at room temperature and an ECL chemiluminescent substrate (GE Healthcare) was used to reveal protein bands through X-ray film exposure.

After ECL detection and scanning of X-ray films by GS-800 densitometer (Bio-Rad), bands were quantified by using Quantity One 4.6.8 Software (Bio-Rad) and normalized to the total protein loading (density protein of interest/density of total protein loaded obtained by Page Blue staining), as previously described (Caldeira et al., 2017). For quantification,

background density value (measured in different area of the membrane) was subtracted from the protein density of each sample.

2.9. RHEOLOGICAL ANALYSIS

Rheological analysis of native and decellularized NPs was performed by using Kinexus Pro rheometer. Four NPs were isolated from the same IVD and a total of three biological replicates were used for the assay. The viscoelastic properties of native tissues were measured by evaluating the amplitude strain sweep and frequency sweep in the same sample and at the same moment. For amplitude strain sweep, a range between 0.10 % to 10 % of shear strain was chosen, while maintaining a constant frequency of 0.2 Hz. For frequency sweep, a range of 0.01 Hz to 30 Hz was chosen, while fixing the shear strain at 5 %.

Before the analysis, samples' height was measured by the help of a digital caliber and the 75 % of the total height was used to determine an accurate gap. The assay was performed at 37 °C in humidified conditions and by using a top geometry of 8 mm. After rheology, native samples were decellularized with the optimal protocol and placed in PBS at 4 °C, overnight. The day after, the viscoelastic properties of decellularized samples were measured as for the native ones. For data analysis, complex shear modulus (G*), were retrieved from the linear viscoelastic region (LVR: 0.04 Hz – 1 Hz) of frequency strain sweep and at 5 % of strain, fixed through LVR of amplitude strain sweep.

2.10. ISOLATION OF BOVINE NUCLEUS PULPOSUS CELLS

Fresh young bovine tails were dissected and NPs were isolated, weighted and kept hydrated in Dulbecco's modified Eagle's medium (DMEM, Gibco) with low glucose supplemented with 5 % *v/v* P/S (Invitrogen) and 10 % *v/v* Amphotericin B (Capricorn Scientific). The NPs were cut in small pieces and digested in DMEM low glucose (Gibco), supplemented with 5 % *v/v* of P/S (Invitrogen), 10 % *v/v* of Amphotericin B (Capricorn Scientific), 2.5 % *v/v* Hepes Buffer (1 M, Lonza), 1.2 % *v/v* of 5 M NaCl/0.4 M KCl solution in order to adjust the osmolarity to 400 mOsm and mimic the IVD physiological conditions, 1.3 µL/mL of DNAse (Promega) and 0.5 mg/mL of Collagenase type IA (Sigma-Aldrich), as previously optimized (M. Molinos et al., 2015). Tissue digestion was performed overnight at 37 °C in humidified and hypoxia environment (5 % O_2 and 8.5 % CO_2) under gentle agitation.

The 10 % of tissue/medium ratio was considered to avoid medium pH dropping below 6.8 during digestion (M. Molinos et al., 2015). After, cell suspension was filtered through a cell strainer to remove any remaining pieces of undigested ECM and centrifuged at 400 g for 15 min to obtain a single and clear cell suspension. Finally, cells were re-suspended in fresh DMEM (Gibco) with low glucose, supplemented with 1 % *v/v* of P/S (Invitrogen), 0.5 % *v/v* of Amphotericin B (Capricorn Scientific), 1.5 % *v/v* of 5 M NaCl/0.4 M KCl solution, 5 % *v/v* of fetal bovine serum (FBS, Biowest), counted and used for the repopulation of decellularized NPs from different ages.

2.11. REPOPULATION OF DECELLULARIZED NPS WITH ADULT BOVINE NP CELLS

Prior to cell seeding, fetus, young and old decellularized NPs were pre-incubated overnight at 37 °C in IVD-culture medium, composed by DMEM (Gibco) with low glucose, supplemented with 1 % *v/v* of P/S (Invitrogen), 0.5 % *v/v* of Amphotericin B (Capricorn Scientific), 1.5 % *v/v* of 5 M NaCl/0.4 M KCl solution, 5 % *v/v* of FBS (Biowest), under humidified and hypoxia conditions (5 % O_2 and 8.5 % CO_2) in order to equilibrate the matrices and facilitate cells penetration. After, decellularized NPs were transferred to a 96-well plate 2-hydroxyethyl methacrylate-coated (polyHEMA, Sigma-Aldrich), to ensure cells adhesion only on the tissue.

For repopulation, adult bovine NP cells were seeded on the decellularized scaffolds by adopting a scaffold turnover method, as already described elsewhere (Xu et al., 2014), to improve cells adhesion and migration. Briefly, 5 µL cells suspension, containing around $5x10^4$ NP cells, was seeded on the top of decellularized NPs by drop-wise addition on the surface of the scaffolds and incubated for 2 h at 37 °C, without medium, under humidified and hypoxia conditions (5 % O_2 and 8.5 % CO_2).

Afterwards, decellularized NPs were turned and another 5 µL cell suspension, containing $5x10^4$ NP cells, was seeded on the other side of the scaffolds and incubated for other 2 h, under the same conditions of the first seeding. Finally, 200 µL of culture medium was added and repopulated NPs were cultured *ex vivo* for 7 days. Media was changed at days 1, 3 and 6 of culture and stored at -80 °C for further analysis.

Decellularized NPs without cells seeding, as well as native bovine IVD organ culture (previously described (Teixeira et al., 2016)), were also maintained in culture for 7 days, under the same conditions of repopulated NPs, and used as controls for the analysis.

2.12. ASSESSMENT OF CELL REPOPULATION EFFICIENCY

Cell repopulation efficiency was assessed by quantification of DNA content, cell metabolic activity, cell viability and histological analysis. DNA content from repopulated NPs scaffolds was analyzed after 24 h of cell seeding upon extraction using PureLink Genomic DNA mini kit (Invitrogen), following the manufacturer's instructions and quantification by Quant-iT™ PicoGreen® dsDNA kit (Invitrogen). Metabolic activity of repopulated NP scaffolds was measured at days 1, 3 and 6 of *ex vivo* culture by resazurin sodium salt assay. After removing the medium, samples were incubated with 10 % of Resazurin solution (Sigma-Aldrich Co.), diluted in DMEM (Gibco) with low glucose, supplemented with 1 % *v/v* of P/S (Invitrogen), 0.5 % *v/v* of Amphotericin B (Capricorn Scientific), 1.5 % *v/v* of 5 M NaCl/0.4 M KCl solution, 5 % *v/v* of FBS (Biowest), for 4 h at 37°C, under humidified and hypoxia conditions (5 % O_2 and 8.5 % CO_2). A blank was included in the analysis. Afterwards, Resazurin solution was transferred to a black well plate and Relative Fluorescence unit (RFU) was measured at excitation 530 nm and emission 590 nm by using Synergy™ Mx multi-mode microplate reader (BioTek). Finally, samples were washed gently with PBS and incubated in fresh medium to proceed with *ex vivo* culture.

For cell viability of *ex vivo* culture repopulated NP scaffolds, Live/Dead staining was performed at day 7. Scaffolds were washed gently with PBS and incubated with a solution of calcein (dilution 1:500; Thermo Fisher Scientific) and Hoestch (dilution 1:1000), prepared in PBS, for 20 min at 37 °C, under humified and hypoxic conditions (5 % O_2 and 8.5 % CO_2). Then, samples were transferred to a petri dish and a solution of propidium iodide (dilution 1:500, Sigma- Aldrich) was added. Finally, NPs were imaged at the confocal microscope (TCS, SP5, Leica Microsystems) using a 10x magnification. At day 7 of *ex vivo* culture, repopulated NPs were processed for histological analysis following the procedure previously described in 2.6. Sections stained with Alcian Blue/Picro-Sirius Red were documented using a 20x objective, while sections stained with Hematoxylin & Eosin (H&E) were imaged at 20x and 40x magnifications.

2.13. CYTOTOXICITY EVALUATION OF REPOPULATED NP SCAFFOLDS

Cytotoxicity analysis of repopulated and control NP scaffolds was performed by measuring the LDH release in sample's conditioned media, collected at days 1, 3 and 6 of *ex vivo* culture. CytoTox 96® Non-Radioactive Cytotoxicity Assay (Promega) was used to perform the analysis, following the manufacturer's instructions. Briefly, conditioned media

was thawed and 50 µL of each sample was transferred to a well plate. Following addition of CytoTox 96® Reagent, the plate was incubated for 30 min at room temperature and protected from light. Stop solution was transferred to each well and absorbance was read at 490 nm through Synergy™ Mx multi-mode microplate reader (BioTek). A positive control, provided by the kit, was included in the analysis as well as a blank sample. For calculation, blank absorbance value was subtracted to the absorbance of each sample and the percentage of cytotoxicity was calculated and normalized by the positive control. Finally, data were normalized by decellularized NPs at the correspondent time point and presented as relative LDH release.

2.14. RNA EXTRACTION AND CDNA SYNTHESIS FOR QUANTITATIVE REAL-TIME REVERSE TRANSCRIPTION–POLYMERASE CHAIN REACTION

At day 7 of *ex vivo* culture, repopulated NP scaffolds and IVD organ culture were washed gently with cold PBS and RNA was extracted as previously described (Ferreira et al., 2021). Briefly, samples were cut in small pieces and digested in DMEM (Gibco), supplemented with 2 mg/mL of Protease from *Streptomyces griseus* (Sigma-Aldrich), for 1 h at 37 °C, under agitation. Following digestion, 1 % FBS (Capricorn) was added to inactivate enzymatic activity. After centrifugation at 400 g for 10 min, tissue pellets were washed twice in PBS, froze in liquid nitrogen and stored at -80 °C, until RNA extraction. For repopulated NP scaffolds, a pull of 5 samples/each age, isolated from the same IVD, were used for digestion and subsequent RNA extraction in order to increase the RNA amount, while for organ culture only one NP was sufficient for the analysis.

For RNA extraction, NPs were thawed and resuspended in Trizol (Invitrogen). After adding chloroform, samples were centrifuged at 12.000 g for 15 min. Then, the aqueous/ transparent phase was collected, re-suspended in isopropanol and transferred to ReliaPrepTM Minicolumn (Promega) to proceed with RNA extraction by using the ReliaPrep RNA Cell Miniprep System kit (Promega), following the manufacturer's instructions, and quantified by a NanoDrop spectrophotometer. RNA from repopulated NP scaffolds and organ culture (concentration of 100 ng) was reverse transcribed in cDNA, by using High Capacity cDNA Reverse Transcription kits (Applied Biosystem). Briefly, a 2X Reverse Transcription (RT) Master Mix was prepared by mixing 10x RT Buffer, 25X Deoxynucleotide (dNTP) Mix (100 mM), 10X RT Random Primers, MultiscribeTM Reverse Transcriptase, RNAse Inhibitor and Nuclease-free water, and added in the RNA samples. Reverse

transcription reaction was run in the thermal cycler (MyCycler Thermo Cycler, Bio-Rad) and the obtained cDNA were used for quantitative real-time reverse transcription–polymerase chain reaction (qRT-PCR).

2.15. QUANTITATIVE REAL-TIME REVERSE TRANSCRIPTION–POLYMERASE CHAIN REACTION

TaqMan Gene expression probes (Applied Biosystem), specific for bovine species, were used to detect gene expression levels of *AGGRECAN* (*ACAN*, (Bt03212186_m1), *COL2A1* (Bt03251861_m1), *GAPDH* (Bt03210913_g1), *MMP1* (Bt03212825_m1) and *MMP3* (Bt04259490_m1) in cDNA obtained from repopulated NP scaffolds and organ culture. The reaction mix was prepared by using TaqMan™ Gene expression Master Mix (Applied biosystem) and the qRT-PCR was carried out in a CFX96 Real-Time qPCR System (BioRad), under the specific conditions required from the Master Mix (Hold: 50 °C for 2 min; Hold: 95 °C for 10 min; Denature: 95 °C for 15 s; Anneal/Extend: 60 °C for 60 s). GAPDH was used as internal control.

Relative expression levels were calculated using the quantification cycle (Cq) method, according to MIQE guidelines (Bustin et al., 2009). Finally, gene expression levels were normalized by control (organ culture).

2.16. HISTOLOGICAL ANALYSIS OF REPOPULATED NPS

Immunofluorescence (IF) for COL2 and immunohistochemistry (IHC) for ACAN and COL1 were performed in 5 µm sections of repopulated NPs and control scaffolds (decellularized NPs cultured under the same experimental conditions of repopulated NPs) at day 7 of *ex vivo* culture. Sections were dewaxed in xylene, re-hydrated through graded alcohols and washed with distilled water.

For IF of COL2, antigen retrieval was performed by immersing sections in microwave-boiled citrate buffer (pH = 6.0) for 1 min, followed by incubation with 20 µg/mL of Proteinase K solution for 15 min at 37 °C. After blocking with 10 % FBS, 4 % bovine serum albumin (BSA, Merck), 0.2 % Triton solution for 1 h at room temperature, sections were incubated with COL2A1 primary antibody (dilution 1:50; anti-COL2A1 monoclonal antibody M2139; sc-52658, Santa Cruz Biotechnology) overnight, at 4 °C. Afterwards, an incubation with Alexa Fluor 594 secondary antibody (dilution: 1:1000; Alexa Fluor™ 594 goat anti-mouse; A11020; Invitrogen) for 1 h was performed. Finally, sections were mounted

in fluoroshield with DAPI mounting media (Sigma- Aldrich) (Ferreira et al., 2021; Pereira et al., 2016).

For IHC, antigen retrieval was performed with 20 µg/mL of Proteinase K solution for 15 min at 37 °C for ACAN followed by microwave-boiled citrate buffer (pH = 6.0) for 1 min and 1.5 U/mL of hyaluronidase for 45 min at 37 °C, for COL1 (Pereira et al., 2016). IHC was performed by using Novolink™ Polymer Detection Kit (Leica Biosystems), following manufacturer's instructions. Briefly, slides were incubated in Peroxidase Block for 5 min to neutralize endogenous peroxidase and in Protein block for other 5 min. Sections were incubated overnight at 4 °C with the optimally diluted primary antibodies: ACAN (dilution: 1:750; anti-ACAN monoclonal antibody BC-3; MA3-16888; Invitrogen) and COL1 (dilution 1:100; anti-COL1; 600-401-103-0.1; Rockland Immunochemicals, Inc.). Following incubation with Post Primary solution for 30 min, a step with Novolink™ Polymer was performed for 30 min, under gentle agitation. Peroxidase activity was developed by using DAB working solution for 5 min. Finally, sections were counterstained with Gill's Hematoxylin (Thermo Fisher Scientific) for 6 min, washed in running tap water, dehydrated and mounted with Entellan (Merck).

For IF of COL2 and IHC of ACAN and COL1, a negative control without primary antibody was included in the same slide. Images were acquired at Apotome microscope (Zeiss) for COL2 and optical microscope (Zeiss) for ACAN and COL1 at 20x objective. To account for all ECM protein pool (both intracellular and extracellularly deposited), percentage area of each image was quantified by Fiji/ImageJ software. For data analysis, percentage area of each image was normalized by the average of the percentage area of the correspondent control (decellularized matrices).

2.17. PICRO-SIRIUS RED STAINING UNDER POLARIZE LIGHT

At day 7 of *ex vivo* culture, 5 µm paraffin sections of repopulated and decellularized NPs were incubated with Picro-Sirius Red solution for 1 h and then washed with acidified water (0.01 N HCl). Images were acquired by using polarized lens at objective 10x in order to characterize different collagen fibers. The percentage of red, yellow and green fibers was quantified by Fiji/ImageJ software.

2.18. *IN VIVO* CAM ASSAY

The *in vivo* angiogenic potential of decellularized NPs from bovine IVDs was assessed by the CAM assay. Fertilized chick (*Gallus gallus*) eggs, obtained from commercial sources, were incubated horizontally at 37.8 °C in a humidified atmosphere and referred to embryonic day (E). On E3 a square window was opened in the shell after removal of 1.5-2 mL of albumen to allow detachment of the developing CAM. The window was sealed with adhesive tape and the eggs returned to the incubator. At E10, eggs were randomly distributed into five groups and, under sterile conditions, a silicone ring was placed on the top of the growing CAM. Four (out of the 5) groups were treated with basic fibroblast growth factor-2 ($bFGF_2$; 400 ng/egg) and the fifth with H_2O, thus the experiment negative control. In three of $bFGF_2$ treated groups, decellularized NPs from animals of different ages (fetus, young and old) were implanted in the treatment site, inside the ring. The last group, $bFGF_2$ alone, was used as positive control. The eggs were re-sealed and returned to the incubator for an additional 3 days. At E13, CAMs were fixed with 10 % of neutral buffered formalin, excised from the embryo and photographed *ex ovo* under a stereoscope, at 20x magnification (Olympus, SZX16 coupled with a DP71 camera). Pictures were used for quantification of new vessels growing towards the site of scaffold implantation in order to evaluate the angiogenic response. Two independent experiments were performed resulting in 9 to 17 samples/eggs per experimental group.

2.19. STATISTICAL ANALYSIS

Results are presented as average ± Standard Error of the Mean (SEM). The normality of the data was tested using a D'Agostine and Pearson normality test. The majority of the data followed a non-normal distribution, a non-parametric paired Friedman test, with Dunn's multiple comparison test as post-hoc, was used. When data followed a parametric distribution (in the case of CAM assay), an unpaired ANOVA test was applied. A confidence level of at least 95 % ($p < 0.05$) was set. Graph Pad Prism v7.01 software was used for the analysis.

3. RESULTS

3.1. A TRANSVERSAL DECELLULARIZATION PROTOCOL EFFICIENTLY REMOVES CELLS AND DNA WHILE PRESERVING ECM INDEPENDENTLY OF DONOR AGE

In order to develop an optimal protocol that would be adequate, independently of donor age, NPs from fetus, young and old bovine IVDs were decellularized by screening a range of features: distinct detergents (SDS and Triton-X-100), at different concentrations and time points (SDS 0.1 % 1 h, 3 h and 24 h; SDS 0.5 % 24 h, Triton 0.6 % 24 h and Triton 1.2 % 24 h). Decellularization efficiency, in terms of DNA and cell removal, was evaluated by PicoGreen DNA quantification and DAPI staining, respectively. As shown in Figure 1a, all protocols tested were able to decrease scaffold DNA content, for all aged donors, when compared to native tissues. However, SDS 0.1 % - based protocols were shown to be more efficient in DNA removal, especially for fetal NPs, in line with DAPI staining (Supplementary Figure 2). The least efficient treatments were those based on Triton 0.6 % and 1.2 %, which still retained numerous cells in both fetal and young matrices.

GAGs and collagen are major components of NP tissue. Specifically, GAGs are essential in maintaining osmotic pressure and hydration of the IVD in order to support compressive loads (Liu et al., 2018), while collagen fibers represent the main structural NP network (Aladin et al., 2010). Since it is known that some decellularization agents can remove (or significantly decrease) GAGs, as well as disrupting collagen organization (Gilbert et al., 2006), we evaluated their retention after decellularization by sGAGs quantification and Alcian Blue/Picro-Sirius red staining, respectively. As expected, decellularization resulted in sGAGs loss for all aged donors (Figure 1b), independently of the decellularization conditions used, as compared to native tissues. However, this effect was even more evident for SDS (0.1 % and 0.5 %) 24 h treatments, which significantly reduced sGAGs content in fetal and young decellularized matrices. No statistically significant differences were observed in terms of NPs COL content between the different experimental methods for all the aged donors (Supplementary Figure 3). This was further confirmed with Alcian Blue and Picro-Sirius Red staining (Figure 1c) which revealed GAGs (blue) loss in fetus, young and old matrices, for all the decellularization conditions. Protocols based on Triton-X-100 1.2 % 24 h and SDS 0.1 % 1 h and 3 h, did not show a statistically significant reduction of sGAGs, indicating a higher retention of these components, which

was corroborated by the bluish coloration in Alcian Blue staining. Collagen content (red) was preserved in all the conditions, with no obvious differences.

Overall, SDS 0.1 % - based protocols were more efficient in decreasing DNA content, while preserving tissue architecture and ECM composition to some extent. Therefore, to ensure minimal exposure to chemical detergents, an SDS 0.1 % for 1 h - based treatment was selected as the optimal procedure. It was then used to further characterize decellularized matrices at the structural, biochemical, and biomechanical level. A summary of the optimal decellularization procedure is illustrated in Figure 1d.

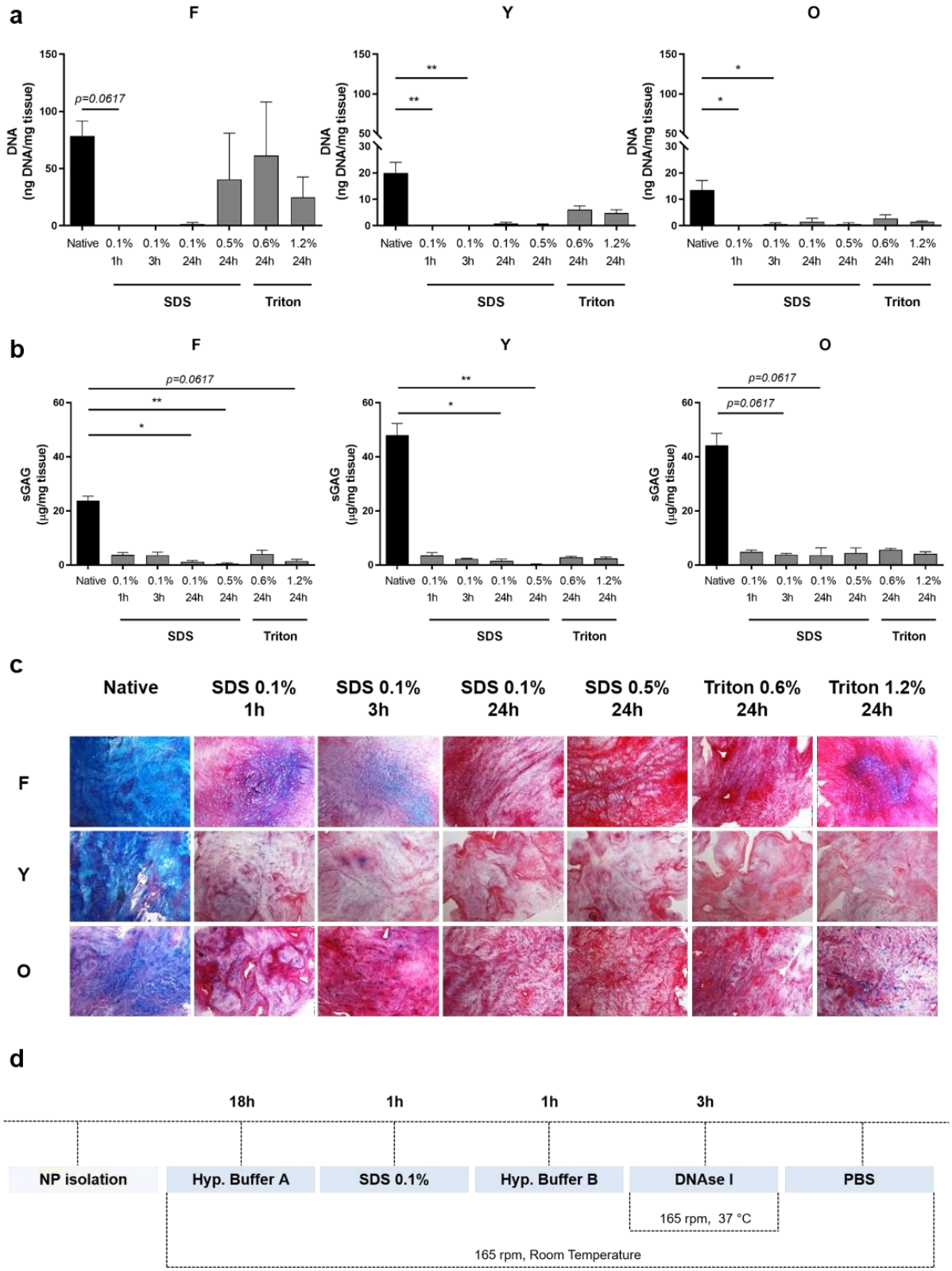
a
F
Y
O
DNA (ng DNA/mg tissue)
p=0.0617
Native
0.1% 1h
0.1% 3h
0.1% 24h
0.5% 24h
0.6% 24h
1.2% 24h
SDS
Triton
b
sGAG (µg/mg tissue)
c
Native
SDS 0.1% 1h
SDS 0.1% 3h
SDS 0.1% 24h
SDS 0.5% 24h
Triton 0.6% 24h
Triton 1.2% 24h
d
18h
1h
1h
3h
NP isolation
Hyp. Buffer A
SDS 0.1%
Hyp. Buffer B
DNAse I
PBS
165 rpm, 37 °C
165 rpm, Room Temperature

Figure 1. Decellularization efficiency of several experimental methods using bovine nucleus pulposus from different ages. (a). Quantification of DNA by PicoGreen assay and **(b)** sulfate sGAGs by Blyscan Sulfate GAGs assay in native and decellularized fetus (F), young (Y) and old (O) NPs. Data from each decellularization treatment and age group were compared to the correspondent control (native) and normalized by wet weight (ng/mg for DNA and µg/mg for sGAGs). For both DNA and sGAGs quantification: Error bars represent mean ± SEM (n=3). Kruskal Wallis test followed by Dunn's multiple comparison test. *p<0.05; **p<0.01. **(c)** Alcian Blue and Picro-Sirius Red staining of tissue sections from native and decellularized F, Y and O NPs. Representative images of three biological replicates. **Red**: collagen; **blue**: GAGs; **purple**: cell nuclei. Magnification 5x; scale bar: 500 µm. **(d)** Schematic workflow of the optimal decellularization procedure.

3.2. DECELLULARIZED NPS FROM DIFFERENT AGED DONORS PRESERVE STRUCTURAL, BIOCHEMICAL AND BIOMECHANICAL CUES

Scaffold structure, which has often been described to be altered as a consequence of decellularization, is known to influence tissue development, homeostasis and regeneration, through several cellular processes (*e.g*. adhesion, survival, migration, proliferation, differentiation, *etc*.) (Caldeira et al., 2018). For that, Cryo-SEM was performed in decellularized NPs from different ages to analyze the effect of decellularization on scaffold topography. All native NPs from different aged donors were characterized by a network of randomly oriented fibers, (Figure 2a), as previously reported (Caldeira et al., 2017). Although general architecture was preserved in all aged donors following decellularization, the collagen network seemed to be sparser, revealing bigger pores than native tissue, particularly for fetus and young NPs. Quantitative analysis using DiameterJ validated the aforementioned observations. Fetus and young decellularized NPs presented less pores (Figure 2b) and increased mean pore area (Figure 2c), when compared to the correspondent native NPs. No major differences were observed for old scaffolds before and after decellularization.

The preservation of COL12 and COL14 in NP decellularized matrices is essential for the pro-regenerative potential of fetal tissues. Since decellularization agents can cause collagen reduction, a western blotting for these two pro-regenerative proteins was performed to evaluate their retention in fetus NPs, after decellularization. Young native NPs

were included in the analysis as negative controls, since COL12 and COL14 are not expressed at this age (Caldeira et al., 2017). As expected COL12 (Figure 2e) and COL14 (Figure 2f) expression was confirmed in fetal native NPs. Both protein levels were higher in fetal decellularized NPs, when compared to either fetus or young native tissues, confirming their preservation after decellularization.

As it is well known, IVD biomechanical properties are essential to allow spine movements, by transferring loads and dissipating energy through the vertebrae (Tomaszewski et al., 2015). Thus, to ascertain if these features were affected by decellularization, viscoelastic properties of fetus, young and old NPs were evaluated by rheological analysis, as described in (Pinto et al., 2017). After decellularization, NPs showed a decrease of complex shear modulus (G*) for all aged donors, demonstrating to be less stiff when compared to the correspondent native tissues (Figure 2g). Moreover, fetus native NPs revealed a tendency of decreased stiffness when compared to young and old NPs, demonstrating a softer-like behavior. This trend was preserved after decellularization. Finally, young and old NPs showed similar stiffness both in native and decellularized samples (Figure 2g).

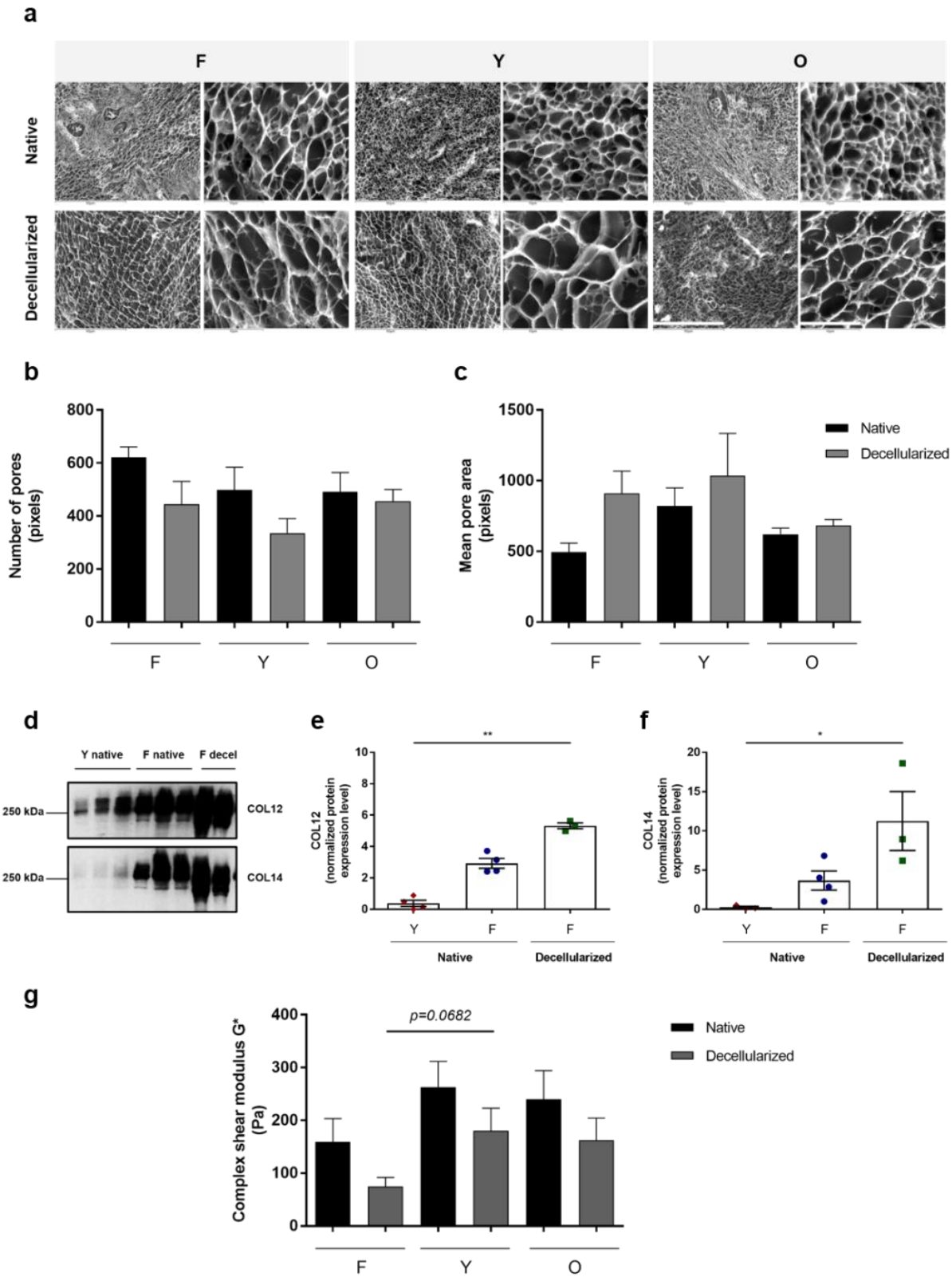
a
F
Y
O
Native
Decellularized
b
Number of pores (pixels)
800
600
400
200
0
F
Y
O
c
Mean pore area (pixels)
1500
1000
500
0
Native
Decellularized
d
Y native
F native
F decel
250 kDa
COL12
250 kDa
COL14
e
COL12 (normalized protein expression level)
**
Native
Decellularized
f
COL14 (normalized protein expression level)
*
Native
Decellularized
g
Complex shear modulus G* (Pa)
p=0.0682
Native
Decellularized

Figure 2. Structural, biochemical and biomechanical characterization of bovine nucleus pulposus from different ages decellularized with the optimal procedure. (a) Representative images of collagen fibers network of native and decellularized fetus (F), young (Y) and old (O) NPs, obtained by Cryo-SEM. Magnification 1000x and scale bar 60 µm (left images); magnification 5000x and scale bar 10 µm (right images). Quantification of number of pores **(b)** and mean pore area **(c)** of decellularized and native F, Y and O NPs by DiameterJ (n=3 to 4). Error bars represent mean ± SEM. Kruskal – Wallis test followed by Dunn's multiple comparison test. **(d)** Collagen type 12 (COL12) **(e)** and Collagen type 14 (COL14) **(f)** western blotting of F decellularized NPs. F native NPs were used as positive control, while Y native NPs as negative one (n=3 to 4). Protein expression levels were normalized by the total protein loading (Page Blue staining). Error bars represent mean ± SEM. Kruskal – Wallis test followed by Dunn's multiple comparison test. * $p<0.05$; ** $p< 0.01$. **(g)** Complex shear modulus (G*) values (at 5 % of strain), retrieved from the linear viscoelastic region (0,04 -1 Hz) of the frequency sweep, performed by rheology, of F, Y and O decellularized NPs, compared to the correspondent native tissues (n=3). Error bars show mean ± SEM. Kruskal – Wallis test followed by Dunn's multiple comparison test.

3.3. ECM DEVELOPMENTAL CUES INFLUENCE ADULT BOVINE NP CELL BEHAVIOR

To evaluate the effect of donor age on cell response and to unveil how developmental - associated ECM features (either biochemical or biomechanical) can affect IVD de/regeneration, decellularized NPs from different ages were repopulated with adult bovine NP cells.

To extrapolate on differences in colonization numbers in the different scaffolds, DNA was quantified 24 h after cell seeding. Fetus, and particularly young repopulated NPs, exhibited higher DNA content, as compared to old ones, although differences were not statistically significant (Figure 3a). Metabolic activity of the *ex vivo* culture, revealed an increased level of RFUs in fetus NPs at day 1, as compared to young and old ones. Despite a slight trend for overall decrease in metabolic activity at day 3 (which was partially recovered at day 6), no major differences were observed between different aged donors at day 3 and 6 of culture (Figure 3b). In addition, no significant cytotoxicity levels were identified in any of the repopulated NPs independently of the time point, except for a modest increase in young-derived scaffolds at day 1 (Figure 3c).

To explore if decellularized NP scaffolds from different aged donors were biocompatible, cell death was assessed after 7 days of culture. More cells and, in particular viable ones were found in fetal and young repopulated NPs, when compared to old ones (Figure 3d). Moreover, seeded cells were characterized by a round morphology, which is typical of chondrocyte–like NP cells (Figure 3e). NP cells repopulating the scaffolds were found inside the hollow spaces left after decellularization (Figure 3f). Notably, in fetal-derived scaffolds, NP seeded cells displayed the capacity to produce GAGs, as inferred by an increase in Alcian blue staining in repopulated cells, which was not observed in cells seeded on young nor on old NPs (Figure 3f).

Altogether, these results suggest that decellularized NPs from all the aged donors were capable of supporting bovine NP cell culture. Nevertheless, younger decellularized matrices were more efficient in promoting adhesion and metabolic activity, as well as in maintaining cell viability, when compared to older microenvironments.

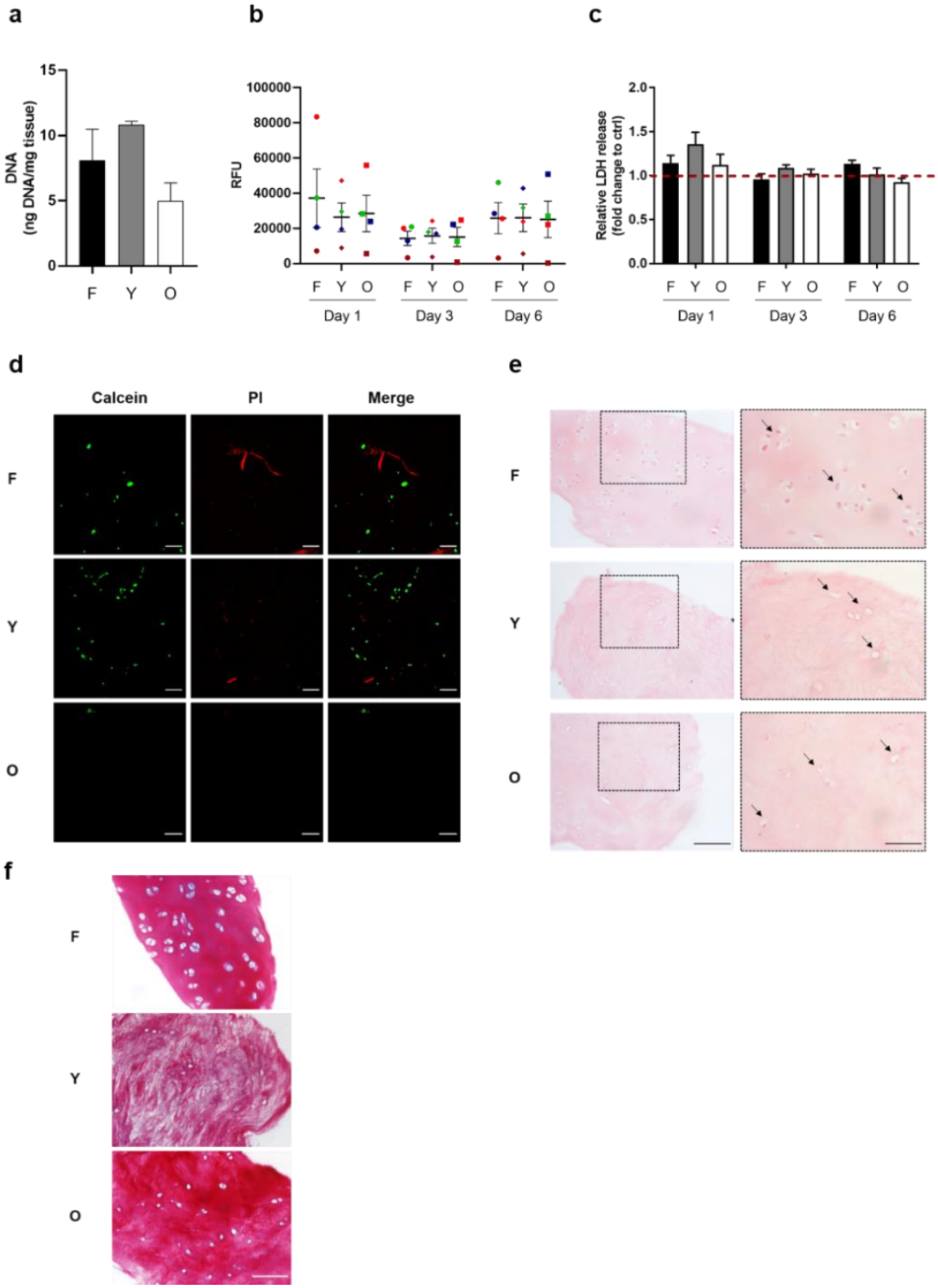
a
DNA (ng DNA/mg tissue)
15
10
5
0
F Y O
b
RFU
100000
80000
60000
40000
20000
0
F Y O F Y O F Y O
Day 1 Day 3 Day 6
c
Relative LDH release (fold change to ctrl)
2.0
1.5
1.0
0.5
0.0
F Y O F Y O F Y O
Day 1 Day 3 Day 6
d
Calcein
PI
Merge
F
Y
O
e
F
Y
O
f
F
Y
O

Figure 3. Repopulation efficiency of decellularized nucleus pulposus from different ages with adult bovine nucleus pulposus cells. (a) Quantification of DNA by PicoGreen assay in fetus (F), young (Y) and old (O) repopulated NPs 24 h after cell seeding. Data were normalized by wet weight (ng DNA/mg tissue). Error bars represent mean ± SEM (n=3). Kruskal Wallis test followed by Dunn's multiple comparison test. **(b)** Metabolic activity of F, Y and O repopulated NPs at day 1, 3 and 6 of *ex vivo* culture (same color dots represent individual experiments). Error bars represent mean ± SEM (n=4). Two-Way Anova followed by Tukey's multiple comparison test. RFU: relative fluorescence units. **(c)** Measurement of relative lactate dehydrogenase (LDH) release in the conditioned media of repopulated NPs at day 1, 3 and 6 of *ex vivo* culture. Data were normalized by the positive control, provided by the kit, and decellularized NPs. Error bars represent mean ± SEM (n=6 technical replicates). Two-Way Anova followed by Tukey's multiple comparison test. **(d)** Calcein (**green**) and propidium iodide (PI; **red**) staining of F, Y and O repopulated NPs after 7 days of *ex vivo* culture. Magnification 10x; scale bar 200 µm. **(e)** Hematoxylin&Eosin (H&E) staining of F, Y and O repopulated NPs after 7 days of *ex vivo* culture. Left images: magnification 20x and scale bar 100 µm; right images: magnification 40x and scale bar 50 µm. Arrows show cell nuclei. **(f)** Alcian Blue and Picro-Sirius Red staining of repopulated F, Y and O NPs after 7 days of *ex vivo* culture. **Red**: collagen; **blue**: GAGs; **purple**: cell nuclei. Magnification 20x; scale bar: 100 µm.

3.4. YOUNGER DECELLULARIZED MATRICES PROMOTE HEALTHY ECM *DE NOVO* SYNTHESIS BY ADULT BOVINE NP CELLS

To understand if ECM-based scaffolds are able to promote tissue regeneration, recellularized NPs matrices from different aged donors were cultured *ex vivo* for 7 days. The ability of seeded cells to synthetize ECM proteins and, thus recover a healthy and functional microenvironment, was investigated at both molecular and protein levels.

As shown in Figure 4, NP cells cultured on fetal decellularized matrices show significant upregulation of *ACAN* (Figure 4a) and *COL2A1* (Figure 4b) when compared to old decellularized matrices. At the protein level, an increase in ACAN production throughout the tissue was observed by IHC in fetal and young matrices, when compared to old donors. (Figure 4c). This was confirmed by percentage of stained area quantification (normalized by the control shown in Supplementary Figure 4a), which showed a significant increase in

ACAN production in fetus and young repopulated NPs, when compared to the old ones (Figure 4d). This increased ACAN synthesis is even more evident in comparison to control decellularized matrices, with almost no ACAN expression at the protein level (Supplementary Figure 4a). Interestingly, non-repopulated fetus decellularized NPs showed a significantly higher amount of ACAN than old scaffolds, and a tendency to increase, as compared to young ones (Supplementary Figure 4b). Thus, cells cultured on younger matrices were able to restore at a higher extent native ACAN expression, which had been lost with the decellularization process.

On the other hand, IF analysis of COL2 expression showed intense staining at the pericellular level in cells repopulating the matrices from all aged donors (Figure 4c), being apparently reduced in young matrices. Upon percentage of area quantification, COL2 was shown to be decreased in all aged donors in comparison to control matrices (fold change <1) (Figure 4e). Still, old repopulated NPs were able to retain a significantly higher amount of COL2, when compared to young ones. Fetal matrices showed a tendency to have increased COL2 content, when compared to young ones, but no significant differences were observed (Figure 4e).

Since COL2 content in non-repopulated young decellularized matrices was significantly higher than fetus and old ones, as revealed by IF (Supplementary Figure 5a) and its subsequent quantification (Supplementary figure 5b), we hypothesized that COL2 decrease upon cell repopulation could be due to increased MMP-mediated matrix degradation. When analyzing *MMP1* and *MMP3* (the most known collagenases present in IVD degeneration) gene expression in repopulated NPs, a trend (although not statistically significant) for higher *MMP1* (Supplementary figure 5c) and *MMP3* (Supplementary figure 5d) gene expression levels was observed in young repopulated NPs, when compared to the other aged donors supporting to some extent the hypothesis that, in the younger matrices, higher COL2 degradation might occur, leading to lower COL2 protein levels.

Our previous work had shown an increased expression of COL1 in fetus native NP matrisome when compared to young and old matrices (Caldeira et al., 2017). Thus, we analyzed COL1 content in repopulated matrices from different ages to understand if the capacity of seeded cells to produce this protein varied with aging. Interestingly, COL1 was present in all recellularized matrices, particularly on those of fetal origin (Figure 4c). Upon area quantification, it was possible to verify that higher COL1 content was present in fetal and young repopulated NPs, although due to high variability of fetal samples, differences were only significant when comparing young and old seeded scaffolds (Figure 4f). These

differences in COL1 were already present in non-repopulated decellularized matrices (Supplementary Figure 6).

Concomitantly, we analyzed collagen fibers' thickness (and maturation) by Picro-Sirius Red staining under polarized light. Quantitative data from normalized coloured area demonstrated that fetal- and old-derived NPs exhibited an increased percentage of thicker/mature fibers (red/yellow colours through birefringence analysis), when compared to young ones (Figure 4c and 4g). Such differences were not observed in what concerns thinner/immature fibers (green colour by birefringence). Interestingly, fetal NPs showed a statistically higher percentage of red fibers when compared to yellow and green ones. In addition, old NPs had a significantly increased percentage of red fibers' when compared to green ones (Figure 4g). Moreover, fetal repopulated NPs showed a higher red/green ratio than young and old NP donors (Figure 4h), in line with the abovementioned COL1 increase in fetal recellularized NP scaffolds. In control decellularized NPs, a higher percentage of intermediate thickness fibers (yellow) was found for all aged donors, with few amounts of thicker fibers detected (red), (Supplementary Figure 6c). When looking into the red/green fiber ratio, we observed a slightly higher value in fetal NP matrices, than in old NPs (Supplementary Figure 6d).

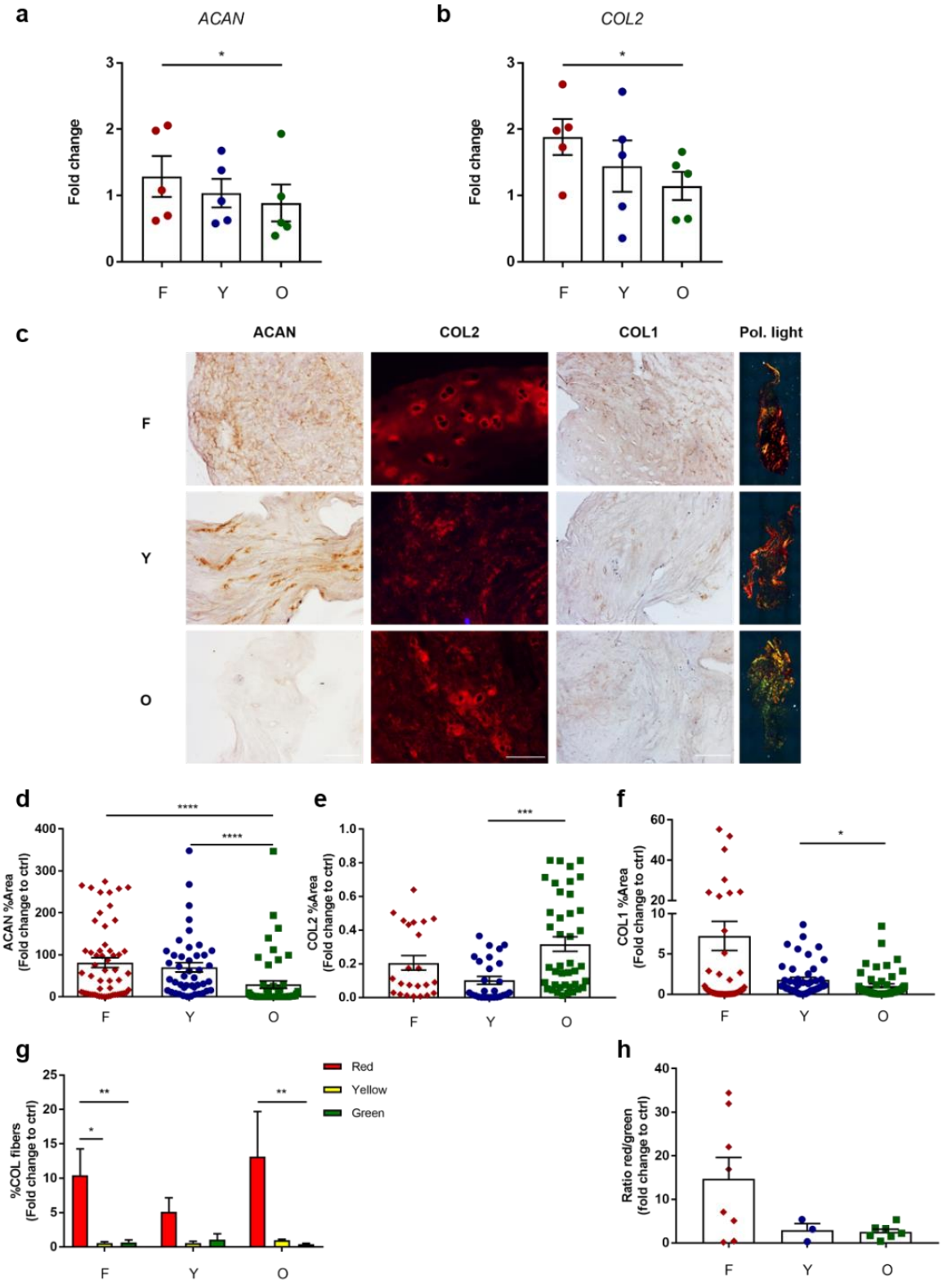
a
ACAN
Fold change
F
Y
O
b
COL2
Fold change
c
ACAN
COL2
COL1
Pol. light
d
ACAN %Area (Fold change to ctrl)
e
COL2 %Area (Fold change to ctrl)
f
COL1 %Area (Fold change to ctrl)
g
%COL fibers (Fold change to ctrl)
Red
Yellow
Green
h
Ratio red/green (fold change to ctrl)

Figure 4. Extracellular matrix *de novo* synthesis of repopulated nucleus pulposus after 7 days of *ex vivo* culture. (a) mRNA expression level of Aggrecan (*ACAN*) and **(b)** Collagen type 2 (*COL2A1*) by quantitative real-time PCR of fetus (F), young (Y) and old (O) repopulated NPs after 7 days of *ex vivo* culture. Fold change to organ culture (native NPs cultured *ex vivo* for 7 days). Error bars represent mean ± SEM (n=5). Friedman test followed by Dunn's multiple comparison test was used for statistical analysis. *p<0.05. **(c)** Representative images of ACAN immunohistochemistry (IHC), COL2 immunofluorescence (IF), Collagen type 1 (COL1) IHC and Picro-Sirius Red staining under polarize light of F, Y, and O repopulated matrices. Magnification 20x; scale bar: 100 µm. **(d)** ACAN, **(e)** COL2 and **(f)** COL1 percentage area quantification of F, Y and O repopulated NPs, obtained by Fiji/ImageJ. Fold change to the correspondent control (ctrl: decellularized matrices cultured *ex vivo* for 7 days). ACAN: n = 6 to 8. COL2A1: n = 4 to 6. COL1: n= 6 to 7. Kruskal – Wallis test followed by Dunn's multiple comparison test. *p<0.05; ** p< 0.01; ***p<0.001; **** p<0.0001. **(g)** Quantification of the relative percentage of collagen fibers, obtained by ImageJ, of F, Y and O repopulated NPs. Fold change to the correspondent controls. Error bars represent mean ± SEM (n=3 to 8). Kruskal – Wallis test followed by Dunn's multiple comparison test. *p<0.05; ** p<0.01. **(h)** Ratio of red/green (mature/immature) collagen fibers of F, Y and O repopulated NPs. Fold change to the correspondent controls. Error bars represent mean ± SEM. (n = 3 to 8). Kruskal – Wallis test followed by Dunn's multiple comparison test.

3.5. FETAL MATRICES INHIBIT THE ANGIOGENIC RESPONSE *IN VIVO*

The CAM assay has been widely used as a first line *in vivo* model to investigate biomaterials' biocompatibility as well as a screening platform to test novel anticancer drugs, tumor cells invasion, metastasis and angiogenesis (Lokman et al., 2012; Marshall et al., 2020). In this study, we used this preclinical animal model to determine the anti-angiogenic capacity of decellularized NPs from different ages (Figure 5a). All the CAMs except the negative control (H_2O), were pre-incubated with $bFGF_2$ (an angiogenic factor), before scaffolds implantation. Our results show that only fetal matrices were capable of reducing the angiogenic response of $bFGF_2$ to levels close to the ones of the negative control (H_2O), when neovascularization was evaluated. CAMs implanted with either young or old decellularized NPs showed angiogenic responses comparable to those of the positive

control ($bFGF_2$) and, thus, significantly higher than H_2O treated eggs. This indicates an inexistent anti-angiogenic potential for young and old matrices (Figure 5b).

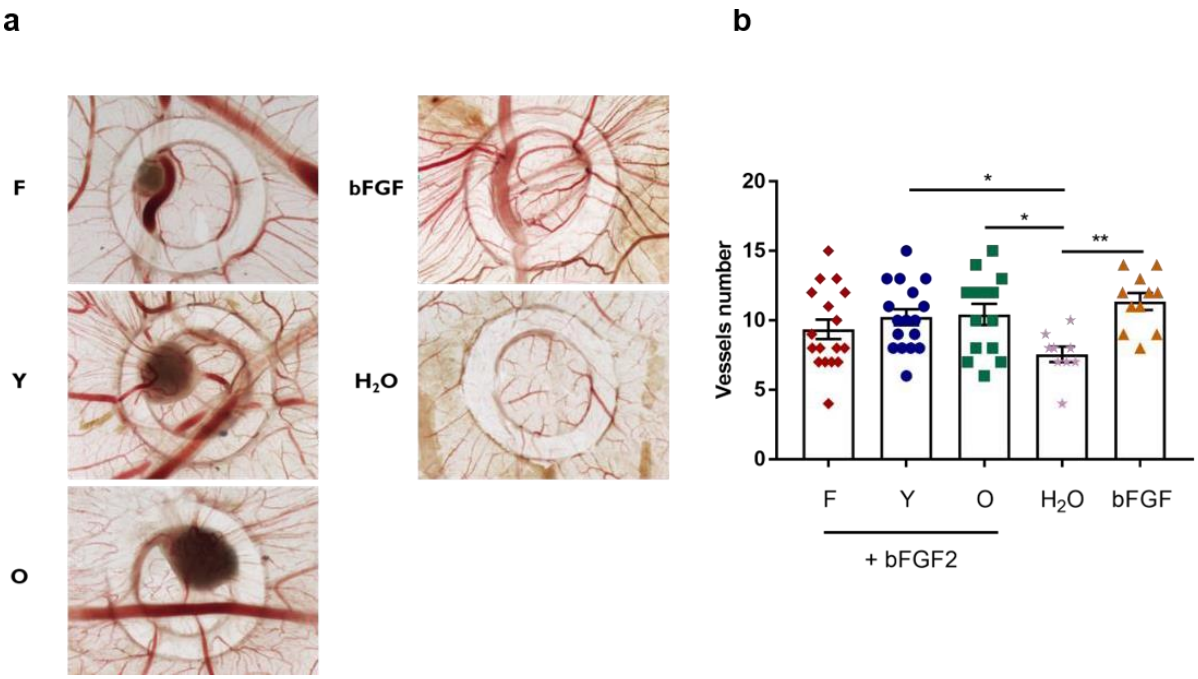

Figure 5. *In vivo* evaluation of anti-angiogenic potential of decellularized nucleus pulposus from different ages. (a) Representative images *in ovo* of chorioallantoic membrane (CAM) treated with basic fibroblast growth factor-2 ($bFGF_2$) and implanted with decellularized matrices from fetus (F), young (Y) and old (O) NPs. **(b)** Quantification of the number of new vessels growing towards the decellularized NPs or the inoculation site in the case of controls. H_20 and $bFGF_2$ represent the negative and positive controls, respectively. Results of decellularized NPs were compared to H_20. Error bars represent mean ± SEM of two independent experiments (n=9 to 17 technical replicates). The One-Way Anova followed by Dunnett's multiple comparison test was used for statistical analysis. Results were considered significant at $p < 0.05$ (*) and $p<0.01$ (**).

4. DISCUSSION

In the last decade, decellularized ECM–based scaffolds have been explored for the regeneration of different tissues (*e.g*. skeletal muscle, esophagus, tendon, lower urinary tract, heart, among others), demonstrating successful tissue remodeling and partial tissue repair both in animal studies and human clinical trials (Cramer & Badylak, 2019). As such, a great number of acellular scaffolds have been approved by Food and Drug Administration (FDA) and commercialized for several clinical applications (*e.g*., AlloDerm, Strattice, Permacol, Surgisis, Veritas) (Kawecki et al., 2018). All in all, the ECM represents a natural biomaterial, which is able to influence cell behavior and contribute to tissue homeostasis. However, to avoid pro-inflammatory response and fibrosis upon *in vivo* implantation (Faulk & Badylak, 2014), decellularization, using chemical, enzymatic or physical agents, is fundamental to remove host cells and DNA, while preserving native ECM structure and composition (Crapo et al., 2011; Gilbert et al., 2006).

With the lack of long-term and effective therapies for LBP, tissue engineering strategies, namely decellularized ECM-based scaffolds, have started to be investigated also for the IVD. These approaches are especially focused on the NP, where the degenerative process is thought to start (Yang & Li, 2009). Such natural biomaterials are very promising given their capacity to recapitulate native biological and functional cues representative of a healthy disc microenvironment. Mercuri and colleagues were the first to define a successful decellularization method for porcine NPs, by using a combination of chemical detergents (Triton-X-100 and deoxycholic acid), ultrasonication and nucleases (Mercuri et al., 2011). Afterwards, many other acellular scaffolds derived from human or animal origin were successfully developed (Fiordalisi et al., 2021) and present a huge potential for disc repair/regeneration.

However, tissue donor age can have a dramatic impact on scaffold properties, by influencing the final outcome of matrix-based therapies (Fiordalisi et al., 2021). Thus, for the development of appropriate biomaterials, it is essential to explore how donor age differences can affect scaffold pro-regenerative potential. Moreover, further studies on the impact of old degenerated microenvironments on cell behavior are needed in order to develop better therapies for IVD degeneration, so we aimed to address these questions.

It is known that a universal decellularization method for different animals or tissues, does not exist, and that different conditions (*e.g*. chemical agents, treatment time, enzyme

exposure, temperature) should be adapted, considering ECM structure and composition. In the present work, we optimized a decellularization protocol (Benedetto et al., 2014; Pinto et al., 2017; Silva et al., 2016) for bovine NPs from different aged donor (fetus, young and old) by using a low detergent concentration and reduced exposure time. This procedure showed to be efficient in removing host cells and DNA from all the aged tissues, while preserving tissue architecture, biomechanical properties and major ECM components. We tested two chemical detergents (SDS and Triton-X- 100) commonly used for tissue decellularization (Crapo et al., 2011), at different concentration and time points. SDS–based protocols were more efficient in cell and DNA removal, as well as in ECM structure preservation, when compared to those that used Triton. Although collagen content was preserved, we detected sGAGs loss for all the decellularization conditions tested. Since GAGs are present in cell membranes, anchoring the cells to the matrix, their partial removal together with cellular components is expected (Pinto et al., 2017).

As it is well described, the NP is mainly constituted by water, PG and collagen fibers (Marcolongo et al., 2017). ACAN, composed by negatively charged GAGs, is the main PG present in the tissue. Such negatively charged molecules are essential for tissue hydration, conferring elastic properties to the NP (Colombier et al., 2014) and enabling the distribution of high loads along the vertebral body (Inoue & Espinoza Orías, 2011). GAGs loss after decellularization has also been reported by other works on IVD decellularization (Fernandez et al., 2016; Illien-Junger et al., 2016; Mercuri et al., 2011) and is caused by the chemical detergents used during the process. It is described that SDS is more effective in decreasing nuclear remnants and cytoplasmatic proteins from the tissue (Keane et al., 2015; Woods & Gratzer, 2005). However, it also induces GAGs and growth factor loss, as well as collagen damage (Crapo et al., 2011; Fu et al., 2014), through a disruption of protein covalent bonds (Keane et al., 2015) and subsequent denaturation (Mendibil et al., 2020). Some studies have shown the efficacy of Triton–based protocols in cell and DNA removal from porcine NPs. Nevertheless, there are references to ECM structure modification (Mercuri et al., 2011) and GAGs loss (Fernandez et al., 2016; Mercuri et al., 2011), likewise SDS. On the contrary, Yuan *et al*. have described complete DNA removal and over 80 % GAG preservation in rabbit NP matrices, by using a combinatorial protocol of Triton-X-200 with sulphobetaine-10 and sulphobetaine-16 (Yuan et al., 2013). In the present study, we observed an opposite effect, with Triton-X-100 being less effective in decreasing DNA levels as well as in preserving GAGs amount. These results may reflect differences in IVD ECM composition and structure between species. Moreover, we only analyzed sGAGs content, thus not considering the non-sulfated GAGs portion that could still be present in the NP, such as

hyaluronic acid (Zhang et al., 2021). Despite the similar DNA decrease observed for the tested SDS 0.1 % - based treatments, only 1 h and 3 h protocols showed a statistically significant DNA reduction in young and old NPs, when compared to the correspondent native controls. Moreover, SDS 0.1 % and 0.5 % 24 h protocols statistically reduced sGAGs amount in fetus and young decellularized matrices, when compared to native NPs. Taking this into account, we selected the lowest SDS concentration and treatment time to minimize exposure to chemical detergents, which could have a cytotoxic effect on the cells (Alizadeh et al., 2019) and induce matrix degeneration (Schmitt et al., 2017). Therefore, the SDS 0.1 % (1 h) – based protocol was identified as the optimal procedure to decellularize bovine NPs from different aged donors. It was then used to further characterize the effect of decellularization on ECM structure, composition and biomechanics.

Given the importance of ECM structure in regulating cell behavior (Wang et al., 2020), we evaluated the retention of collagen network after NP decellularization, by using Cryo-SEM. Native bovine NPs from different ages were characterized by the presence of randomly oriented collagen fibers, as previously observed (Caldeira et al., 2017). After decellularization, we could confirm the preservation of matrix overall structure. However, collagen network seemed to be more opened, especially for fetus and young donors, when compared to the corresponding native controls. We hypothesize that this effect may result from the exposure to decellularization solutions during tissue processing. Quantitative data was indicative of a sparser matrix (reduced number of pores) and increased mean pore area in all decellularized NPs, except for old donors, probably due to the differences in ECM architecture and composition. During ageing IVDs become less hydrated, stiffer and more fibrotic, as observed macroscopically by Caldeira *et al*. (Caldeira et al., 2017), eventually rendering problematic the penetration of decellularization solutions deeper in the tissues. Interestingly, Caldeira *et al*., showed reduced but bigger pores in old bovine NPs when compared to young ones, as well as pores with increased mean pore area in fetal NPs (Caldeira et al., 2017). On the contrary, we observed increased number of pores and decreased mean pore area in fetus NP, when compared to young ones, although not statistically significant. These differences are most probably justified by distinct techniques used to analyze ECM structure. Since the NP is a highly hydrated hydrogel-like tissue, we adopted a Cryo-SEM to evaluate collagen network of NPs before and after decellularization, instead of Scanning Electron Microscopy, used by Caldeira *et al*. (Caldeira et al., 2017). This technology keeps samples hydrated and makes use of fast freezing in liquid nitrogen, avoiding tissue distortion and collapse during the analysis (effects observed with the traditional Scanning Electron Microscopy).

By dissecting the matrisome of bovine NPs from fetus, young and old IVDs, previous work from our group has demonstrated that the pro-regenerative proteins, COL12 and COL14, are uniquely expressed in fetal bovine NPs (Caldeira et al., 2017). To understand if these pivotal molecules were not affected by decellularization, we explored their expression following tissue processing. After decellularization, both proteins were detected in fetal-derived NPs, being expressed at levels that were not statistically different from native tissues, thus confirming protein preservation in the acellular scaffolds. In fact, there was a slight tendency of COL12 and COL14 to be present at higher levels in decellularized fetal samples rather than in native ones. This effect, had already been observed for other ECM constituents like collagen (Mercuri et al., 2011), and is a result of data normalization by the total protein loading. As a consequence of nuclear and perinuclear protein removal, the overall proportion of ECM increases after decellularization, as well as the ratio of COL12 and COL14. Preservation of COL12 and COL14 is crucial to maintain the pro-regenerative cues of fetal ECM–based scaffolds, which are expected to provide the enhanced potential for IVD repair, as in other tissue contexts (Marro et al., 2016; Nauroy et al., 2019; Schönborn et al., 2020; Wehner et al., 2017).

Given the importance of IVD biomechanics, we analyzed the viscous-elastic properties of NPs from different aged donors before and after decellularization, by rheology. It is known that healthy NPs are composed by higher level of water and PG which ensure the maintenance of pressure within the tissue, as well as higher hydration. With ageing the water and PG content start to decrease, leading to a reduction of NP pressure. As a consequence, NP became a solid-like tissue (Newell et al., 2017). Herein, fetal scaffolds showed to have a softer-like behavior, when compared to young/old tissues, thus confirming what happen in an age-associated IVD degenerative scenario.

Biomaterial biocompatibility is fundamental for the development of accurate 3D models to study diseases and to understand the role of ECM-cell crosstalk in pathological scenarios. In this context, IVD 3D scaffolds should be able to support cell survival and integration as well as to maintain native cells phenotype (Stergar et al., 2019). Moreover, envisaging future therapeutic applications, it is fundamental that the developed scaffolds are well tolerated by host cells. In the present work, after repopulation of decellularized matrices from different aged donors with adult bovine NPs cells, ECM-based scaffolds were able to support NP *ex vivo* cell culture, demonstrating good biocompatibility. Both fetal- and young-derived matrices showed slightly higher DNA content after 24 h of cell seeding and increased cell viability after 7 days in culture, when compared to old tissues. Interestingly,

a higher repopulation efficacy had been detected also for fetal heart bioscaffolds, when compared to adult ones (Silva et al., 2016), as a reflex of increased cell migration and proliferation.

It is well recognized that degenerated IVDs are affected by several ECM modifications (Pereira et al., 2016), which negatively affect tissue biology and function. Specifically, the reduction of ACAN and other chondroitin sulfate PG is associated with disc ageing and degeneration (Collin et al., 2017; Ohnishi et al., 2020). Moreover, Lian *et al*., showed downregulation of COL2 in human NPs derived from patients with disc degenerative disease, at both molecular and protein levels, when compared to healthy ones (Lian et al., 2017). Therefore, we evaluated matrix deposition in repopulated NPs to understand if seeded cells were able to recover a healthy microenvironment by ECM *de novo* synthesis, thus reverting the degenerative process. At day 7 of *ex vivo* culture, we were able to detect several differences at the molecular level when comparing *COL2* and *ACAN* gene expression from different aged donors. Fetal matrices showed higher *COL2* and *ACAN* expression than old donors, demonstrating a pro- regenerative potential. At the protein level, we detected an increased ACAN production in fetus and young repopulated matrices, when compared to old donors. ACAN represents one of the major components of NPs (Sivan et al., 2014) and its higher synthesis can be associated to matrix restoration. Therefore, our results demonstrate that younger matrices have an enhanced ability to recover a healthy and functional ECM microenvironment, guiding IVD through repair/regeneration.

While ACAN increased, we observed a statistically significant reduction of COL2 in young matrices as well as a tendency in decreasing COL2 levels in fetal NPs, when compared to old ones, probably due to increased MMPs-mediated protein breakdown. In particular, MMPs are involved in tissue remodeling through proteolytic degradation of ECM proteins, such as collagen (Stamenkovic, 2003). They are also implicated in other fundamental processes, such as cell migration, production of fragments with biological activity, regulation of tissue architecture, activation, inhibition or modification of signaling molecules' activity and cell function (Page-McCaw et al., 2007). MMPs activity is regulated by TIMPs (Carmeli et al., 2004) and the balance between MMPs and TIMPs expression is critical for maintaining tissue homeostasis. In this work, we analyzed *MMP1* and *MMP3* gene expression, which are known to specifically degrade COL2, to unravel their implication in COL2 decrease. Although not statistically significant, young NPs showed an upregulation of *MMP1* and *MMP3*, when compared to fetus and old aged donors. The overexpression of

MMP1 and *MMP3* in young NPs may explain the decrease of COL2, observed at the protein level. However, differences on MMPs activities or even their regulation through TIMPs could be implicated in this phenomenon and should be further explored to dissect their roles in this complex scenario.

Furthermore, fetal matrices showed a tendency to have higher COL1 content, than young-and old-derived NPs, as already shown in native NPs by Caldeira *et al*. (Caldeira et al., 2017). These results were further confirmed by Picro-Sirius Red staining under polarized light, which showed an increased red/green ratio (associated with COL1 expression) in fetal NPs, when compared to young and old ones. Although COL1 expression has been correlated with progressive disc degeneration and found in NP lesioned sites (Pereira et al., 2016), it has also been associated with beneficial effects for the IVD. A recent study has shown that Transforming growth factor – beta (TGF-β) signaling is essential for IVD development and growth, and has an important role in different processes, such as matrix synthesis, inhibition of matrix catabolism, inflammatory response and cell loss (Chen et al., 2019; Hu et al., 2020). In spite of higher expression of TGF-β1 being often associated with IVD degeneration (Chen et al., 2019; Nerlich et al., 2005) and its pathological grade (Chen et al., 2019; Li et al., 2014; Yang et al., 2012), a correlation between TFG-β signaling pathway and disc regeneration has also been shown. Interestingly, several studies have revealed a higher PG and collagen synthesis in degenerated IVD cells transfected with TGF-β1 (Maria Molinos et al., 2015; Tan et al., 2003), demonstrating the beneficial effect of TGF-β1 signaling. Recently, Lehmann *et al* have shown that TGF-β signaling pathway increased the expression of *COL1A1*, *ACAN* and *SOX9* genes in mesenchymal stem cells co- cultured with NP cells (Lehmann et al., 2018). Thus, a tight control on TGF-β activation and inhibition must exist to preserve tissue function and, as a consequence, with implications on COL1 regulation in the IVD environment.

Vascularization is also an important step of the degenerative cascade. It is well known that healthy IVDs are avascular tissues, receiving nutrient supply by diffusion through endplates (Whatley & Wen, 2012). With degeneration, neovascularization starts to be found within the tissue with consequent immune cell migration, and stimulation of an inflammatory response (Dou et al., 2021). Interestingly, higher levels of thrombospondin-1 (TSP1), an angiogenesis inhibitor (Rohrs et al., 2016), were detected at higher levels in fetal bovine NPs, when compared to young and old ones (Caldeira et al., 2017). Thus, we performed a CAM assay as a first *in vivo* proof of concept of the anti-angiogenic potential of decellularized matrices from different aged donors. As expected, fetal scaffolds were the

only ones capable of reducing the angiogenic response of $bFGF_2$ to negative control levels, thus demonstrating an anti-angiogenic capacity. Therefore, fetal matrices were able to mimic a microenvironment closer to a healthy IVD, considering the avascular nature of this tissue. On the contrary, young and old NPs did not show any anti-angiogenic capability given that their angiogenic response was similar to that of $bFGF_2$ alone, physiologically resembling a degenerative scenario.

Nowadays, there are no ideal animal models to study IVD degeneration. Thus, there is an urgent need to develop suitable 3D platforms to screen for novel cues involved in IVD pathology and to investigate innovative therapeutic solutions (Daly et al., 2016). Human IVDs would be ideal, however they are limited in numbers and difficult to harvest for several ethical and governmental restrictions (Alini et al., 2008). Although animal tissues have shown to be a great alternative to study IVD degeneration/regeneration (Alini et al., 2008; Pereira et al., 2016; Teixeira et al., 2016), the creation of an appropriate 3D scaffold is challenging for the complexity of IVD etiology and pathogenesis (Jin et al., 2018). Specifically, to choose an adequate animal donor species, several aspects need to be considered, including persistence of notochordal cells, disc geometry and size, disc mechanical loading, among others (Daly et al., 2016). Herein, we have shown that bovine NPs are characterized by several changes along ageing. Specifically, our findings demonstrate that younger matrices provide a more favorable microenvironment for cell adhesion. Adhered cells were kept viable within the scaffolds and able to synthesize new ECM components like ACAN, thus inducing tissue restoration. On the contrary, cells in contact with an old and degenerated tissue did not remain viable nor able to synthesize new matrix proteins. It has been reported that old and degenerated IVD matrices are characterized by the expression of several fibrotic–like proteins (COL1, fibronectin, cartilage intermediate layered protein (CILP) and HTRA1) (Yee et al., 2016). Moreover, Caldeira *et al*., have reported higher content of fibronectin in aged bovine NPs, which is associated with tissue fibrosis (Caldeira et al., 2017). Therefore, old NPs could be a valuable 3D model to study age-associated degenerative features of IVD pathology and their implication in the crosstalk between cells and the ECM.

To the best of our knowledge, this is the first report comparing decellularized NPs scaffolds from different aged donors. Overall, we demonstrate that donor age matters and that younger matrices have an increased potential to both induce ECM *de novo* synthesis after repopulation and to inhibit vessel formation *in vivo*. Nevertheless, some limitations of the work should be discussed envisaging future studies. Firstly, a milder and faster

decellularization protocol could be investigated to benefit scale up production and to minimize GAGs loss, such as a vacuum-assisted method. Alternatively, supplementation of decellularized matrices with chondroitin sulphate could be a promising strategy to replace lost GAGs, as described by Zhou and colleagues (Zhou et al., 2018). If not feasible, cells (either exogenous or endogenous) seeded on the ECM-based scaffolds are expected to produce GAGs *in situ*, as we have shown for ACAN, and thus compensate for their loss with decellularization.

Despite the promising results obtained after adult bovine NP cell seeding, recellularization with human cells, derived from degenerated IVDs, should be pursued in order to explore the potential of younger matrices to rejuvenate endogenous disc cells and restore a healthy ECM *in situ*, regenerating the IVD. Moreover, further *in vivo* studies should be performed to evaluate scaffolds' biocompatibility by using an adequate animal model. The use of rodent models (mice and rats) have several limitations, such as the preservation of notochordal cells, which are lost in human IVDs after birth, as well as the different disc biomechanics and size (Daly et al., 2016; Fiordalisi et al., 2021), rendering problematic the clinical relevance of the study. Therefore, chondrodystrophic (CD) dogs, that spontaneously develop IVD degeneration with aging (Daly et al., 2016), could be a better alternative. Finally, a non-disruptive sterilization method should be investigated to remove any contaminants from the scaffolds prior to *in vivo* implantation, in order to avoid a host adverse response and unwanted inflammatory reaction, while maintaining favorable biomaterial properties.

All in all, this work supports the notion that the recapitulation of a healthy and pro-regenerative microenvironment, similar to early developmental stages, is necessary and sufficient to rejuvenate native disc cells and revert the degenerative process, through ECM remodeling and angiogenesis inhibition. Moreover, old-derived decellularized NP scaffolds have the potential to be used as a novel model to study age-associated disc degeneration. Overall, we demonstrated that donor age strongly impacts on IVD cell behavior, which is of utmost importance for tissue regeneration. In the future, a deeper understanding of which developmental-associated biochemical and biomechanical ECM features influence cell behavior, is envisaged. Moreover, the creation of an injectable hydrogel from decellularized fetal ECM-based scaffolds could be a promising minimally invasive strategy to treat IVD degeneration.

5. DECLARATION OF COMPETING INTEREST

The co-authors Mário Adolfo Barbosa, Joana Caldeira, Raquel Madeira Gonçalves and Morena Francesca Fiordalisi, has a patent application for fetal decellularization procedure (WO2021118379 – 17.06.2021): “Fetal decellularized nucleus pulposus material and methods for obtaining pharmaceutic compositions to be used in the treatment of intervertebral disc degeneration and low back pain). The remaining co-authors have no conflict of interest to declare.

6. ACKNOWLEDGEMENTS

This work was supported by Fundação para a Ciência e a Tecnologia (FCT) through FETBIO project (FCT-2020-PTDC/BTM-MAT/0438/2020) and (UIDB/04293/2020) and FEedIT (EXPL/BTM-ORG/0880/2021). It was also financed by QREN and a grant (20-165) from EUROSPINE/ON Foundation. The authors would like to acknowledge FCT for their grants: FCT/DL57/2016/CP1360/CT0005-JC, PhD grant (PD/BD/135544/2018-MF). We would like to thank Daniela Silva (CEMUP) for the technical support in the Cryo-Scanning electron microscopy analysis. The authors acknowledge the support of the i3S Scientific Platform (Advanced Light Microscopy (ALM), BioSciences Screening (BS), Bioimaging, and Histology and Electron Microscopy), member of the PPBI (PPBI-POCI-01-0145-FEDER-022122). Finally, the authors would like to thank Ana Joao Silva for the help in the collection of IVD samples and in the decellularization optimization.

7. AUTHORS’ CONTRIBUTIONS

M.F.F performed the experimental work, data analysis and participated in the design of the experiments as well as prepared the manuscript. J.R.F. helped in the RNA extraction, samples collection and in the discussion of the results. M.L.P. participated in the decellularization optimization. C.R.M. helped in the optimization of histological staining and sample processing, and developed the Fiji/ImageJ macro adopted for images quantification. M.T.P. designed, performed and analyzed the *in vivo* CAM assay of decellularized matrices. M.J.O. participated in the design of the strategy. M.A.B, J.C. and R.M.G, provided the funding, participated in the design of the experiments, data analysis and interpretation of the results, as well as in the preparation of the manuscript.

8. REFERENCES

Aladin, D. M. K., Cheung, K. M. C., Ngan, A. H. W., Chan, D., Leung, V. Y. L., Lim, C. T., Luk, K. D. K., & Lu, W.W. (2010). Nanostructure of collagen fibrils in human nucleus pulposus and its correlation with macroscale tissue mechanics. Journal of Orthopaedic Research, 28(4), 497-502. https://doi.org/https://doi.org/10.1002/jor.21010

Alini, M., Eisenstein, S. M., Ito, K., Little, C., Kettler, A. A., Masuda, K., Melrose, J., Ralphs, J., Stokes, I.,& Wilke, H. J. (2008). Are animal models useful for studying human disc disorders/degeneration? European Spine Journal, 17(1), 2-19. https://doi.org/10.1007/s00586-007-0414-y

Alizadeh, M., Rezakhani, L., Soleimannejad, M., Sharifi, E., Anjomshoa, M., & Alizadeh, A. (2019). Evaluation of vacuum washing in the removal of SDS from decellularized bovine pericardium: method and device description. Heliyon, 5(8), e02253-e02253. https://doi.org/10.1016/j.heliyon.2019.e02253

Anderson, D. G., & Tannoury, C. (2005). Molecular pathogenic factors in symptomatic disc degeneration. Spine J, 5(6 Suppl), 260s-266s. https://doi.org/10.1016/j.spinee.2005.02.010

Benedetto, C. D., Barbaglio, A., Martinello, T., Alongi, V., Fassini, D., Cullorà, E., Patruno, M., Bonasoro, F., Barbosa, M. A., Carnevali, M. D. C., & Sugni, M. (2014). Production, characterization and biocompatibility of marine collagen matrices from an alternative and sustainable source: the sea urchin Paracentrotus lividus. Marine drugs, 12(9), 4912-4933. https://doi.org/10.3390/md12094912

Bustin, S. A., Benes, V., Garson, J. A., Hellemans, J., Huggett, J., Kubista, M., Mueller, R., Nolan, T., Pfaffl, M.W., Shipley, G. L., Vandesompele, J., & Wittwer, C. T. (2009). The MIQE Guidelines: Minimum Information for Publication of Quantitative Real-Time PCR Experiments. Clinical Chemistry, 55(4), 611-622. https://doi.org/10.1373/clinchem.2008.112797

Caldeira, J., Santa, C., Osório, H., Molinos, M., Manadas, B., Gonçalves, R., & Barbosa, M. (2017). Matrisome Profiling During Intervertebral Disc Development And Ageing. Scientific reports, 7(1), 11629-11629. https://doi.org/10.1038/s41598-017-11960-0

Caldeira, J., Sousa, A., Sousa, D. M., & Barros, D. (2018). 2 - Extracellular matrix constitution and function for tissue regeneration and repair. In M. A. Barbosa & M. C. L. Martins (Eds.), Peptides and Proteins as Biomaterials for Tissue Regeneration and Repair (pp. 29-72). Woodhead Publishing. https://doi.org/https://doi.org/10.1016/B978-0-08-100803-4.00002-4

Carmeli, E., Moas, M., Reznick, A. Z., & Coleman, R. (2004). Matrix metalloproteinases and skeletal muscle: A brief review [https://doi.org/10.1002/mus.10529]. Muscle & Nerve, 29(2), 191-197. https://doi.org/https://doi.org/10.1002/mus.10529

Chen, S., Chen, M., Wu, X., Lin, S., Tao, C., Cao, H., Shao, Z., & Xiao, G. (2022). Global, regional and national burden of low back pain 1990–2019: A systematic analysis of the Global Burden of Disease study 2019. Journal of Orthopaedic Translation, 32, 49-58. https://doi.org/https://doi.org/10.1016/j.jot.2021.07.005

Chen, S., Liu, S., Ma, K., Zhao, L., Lin, H., & Shao, Z. (2019). TGF-β signaling in intervertebral disc health and disease. Osteoarthritis Cartilage, 27(8), 1109-1117. https://doi.org/10.1016/j.joca.2019.05.005

Collin, E. C., Carroll, O., Kilcoyne, M., Peroglio, M., See, E., Hendig, D., Alini, M., Grad, S., & Pandit, A. (2017). Ageing affects chondroitin sulfates and their synthetic enzymes in the intervertebral disc. Signal Transduction and Targeted Therapy, 2(1), 17049. https://doi.org/10.1038/sigtrans.2017.49

Colombier, P., Clouet, J., Hamel, O., Lescaudron, L., & Guicheux, J. (2014). The lumbar intervertebral disc: from embryonic development to degeneration. Joint Bone Spine, 81(2), 125-129. https://doi.org/10.1016/j.jbspin.2013.07.012

Cramer, M. C., & Badylak, S. F. (2019). Extracellular Matrix-Based Biomaterials and Their Influence Upon Cell Behavior. Annals of Biomedical Engineering. https://doi.org/10.1007/s10439-019-02408-9

Crapo, P. M., Gilbert, T. W., & Badylak, S. F. (2011). An overview of tissue and whole organ decellularization processes. Biomaterials, 32(12), 3233-3243. https://doi.org/https://doi.org/10.1016/j.biomaterials.2011.01.057

Daly, C., Ghosh, P., Jenkin, G., Oehme, D., & Goldschlager, T. (2016). A Review of Animal Models of Intervertebral Disc Degeneration: Pathophysiology, Regeneration, and Translation to the Clinic. BioMed research international, 2016, 5952165. https://doi.org/10.1155/2016/5952165

Dou, Y., Sun, X., Ma, X., Zhao, X., & Yang, Q. (2021). Intervertebral Disk Degeneration: The Microenvironment and Tissue Engineering Strategies [Review]. Frontiers in Bioengineering and Biotechnology, 9(490) https://doi.org/10.3389/fbioe.2021.592118

Dowdell, J., Erwin, M., Choma, T., Vaccaro, A., Iatridis, J., & Cho, S. K. (2017). Intervertebral Disk Degeneration and Repair. Neurosurgery, 80(3S), S46-S54. https://doi.org/10.1093/neuros/nyw078

Fatoye, F., Gebrye, T., & Odeyemi, I. (2019). Real-world incidence and prevalence of low back pain using routinely collected data. Rheumatol Int, 39(4), 619-626. https://doi.org/10.1007/s00296-019-04273-0

Faulk, D. M., & Badylak, S. F. (2014). Chapter 8 - Natural Biomaterials for Regenerative Medicine Applications. In G. Orlando, J. Lerut, S. Soker, & R. J. Stratta (Eds.), Regenerative Medicine Applications in Organ Transplantation (pp. 101-112). Academic Press. https://doi.org/https://doi.org/10.1016/B978-0-12-398523-1.00008-2

Fernandez, C., Marionneaux, A., Gill, S., & Mercuri, J. (2016). Biomimetic nucleus pulposus scaffold created from bovine caudal intervertebral disc tissue utilizing an optimal decellularization procedure. J Biomed Mater Res A, 104(12), 3093-3106. https://doi.org/10.1002/jbm.a.35858

Ferreira, J. R., Teixeira, G. Q., Neto, E., Ribeiro-Machado, C., Silva, A. M., Caldeira, J., Leite Pereira, C., Bidarra, S., Maia, A. F., Lamghari, M., Barbosa, M. A., & Gonçalves, R. M. (2021). IL-1β-pre- conditioned mesenchymal stem/stromal cells' secretome modulates the inflammatory response and aggrecan deposition in intervertebral disc. Eur Cell Mater, 41, 431-453. https://doi.org/10.22203/eCM.v041a28

Fiordalisi, M., Silva, A. J., Barbosa, M., Gonçalves, R., & Caldeira, J. (2020). Decellularized Scaffolds for Intervertebral Disc Regeneration. Trends in Biotechnology, 38(9), 947-951. https://doi.org/https://doi.org/10.1016/j.tibtech.2020.05.002

Fiordalisi, M. F., Silva, A. J., Barbosa, M., Gonçalves, R. M., & Caldeira, J. (2021). Intervertebral disc decellularisation: progress and challenges. Eur Cell Mater, 41, 196-219. https://doi.org/10.22203/eCM.v042a15

Fu, R. H., Wang, Y. C., Liu, S. P., Shih, T. R., Lin, H. L., Chen, Y. M., Sung, J. H., Lu, C. H., Wei, J. R., Wang, Z. W., Huang, S. J., Tsai, C. H., Shyu, W. C., & Lin, S. Z. (2014). Decellularization and recellularization technologies in tissue engineering. Cell Transplant, 23(4-5), 621-630. https://doi.org/10.3727/096368914x678382

Gilbert, T. W., Sellaro, T. L., & Badylak, S. F. (2006). Decellularization of tissues and organs. Biomaterials, 27(19), 3675-3683. https://doi.org/https://doi.org/10.1016/j.biomaterials.2006.02.014

Gilpin, A., & Yang, Y. (2017). Decellularization Strategies for Regenerative Medicine: From Processing Techniques to Applications. BioMed research international, 2017,9831534-9831534. https://doi.org/10.1155/2017/9831534

Hu, S., Fu, Y., Yan, B., Shen, Z., & Lan, T. (2020). Analysis of key genes and pathways associated with the pathogenesis of intervertebral disc degeneration. Journal of Orthopaedic Surgery and Research,15(1), 371. https://doi.org/10.1186/s13018-020-01902-4

Illien-Junger, S., Sedaghatpour, D. D., Laudier, D. M., Hecht, A. C., Qureshi, S. A., & Iatridis, J. C. (2016). Development of a bovine decellularized extracellular matrix-biomaterial for nucleus pulposus regeneration. J Orthop Res, 34(5), 876-888. https://doi.org/10.1002/jor.23088

Inoue, N., & Espinoza Orías, A. A. (2011). Biomechanics of intervertebral disk degeneration. The Orthopedic clinics of North America, 42(4), 487-vii. https://doi.org/10.1016/j.ocl.2011.07.001

Jin, L., Balian, G., & Li, X. J. (2018). Animal models for disc degeneration-an update. Histology and histopathology, 33(6), 543-554. https://doi.org/10.14670/HH-11-910

Kajbafzadeh, A. M., Khorramirouz, R., Masoumi, A., Keihani, S., & Nabavizadeh, B. (2018). Decellularized human fetal intestine as a bioscaffold for regeneration of the rabbit bladder submucosa. J Pediatr Surg, 53(9), 1781-1788. https://doi.org/10.1016/j.jpedsurg.2018.01.018

Kawecki, M., Łabuś, W., Klama-Baryla, A., Kitala, D., Kraut, M., Glik, J., Misiuga, M., Nowak, M., Bielecki, T., & Kasperczyk, A. (2018). A review of decellurization methods caused by an urgent need for quality control of cell-free extracellular matrix' scaffolds and their role in regenerative medicine. Journal of Biomedical Materials Research Part B: Applied Biomaterials, 106(2), 909-923. https://doi.org/10.1002/jbm.b.33865

Keane, T. J., Swinehart, I. T., & Badylak, S. F. (2015). Methods of tissue decellularization used for preparation of biologic scaffolds and in vivo relevance. Methods, 84, 25-34. https://doi.org/https://doi.org/10.1016/j.ymeth.2015.03.005

Lehmann, T. P., Jakub, G., Harasymczuk, J., & Jagodziński, P. P. (2018). Transforming growth factor β mediates communication of co-cultured human nucleus pulposus cells and mesenchymal stem cells. J Orthop Res, 36(11), 3023-3032. https://doi.org/10.1002/jor.24106

Li, N., Xiu, L., Guan, T., Hu, Z., & Jin, Q. (2014). [EXPRESSIONS OF TRANSFORMING GROWTH FACTOR B1 AND CONNECTIVE TISSUE GROWTH FACTOR IN HUMAN LUMBAR INTERVERTEBRAL DISCS IN DIFFERENT DEGREES OF DEGENERATION]. Zhongguo Xiu Fu Chong Jian Wai Ke Za Zhi, 28(7), 891-895.

Lian, C., Gao, B., Wu, Z., Qiu, X., Peng, Y., Liang, A., Xu, C., Su, P., & Huang, D. (2017). Collagen type II is downregulated in the degenerative nucleus pulposus and contributes to the degeneration and apoptosis of human nucleus pulposus cells. Molecular medicine reports, 16(4), 4730-4736. https://doi.org/10.3892/mmr.2017.7178

Liu, X., Krishnamoorthy, D., Lin, L., Xue, P., Zhang, F., Chi, L., Linhardt, R. J., & Iatridis, J. C. (2018). Method for characterising human intervertebral disc glycosaminoglycan disaccharides using liquid chromatography-mass spectrometry with multiple reaction monitoring. Eur Cell Mater, 35, 117- 131. https://doi.org/10.22203/eCM.v035a09

Lokman, N. A., Elder, A. S. F., Ricciardelli, C., & Oehler, M. K. (2012). Chick chorioallantoic membrane (CAM) assay as an in vivo model to study the effect of newly identified molecules on ovarian cancer invasion and metastasis. International journal of molecular sciences, 13(8), 9959-9970. https://doi.org/10.3390/ijms13089959

Marcolongo, M., Sarkar, S., & Ganesh, N. (2017). 7.11 Trends in Materials for Spine Surgery. In P. Ducheyne (Ed.), Comprehensive Biomaterials II (pp. 175-198). Elsevier. https://doi.org/https://doi.org/10.1016/B978-0-08-100691-7.00269-X

Marro, J., Pfefferli, C., de Preux Charles, A.-S., Bise, T., & Jaźwińska, A. (2016). Collagen XII Contributes to Epicardial and Connective Tissues in the Zebrafish Heart during Ontogenesis and Regeneration. PLOS ONE, 11(10), e0165497. https://doi.org/10.1371/journal.pone.0165497

Marshall, K. M., Kanczler, J. M., & Oreffo, R. O. (2020). Evolving applications of the egg: chorioallantoic membrane assay and ex vivo organotypic culture of materials for bone tissue engineering. Journal of tissue engineering, 11, 2041731420942734-2041731420942734. https://doi.org/10.1177/2041731420942734

McCann, R. M., & Séguin, A. C. (2016). Notochord Cells in Intervertebral Disc Development and Degeneration. Journal of Developmental Biology, 4(1). https://doi.org/10.3390/jdb4010003

Mendibil, U., Ruiz-Hernandez, R., Retegi-Carrion, S., Garcia-Urquia, N., Olalde-Graells, B., & Abarrategi, A. (2020). Tissue-Specific Decellularization Methods: Rationale and Strategies to Achieve Regenerative Compounds. Int J Mol Sci, 21(15). https://doi.org/10.3390/ijms21155447

Mercuri, J. J., Gill, S. S., & Simionescu, D. T. (2011). Novel tissue-derived biomimetic scaffold for regenerating the human nucleus pulposus. Journal of Biomedical Materials Research Part A, 96A(2), 422-435. https://doi.org/10.1002/jbm.a.33001

Molinos, M., Almeida, C. R., Caldeira, J., Cunha, C., Gonçalves, R. M., & Barbosa, M. A. (2015). Inflammation in intervertebral disc degeneration and regeneration. Journal of the Royal Society, Interface, 12(104), 20141191-20141191. https://doi.org/10.1098/rsif.2014.1191

Molinos, M., Almeida, C. R., Gonçalves, R. M., & Barbosa, M. A. (2015). Improvement of Bovine Nucleus Pulposus Cells Isolation Leads to Identification of Three Phenotypically Distinct Cell Subpopulations. Tissue Eng Part A, 21(15-16), 2216-2227. https://doi.org/10.1089/ten.TEA.2014.0461

Nakayama, K. H., Batchelder, C. A., Lee, C. I., & Tarantal, A. F. (2011). Renal tissue engineering with decellularized rhesus monkey kidneys: age-related differences. Tissue Eng Part A, 17(23-24), 2891-2901. https://doi.org/10.1089/ten.TEA.2010.0714

Nauroy, P., Guiraud, A., Chlasta, J., Malbouyres, M., Gillet, B., Hughes, S., Lambert, E., & Ruggiero, F. (2019). Gene profile of zebrafish fin regeneration offers clues to kinetics, organization and biomechanics of basement membrane. Matrix Biology, 75-76, 82-101. https://doi.org/https://doi.org/10.1016/j.matbio.2018.07.005

Nerlich, A. G., Bachmeier, B. E., & Boos, N. (2005). Expression of fibronectin and TGF-beta1 mRNA and protein suggest altered regulation of extracellular matrix in degenerated disc tissue. Eur Spine J, 14(1), 17-26. https://doi.org/10.1007/s00586-004-0745-x

Newell, N., Little, J. P., Christou, A., Adams, M. A., Adam, C. J., & Masouros, S. D. (2017). Biomechanics of the human intervertebral disc: A review of testing techniques and results. Journal of the Mechanical Behavior of Biomedical Materials, 69, 420-434. https://doi.org/https://doi.org/10.1016/j.jmbbm.2017.01.037

Ohnishi, T., Novais, E. J., & Risbud, M. V. (2020). Alterations in ECM signature underscore multiple subphenotypes of intervertebral disc degeneration. Matrix Biology Plus, 6-7, 100036. https://doi.org/https://doi.org/10.1016/j.mbplus.2020.100036

Page-McCaw, A., Ewald, A. J., & Werb, Z. (2007). Matrix metalloproteinases and the regulation of tissue remodelling. Nature Reviews Molecular Cell Biology, 8(3), 221-233. https://doi.org/10.1038/nrm2125

Pereira, C. L., Teixeira, G. Q., Ribeiro-Machado, C., Caldeira, J., Costa, M., Figueiredo, F., Fernandes, R., Aguiar, P., Grad, S., Barbosa, M. A., & Gonçalves, R. M. (2016). Mesenchymal Stem/Stromal Cells seeded on cartilaginous endplates promote Intervertebral Disc Regeneration through Extracellular Matrix Remodeling. Scientific reports, 6(1), 33836. https://doi.org/10.1038/srep33836

Pinto, M. L., Rios, E., Silva, A. C., Neves, S. C., Caires, H. R., Pinto, A. T., Duraes, C., Carvalho, F. A., Cardoso, A. P., Santos, N. C., Barrias, C. C., Nascimento, D. S., Pinto-do, O. P., Barbosa, M. A., Carneiro, F., & Oliveira, M. J. (2017). Decellularized human colorectal cancer matrices polarize macrophages towards an anti-inflammatory phenotype promoting cancer cell invasion via CCL18. Biomaterials, 124, 211-224. https://doi.org/10.1016/j.biomaterials.2017.02.004

Ren, T., Faust, A., van der Merwe, Y., Xiao, B., Johnson, S., Kandakatla, A., Gorantla, V. S., Badylak, S. F., Washington, K. M., & Steketee, M. B. (2018). Fetal extracellular matrix nerve wraps locally improve peripheral nerve remodeling after complete transection and direct repair in rat. Scientific reports,8(1), 4474. https://doi.org/10.1038/s41598-018-22628-8

Rohrs, J. A., Sulistio, C. D., & Finley, S. D. (2016). Predictive model of thrombospondin-1 and vascular endothelial growth factor in breast tumor tissue. npj Systems Biology and Applications, 2(1), 16030. https://doi.org/10.1038/npjsba.2016.30

Schmitt, A., Csiki, R., Tron, A., Saldamli, B., Tübel, J., Florian, K., Siebenlist, S., Balmayor, E., & Burgkart, R. (2017). Optimized protocol for whole organ decellularization. European journal of medical research, 22(1), 31-31. https://doi.org/10.1186/s40001-017-0272-y

Schönborn, K., Willenborg, S., Schulz, J. N., Imhof, T., Eming, S. A., Quondamatteo, F., Brinckmann, J., Niehoff, A., Paulsson, M., Koch, M., Eckes, B., & Krieg, T. (2020). Role of collagen XII in skin homeostasis and repair. Matrix Biol, 94, 57-76. https://doi.org/10.1016/j.matbio.2020.08.002

Schutgens, E. M., Tryfonidou, M. A., Smit, T. H., Öner, F. C., Krouwels, A., Ito, K., & Creemers, L. B. (2015). Biomaterials for intervertebral disc regeneration: past performance and possible future strategies. Eur Cell Mater, 30, 210-231. https://doi.org/10.22203/ecm.v030a15

Shiri, R., Falah-Hassani, K., Heliövaara, M., Solovieva, S., Amiri, S., Lallukka, T., Burdorf, A., HusgafvelPursiainen, K., & Viikari-Juntura, E. (2019). Risk Factors for Low Back Pain: A Population-Based Longitudinal Study. Arthritis Care & Research, 71(2), 290-299. https://doi.org/10.1002/acr.23710

Sicari, B. M., Johnson, S. A., Siu, B. F., Crapo, P. M., Daly, K. A., Jiang, H., Medberry, C. J., Tottey, S., Turner, N. J., & Badylak, S. F. (2012). The effect of source animal age upon the in vivo remodelling characteristics of an extracellular matrix scaffold. Biomaterials, 33(22), 5524-5533. https://doi.org/https://doi.org/10.1016/j.biomaterials.2012.04.017

Silva, A. C., Rodrigues, S. C., Caldeira, J., Nunes, A. M., Sampaio-Pinto, V., Resende, T. P., Oliveira, M. J., Barbosa, M. A., Thorsteinsdóttir, S., Nascimento, D. S., & Pinto-do-Ó, P. (2016). Three-dimensional scaffolds of fetal decellularized hearts exhibit enhanced potential to support cardiac cells in comparison to the adult. Biomaterials, 104, 52-64. https://doi.org/https://doi.org/10.1016/j.biomaterials.2016.06.062

Sivan, S. S., Wachtel, E., & Roughley, P. (2014). Structure, function, aging and turnover of aggrecan in the intervertebral disc. Biochim Biophys Acta, 1840(10), 3181-3189. https://doi.org/10.1016/j.bbagen.2014.07.013

Smith, L. J., Nerurkar, N. L., Choi, K.-S., Harfe, B. D., & Elliott, D. M. (2011). Degeneration and regeneration of the intervertebral disc: lessons from development. Disease Models & Mechanisms, 4(1), 31-41. https://doi.org/10.1242/dmm.006403

Stamenkovic, I. (2003). Extracellular matrix remodelling: the role of matrix metalloproteinases [https://doi.org/10.1002/path.1400]. The Journal of Pathology, 200(4), 448-464. https://doi.org/https://doi.org/10.1002/path.1400

Stergar, J., Gradisnik, L., Velnar, T., & Maver, U. (2019). Intervertebral disc tissue engineering: A brief review. Bosnian journal of basic medical sciences, 19(2), 130-137. https://doi.org/10.17305/bjbms.2019.3778

Tan, Y., Hu, Y., & Tan, J. (2003). Extracellular matrix synthesis and ultrastructural changes of degenerative disc cells transfected by Ad/CMV-hTGF-beta 1. Chin Med J (Engl), 116(9), 1399-1403.

Taylor, D. A., Lee, P.-F., Barac, Y., Hochman-Mendez, C., & Sampaio, L. C. (2020). Chapter 15 - Decellularization of whole hearts for cardiac regeneration. In U. Nussinovitch (Ed.), Emerging Technologies for Heart Diseases (pp. 291-310). Academic Press. https://doi.org/https://doi.org/10.1016/B978-0-12-813706-2.00015-4

Teixeira, G. Q., Boldt, A., Nagl, I., Pereira, C. L., Benz, K., Wilke, H.-J., Ignatius, A., Barbosa, M. A., Gonçalves, R. M., & Neidlinger-Wilke, C. (2016). A Degenerative/Proinflammatory Intervertebral Disc Organ Culture: An Ex Vivo Model for Anti-inflammatory Drug and Cell Therapy. Tissue Eng Part C Methods, 22 1, 8-19.

Tomaszewski, K. A., Saganiak, K., Gladysz, T., & Walocha, J. A. (2015). The biology behind the human intervertebral disc and its endplates. Folia Morphol (Warsz), 74(2), 157-168. https://doi.org/10.5603/fm.2015.0026

Urban, J. P. G., & Fairbank, J. C. T. (2020). Current perspectives on the role of biomechanical loading and genetics in development of disc degeneration and low back pain; a narrative review. Journal of Biomechanics, 102, 109573. https://doi.org/https://doi.org/10.1016/j.jbiomech.2019.109573

van Uden, S., Silva-Correia, J., Oliveira, J. M., & Reis, R. L. (2017). Current strategies for treatment of intervertebral disc degeneration: substitution and regeneration possibilities. Biomaterials Research, 21(1), 22. https://doi.org/10.1186/s40824-017-0106-6

Vo, N. V., Hartman, R. A., Yurube, T., Jacobs, L. J., Sowa, G. A., & Kang, J. D. (2013). Expression and regulation of metalloproteinases and their inhibitors in intervertebral disc aging and degeneration. Spine J, 13(3), 331-341. https://doi.org/10.1016/j.spinee.2012.02.027

Wang, T., Nanda, S. S., Papaefthymiou, G. C., & Yi, D. K. (2020). Mechanophysical Cues in Extracellular Matrix Regulation of Cell Behavior. Chembiochem, 21(9), 1254-1264. https://doi.org/10.1002/cbic.201900686

Wehner, D., Tsarouchas, T. M., Michael, A., Haase, C., Weidinger, G., Reimer, M. M., Becker, T., & Becker, C. G. (2017). Wnt signaling controls pro-regenerative Collagen XII in functional spinal cord regeneration in zebrafish. Nature Communications, 8(1), 126. https://doi.org/10.1038/s41467-017-00143-0

Whatley, B. R., & Wen, X. (2012). Intervertebral disc (IVD): Structure, degeneration, repair and regeneration. Materials Science and Engineering: C, 32(2), 61-77. https://doi.org/https://doi.org/10.1016/j.msec.2011.10.011

Woods, B. I., Sowa, G., Vo, N., & Kang, J. D. (2010). A Change in Strategy: The Use of Regenerative Medicine and Tissue Engineering to Augment the Course of Intervertebral Disc Degeneration. Operative Techniques in Orthopaedics, 20(2), 144-153. https://doi.org/https://doi.org/10.1053/j.oto.2009.10.009

Woods, T., & Gratzer, P. F. (2005). Effectiveness of three extraction techniques in the development of a decellularized bone–anterior cruciate ligament–bone graft. Biomaterials, 26(35), 7339-7349. https://doi.org/https://doi.org/10.1016/j.biomaterials.2005.05.066

Wu, A., March, L., Zheng, X., Huang, J., Wang, X., Zhao, J., Blyth, F. M., Smith, E., Buchbinder, R., & Hoy, D. (2020). Global low back pain prevalence and years lived with disability from 1990 to 2017: estimates from the Global Burden of Disease Study 2017. Annals of Translational Medicine, 8(6),299. https://doi.org/10.21037/atm.2020.02.175

Xu, H., Xu, B., Yang, Q., Li, X., Ma, X., Xia, Q., Zhang, Y., Zhang, C., Wu, Y., & Zhang, Y. (2014). Comparison of decellularization protocols for preparing a decellularized porcine annulus fibrosus scaffold. PLOS ONE, 9(1), e86723. https://doi.org/10.1371/journal.pone.0086723

Yang, X., & Li, X. (2009). Nucleus pulposus tissue engineering: a brief review. European spine journal: official publication of the European Spine Society, the European Spinal Deformity Society, and the European Section of the Cervical Spine Research Society, 18(11), 1564-1572. https://doi.org/10.1007/s00586-009-1092-8

Yang, Y., He, X., Li, Y., Feng, J., Pang, H., Wang, J., & Liu, Q. (2012). [Association of transforming growth factor-β1 with pathological grading of intervertebral disc degeneration]. Nan Fang Yi Ke Da Xue Xue Bao, 32(6), 897-900.

Yee, A., Lam, M. P., Tam, V., Chan, W. C., Chu, I. K., Cheah, K. S., Cheung, K. M., & Chan, D. (2016). Fibroticlike changes in degenerate human intervertebral discs revealed by quantitative proteomic analysis. Osteoarthritis Cartilage, 24(3), 503-513. https://doi.org/10.1016/j.joca.2015.09.020

Yuan, M., Yeung, C. W., Li, Y. Y., Diao, H., Cheung, K. M. C., Chan, D., Cheah, K., & Chan, P. B. (2013). Effects of nucleus pulposus cell-derived acellular matrix on the differentiation of mesenchymal stem cells. Biomaterials, 34(16), 3948-3961. https://doi.org/10.1016/j.biomaterials.2013.02.004

Zhang, F., Liu, X., Li, B., Li, Z., Grad, S., Chen, D., Gao, M., & Liu, S. (2021). The effect of hyaluronic acid on nucleus pulposus extracellular matrix production through hypoxia-inducible factor-1α transcriptional activation of CD44 under hypoxia. Eur Cell Mater, 41, 142-152. https://doi.org/10.22203/eCM.v041a10

Zhou, X., Wang, J., Huang, X., Fang, W., Tao, Y., Zhao, T., Liang, C., Hua, J., Chen, Q., & Li, F. (2018). Injectable decellularized nucleus pulposus-based cell delivery system for differentiation of adipose- derived stem cells and nucleus pulposus regeneration. Acta Biomater, 81, 115-128. https://doi.org/10.1016/j.actbio.2018.09.044

CHAPTER V

CHAPTER V – SUPPLEMENTARY DATA

THE IMPACT OF MATRIX AGE ON INTERVERTEBRAL DISC REGENERATION

Published in Biomaterial Advances

doi: 10.1016/j.bioadv.2022.213192

SUPPLEMENTARY DATA

SUPPLEMENTARY FIGURE 1 - OPTIMIZATION OF STORAGE METHODS FOR THE DECELLULARIZED MATRICES.

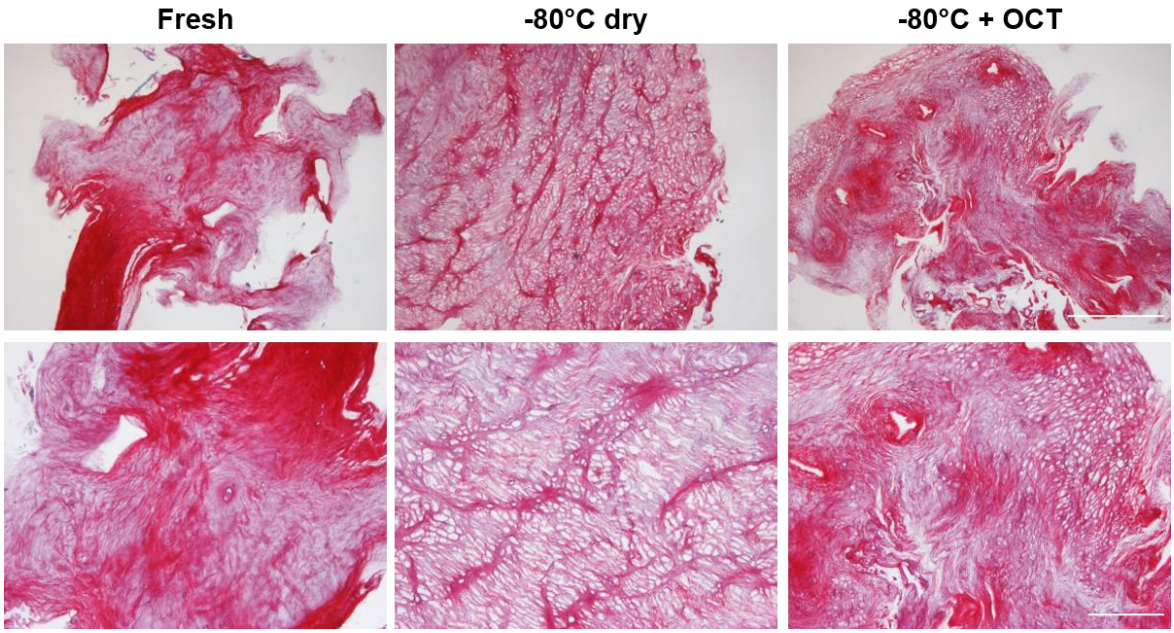

Supplementary Figure 1. Evaluation of several freezing methods of decellularized young matrices, in comparison with fresh tissue, by Alcian Blue and Picro-Sirius Red staining. Upper images: magnification 5x and scale bar 500 µm. Lower images: magnification 10x and scale bar 200 µm.

SUPPLEMENTARY FIGURE 2 - NUCLEAR STAINING OF NATIVE AND DECELLULARIZED NPS.

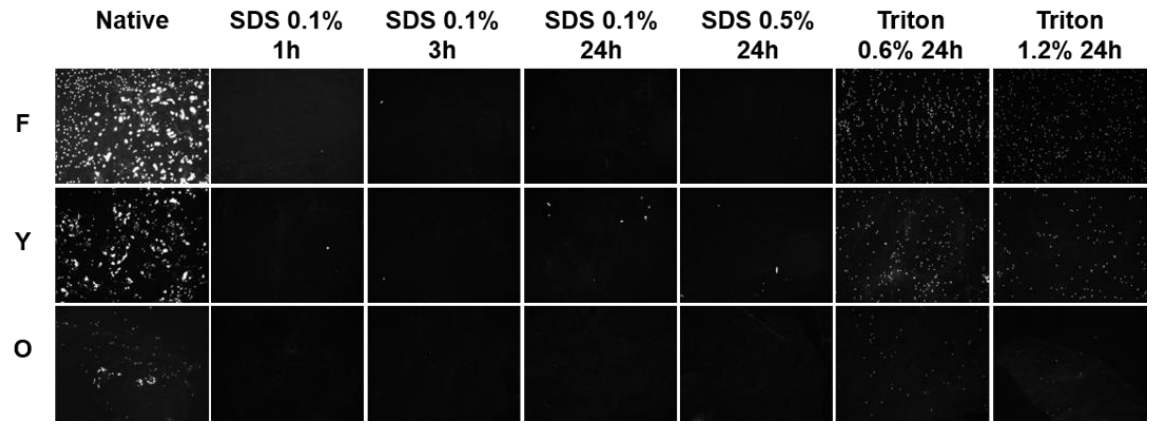

Supplementary Figure 2. Evaluation of cell removal by DAPI staining in NPs from different aged donors, decellularized with different protocols. Magnification 5x.

SUPPLEMENTARY FIGURE 3 - SOLUBLE COLLAGEN CONTENT IN DECELLULARIZED NPS.

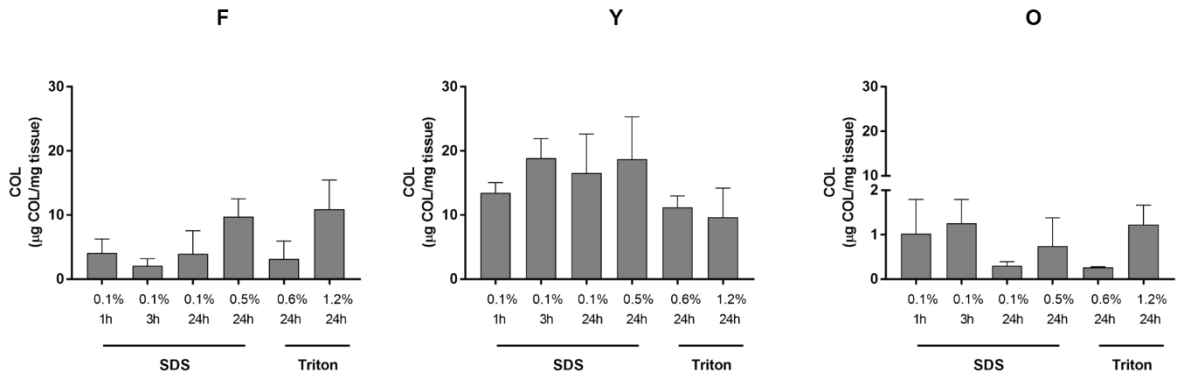

Supplementary Figure 3. Quantification of soluble collagen by Sircol Soluble Collagen Assay in fetus (F), young (Y) and old (O) NPs after decellularization with different experimental methods. Error bars represent mean ± SEM (n=3). Kruskal – Wallis test followed by Dunn's multiple comparison test.

SUPPLEMENTARY FIGURE 4 - AGGRECAN PROTEIN EXPRESSION IN NON-REPOPULATED DECELLULARIZED NPS.

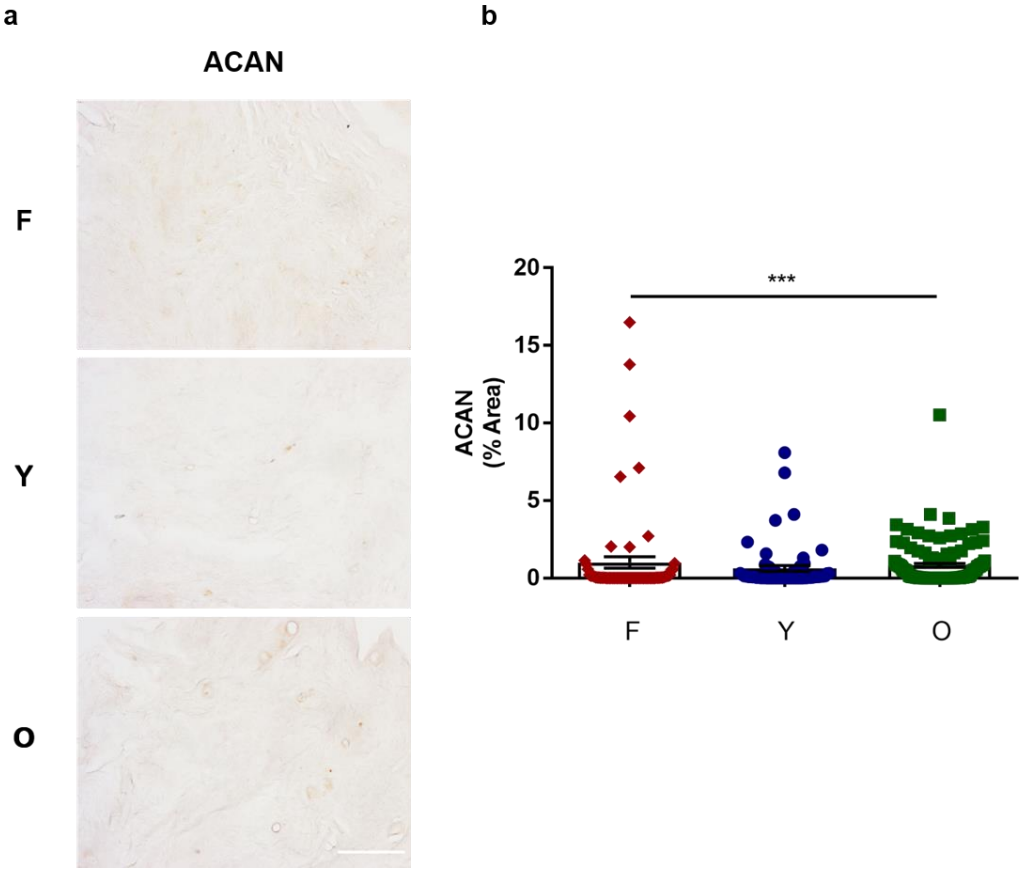

Supplementary Figure 4. (a) Representative images of aggrecan (ACAN) immunohistochemistry (IHC) from fetus (F), young (Y) and old (O) decellularized control matrices. Magnification 20x; scale bar: 100 µm. **(b)** ACAN (n=7 to 8) percentage area quantification of F, Y and O decellularized control NPs, obtained by Fiji/ImageJ. Error bars represent mean ± SEM. Kruskal – Wallis test followed by Dunn's multiple comparison test. ***p<0.001.

SUPPLEMENTARY FIGURE 5 - COLLAGEN TYPE II PROTEIN EXPRESSION IN NON-REPOPULATED DECELLULARIZED NPS AND MMP-MEDIATED MATRIX REMODELING AFTER REPOPULATION.

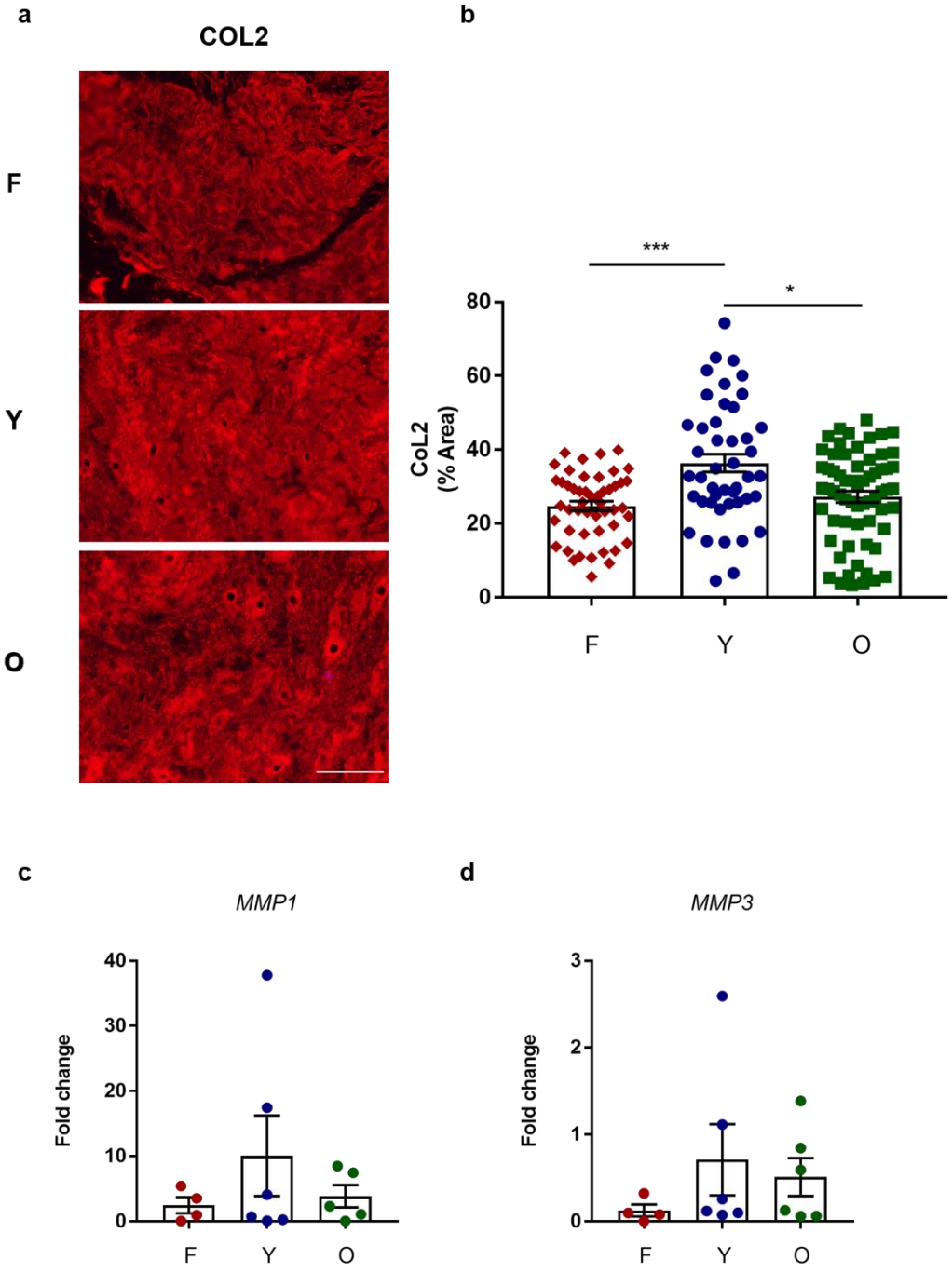

Supplementary Figure 5. (a) Representative images of Collagen type 2 (COL2) immunofluorescence (IF) of fetus (F), young (Y) and old (O) decellularized control matrices. Magnification 20x; scale bar: 100 µm. **(b)** COL2 IF (n=4 to 6) percentage area quantification of F, Y and O decellularized NPs, obtained by Fiji/ImageJ. Error bars represent mean ± SEM. Kruskal – Wallis test followed by Dunn's multiple comparison test. *p<0.05, ***p<0.001. **(c)** mRNA expression level of metalloproteinase 1 (*MMP1*) and **(d)** metalloproteinase 3 (*MMP3*) obtained by quantitative real-time PCR from F, Y and O repopulated NPs after 7 days of *ex vivo* culture. Fold change to organ culture (native NPs cultured *ex vivo* for 7 days). Error bars represent mean ± SEM (n= 4 to 6).

SUPPLEMENTARY FIGURE 6 - COLLAGEN TYPE I PROTEIN EXPRESSION AND BIREFRINGENCY ANALYSIS IN NON-REPOPULATED DECELLULARIZED NPS.

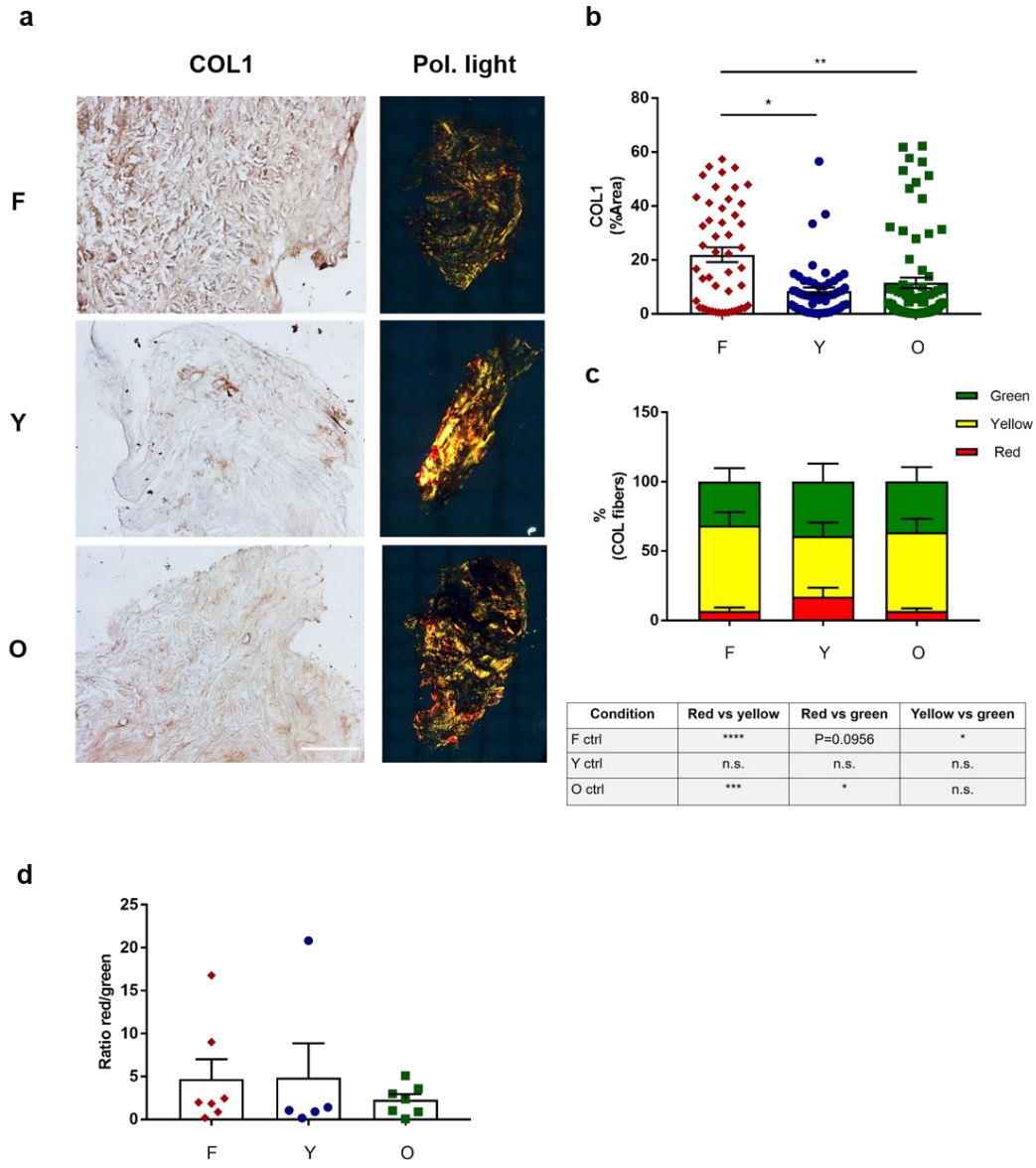

Condition	Red vs yellow	Red vs green	Yellow vs green
F ctrl	****	P=0.0956	*
Y ctrl	n.s.	n.s.	n.s.
O ctrl	***	*	n.s.

Supplementary Figure 6. (a) Representative images of Collagen type 1 (COL1) IHC and Picro-Sirius Red staining under polarized light obtained from fetus (F), young (Y), and old (O) decellularized matrices. Magnification 20x; scale bar: 100 µm. **(b)** COL1 (n=7) percentage area quantification of F, Y and O decellularized NPs, obtained by Fiji/ImageJ. Error bars represent mean ± SEM. Kruskal – Wallis test followed by Dunn's multiple comparison test. *p<0.05; **p<0.01. **(c)** Quantification of collagen fibers relative percentage (n=6 to 8), acquired by Fiji/ImageJ. Error bars represent mean ± SEM. Two-Way Anova followed by Tukey's multiple comparison test. Table reports the statistical differences between % Collagen (COL) fibers of each aged group: *p<0.05; ***p<0.001; ****p<0.0001; n.s: not significant. **(d)** Ratio of thicker/thinner (red/green) collagen fibers (n=5 to 7) in F, Y and O decellularized NPs. Error bars represent mean ± SEM. Kruskal – Wallis test followed by Dunn's multiple comparison test.

CHAPTER VI

CHAPTER VI – DISCLOSE THE MECHANISM BEHIND THE ENHANCED IVD REGENERATIVE POTENTIAL OF FETAL DECELLULARIZED MATRICES

The content of this chapter was not published.

ABSTRACT

The intervertebral disc (IVD) is an avascular tissue and the presence of neo-angiogenesis, which occurs with degeneration, is associated with inflammatory and immune cells migration, leading to pain. Recently, we have obtained decellularized extracellular matrix (ECM)-based biomaterials from bovine nucleus pulposus (NP) of different donor ages (fetus, young and old). Through *in vitro* assays with bovine NP cell cultures and an *in vivo* chick embryo chorioallantoic membrane (CAM) assay, we have detected enhanced *de novo* matrix synthesis by bovine NP cells and a superior anti-angiogenic potential of fetus decellularized NPs. However, an increased inflammation score was also observed in the fetal matrices, when compared to young and old ones. Therefore, here we aim to go further and investigate the mechanisms behind the enhanced IVD regenerative potential of fetal ECM decellularized matrices.

For that, we investigated the mechanism behind the increased ECM production in fetal decellularized NPs by blocking CD44 in bovine NP cells prior to cell seeding on the top of NP-based scaffolds. After 7 days of *ex vivo* culture, Hematoxylin&Eosin (H&E) staining, as well as Aggrecan (ACAN) and SRY-box transcription factor 9 (Sox9) immunohistochemistry (IHC) were performed in order to unravel factors involved in this specific process. Next, we have focused on understanding the molecules involved in the pro-inflammatory and anti-angiogenic responses, previously observed in fetal scaffolds. Thus, we evaluated inflammatory cytokines, angiogenic factors and other molecules in the conditioned media from decellularized NPs of different donor ages, after 3 days of *ex vivo* culture, by using a commercial semi-quantitative bovine array. Furthermore, we validated the anti-angiogenic potential of fetal matrices with human NP cells. For that, we performed an *in vivo* CAM assay with decellularized NPs of different donor ages seeded with human immortalized NP (iNP) cells. Finally, we evaluated cells infiltration (both inflammatory and blood cells) inside the scaffolds, as well as glycosaminoglycans (GAGs) production by seeded cells, by histological analysis.

As a result, no major differences were detected in terms of Sox9 and ACAN protein content in fetal matrices seeded with CD44-knockout cells, when compared to the CD44-wildtype cells (without blocking). Regarding the cytokine array, conditioned media from decellularized NPs of different ages did not show significant changes of inflammatory and angiogenic cytokines between ages. After *in vivo* CAM assay, fetal matrices were the only ones that did not exhibit a significant increase in neovessels number after human iNP cell

seeding, therefore preserving an anti-angiogenic potential. Moreover, iNP cells seeded on the top of fetal decellularized NPs were able to produce GAGs, which was detected by Alcian Blue and Picro-Sirius Red staining, which was not observed in young and old ones.

Overall, this work provides a preliminary understanding of the mechanisms that may be responsible for the enhanced pro-regenerative potential of fetal matrices. Moreover, it gave a first comprehension of inflammatory response in bovine decellularized-based biomaterials, opening the door for the evaluation of host response in other animal models more appropriate to evaluate inflammation. Finally, it constitutes the first *in vivo* proof-of-concept of the anti-angiogenic potential of fetal matrices with human IVD cells.

1. MATERIAL AND METHODS

1.1. CD44-BLOCKING IN FETAL REPOPULATED MATRICES

Fetal (~8 months of gestation) bovine tails were obtained from local abattoirs (Carnes Landeiro, Barcelos, Portugal) within 2 h of animal sacrifice, under the approval of the Portuguese National Authority for Animal Health, and transported at the lab on ice. Fetal nucleus pulposus (NPs) were isolated from bovine intervertebral disc (IVDs) and decellularized by using an optimal protocol (Sodium dodecyl sulphate [SDS] 0.1 %, 1 h), as previously optimized (Fiordalisi et al., 2022).

Fresh NPs cells were isolated from adult bovine IVDs by adopting a collagenase-based digestion (Fiordalisi et al., 2022) and used for the repopulation of fetal decellularized matrices. Prior to cell seeding, fresh bovine NP cells were re-suspended in IVD culture media, composed by Dulbecco's modified Eagle's medium (DMEM, Gibco) with low glucose, supplemented with 1 % *v*/v of Penicillin/Streptomycin (P/S, Invitrogen), 0.5 % *v/v* of Amphotericin B (Capricorn Scientific), 1.5 % *v/v* of 5 M NaCl/0.4 M KCl solution, 5 % *v/v* of fetal bovine serum (FBS, Biowest) and supplemented with 10 µg/mL of CD44-blocking antibody (CD44 Ab, Hermes-1, NBP2-22530, Bio-Techne), in order to neutralize CD44 in the cells. For repopulation, NP cells were seeded on the decellularized fetal matrices by adopting a scaffold turnover method, as previously optimized (Fiordalisi et al., 2022). Decellularized fetal scaffolds seeded with wildtype bovine NP cells (without CD44 blocking), as well as decellularized NPs (without cell seeding), were used as experimental control. All the scaffolds were cultured *ex vivo* for 7 days, under humidified and hypoxia conditions (5% O_2 and 8.5 % CO_2).

During *ex vivo* culture, media was changed at day 1 and 3 and re-supplemented with 10 µg/mL of CD44-blocking antibody in order to ensure a constant neutralization of the protein of interest. After 7 days of *ex vivo* culture, all NP-based scaffolds were fixed in 10% formalin (Bio-Optica) overnight and transferred in Phosphate-buffered saline (PBS) to be processed for paraffin embedding. Hematoxylin & Eosin (H&E) staining and immunohistochemistry (IHC) for SRY-box transcription factor 9 (Sox9) and aggrecan (ACAN) were performed in sections of 5 µm to evaluate the CD44 blocking's efficiency.

1.2. HISTOLOGICAL STAINING

For H&E staining, sections were incubated in hematoxylin for 3 min followed by eosin for 1 min.

For IHC, antigen retrieval was performed by using 20 µg/mL of Proteinase K solution for 15 min at 37 °C for both Sox9 and ACAN. The NovolinkTM Polymer Detection Kit (Leica Biosystems), was used to perform the IHC, following manufacturer's instructions. Sections were incubated overnight at 4 °C with the optimally diluted primary antibodies: Sox9 (dilution: 1:500; anti-Sox9 polyclonal antibody, NBP2-24659, Biotechne) and ACAN (dilution: 1:750; anti-ACAN monoclonal antibody BC-3; MA3–16888; Invitrogen). After, slides were incubated for 5 min in DAB working solution and counterstained with Gill's Hematoxylin (Thermo Fisher Scientific) for 6 min, washed in running tap water, dehydrated and mounted with Entellan (Merck). Images were acquired at optical microscope (Zeiss) at 20x objective.

1.3. INFLAMMATION SCORE OF DECELLULARIZED NPS ASSESSED THROUGH AN *IN VIVO* CAM ASSAY

The inflammation score of decellularized bovine NPs of different donor ages (fetus, young and old), was assessed after the *in vivo* chick embryo chorioallantoic membrane (CAM) assay, performed in the Chapter IV of this thesis (Fiordalisi et al., 2022). At embryonic day 13, CAMs were fixed with 10 % of neutral buffered formalin, excised from the embryo and photographed *ex ovo* under a stereoscope, at 20× magnification (Olympus, SZX16 coupled with a DP71 camera). Pictures were used for the quantification of new vessels growth towards the site of scaffold implantation in order to evaluate the angiogenic response (Fiordalisi et al., 2022), as well as to analyze the inflammatory response.

The inflammatory score was assessed by a qualitative observation of the scaffold inside the inoculation site in a blind fashion way, as previously described (Coelho et al., 2020; Loureiro et al., 2019). Briefly, the appearance of a clear dense area around the scaffolds, suggestive of a consistent inflammatory response, was reported by score 2. The absence of a dense area around the scaffold was a sign of absent inflammation and was reported by score 0. When the dense zone was less evident but present next to the scaffolds, the attributed score was 1. Examples of decellularized NPs from different donor

ages implanted in the CAMs with score 0, 1 and 2 are reported in Figure 3a. The percentage of inflammatory score was calculated by dividing the number of scaffolds with the specific score by the total number of scaffolds per age group. The number of samples/eggs used for the experimental assay were: 19 for fetus NPs, 21 for young NPs, 18 for old NPs, 11 for H_2O and 10 for basic fibroblast growth factor 2 ($bFGF_2$).

1.4. COLLECTION AND PREPARATION OF *EX VIVO* DECELLULARIZED AND REPOPULATED NPS CONDITIONED MEDIA FOR CYTOKINE ARRAY ANALYSIS

For cytokine array analysis**,** the conditioned media was collected from the decellularized and repopulated matrices of different donor ages, after performing the recellularization experiments reported in the Chapter IV of this thesis (Fiordalisi et al., 2022). Briefly, decellularized NPs from fetus, young and old animals were maintained in culture for 7 days in IVD culture medium, under humidified and hypoxia conditions (5 % O_2 and 8.5 % CO_2). In parallel, decellularized NPs from different donor ages repopulated with bovine NP cells were also cultured *ex vivo* for 7 days, as reported in (Fiordalisi et al., 2022). Conditioned media from both decellularized and repopulated NPs was changed and collected at day 1, 3 and 7 of *ex vivo* culture and stored at -80°C for further studies. For the cytokine array analysis, conditioned media derived from day 3 of *ex vivo* culture were centrifuged at 13.000 rpm and 4 °C for 5 min in order to remove cell debris, and supernatants were collected and stored at -20 °C.

For decellularized NPs, conditioned media derived from three biological replicates of three independent experiments, were pooled together for each of the aged donors (fetus, young and old) for a total of n=2 samples. For repopulated NPs, conditioned media derived from six technical replicates, were pulled together for each of the aged donors (fetus, young and old) for a total of n=3 biological replicates. Afterwards, conditioned media, with an initial volume of 330 µL, was concentrated by using SpeedVac vacuum concentrator (Thermo Scientific™) at 37 °C for around 25 min. The final volume of the concentrated samples was 160/170 µL. Finally, concentrated samples were stored at -20 °C until cytokine array analysis.

1.5. CYTOKINE ARRAY

Cytokine analysis was performed by using a commercially available array kit (G-Series Bovine Cytokine Array 30, Ray Biotech), according to the manufactures' instructions. This array consisted in a combination of 3 non-overlapping glass slide-based antibody arrays, which is able to measure the relative expression levels of 30 bovine cytokines. Conditioned media derived from both decellularized and repopulated NPs of different donor ages, were diluted 2x with sample diluent, provided by the kit, to minimize the background of the medium-containing serum. Moreover, IVD culture medium was also diluted 2x and included in the analysis as a control. After the procedure, slides were completely dried by using compressed N_2 stream and stored at 4 °C. Ray Biotech company measured the fluorescence intensity of the array, by using a specific laser scanner. The company also performed data analysis. Samples resulted stable to conditions of the test. Row data were normalized by the positive control of the reference array, which was arbitrarily defined by the company. For data analysis, the fluorescence value of the media was subtracted from the fluorescence values of each sample, in order to remove the cytokine background of the media. For repopulated NPs, fluorescence values of the decellularized matrices were subtracted from the fluorescence of each sample in order to consider only the cytokine produced by seeded cells. Data are presented in fluorescence intensity.

1.6. IMMORTALIZED NUCLEUS PULPOSUS CELL CULTURE

Human immortalized NP (iNP) cells (clone GA094 and clone GA111) were obtained from Tim Welting's group (CAPHRI/Orthopedic surgery of the Faculty of Health Medicine and Life Sciences) in dry ice and stored in the biobank under liquid nitrogen. Specifically, iNP cells were obtained from healthy human disc as excess material from correction surgery, and immortal clones were generated by retroviral transduction (van den Akker et al., 2014). The differences in the two clones are reported in Table 1 (van den Akker et al., 2020).

iNP cells were unfrozen and maintained in culture in Dulbecco's Modified Eagle Medium/Nutrient Mixture F-12 (DMEM/F12, Alfagene) supplemented with 10 % *v/v* FBS (Biowest), 1 % *v/v* P/S (Invitrogen), 1 % *v/v* non-essential amminoacid (NEEA), until they reached confluency. Then, cells were trypsinized, counted and used for the *in vivo* CAM assay.

Table 1. Immortalized nucleus pulposus cells.

Clone	Code clone	Features
GA111	DISC hTERT of SV40 clones 105 nR GA111	CD24 Non-Responder
GA094	DISC hTERT of SV40 clones 114 GA094	CD24 - Responder

1.7. *IN OVO* EVALUATION OF HUMAN iNPS CELLS ANGIOGENIC POTENTIAL

A first *in vivo* CAM assay was conducted to analyze the angiogenic capacity of human iNP cells from different clones (GA094: clone 1 and GA111: clone 2). Fertilized chick (*Gallus gallus*), were obtained from commercial source and incubated at 37.8 °C under humified atmosphere, as described in (Fiordalisi et al., 2022). At embryonic day 10, a silicone ring was placed on the top of the CAM under sterile conditions. Then, $1x10^5$ cells of each clone were resuspended in 5 µL of culture media and inoculated inside the ring. The eggs were then re-sealed and returned to the incubator. At embryonic day 13, CAMs were processed for neovessel quantification as described in 1.3 and (Fiordalisi et al., 2022).

Human iNP cells from clone GA094 were selected as those inducing a higher angiogenic response. As so, they were used for another *in vivo* CAM assay screening by using a higher cell density ($5x10^5$) in order to potentiate the angiogenic response. Also, in this case, vessel number was quantified to evaluate the angiogenic capacity.

1.8. ANGIOGENIC *IN OVO* ASSESSMENT OF DECELLULARIZED NUCLEUS PULPOSUS FROM DIFFERENT DONOR AGE WITH HUMAN IMMORTALIZED NUCLEUS PULPOSUS CELLS

Fetus, young and old bovine NPs were decellularized as in (Fiordalisi et al., 2022) and stored in PBS overnight at 4 °C, prior to *in vivo* CAM assay. Human iNP cells (clone GA094) were trypsinized, counted and $4x10^5$ cells were resuspended in 5 µL of fresh culture medium, prior to inoculation in the CAMs. At embryonic day 10, decellularized NPs from

different donor ages were implanted inside the silicone ring of the CAMs and human iNP cells were seeded on top. Moreover, a group of eggs was inoculated only with human iNP cells, and used as control. Then, eggs were re-sealed and incubated at 37 °C. At embryonic day 13, the CAMs were fixed in 10 % of neutral buffered formalin and neovessels were quantified as described in 1.3 and (Fiordalisi et al., 2022). Two independent experiments were performed. H_2O and $bFGF_2$ were used as negative and positive controls, respectively.

A schematic representation of the experimental strategy for the *in vivo* CAM assay is reported in the following scheme (Figure 1).

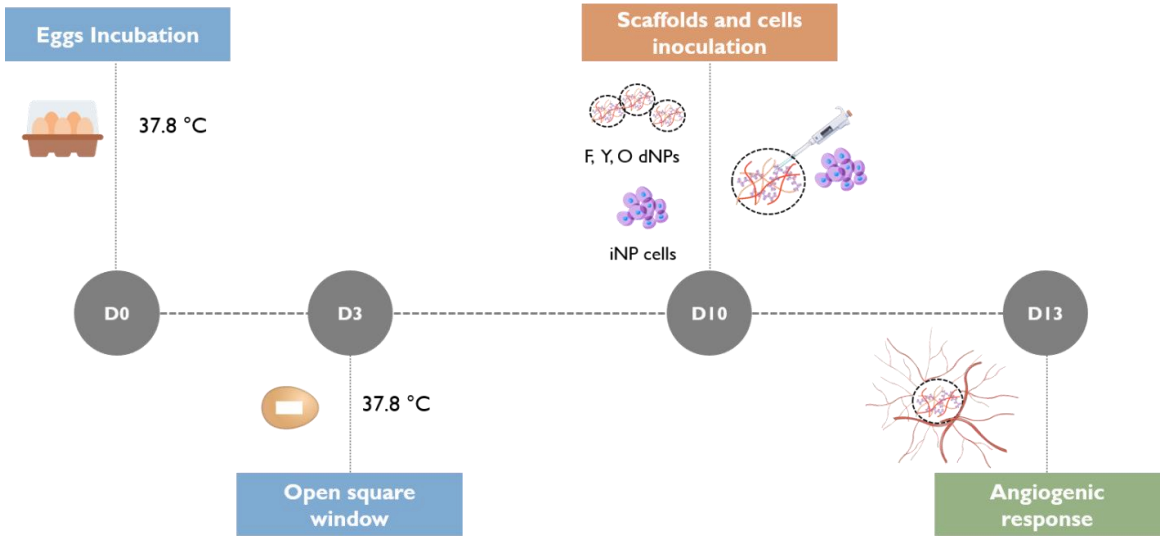

Figure 1. Schematic workflow of the experimental procedure for *in vivo* CAM assay of decellularized NPs from different donor ages in combination with human iNP cells.

1.9. HISTOLOGICAL EVALUATION OF CAMS

CAMs were excised from the eggs, fixed in 10 % neutral buffered/formalin (Bio-Optica) overnight and embedded in paraffin. H&E (to evaluate the sample morphology) and Alcian Blue/Picro-Sirius Red (to specifically stain glycosaminoglycans [GAGs]: blue and Collagen [COL]: red) staining were performed in sections of 5 µm. Histological processing as well as the staining were conducted by Histology and Electron Microscopy (HEMS) Scientific Platform at Instituto de Investigação e Inovação em Saúde da Universidade do Porto (i3S, Porto, Portugal). Pictures from sections stained with H&E and Alcian Blue/Picro-

Sirius Red were acquired at 5x and 20x magnification. Finally, a qualitative analysis of the sections stained with H&E was performed, analyzing the following parameters:

- Presence/absence of the decellularized scaffold
- Presence/absence of inflammatory cells
- Presence/absence of blood cells inside the scaffold

Data were presented as a percentage score, obtained by dividing the number of scaffolds with presence of scaffold and/or inflammatory and/or blood cells by the total number of scaffolds per age.

1.10. STATISTICAL ANALYSIS

Statistical analysis was performed using Kruskal-Wallis test followed by Dunn's multiple comparison test in GraphPad Prism Software 7.03. Data were reported as average ± Standard Error of the Mean (SEM). Values from $p \leq 0.05$ were considered statistically significant.

2. RESULTS

2.1. FETAL MATRICES SEEDED WITH BOVINE CD44-KNOCKOUT NP CELLS DID NOT EXHIBIT SIGNIFICANT DIFFERENCES IN PROTEIN EXPRESSION.

In order to evaluate changes of Sox9 expression along ageing, we firstly performed an IHC in repopulated and decellularized matrices (experimental controls) from different donor ages. After 7 days of *ex vivo* culture, fetus and young matrices seemed to have an increased number of positive cells for Sox9 (brown staining), when compared to old ones. Therefore, seeded cells appeared to produce higher amount of Sox9 when in contact with younger NP-based scaffolds. Decellularized matrices from different donor ages did not exhibit significant staining, indicating absence of Sox9 (Figure 2a).

Afterwards, bovine NP cells knockout for CD44, were seeded on the top of the fetal decellularized matrices and the efficiency of the process was evaluated by H&E, IHC for Sox9 and ACAN, as summarized in Figure 2b. Since we hypothesized that CD44 is involved in the increased protein production of the fetal matrices (described in the Chapter IV of this thesis), we were expected a decrease of ACAN and Sox9 after blocking CD44. However, we did not detect major differences in ACAN expression when comparing fetal matrices repopulated with CD44-knockout and CD44-wildtype cells (without blocking), as shown in Figure 2c. Fetal repopulated matrices showed increased ACAN levels, when compared to the negative control (decellularized matrices without cell seeding). Moreover, Sox9 was not detected in any of the conditions tested. H&E staining showed that the neutralization of CD44 did not affect cell adhesion in the extracellular matrices (ECMs), when compared to the wildtype condition (Figure 2c).

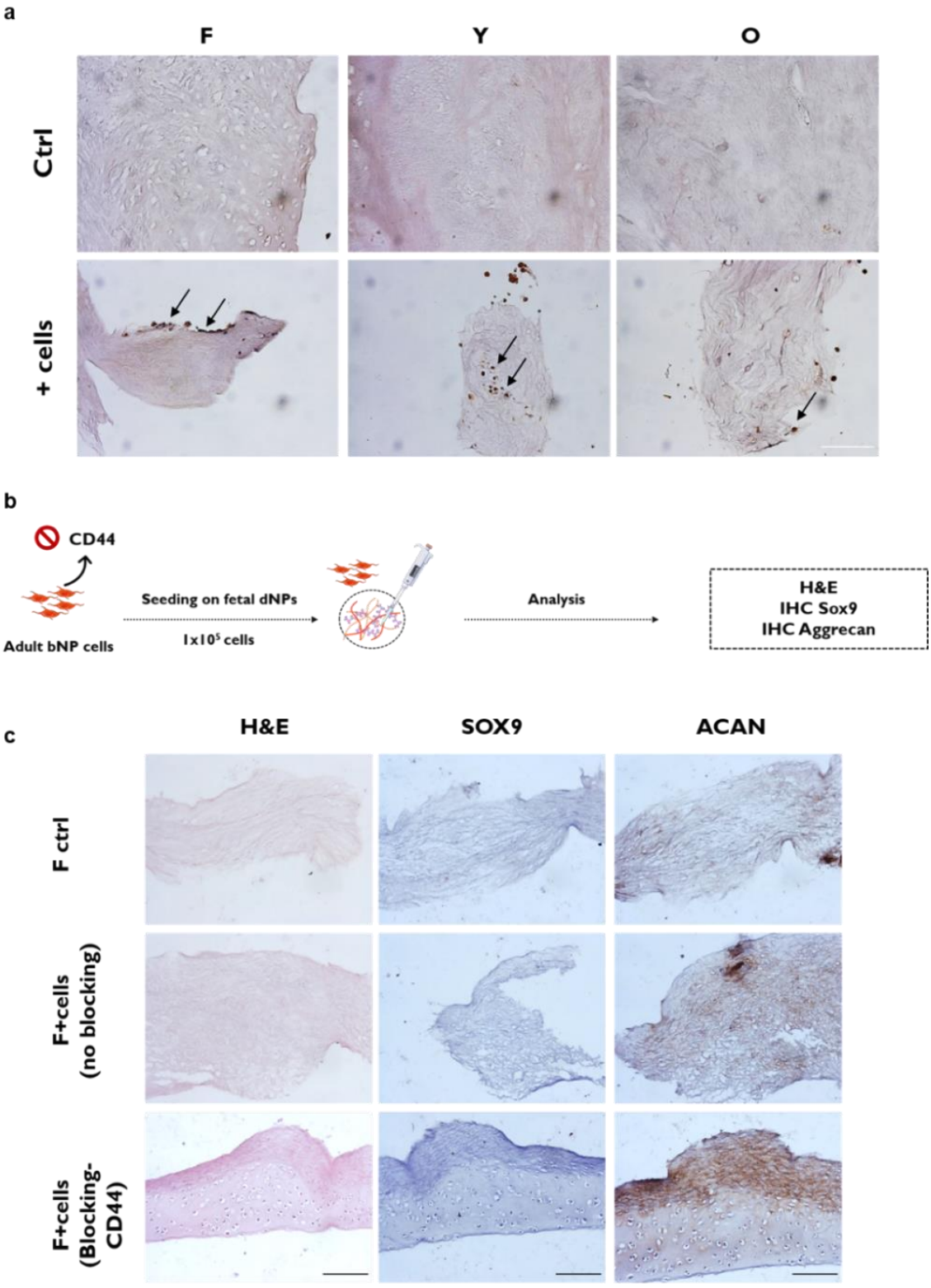
a
F
Y
O
Ctrl
+ cells
b
CD44
Adult bNP cells
Seeding on fetal dNPs
1x10⁵ cells
Analysis
H&E
IHC Sox9
IHC Aggrecan
c
H&E
SOX9
ACAN
F ctrl
F+cells (no blocking)
F+cells (Blocking-CD44)

Figure 2. Evaluation of protein expression in decellularized fetal matrices repopulated with CD44-knockout and CD44-wildtype NP cells. a. Sox9 immunohistochemistry (IHC) of repopulated matrices from different donor ages, compared to the correspondent control (ctrl: decellularized matrices without cell seeding). Arrows represents positive cells for Sox9 (brown staining). Magnification 20x and scale bar 100 µm. **b.** Schematic workflow of the experimental procedure for blocking CD44 in fetal repopulated matrices. **c.** Hematoxylin&Eosin (H&E) staining and Aggrecan (ACAN) and Sox9 IHC of fetal decellularized matrices (ctrl), fetal ECMs repopulated with CD44-wildtype cells (no blocking) and with CD44-knockout cells (blocking-CD44). Magnification 20x and scale bar 100 µm. F: fetus; bNP: bovine NP; ctrl: control.

2.2. DECELLULARIZED NUCLEUS PULPOSUS FROM DIFFERENT DONOR AGES DID NOT SHOW SIGNIFICANT INFLAMMATORY RESPONSE

It is known that materials, upon implantation, can provoke an inflammatory reaction, which can evolve in a chronic inflammatory immune response. Although the host foreign body reaction should be limited by using natural-derived ECM-based biomaterials (Aamodt & Grainger, 2016), it is essential to deeply investigate any response, prior to clinical applications, in order to ensure successful scaffolds' performance. Therefore, we have analyzed the inflammatory response in decellularized matrices from different donor ages, by an *in vivo* CAM assay. After 3 days of scaffolds implantation in the CAMs, the presence of a clear dense area around the decellularized scaffolds, especially when using fetal-derived scaffolds (Figure 3a), was detected. Qualitative scoring confirmed the higher inflammatory potential of fetal matrices when compared to young and old ones (Figure 3b).

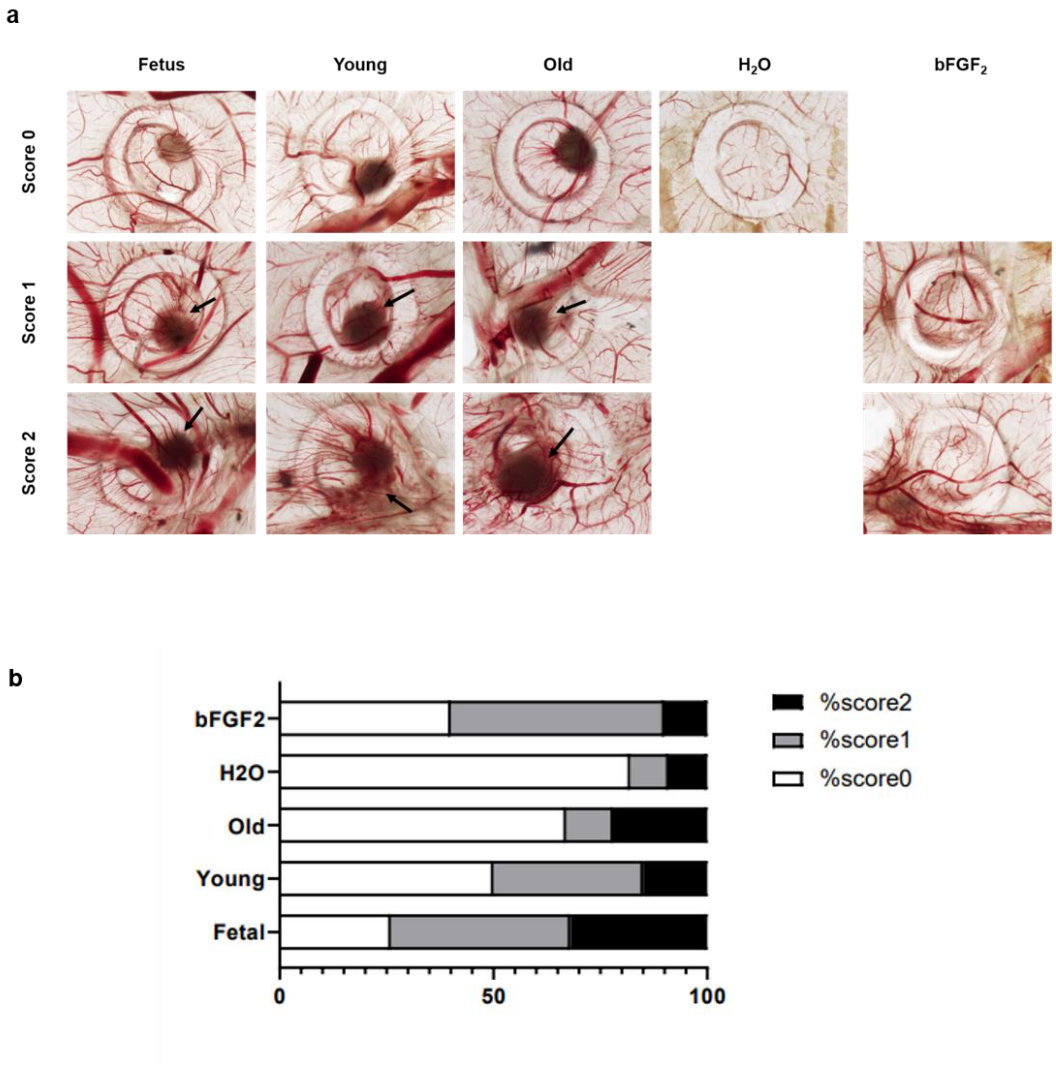

Figure 3. *In vivo* evaluation of the inflammatory score obtained after implantation of decellularized matrices from different aged donors. (a) Representative images of CAMs' with different scores of inflammations, after basic fibroblast growth factor-2 ($bFGF_2$) treatment and implantation with decellularized matrices from fetus (F), young (Y) and old (O) NPs. **(b)** Percentage of inflammatory score, evaluated on images of excised CAMs. Score 0: absence of inflammatory reaction; score 1: presence of inflammatory reaction; score 2: higher inflammatory reaction. H_20 and $bFGF_2$ represent the negative and positive controls, respectively.

Therefore, inflammatory cytokine levels released by decellularized NPs from different donor ages were further analyzed by using a commercially semi-quantitative array kit in order to validate the aforementioned results. Several factors, including interferons (IFN), transforming growth factor (TNF) and interleukin (IL), were evaluated in the conditioned media derived from decellularized NPs at day 3 of *ex vivo* culture (same time point used for CAMs). As a complementary study, cytokine levels were also analyzed in conditioned media derived from decellularized matrices repopulated with adult bovine NP cells, at the same time point (3 days of *ex vivo* culture).

As shown in Figure 4a, fetal decellularized NPs showed a tendency to increase IFN-α levels, when compared to young and old ones, although not statistically significant and this trend was also preserved after repopulation, although with higher variability (Supplementary figure 1a). No major differences were observed in IFN-β in any of the aged groups, while its amount increased in young NPs after repopulation, when compared to fetus and old ones (Supplementary figure 1a). On the contrary, IFN-γ showed a tendency to increase in fetal decellularized NPs (Figure 4a), as compared to young ones, while after repopulation its level was higher in young NPs (Supplementary figure 1a). TNF-α was not expressed in decellularized matrices with values close to zero (Figure 4a). The same was observed after repopulation except for one donor when repopulated in fetal or young scaffolds (Supplementary figure 1a).

Regarding IL expression, IL-1β showed a tendency to increase its levels in young NPs when compared to old ones (Figure 4b). However, after repopulation its expression was significantly higher in fetus matrices when compared to young ones (Supplementary Figure 1b), indicating that a higher inflammatory response could occur when fetus NPs were in contact with bovine NP cells. A similar trend was observed for IL-1α after repopulation. IL-1α, IL-4, and IL-15 were detected at higher levels in old decellularized NPs only for one replicate, when compared to fetus and young ones, while IL-17A and IL-18 expression was greatest in fetus NPs (Figure 4b). Also, in this case, high variability between samples was detected. An increase of IL-10 content was also revealed in old decellularized NPs, when compared to young ones. After repopulation, no major differences were observed for what concern IL-4 (highly variable), IL-13, IL-15 and IL-17A levels, while both IL-10 and IL-18 were higher in young NPs when compared to the other aged group (Supplementary figure 1b).

Overall, decellularized NPs from different donor ages did not exhibit a consistent inflammatory response, since no statistical differences were detected between ages for the different cytokines analyzed. However, we cannot exclude cytokine removal after media changes at day 1 of *ex vivo* culture. Overall, inflammation increased after repopulation as demonstrated by an overexpression of several cytokines, indicating that seeded cells could release inflammatory factors when in contact with different tissue microenvironments, particularly in fetus matrices as revealed by a statistically significant increase of IL-1β.

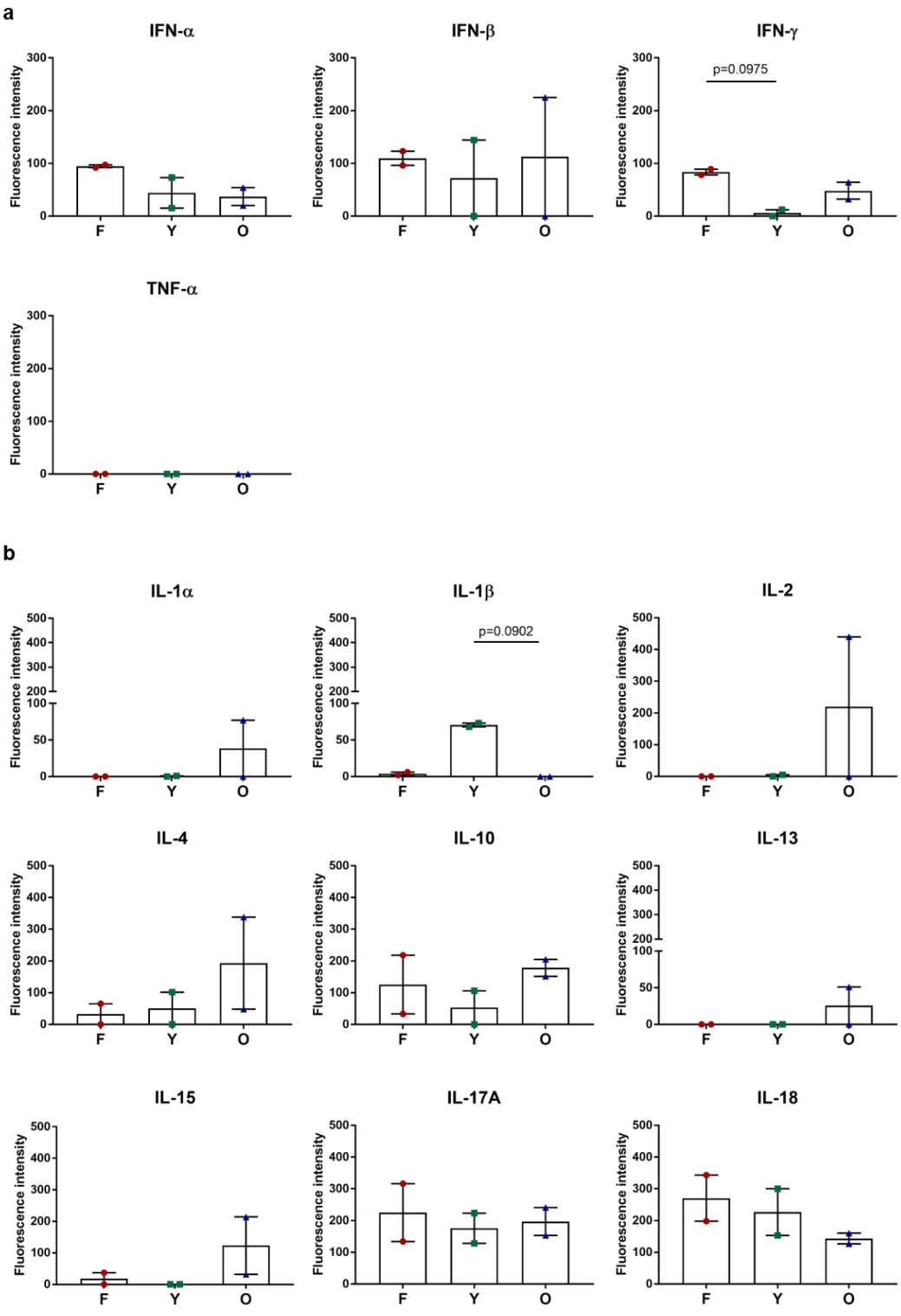
a
IFN-α
IFN-β
IFN-γ
p=0.0975
TNF-α
Fluorescence intensity
F
Y
O
b
IL-1α
IL-1β
p=0.0902
IL-2
IL-4
IL-10
IL-13
IL-15
IL-17A
IL-18

Figure 4. Evaluation of inflammatory cytokine levels in conditioned media derived from decellularized NPs of different donor ages. (a). Interferon (IF)-α, IFN-β, IFN-γ, transforming growth factor-α (TNF-α) and **(b)** several interleukins (ILs) expression in conditioned media from decellularized fetus (F), young (Y) and old (O) matrices. Data are presented as fluorescence intensity. Error bars represent mean ± SEM (n = 2 indicates a pool of three different experiments each). Kruskal Wallis test followed by Dunn's multiple comparison test was performed.

2.3. DECELLULARIZED MATRICES FROM DIFFERENT DONOR AGES DID NOT SHOW SIGNIFICANT CHANGES IN ANGIOGENIC CYTOKINES, GROWTH FACTORS OR CHEMOKINES

A screening of several factors involved in angiogenesis was performed in conditioned media derived from decellularized matrices of different donor ages, to understand their role in this precise process.

Although not statically significant and highly variable, old decellularized NPs showed a tendency to increase vascular endothelial growth factor (VEGF-A), angiopoietin-1 (ANG-1), bFGF levels for only one replicate, when compared to fetus and young ones (Figure 5a). However, the analysis should be repeated with higher number of replicates in order to validate these results. Surprisingly, VEGF-A increased in both fetus and young NPs after repopulation, when compared to old ones. Thus, it seems that conditioned media from younger decellularized matrices acquired a pro-angiogenic signature after repopulation with bovine NP cells. No major differences were observed in ANG-1, a part for an increase for only one replicate in fetus matrix, while young and old matrices showed a greatest amount of bFGF (Supplementary Figure 2a). Overall, we did not detect statistically significant changes in the angiogenic factors released by any of the decellularized NPs from different aged donors, but we cannot exclude that other molecules could be involved in the observed effect.

Expression of growth factor, including fibroblast growth factor-1 (FGF-1) and Insulin-like growth factor-1 (IGF-1) were also analyzed, demonstrating a tendency to increase in old decellularized NPs (Figure 5a), but variability between sample was very high, thus not reaching statistical significance.

Other factors analyzed were: interferon γ-induced protein-10 (IP-10), monocyte chemoattractant protein-1 (MCP-1), monokine induced by gamma interferon (MIG), growth and differentiation factor-associated serum protein-1 (GASP-1), neural cell adhesion molecule (NCAM-1), leukemia inhibitory factor (LIF), regulated on activation, normal T cell expressed and secreted (RANTES) and CD40 ligand (CD40L). In particular, conditioned media derived from old decellularized NPs showed a tendency in increasing MCP-1, GASP-1, NCAM-1, and Decorin when compared to fetus and young ones, while LIF and RANTES were higher in fetal matrices (Figure 5b). After repopulation, GASP-1, MCP-1 and MIG showed an opposite tendency being highly expressed in young and fetal NPs, respectively, while LIF and RANTES increased in older matrices (Supplementary figure 2b). No major differences in IP-10 and MIG levels were detected in decellularized NPs from different donor ages, while CD40L was highly variable (Figure 5b).

Finally, old decellularized matrices showed the highest levels of decorin (Figure 5b), thus confirming previous observations in old native NPs (Caldeira et al., 2017). However, after repopulation an opposite trend was observed with an increase of decorin in younger matrices when compared to old ones (Supplementary figure 2b), therefore demonstrating that seeded cells are able to release this protein.

Other cytokines, namely IL-1 F5, IL-21 and MIP-1b (data not shown) were also evaluated but were never expressed (values equal to zero) in any of the decellularized samples.

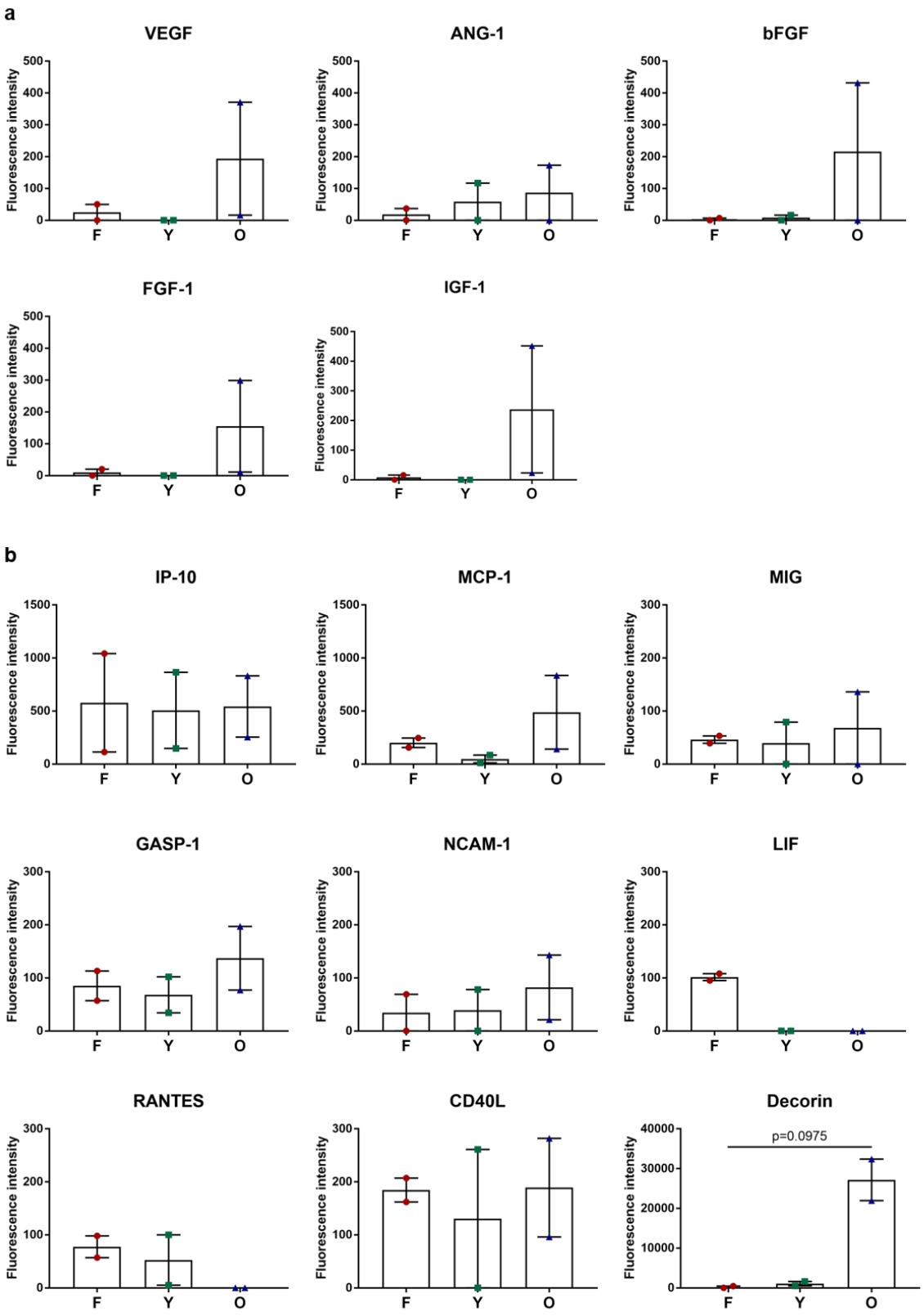
a
VEGF
ANG-1
bFGF
FGF-1
IGF-1
b
IP-10
MCP-1
MIG
GASP-1
NCAM-1
LIF
RANTES
CD40L
Decorin
p=0.0975
Fluorescence intensity
F
Y
O

Figure 5. Analysis of angiogenic molecules, growth factors and other cytokines in conditioned media of decellularized NPs from different aged donors. (a) Vascular endothelial growth factor (VEGF-A), angiopoietin-1 (ANG-1), basic fibroblast growth factor (bFGF), fibroblast growth factor-1 (FGF-1) and insulin-like growth factor (IGF-1) expression levels in decellularized fetus (F), young (Y) and old (O) NPs. **(b)** Interferon γ-induced protein-10 (IP-10), monocyte chemoattractant protein-1 (MCP-1), monokine induced by gamma interferon (MIG), growth and differentiation factor-associated serum protein-1 (GASP-1), neural cell adhesion molecule (NCAM-1), leukemia inhibitory factor (LIF), regulated on activation, normal T cell expressed and secreted (RANTES) and CD40 ligand (CD40L) expression levels in F, Y and O decellularized NPs. Data are presented as fluorescence intensity. Error bars represent mean ± SEM (n = 2 indicates a pool of three different experiments each). Kruskal Wallis test followed by Dunn's multiple comparison test was performed.

2.4. FETAL MATRICES MAINTAINED AN ANTI-ANGIOGENIC POTENTIAL AFTER REPOPULATION WITH HUMAN IMMORTALIZED NUCLEUS PULPOSUS CELLS

An *in vivo* CAM assay with decellularized bovine NPs from different donor ages in contact with human iNP cells was performed as a first *in vivo* proof-of-concept of scaffolds anti-angiogenic potential after cell seeding. A first experiment with iNP cells from two different clones (clone 1: GA094 and clone 2: GA111), with a cell density of $1x10^5$, was performed in order to evaluate their angiogenic response. Clone 1 was able to induce a superior pro-angiogenic response, when compared to clone 2 (Supplementary Figure 3a). Moreover, CAMs inoculated with clone 1, with higher cells density ($5x10^5$ cells), showed a statistically significant increase of vessels number, when compared to the negative control (H_2O), and a tendency to be higher rather than clone 1 and 2 with lower cell density ($1x10^5$ cells). However, considering the observed increased toxicity with higher number of cells (data not shown), following experiments were performed with $4x10^5$ cells of clone 1.

Decellularized NPs from different donor ages (fetus, young and old) were implanted in the CAMs and iNP cells were seeded on top (Figure 6a). After three days of implantation, fetal matrices were the only ones that in the presence of human iNP cells, were not able to promote angiogenesis, showing no statistically differences when compared to the negative

control (H_2O) in terms of vessels number. On the other hand, both young and old matrices showed a statistically significant increase in vessels number when compared to the negative control (H_20), demonstrating a higher pro-angiogenic response (Figure 6b). These results validated our previous observations, in which fetal decellularized NPs showed a superior anti-angiogenic potential when compared to young and old ones (Fiordalisi et al., 2022). Thus, fetus scaffolds retained a low angiogenic potential in the presence of human NP cells.

With H&E staining, different parameters were evaluated including: presence/absence of scaffold in the CAM; presence/absence of inflammatory and/or blood cells within the scaffolds (Figure 6c). As shown in Figure 6d old decellularized NP scaffolds were often absent, indicating that they were not able to strongly adhere to the CAMs, when compared to fetus and young ones. Moreover, fetal decellularized NPs showed a slight tendency to have decreased number of inflammatory cells, when compared to young and old ones (Figure 6e). This is probably due to the decreased vessels number growing towards the fetal NPs, which did not allow the migration of the inflammatory cells inside the scaffolds.

Finally, blood cells were absent from fetal NPs but present at similar ranges in both young and old scaffolds, thus validating our observation of the anti-angiogenic potential of fetal matrices (Figure 6f). Interestingly, human iNP cells seeded on the top of fetal decellularized NPs showed higher production of GAGs (in blue) after 3 days of *in vivo* culture. This production was not observed for young and old NPs, suggesting that fetal NPs provide a more favorable microenvironment for the cells to start producing healthy matrix proteins (Figure 6c).

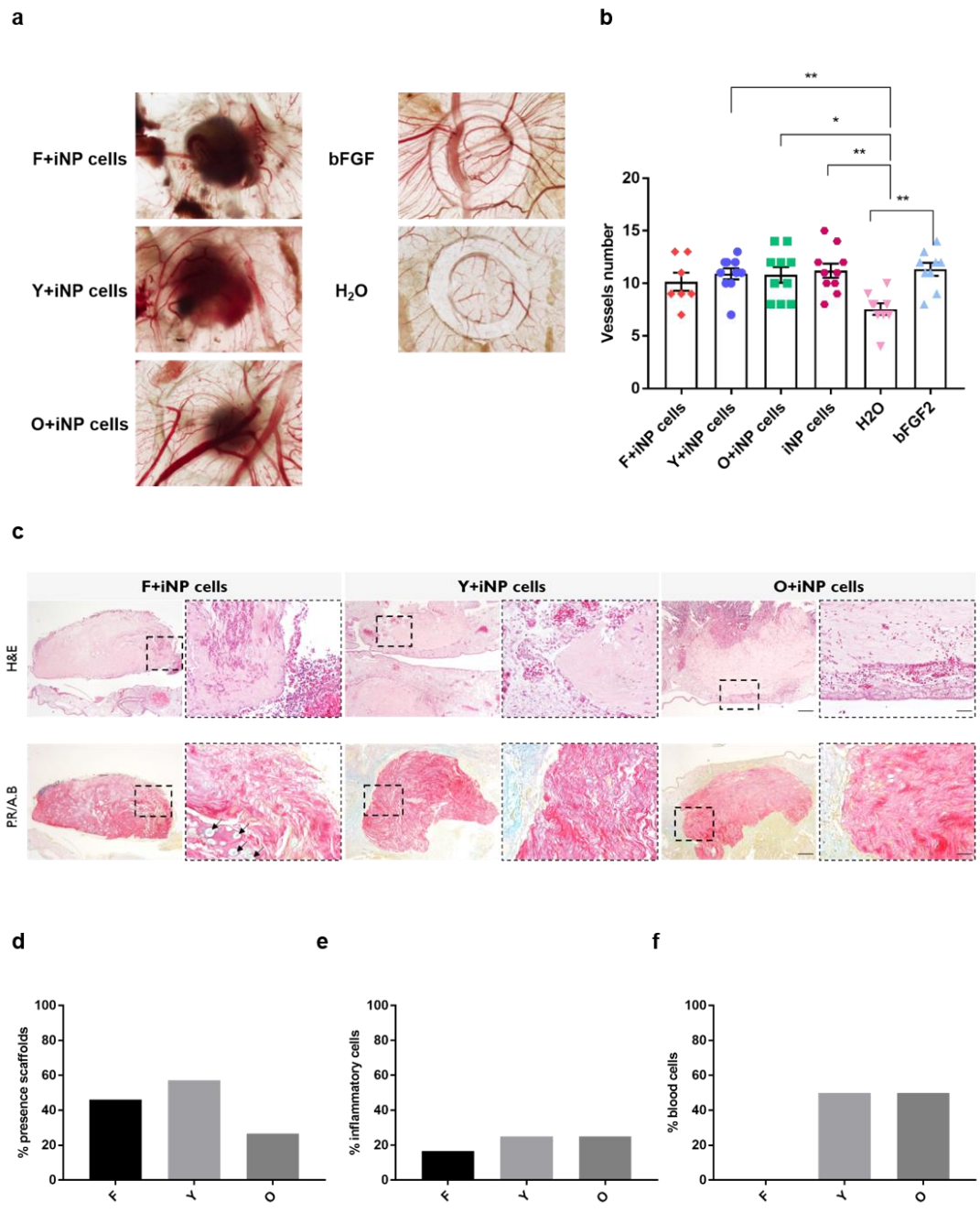
a
b
F+iNP cells
Y+iNP cells
O+iNP cells
bFGF
H2O
Vessels number
F+iNP cells
Y+iNP cells
O+iNP cells
iNP cells
H2O
bFGF2
c
F+iNP cells
Y+iNP cells
O+iNP cells
H&E
PR/A.B
d
e
f
% presence scaffolds
% inflammatory cells
% blood cells
F
Y
O

Figure 6. *In vivo* CAM assays of decellularized NPs from different aged donors seeded with human immortalized nucleus pulposus cells. (a). Representative images of CAMs implanted with decellularized fetal (F), young (Y) and old (O) NPs in combination with immortalized nucleus pulposus (iNP) cells. **(b).** Quantification of new vessel formation towards the inoculation site. H_20 and $bFGF_2$ represent the negative and positive controls, respectively. Error bars represent mean ± SEM. One-Way Anova followed by Sidak's multiple comparison test. (*) $p < 0.05$ and (**) $p < 0.01$. **(c).** Representative images of Hematoxylin&Eosin (H&E) and Picro-Sirius Red and Alcian Blue (P.R/A.B) staining of CAMs implanted with F, Y and O decellularized matrices in combination with iNP cells. Left images: magnification 5x and scale bar: 200 µm. Right images: magnification 20x and scale bar: 50 µm. Arrows show glycocaminoglycans (GAGs) production by seeded cells. For P.R/A.B staining, red: collagen [COL]; blue: GAGs; purple: cell nuclei. **(d).** Qualitative evaluation of scaffold presence in the CAMs, **(e)** inflammatory and blood **(f)** cells presence in the scaffold after H&E staining. Data are presented as a percentage score.

3. DISCUSSION

In the Chapter IV of this thesis, we have demonstrated the superior potential of younger decellularized matrices in inducing *de novo* matrix production (ACAN increase) and ECM remodeling (COL2 reduction), after repopulation with bovine NP cells. Moreover, fetal matrices showed the greatest ACAN and COL2 expression, at molecular levels and decreased angiogenic response after *in vivo* CAM assay (Fiordalisi et al., 2022). Therefore, we have hypothesized that fetal matrices could have a superior pro-regenerative capacity for IVD repair, but the specific mechanism behind this scenario was not addressed. Moreover, an *in vivo* proof of concept of the capacity of fetal matrices to reduce angiogenic response in the presence of human IVD cells, was still lacking. Herein, we aimed to address these questions.

Firstly, we have tried to dissect the mechanism behind the increased protein production in fetal matrices, by repopulating the scaffolds with CD44-knockout or CD44-wildtype bovine NP cells. CD44 was chosen as protein target, since a chondroitin/dermatan sulfate form of CD44 was previously described as a receptor for COL14 (Ehnis et al., 1996), which is mainly expressed in fetal bovine NPs (Caldeira et al., 2017). CD44 is involved in several signaling, including β-catenin activation (Orian-Rousseau, 2015), which can in turn activate Sox-9 transcription (Aguilar-Medina et al., 2019). Sox-9 is able to activate several genes, including ACAN and COL2 (Zhang et al., 2015). Thus, we hypothesized that seeded cells could sense the presence of COL14 in fetal matrices and increase ACAN production through activation of β-catenin and Sox-9 transcription. Firstly, we confirmed the presence of Sox9 in fetal NPs, by analyzing its levels in repopulated matrices from different donor ages, compared to the correspondent controls (decellularized NPs without cells seeding). As results, it seemed that higher number of positive cells for Sox9 were present in both fetus and young NPs, when compared to the old ones. Despite these data need a further confirmation by quantitative analysis, these results gave a first proof of the bovine NP cells' ability to produce Sox9, especially when in contact with younger decellularized matrices. Afterwards, we neutralized CD44 in adult bovine NP cells, by using a specific blocking-antibody, prior to cells seeding on the top of fetal decellularized NPs. We expected a decrease of ACAN and Sox9 in NPs seeded with CD44-knockout cells, when compared to the wildtype condition (without blocking). However, we were not able to detect major changes between conditions, in terms of ACAN content. Moreover, Sox9 was not expressed in all the samples. This could be due to a technical issue, regarding the antibody specificity

and therefore being unable to bind/neutralize the protein of interest, or the signaling pathway analyzed not being involved in this mechanism.

It is well known that biomaterials need to be well tolerated by the human body in order to achieve successful tissue regeneration upon implantation. Specifically, scaffolds (either natural or synthetic) are able to interact with the local microenvironment, particularly the surrounding ECM. Therefore, it is essential to address tissue – mediated host response to biomaterials in terms of inflammatory response and immune reaction, envisaging clinical application. Nowadays, several biomaterials are already being used for tissue replacement, including glucose biosensors, heart valves, cardiac pacemakers, stents, catheters, among others (Zhou & Groth, 2018), showing good outcomes. In the IVD context, several cages exist as implants for spinal fusion, including metal (pure titanium and titanium composite/alloy), ceramic (*e.g.*, silicon nitride), plastic (*e.g.*, polyetheretherketone [PEEK]). PEEK and titanium alloys are the most frequently used (Veronesi et al., 2022). Given that chronic inflammation and fibrosis are the most common cause of implants' failure (Zhou & Groth, 2018), it is fundamental to evaluate factors involved in this cascade.

We have previously demonstrated that decellularized ECM-based scaffolds obtained from bovine NPs of different donor ages (fetus, young and old), were cytocompatible and not toxic *in vitro* after repopulation with adult bovine NP cells. Moreover, fetal decellularized NPs showed a superior anti-angiogenic potential *in vivo* in a CAM assay, being able to better mimic the avascular nature of the IVD, when compared to older matrices (Fiordalisi et al., 2022). Fetal decellularized NPs have also shown an increased inflammatory score, rather than the other aged groups, after *in vivo* CAM assay. However, a deeper understanding of the soluble factors involved in both inflammatory and angiogenic processes was missing.

Thus, several cytokines were evaluated in the conditioned media derived from decellularized NPs of different aged donors, at day 3 of *ex vivo* culture, by using a commercially available array kit, specific for bovine species. As a complementary study, cytokine levels were also evaluated in the conditioned media from repopulated NPs of different donor ages, at the same time point of decellularized scaffolds. Among the cytokines analyzed, the levels of several IFN and ILs were measured. As it is known, IFNs are involved in several processes, including antiviral, antitumoral and immunomodulatory responses (Kline & Kitagaki, 2006). Herein, we have shown a tendency for IFN-α and IFN-γ to be expressed at higher levels in fetal decellularized NPs when compared to young and

old ones. While no major changes were detected for IFN-β in decellularized matrices, the levels increased after repopulation, especially in young NPs. Moreover, TNF-α, which is widely associated with IVD degeneration, was not expressed in any of the aged groups, with values close to zero, indicating an absent TNF-mediated inflammatory response.

As widely described, ILs are involved in the regulation of several processes related to inflammatory and immune response, including growth, differentiation and activation of immune cells. Moreover, IL can have pro- or anti-inflammatory roles (Justiz Vaillant & Qurie, 2022), depending on the type of ILs and on the context in which they are expressed. Herein, we evaluated several ILs (IL-1α, IL-1β, IL-2, IL-4, IL-10, IL-13, IL-15, IL-17A and IL-18) in order to understand if they could be released by decellularized matrices and trigger an inflammatory response. IL-1α and IL-1β are known pro-inflammatory cytokines and the alteration of their associated signaling can induce several pathologies, which are characterized by acute or chronic inflammation (Di Paolo & Shayakhmetov, 2016). IL-1β and TNF-α are widely explored in the IVD for their role in disc degeneration and herniation (Le Maitre et al., 2007). Moreover, it has been shown that the risk of IVD degeneration is highly associated with polymorphism of IL-1α (Wang et al., 2016). Herein, we did not detect major changes in IL-1α levels between ages. However, we observed an increase of IL-1β in young decellularized matrices when compared to fetal and old ones, being close to statistical significance. Surprisingly, after repopulation, fetal NPs displayed a statistically significant higher expression of IL-1β when compared to young NPs, demonstrating an increased inflammatory response. Previous work from our group has demonstrated the presence of thrombospondin (TSP) in the matrisome profiling of fetal bovine NPs (Caldeira et al., 2017), which is involved in inflammation (Lopez-Dee et al., 2011). Therefore, the higher inflammation in fetal NPs could be mediated by this factor. Also, adult bovine NP cells may start to produce more IL-1β when they are in contact with fetal matrices, due to the differences in tissue microenvironment, namely structure and composition. Thus, IL-1β expression should be analyzed at longer time points to understand if its production can be associated to a prolonged inflammatory response. Finally, fetal matrices may also be characterized by the presence of a higher number of endotoxins, thus leading to an increase of IL-1β expression. Regarding the other ILs analyzed, we have observed an increase of IL-4, IL-10 and IL-15 in old decellularized matrices when compared to the other aged groups. On the contrary, IL-17A and IL-18 were both higher in fetal NPs. However, the variability between samples was too high to consider these results consistent.

Overall, inflammatory cytokines did not significantly increase in decellularized matrices from different ages, however we cannot exclude that this is due to the change of media after 24 hours of *ex vivo* culture.

Apart from the cytokines involved in the inflammatory response, angiogenic factors, including VEGF, ANG-1 and bFGF, were also analyzed in order to validate our previous observation on the anti-angiogenic potential of fetal matrices. It is known that VEGF is able to bind a specific receptor localized on endothelial cells' surface, thus inducing vasculogenesis (Goodsell, 2003). Other glycoproteins involved on the regulation of blood vessel formation and stability, are the ANGs (Fagiani & Christofori, 2013). bFGF is another pro-angiogenic molecule which belongs to the family of FGF and participates in several processes, such as cell differentiation, angiogenesis, mitogenesis and wound healing (Cortina & Azar, 2010).

In the present work, VEGF, ANG-1 and bFGF showed a tendency in increasing in old matrices, when compared to both fetal and young ones. Although these results could confirm our previous observations on the higher pro-angiogenic potential of older matrices (Fiordalisi et al., 2022), the variability between samples was too high and therefore further analysis should be performed to validate them. Surprisingly, higher levels of VEGF-A were found in the conditioned media of repopulated fetus and young NPs, when compared to old ones. These data are in contrast with our previous observation on the anti-angiogenic role of fetal matrices. Fujita and colleagues have previously reported the high expression of VEGF-A in the NP and uncovered its role in tissue survival through an autocrine/paracrine way (Fujita et al., 2008). Furthermore, another study had also correlated the expression of ANG-1, which is also a ligand of Tie2, with NP cells survival (Sakai et al., 2012). Although VEGF and ANG-1 are primarily associated with angiogenesis, which is not beneficial for IVD, their expression seems to have also an essential role in IVD cell survival (Sakai & Grad, 2015). Thus, the increased expression of pro-angiogenic factors in fetal matrices after repopulation could be also correlated to the activation of specific mechanisms to ensure cells survival. Furthermore, young and old repopulated matrices showed an increased expression of bFGF, when compared to fetal NPs, demonstrating a superior pro-angiogenic response. Therefore, this observation could support our previous data on the anti-angiogenic potential of fetal matrices in CAMs $bFGF_2$-treated (Fiordalisi et al., 2022).

Other growth factors, including FGF-1 and IGF-1, were also analyzed. FGF-1 is involved in cell cycle regulation, cell differentiation, survival and apoptosis (Ornitz & Itoh,

2015). IGF-1 signaling is able to prevent IVD degeneration through activation of cell proliferation and ECM synthesis, as well as inhibition of matrix degradation, apoptosis and senescence. However, it can also induce disc degeneration when the signaling is abnormally activated (Lin et al., 2021). Le Maitre and colleagues have previously demonstrated the presence of IGF-1 receptor in healthy and degenerated NP and AF cells, thus indicating its role in IVD homeostasis (Le Maitre et al., 2005). Herein, we have detected a tendency of higher levels of both FGF-1 and IGF-1 in old decellularized NP when compared to fetus and young ones, although only for one replicate. Although this effect could be correlated with an abnormal activation of growth factor signaling pathways, the variability between samples was too high to take any definitive conclusion.

Other cytokines (IP-10, MCP-1, MIG, GASP-1, NCAM-1, LIF, RANTES, CD40L and decorin), involved in pathological processes, immune response, inflammation or IVD degeneration, were also evaluated. The chemokine IP-10, also known as CXCL-10, participate in the recruitment of leukocytes, eosinophils, monocytes and natural killer cells, thus regulating the immune response (Vazirinejad et al., 2014). However, this small protein has other functions, regulating chemotaxis, activation of apoptosis, modulation of cell growth and angiostatic effects (Liu et al., 2011). Moreover, it is also involved in several pathological conditions, including disc degeneration. Specifically, high levels of CXCL10 were found in the serum of patients with IVD degeneration, and positively correlated with the clinical severity of the condition (Yang et al., 2022). Therefore, CXCL10 seems to have a role in the progression of IVD degeneration. Herein, we did not detect major changes of IP-10 between ages.

MCP-1, also known as CCL2, is part of a chemokine family and has been recognized as a potent chemoattractant factor for monocytes and macrophages, controlling their migration and infiltration and being involved in several pathologies (Deshmane et al., 2009). MIG (or CXCL-9) is a chemokine activated by IFN-γ (Tokunaga et al., 2018) and is able to modulate cell recruitment on the site of inflammation, particularly by attracting T-lymphocytes (Fulkerson & Rothenberg, 2006). Herein, conditioned media derived from old decellularized NPs has shown a tendency in increasing levels of MCP-1, when compared to the other ages. No major differences were observed for MIG between samples, due to the high variability. After repopulation MCP-1 increased in young NPs, while MIG was higher in fetal matrices. Nevertheless, neither cytokines' levels showed a statistical significance, their increase in younger matrices could be an adaptive response to the seeded cells.

GASPs are proteins able to bind and inhibit factors of the TGF-β family. GASP-1 is present in several tissues during fetal stages, including skeletal muscle (Parenté et al., 2020). NCAM-1 (or CD56) plays an essential role in cell-cell interactions (Rutishauser et al., 1988) and its expression is also important during embryonic development (Rutishauser, 1992). Despite being predominately expressed by neural cells, Sakai and colleagues have previously shown NCAM-1 mRNA overexpression in canine coccygeal NP, when compared to lumbar NP and AF, which was further confirmed at protein level (Sakai et al., 2009). Our results have shown higher amount of GASP-1 and NCAM-1 in old decellularized NPs when compared to the other ages, however not statistically significant. After repopulation, GASP-1 levels were greatest in young NPs.

LIF is a member of the IL-6 cytokine family, which is involved in different cellular processes, such as cell proliferation, differentiation and survival. It has an important role in several organs (*e.g.*, hemopoietic, bone remodeling, neural, muscular, endocrine and reproductive system) and is able to induce different signaling pathways (Nicola & Babon, 2015). LIF has been described as an anti-inflammatory cytokine in axon regeneration (Vidal et al., 2013) and during cutaneous inflammation (Banner et al., 1998). However, it also seems to have a pro-inflammatory role, being involved in osteoarthritis pathology (Kapoor et al., 2011; Lotz et al., 1992). RANTES is a small chemokine, involved in acute infection by inducing migration and homing of lymphoid cells, such as T cells and monocytes (Appay & Rowland-Jones, 2001; Crawford et al., 2011), as well as in inflammatory response through leukocytes recruitment (Appay & Rowland-Jones, 2001). In the context of IVD, Kepler and colleagues have detected overexpression of RANTES in painful IVDs, isolated from patients undergoing surgery, which was also correlated to IL-1β expression (Kepler et al., 2013). In the present work, both LIF and RANTES have shown higher level in fetal decellularized NPs when compared to the other aged donors. The role of LIF as and anti or pro-inflammatory cytokine is controversial in the literature and it depends on the biological context in which it is expressed. Regarding the high levels of RANTES in fetal NPs, it may be that remaining endotoxin in the fetal tissue are responsible for the increase of this inflammatory and infection-related cytokine. Thus, an analysis of the remaining endotoxin, within the decellularized tissue, should be performed to validate these data. Interestingly, after repopulation both LIF and RANTES levels decreased in fetal matrices and increased in older ones. Therefore, there might be a different mechanism activated before and after decellularization that could regulate the expression of both cytokines.

CD40L is a transmembrane glycoprotein, which is present on T cells surface and is involved in the inflammatory response through the regulation of cytokine and chemokines release (Chan & Rainer, 2013). Herein, no significant changes were detected in CD40L levels between different aged donors.

Finally, decorin is included in the small leucin-rich proteoglycan family and is able to modulate growth factors and matrix formation. Moreover, it can bind several cytokines and growth factors, participating in different processes, such as cancer cells proliferation, pro-inflammatory response and anti-fibrillogenesis (Zhang et al., 2018). As it is well described, decorin levels increase in the ECM with ageing (Frantz et al., 2010). In the IVD context, higher expression levels of decorin were previously detected in the matrisome of old native NPs, when compared to fetal and young ones (Caldeira et al., 2017). Herein, array analysis has demonstrated increased levels of decorin in the conditioned media derived from old decellularized matrices, thus validating the previous observations. After repopulation, the levels of decorin increased in younger matrices. This effect might be due to an increased release of specific matrix metalloproteinases (MMPs) by seeded cells in fetal and young matrices, that could induce decorin release. It was previously shown that decorin is proteolytically degraded by MMP-2, MMP-3 and MMP-7 (Imai et al., 1997). This is in line with our previous observation where we saw an overexpression of MMP-1 and MMP-3 in young repopulated matrices, but only at the molecular level (Fiordalisi et al., 2022). However, we cannot exclude that other MMPs may be expressed in decellularized NPs and should be further explored in terms of expression as well as activity.

As it is known, angiogenesis plays an essential role in tissue regeneration. In particular, therapeutic biomaterials for tissue repair should be able to induce the formation of blood vessels in order to achieve their clinical success (Lee et al., 2021). However, IVDs are avascular tissues in physiological conditions and neovascularization is associated with degeneration. In the present work we have investigated the angiogenic response of decellularized matrices from different donor ages (fetus, young and old) after seeding with human iNP cells. After inoculating iNP cells from different clones in CAMs, we demonstrated a superior pro-angiogenic response of clone GA094, when compared to the negative control (H_2O) and to the other cell clone (GA111). Thus, this preliminary result unveiled the angiogenic potential of human iNP cells. When these cells were seeded on the top of decellularized NPs from different donor ages, fetal scaffolds were the only ones that did not significantly increase neovessels formation, when compared to the negative control (H_2O), in a CAM assay. These observations provided the first *in vivo* proof-of-concept of the

capacity of fetal matrices to reduce the angiogenic response induced by human cells, recapitulating a healthy and physiologic IVD microenvironment. Moreover, by H&E staining, we could observe that old decellularized matrices were detached from the CAMs, when compared to fetus and young ones, indicating that their composition did not enable scaffold integration. Also, fetal matrices showed a tendency to decrease the number of inflammatory cells, but more importantly absence of blood cells within the scaffolds. Both inflammatory and blood cells were detected at higher levels in young and old matrices. These results confirmed the anti-angiogenic potential of fetal matrices and showed that they are more appropriate scaffolds to mimic a healthy and physiological IVD microenvironment. Interestingly, iNP cells seeded on fetal NPs were also able to produce GAGs after only 3 days of seeding, which was not observed for young nor old ones. These data suggest the superior capacity of fetal matrices to provide a more favorable microenvironment for human cells to produce matrix proteins, which had been already observed with bovine NP cells (Fiordalisi et al., 2022).

Despite the promising results on an absent inflammatory response when using decellularized matrices, in the future, further studies need to be conducted to validate the aforementioned observations. Specifically, cytokine levels should be evaluated with an increased number of replicates in order to have consistent results and reduce the variability between samples. Moreover, cytokines levels should be evaluated after 24h of *ex vivo* culture, to make sure that cytokines are not removed by media changes, as well as at longer time points to assess long term inflammatory response.

In the future, it is essential to explore the inflammatory response and immune reaction of decellularized NPs in a specific animal model of inflammation (mice air pouch model). Finally, angiogenesis as well as matrix restoration should be further addressed in a specific animal model of disc degeneration (*e.g*. rat) envisaging future clinical applications.

4. ACKNOWLEDGMENTS

This work was supported by Fundação para a Ciência e a Tecnologia (FCT) through FETBIO project (FCT-2020-PTDC/BTM-MAT/0438/2020). We would like to acknowledge Marta Teixeira Pinto for performing the *in vivo* CAM assays of this work and Ana Luisa Castro for the help with cytokine array.

5. REFERENCES

Aamodt, J. M., & Grainger, D. W. (2016). Extracellular matrix-based biomaterial scaffolds and the host response. *Biomaterials*, *86*, 68-82. https://doi.org/https://doi.org/10.1016/j.biomaterials.2016.02.003

Aguilar-Medina, M., Avendaño-Félix, M., Lizárraga-Verdugo, E., Bermúdez, M., Romero-Quintana, J. G., Ramos-Payan, R., Ruíz-García, E., & López-Camarillo, C. (2019). SOX9 Stem-Cell Factor: Clinical and Functional Relevance in Cancer. *Journal of Oncology*, *2019*, 6754040. https://doi.org/10.1155/2019/6754040

Appay, V., & Rowland-Jones, S. L. (2001). RANTES: a versatile and controversial chemokine. *Trends Immunol*, *22*(2), 83-87. https://doi.org/10.1016/s1471-4906(00)01812-3

Banner, L. R., Patterson, P. H., Allchorne, A., Poole, S., & Woolf, C. J. (1998). Leukemia inhibitory factor is an anti-inflammatory and analgesic cytokine. *J Neurosci*, *18*(14), 5456-5462. https://doi.org/10.1523/jneurosci.18-14-05456.1998

Caldeira, J., Santa, C., Osório, H., Molinos, M., Manadas, B., Gonçalves, R., & Barbosa, M. (2017). Matrisome Profiling During Intervertebral Disc Development And Ageing. *Sci Rep*, *7*(1), 11629. https://doi.org/10.1038/s41598-017-11960-0

Chan, C. P.-y., & Rainer, T. H. (2013). Chapter Two - Pathophysiological Roles and Clinical Importance of Biomarkers in Acute Coronary Syndrome. In G. S. Makowski (Ed.), *Advances in Clinical Chemistry* (Vol. 59, pp. 23-63). Elsevier. https://doi.org/https://doi.org/10.1016/B978-0-12-405211-6.00002-4

Coelho, C. C., Padrão, T., Costa, L., Pinto, M. T., Costa, P. C., Domingues, V. F., Quadros, P. A., Monteiro, F. J., & Sousa, S. R. (2020). The antibacterial and angiogenic effect of magnesium oxide in a hydroxyapatite bone substitute. *Scientific Reports*, *10*(1), 19098. https://doi.org/10.1038/s41598-020-76063-9

Cortina, M. S., & Azar, D. T. (2010). Corneal Angiogenesis. In D. A. Dartt (Ed.), *Encyclopedia of the Eye* (pp. 408-415). Academic Press. https://doi.org/https://doi.org/10.1016/B978-0-12-374203-2.00145-7

Crawford, A., Angelosanto, J. M., Nadwodny, K. L., Blackburn, S. D., & Wherry, E. J. (2011). A Role for the Chemokine RANTES in Regulating CD8 T Cell Responses during Chronic Viral Infection. *PLOS Pathogens*, *7*(7), e1002098. https://doi.org/10.1371/journal.ppat.1002098

Deshmane, S. L., Kremlev, S., Amini, S., & Sawaya, B. E. (2009). Monocyte chemoattractant protein-1 (MCP-1): an overview. *J Interferon Cytokine Res*, *29*(6), 313-326. https://doi.org/10.1089/jir.2008.0027

Di Paolo, N. C., & Shayakhmetov, D. M. (2016). Interleukin 1α and the inflammatory process. *Nat Immunol*, *17*(8), 906-913. https://doi.org/10.1038/ni.3503

Ehnis, T., Dieterich, W., Bauer, M., Lampe, B., & Schuppan, D. (1996). A chondroitin/dermatan sulfate form of CD44 is a receptor for collagen XIV (undulin). *Exp Cell Res*, *229*(2), 388-397. https://doi.org/10.1006/excr.1996.0384

Fagiani, E., & Christofori, G. (2013). Angiopoietins in angiogenesis. *Cancer Letters*, *328*(1), 18-26. https://doi.org/https://doi.org/10.1016/j.canlet.2012.08.018

Fiordalisi, M. F., Ferreira, J. R., Pinto, M. L., Ribeiro-Machado, C., Teixeira Pinto, M., Oliveira, M. J., Barbosa, M. A., Madeira Gonçalves, R., & Caldeira, J. (2022). The impact of matrix age on intervertebral disc regeneration. *Biomaterials Advances*, *143*, 213192. https://doi.org/https://doi.org/10.1016/j.bioadv.2022.213192

Frantz, C., Stewart, K. M., & Weaver, V. M. (2010). The extracellular matrix at a glance. *Journal of Cell Science*, *123*(24), 4195-4200. https://doi.org/10.1242/jcs.023820

Fujita, N., Imai, J.-i., Suzuki, T., Yamada, M., Ninomiya, K., Miyamoto, K., Iwasaki, R., Morioka, H., Matsumoto, M., Chiba, K., Watanabe, S., Suda, T., Toyama, Y., & Miyamoto, T. (2008). Vascular endothelial growth factor-A is a survival factor for nucleus pulposus cells in the intervertebral disc. *Biochemical and Biophysical Research Communications*, *372*(2), 367-372. https://doi.org/https://doi.org/10.1016/j.bbrc.2008.05.044

Fulkerson, P. C., & Rothenberg, M. E. (2006). CHEMOKINES, CXC | CXCL9 (MIG). In G. J. Laurent & S. D. Shapiro (Eds.), *Encyclopedia of Respiratory Medicine* (pp. 398-402). Academic Press. https://doi.org/https://doi.org/10.1016/B0-12-370879-6/00471-3

Goodsell, D. S. (2003). The Molecular Perspective: VEGF and Angiogenesis. *Stem Cells*, *21*(1), 118-119. https://doi.org/10.1634/stemcells.21-1-118

Imai, K., Hiramatsu, A., Fukushima, D., Pierschbacher, M. D., & Okada, Y. (1997). Degradation of decorin by matrix metalloproteinases: identification of the cleavage sites, kinetic analyses and transforming growth factor-β1 release. *Biochemical Journal*, *322*(3), 809-814. https://doi.org/10.1042/bj3220809

Justiz Vaillant, A. A., & Qurie, A. (2022). Interleukin. In *StatPearls*. StatPearls Publishing

Kapoor, M., Martel-Pelletier, J., Lajeunesse, D., Pelletier, J. P., & Fahmi, H. (2011). Role of proinflammatory cytokines in the pathophysiology of osteoarthritis. *Nat Rev Rheumatol*, *7*(1), 33-42. https://doi.org/10.1038/nrrheum.2010.196

Kepler, C. K., Markova, D. Z., Dibra, F., Yadla, S., Vaccaro, A. R., Risbud, M. V., Albert, T. J., & Anderson, D. G. (2013). Expression and relationship of proinflammatory chemokine RANTES/CCL5 and cytokine IL-1β in painful human intervertebral discs. *Spine (Phila Pa 1976)*, *38*(11), 873-880. https://doi.org/10.1097/BRS.0b013e318285ae08

Kline, J. N., & Kitagaki, K. (2006). INTERFERONS. In G. J. Laurent & S. D. Shapiro (Eds.), *Encyclopedia of Respiratory Medicine* (pp. 346-350). Academic Press. https://doi.org/https://doi.org/10.1016/B0-12-370879-6/00190-3

Le Maitre, C. L., Hoyland, J. A., & Freemont, A. J. (2007). Catabolic cytokine expression in degenerate and herniated human intervertebral discs: IL-1β and TNFα expression profile. *Arthritis Research & Therapy*, *9*(4), R77. https://doi.org/10.1186/ar2275

Le Maitre, C. L., Richardson, S. M. A., Baird, P., Freemont, A. J., & Hoyland, J. A. (2005). Expression of receptors for putative anabolic growth factors in human intervertebral disc: implications for repair and regeneration of the disc [https://doi.org/10.1002/path.1862]. *The Journal of Pathology*, *207*(4), 445-452. https://doi.org/https://doi.org/10.1002/path.1862

Lee, J.-H., Parthiban, P., Jin, G.-Z., Knowles, J. C., & Kim, H.-W. (2021). Materials roles for promoting angiogenesis in tissue regeneration. *Progress in Materials Science*, *117*, 100732. https://doi.org/https://doi.org/10.1016/j.pmatsci.2020.100732

Lin, H., Tian, S., Peng, Y., Wu, L., Xiao, Y., Qing, X., & Shao, Z. (2021). IGF Signaling in Intervertebral Disc Health and Disease. *Front Cell Dev Biol*, *9*, 817099. https://doi.org/10.3389/fcell.2021.817099

Liu, M., Guo, S., & Stiles, J. K. (2011). The emerging role of CXCL10 in cancer (Review). *Oncol Lett*, *2*(4), 583-589. https://doi.org/10.3892/ol.2011.300

Lopez-Dee, Z., Pidcock, K., & Gutierrez, L. S. (2011). Thrombospondin-1: multiple paths to inflammation. *Mediators Inflamm*, *2011*, 296069. https://doi.org/10.1155/2011/296069

Lotz, M., Moats, T., & Villiger, P. M. (1992). Leukemia inhibitory factor is expressed in cartilage and synovium and can contribute to the pathogenesis of arthritis. *J Clin Invest*, *90*(3), 888-896. https://doi.org/10.1172/jci115964

Loureiro, J., Torres, A. L., Neto, T., Aguiar, P., Barrias, C. C., Pinto, M. T., & Amaral, I. F. (2019). Conjugation of the T1 sequence from CCN1 to fibrin hydrogels for therapeutic vascularization. *Materials Science and Engineering: C*, *104*, 109847. https://doi.org/https://doi.org/10.1016/j.msec.2019.109847

Nicola, N. A., & Babon, J. J. (2015). Leukemia inhibitory factor (LIF). *Cytokine & Growth Factor Reviews*, *26*(5), 533-544. https://doi.org/https://doi.org/10.1016/j.cytogfr.2015.07.001

Orian-Rousseau, V. (2015). CD44 Acts as a Signaling Platform Controlling Tumor Progression and Metastasis [Mini Review]. *Frontiers in immunology*, *6*. https://www.frontiersin.org/articles/10.3389/fimmu.2015.00154

Ornitz, D. M., & Itoh, N. (2015). The Fibroblast Growth Factor signaling pathway [https://doi.org/10.1002/wdev.176]. *WIREs Developmental Biology*, *4*(3), 215-266. https://doi.org/https://doi.org/10.1002/wdev.176

Parenté, A., Di Meo, F., Lapeyronie, E., Al Mansi, M., Delourme, D., Pélissier, P., Brémaud, L., Trouillas, P., & Blanquet, V. (2020). GASP-1 and GASP-2, two closely structurally related proteins with a functional duality in antitrypsin inhibition specificity: a mechanistic point of view [https://doi.org/10.1111/febs.15072]. *The FEBS Journal*, *287*(5), 909-924. https://doi.org/https://doi.org/10.1111/febs.15072

Rutishauser, U. (1992). NCAM and its polysialic acid moiety: a mechanism for pull/push regulation of cell interactions during development? *Dev Suppl*, 99-104.

Rutishauser, U., Acheson, A., Hall, A. K., Mann, D. M., & Sunshine, J. (1988). The neural cell adhesion molecule (NCAM) as a regulator of cell-cell interactions. *Science*, *240*(4848), 53-57. https://doi.org/10.1126/science.3281256

Sakai, D., & Grad, S. (2015). Advancing the cellular and molecular therapy for intervertebral disc disease. *Advanced Drug Delivery Reviews*, *84*, 159-171. https://doi.org/https://doi.org/10.1016/j.addr.2014.06.009

Sakai, D., Nakai, T., Mochida, J., Alini, M., & Grad, S. (2009). Differential Phenotype of Intervertebral Disc Cells: Microarray and Immunohistochemical Analysis of Canine Nucleus Pulposus and Anulus Fibrosus. *Spine*, *34*(14). https://journals.lww.com/spinejournal/Fulltext/2009/06150/Differential_Phenotype_of_Intervertebral_Disc.5.aspx

Sakai, D., Nakamura, Y., Nakai, T., Mishima, T., Kato, S., Grad, S., Alini, M., Risbud, M. V., Chan, D., Cheah, K. S. E., Yamamura, K.-i., Masuda, K., Okano, H., Ando, K., & Mochida, J. (2012). Exhaustion of nucleus pulposus progenitor cells with ageing and degeneration of the intervertebral disc. *Nature Communications*, *3*(1), 1264. https://doi.org/10.1038/ncomms2226

Tokunaga, R., Zhang, W., Naseem, M., Puccini, A., Berger, M. D., Soni, S., McSkane, M., Baba, H., & Lenz, H. J. (2018). CXCL9, CXCL10, CXCL11/CXCR3 axis for immune activation - A target for novel cancer therapy. *Cancer Treat Rev*, *63*, 40-47. https://doi.org/10.1016/j.ctrv.2017.11.007

van den Akker, G. G. H., Eijssen, L. M. T., Richardson, S. M., Rhijn, L. W. V., Hoyland, J. A., Welting, T. J. M., & Voncken, J. W. (2020). A Membranome-Centered Approach Defines Novel Biomarkers for Cellular Subtypes in the Intervertebral Disc. *Cartilage*, *11*(2), 203-220. https://doi.org/10.1177/1947603518764260

van den Akker, G. G. H., Surtel, D. A. M., Cremers, A., Rodrigues-Pinto, R., Richardson, S. M., Hoyland, J. A., van Rhijn, L. W., Welting, T. J. M., & Voncken, J. W. (2014). Novel immortal human cell lines reveal subpopulations in the nucleus pulposus. *Arthritis Research & Therapy*, *16*(3), R135. https://doi.org/10.1186/ar4597

Vazirinejad, R., Ahmadi, Z., Kazemi Arababadi, M., Hassanshahi, G., & Kennedy, D. (2014). The biological functions, structure and sources of CXCL10 and its outstanding part in the pathophysiology of multiple sclerosis. *Neuroimmunomodulation*, *21*(6), 322-330. https://doi.org/10.1159/000357780

Veronesi, F., Sartori, M., Griffoni, C., Valacco, M., Tedesco, G., Davassi, P. F., Gasbarrini, A., Fini, M., & Barbanti Brodano, G. (2022). Complications in Spinal Fusion Surgery: A Systematic Review of Clinically Used Cages. *Journal of Clinical Medicine*, *11*(21).

Vidal, P. M., Lemmens, E., Dooley, D., & Hendrix, S. (2013). The role of "anti-inflammatory" cytokines in axon regeneration. *Cytokine & Growth Factor Reviews*, *24*(1), 1-12. https://doi.org/https://doi.org/10.1016/j.cytogfr.2012.08.008

Wang, Z., Qu, Z., Fu, C., Xu, F., Chen, Y., Wang, Z., & Liu, Y. (2016). Interleukin 1 Polymorphisms Contribute to Intervertebral Disc Degeneration Risk: A Meta-Analysis. *PLOS ONE*, *11*(6), e0156412. https://doi.org/10.1371/journal.pone.0156412

Yang, J.-E., Zhao, K.-H., Qu, Y., & Zou, Y.-C. (2022). Increased serum CXCL10 levels are associated with clinical severity and radiographic progression in patients with lumbar disc degeneration. *Clinica Chimica Acta*, *525*, 15-22. https://doi.org/https://doi.org/10.1016/j.cca.2021.12.006

Zhang, Q., Ji, Q., Wang, X., Kang, L., Fu, Y., Yin, Y., Li, Z., Liu, Y., Xu, X., & Wang, Y. (2015). SOX9 is a regulator of ADAMTSs-induced cartilage degeneration at the early stage of human osteoarthritis. *Osteoarthritis Cartilage*, *23*(12), 2259-2268. https://doi.org/10.1016/j.joca.2015.06.014

Zhang, W., Ge, Y., Cheng, Q., Zhang, Q., Fang, L., & Zheng, J. (2018). Decorin is a pivotal effector in the extracellular matrix and tumour microenvironment. *Oncotarget; Vol 9, No 4*. https://www.oncotarget.com/article/23869/text/

Zhou, G., & Groth, T. (2018). Host Responses to Biomaterials and Anti-Inflammatory Design—a Brief Review [https://doi.org/10.1002/mabi.201800112]. *Macromolecular Bioscience*, *18*(8), 1800112. https://doi.org/https://doi.org/10.1002/mabi.201800112

6. SUPPLEMENTARY FIGURES

SUPPLEMENTARY FIGURE 1. EVALUATION OF INFLAMMATORY CYTOKINE LEVELS IN CONDITIONED MEDIA FROM REPOPULATED NPS OF DIFFERENT AGED DONORS.

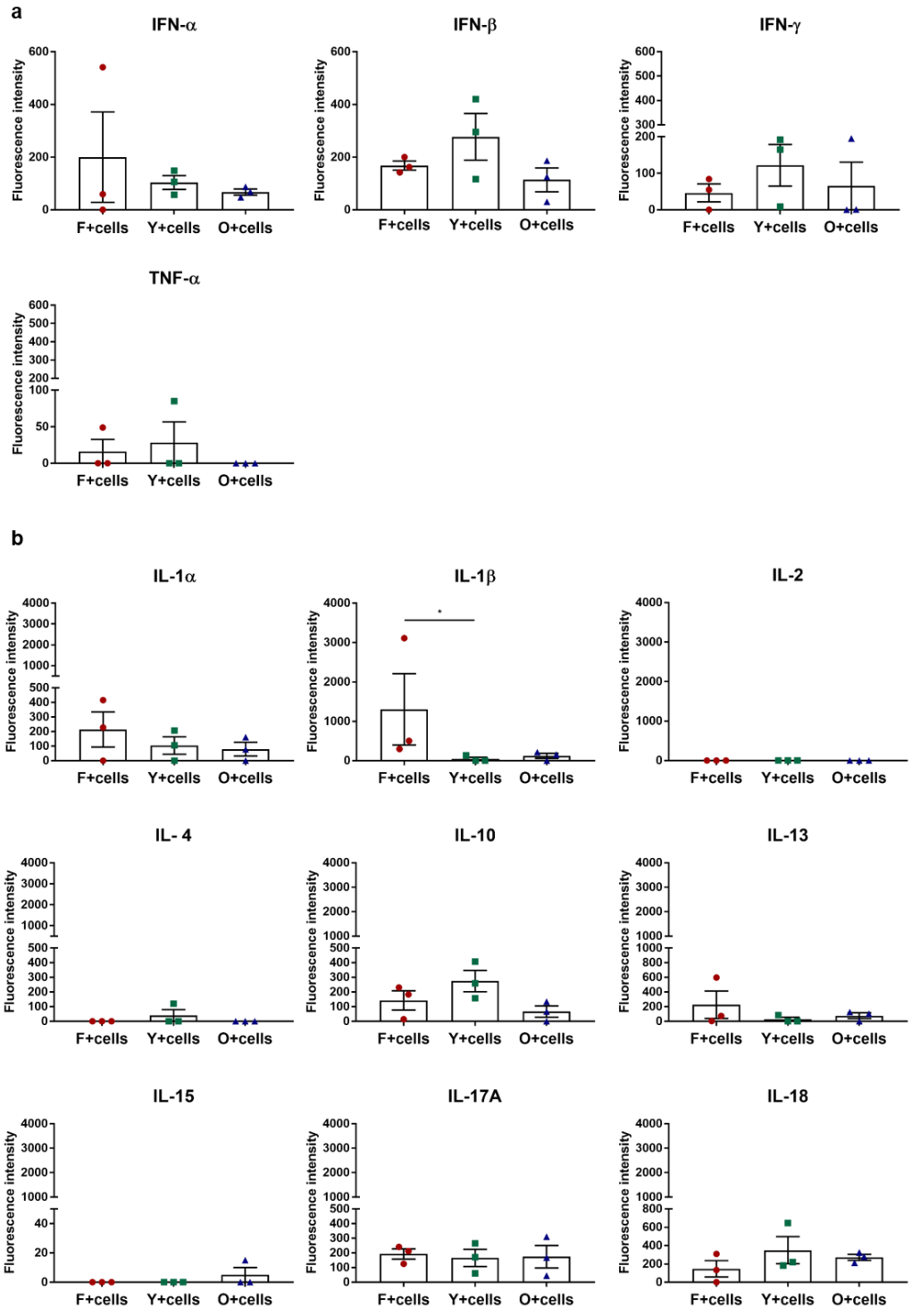

Supplementary figure 1. (a). Interferon (IF)-α, IFN-β, IFN-γ, transforming growth factor-α (TNF-α) and **(b)** several interleukins (ILs) expression in conditioned media from repopulated fetus (F), young (Y) and old (O) matrices. Data are presented as fluorescence intensity. Error bars represent mean ± SEM (n=3 biological replicates). Kruskal Wallis test followed by Dunn's multiple comparison test was performed. *p<0.05.

SUPPLEMENTARY FIGURE 2. ASSESSMENT OF ANGIOGENIC MOLECULES, GROWTH FACTORS AND OTHER CYTOKINES IN CONDITIONED MEDIA FROM REPOPULATED NPS OF DIFFERENT AGED DONORS.

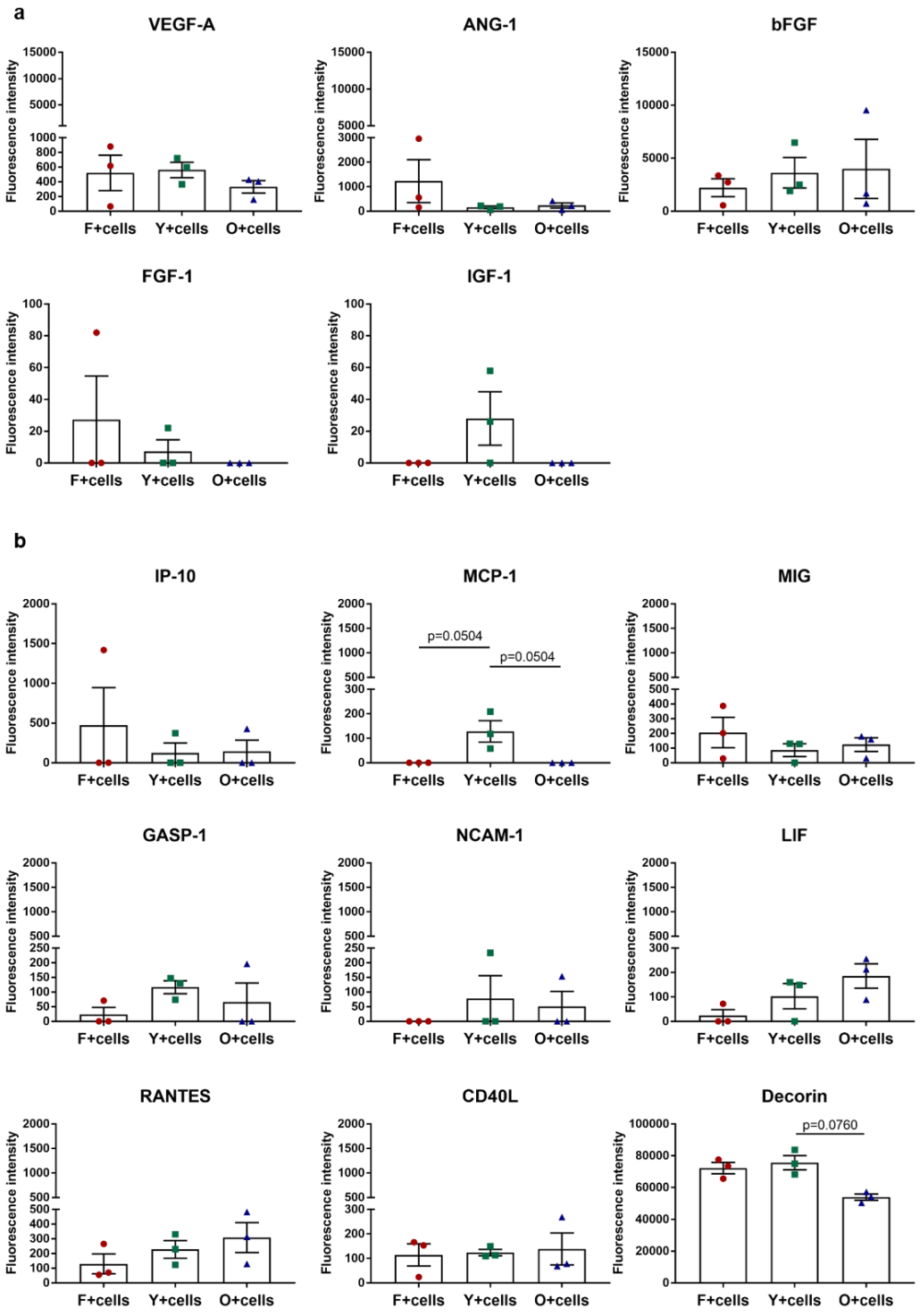

Supplementary figure 2. Vascular endothelial growth factor (VEGF-A), angiopoietin-1 (ANG-1), basic fibroblast growth factor (bFGF), fibroblast growth factor-1 (FGF-1) and insulin-like growth factor (IGF-1) expression levels in repopulated fetus (F), young (Y) and old (O) NPs. **(b)** Interferon γ-induced protein-10 (IP-10), monocyte chemoattractant protein-1 (MCP-1), monokine induced by gamma interferon (MIG), growth and differentiation factor-associated serum protein-1 (GASP-1), neural cell adhesion molecule (NCAM-1), leukemia inhibitory factor (LIF), regulated on activation, normal T cell expressed and secreted (RANTES) and CD40 ligand (CD40L) expression levels in repopulated F, Y and O NPs. Data are presented as fluorescence intensity. Error bars represent mean ± SEM (n=3 biological replicates). Kruskal Wallis test followed by Dunn's multiple comparison test was performed.

SUPPLEMENTARY FIGURE 3. SCREENING OF THE ANGIOGENIC POTENTIAL OF HUMAN IMMORTALIZED NP CELLS BY *IN VIVO* CAM ASSAY.

a

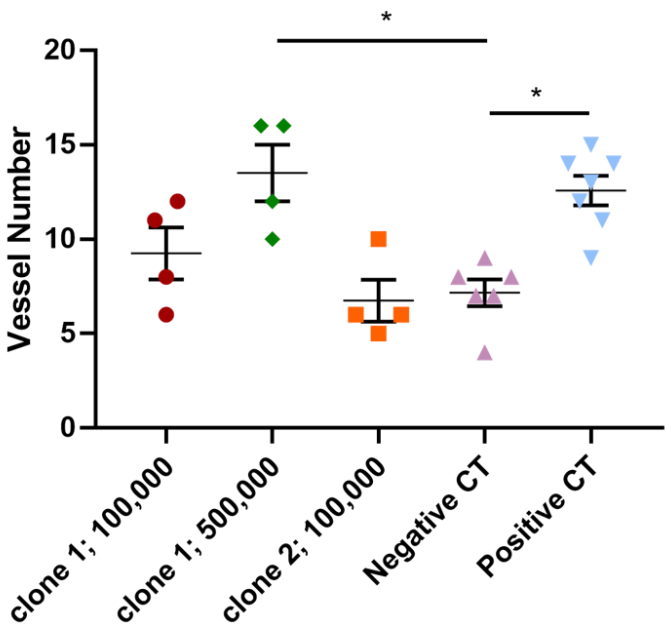

Supplementary figure 3. (a). Quantification of new vessels growing towards the chorioallantoic membrane (CAM) inoculated with different clones of immortalized nucleus pulposus (iNP) cells (clone 1: GA094 and clone 2: GA111), with $1x10^5$ cells or $5x10^5$ cells (clone 1), compared to the negative control (CT: H_2O) and the positive one ($bFGF_2$). Error bars represent mean ± SEM. Kruskal Wallis test followed by Dunn's multiple comparison test was performed. *$p<0.05$.

CHAPTER VII

CHAPTER VII – GENERAL DISCUSSION AND FUTURE PERSPECTIVES

1. GENERAL DISCUSSION

The work developed under the scope of this thesis aimed to recapitulate a pro-regenerative microenvironment, by using fetal-derived biomaterials, to develop efficient therapies for inducing endogenous repair of intervertebral disc (IVD).

As extensively reported, IVD degeneration occurs naturally with aging as a consequence of physiological changes at cellular, biochemical and structural levels, finally leading to low back pain (LBP). Despite disc degeneration having been widely correlated to age-associated alterations, further studies are needed to understand the complex mechanism underlying this pathological scenario (Colombier et al., 2014). As described in Chapter I, IVD is characterized by a harsh microenvironment, which leads to scarcer cell survival. Thus, adult IVDs have a decreased ability to self-regenerate, due to the limited number of progenitor cells (Tessier & Risbud, 2021), rendering problematic the regression of the degenerative cascade (Ma et al., 2019). Indeed, IVD is the tissue that undergoes degeneration earliest in the human body, when compared to other connective tissues (Urban & Roberts, 2003). However, during embryonic development IVDs are characterized by a more pro-regenerative – like phenotype due to their unique cellular and biochemical composition, as widely described in Chapter I. Although several researchers have tried to dissect the protein profile of fetal IVD matrices, still few studies currently exist in the literature, and the role of all the different molecules involved is yet to be defined.

As it is well known, current available treatments for IVD degeneration (both conservative therapies and surgical approaches) focus only on relieving patient's symptoms (Dou et al., 2021), being enable to reconstitute a healthy tissue microenvironment. Thus, new alternatives are needed. Decellularized extracellular matrix (ECM)-based biomaterials has been proposed for tissue regeneration, including IVD, as addressed in Chapter II of this thesis. These naturally-derived biomaterials represent a huge promise for the treatment of IVD degeneration, because of the possibility to mimic native structural, biochemical and biomechanical cues, which can ultimately lead to tissue repair. However, in order to develop efficient therapy to specifically trigger IVD repair, a deeper understanding of the impact of development and aging, as well as their associated microenvironmental cues, on tissue degeneration and regeneration is needed.

The main hypothesis of this thesis, as defined in Chapter III, was that fetal decellularized nucleus pulposus (NP) ECM would have a superior potential for IVD regeneration. This hypothesis was based on our previous assumption of the superior pro-regenerative potential of fetal bovine NP, when compared to young and old ones, due to the expression of specific proteins (Collagen [COL] 12 and COL14), which were lost with ageing (Caldeira et al., 2017).

To address this question, we selected caudal bovine IVDs as tissue source due to its similarity in size (Alini et al., 2008), ECM composition and cell content to human tissues. In particular, bovine IVD are characterized by a decrease and disappearance of notochordal cells (NC) in the NP after birth, like humans. Contrarily, other species (*e.g*. mouse, rat, cat, mink, dog, pig and rabbit) had demonstrated the persistence of NC after birth (Alini et al., 2008), thus reducing the clinical relevance of those models for the study of pathological features involved in IVD degeneration. Moreover, bovine IVDs are available and easier to access, when compared to human ones, due to ethical governmental restrictions in collecting tissues from cadaveric origin, especially from fetal origin. Therefore, cow tissues have been widely used as *ex vivo* models to investigate suitable therapeutic strategies for IVD degeneration (Antunes et al., 2017; Ferreira et al., 2021; Lang et al., 2018; Li et al., 2020; Pereira et al., 2016; Teixeira et al., 2016).

In Chapter IV, we have developed decellularized ECM-based scaffolds from bovine NPs of different aged donors (fetus, young and old). We have selected a decellularization method for different reasons. Firstly, this technique offers the possibility to create 3D models and therapeutic solutions, which are closer to the native tissue, since it is able to remove cells and DNA without dramatically affecting matrix structure and composition. In particular, the ECM represents the 3D network of tissues and organs, providing structural support to resident cells (Caldeira et al., 2018). Moreover, it also acts as a dynamic template, regulating essential cellular processes, including morphogenesis, differentiation, homeostasis, among others, thanks to its intrinsic biochemical and biomechanical features (Caldeira et al., 2018; Hussey et al., 2018). Thus, mimicking the unique ECM microenvironmental features represents a promising strategy to unravel specific cues involved in pathological progression, but also as a novel therapeutic strategy for tissue regeneration (Hussey et al., 2018). Although the development of decellularized IVD-based scaffolds has been widely attempted by several researchers, as extensively described in Chapter II of this thesis, the impact of tissue donor age on biomaterials development had never been explored before in the disc field.

The first contribution of this thesis was the development, for the first time, of a transversal and standardized sodium dodecyl sulphate (SDS) 0.1 % (1 h) – based protocol, efficient at removing host cells and DNA from bovine NPs of different donor ages (fetus, young and old), while preserving structural, biochemical and biomechanical cues of native tissues. Importantly, the decellularization protocol herein developed is under a provisional patent application ("Fetal decellularized nucleus pulposus material and methods for obtaining pharmaceutic compositions to be used in the treatment of intervertebral disc degeneration and low back pain" - WO2021118379; 17.06.2021). Moreover, it is also being used by our group for the decellularization of other tissues (*e.g*. mice intestines), after some required adaptations, considering the different ECM structure and composition between organs and species.

In order to optimize the decellularization process, we tested two detergents, SDS and Triton X-100, at different concentration and time points. SDS - based protocol showed to be more efficient in removing host cells and decreasing DNA content from all NPs of different donor ages, as compared to Triton X-100. It is known that SDS can have adverse effects on ECM composition, structure and biomechanical properties, which may be influenced by the detergent concentration and time of exposure (Friedrich et al., 2018). The majority of the SDS-based protocols applied to the IVD adopt long exposure to detergents (Chan et al., 2013; Wu et al., 2014; Wu et al., 2017). The novelty of the decellularization protocol, herein developed, is the use of lower SDS concentration (0.1 %) as well as the reduction of exposure time to only 1 h, which may decrease the risk of toxicity due to remaining detergent within the tissue. Although in the present study we did not investigate the presence of SDS in the tissues, preliminary data from our group showed detergent absence in the NPs, which were decellularized by adopting the SDS-based protocol herein optimized. This is essential, envisaging biomaterials translation for clinical applications. In particular, SDS can have a cytotoxic effect on cells (Alizadeh et al., 2019) and if not properly removed, may provoke an adverse host response upon scaffolds' implantation (Friedrich et al., 2018). Syed *et al*. showed that a protocol based on a combination of SDS and Triton X-100 was the most efficient in decreasing DNA content from porcine small intestine submucosa. However, after repopulation, metabolic activity of seeded cells decreased and this higher cytotoxic effect was associated to residual detergents within the tissue (Syed et al., 2014). Alizabeh *et al.* (2019) investigated a novel and rapid vacuum-based method for washing out any remaining SDS from bovine pericardium after decellularization. They demonstrated that the vacuum methods were more successful in removing SDS from

decellularized tissues, as well as in decreasing the toxicity for cells, by increasing their survival and metabolic properties, when compared to normal washing procedures (Alizadeh et al., 2019).

A limitation of our protocol is the loss of glycosaminoglycans (GAGs) detected in all the NPs from different aged donors after decellularization. Therefore, a milder procedure which would be able to preserve higher GAGs content, should be investigated, knowing their essential role in the disc. A vacuum-assisted decellularization could be the solution to avoid the loss of large number of GAGs as well as to accelerate and scale-up the procedure. This is particularly important for industrial manufacturing, envisaging clinical application. In the last decade, this process is started to be investigated for tissues requiring longer treatment cycles to remove cells, including human (Butler et al., 2017) and porcine trachea (Lange et al., 2017), porcine urinary bladder (Ren et al., 2018), *etc*. To the best of our knowledge, vacuum-assisted decellularization has not been applied yet to the IVD and this would be particularly interesting for the decellularization of whole discs. Indeed, obstacles in solution penetration inside the IVD can be encountered during standard decellularization procedure, knowing the denser nature of this tissue. Currently, we are exploring this procedure to scale up the decellularization of larger bovine NP specimens, by using the SDS-based protocol herein developed. Another option to replace the GAGs loss after decellularization could be the supplementation of the scaffolds with chondroitin sulphate, as others had done previously (Zhou et al., 2018). In the present work, we decided to not supplement decellularized NP matrices with chondroitin sulphate, since our aim was to use naturally-derived scaffolds and maintain their structure, composition and biomechanical properties as close as possible to native environment. This is essential for preserving the pro-regenerative cues of fetal native matrices (*e.g.,* COL12 and COL14).

In recent years, the interest for detergent-free strategies for tissue decellularization has increased, since these approaches are able to separate cell and proteins, without dramatically affecting native ECM features. Among these methods, the supercritical carbon dioxide (CO_2)-based approach has gained significant attention and has been applied for the decellularization of different tissues and organs (*e.g*., porcine trabecular bone (Duarte et al., 2021), porcine trachea (de Wit et al., 2023), ovine aorta and bovine cornea (Guler et al., 2017), bovine articular cartilage, horse tendons and human skin (Antons et al., 2018), *etc)*, as well as apoptosis-assisted approach (*e.g*., lung (Song et al., 2021), nerve (Cornelison et al., 2018), *etc*). To the best of our knowledge these methods have not been applied yet to the IVD and could be beneficial for the decellularization of this dense tissue.

The second contribution of this thesis was to uncover the superior pro-regenerative potential of fetal decellularized matrices. In Chapter IV, we repopulated decellularized matrices from different donor ages with adult bovine NP cells. The rationale behind the selection of this cell source was to understand if adult cells, which are characterized by a limited capacity to proliferate and produce proteins, were rejuvenated by a more pro-regenerative tissue. Indeed, cells were able to sense the surrounding microenvironment, particularly the ECM, behaving differently in contact with a pro-regenerative or degenerated tissue, especially in terms of viability and protein production. We have demonstrated that cells were able to adhere to a higher degree, as well as to remain more viable, in younger decellularized NPs when compared to old ones. Moreover, seeded cells started to produce GAGs in fetal NPs which is of utmost of importance for our work, since the decellularization procedure lead to a loss of these proteins, fundamental for IVD function. More importantly, at the molecular level we observed the greatest Collagen type 2 (*COL2)* and aggrecan (*ACAN*) gene expression levels in fetal scaffolds. At the protein level, ACAN increased in both fetus and young matrices, when compared to the old ones, while COL2 decreased, which may be indicative of matrix remodeling. Therefore, younger matrices were able to rejuvenate the cellular and biochemical signals of adult NP cells, through matrix reconstruction. Although the enhanced pro-regenerative potential of fetal matrices could be associated to the presence of COL12 and COL14, other factors may be involved in this precise process. In Chapter VI of this thesis we have performed a preliminary study to explore the mechanisms behind the increased ACAN production in fetal NP-based scaffolds. Given that a form of CD44 was described as a receptor for COL14 (Ehnis et al., 1996), we have neutralized this protein in bovine NP cells, before the seeding on fetal decellularized matrices. We were expecting a decrease of ACAN in fetal NPs repopulated with CD44-knockout cells, when compared to the scaffolds recellularized with CD44-wildtype cells. Results did not show significant changes in ACAN content between the tested conditions. We hypothesized that this could be due to the inefficiency of the antibody to neutralize CD44. Therefore, CD44 should be neutralized by using RNA signaling-based approach in order to induce the blocking of the target protein in a more specific manner.

Nevertheless, other factors and signaling pathways (described in the Chapter I) herein not explored, could have a role in the increased regenerative response of fetal matrices, such as Wnt signaling. Interestingly, Pizzute *et al*. (2018) were able to demonstrate that overexpression of WNT factors in NP cells, isolated from human herniated IVDs, lead to an increase of GAGs deposition and over-expression of NP re-differentiation

genes (*PAX-1, FOXF-1, COL2A1, ACAN*), although the effect ameliorates after 28 days (Pizzute et al., 2018). Moreover, it has also been shown that COL12 deposition is regulated by Wnt/β-catenin signaling and that over-expression of *Col12a1* is able to accelerate axon regeneration and rescue Wnt/β-catenin signaling pathway inhibition, at least for zebrafish species (Wehner et al., 2017). Therefore, Wnt signaling could be involved in the observed fetal matrices outcomes, knowing the higher expression of COL12 at this age. Taking this in account, one limitation of the present work was the lack of a deeper understanding of the composition of decellularized matrices from different donor ages, as well as of the pathways that could orchestrate the regenerative cascade, which could be conducted by proteomic analysis.

An intrigued question that remain also opened is to understand if fetal matrices could be ideal substrates to re-activate the reminiscent NC sub-population in adult NPs, which is of utmost importance for inducing endogenous IVD regeneration, in the case of a mild tissue degeneration. As described in the Chapter I, NC are involved in disc homeostasis and repair. Interestingly, Tryfonidou's group was able to demonstrate the enhanced capacity of porcine NC-derived matrices in increasing both DNA and GAGs content of human and canine chondrocyte-like cells, as well as GAGs and COL2 production. Moreover, it was also able to induce chondrogenic differentiation of canine mesenchymal stromal cells (MSCs). More interestingly, after injection of NC-derived matrix in a canine model of moderate disc degeneration, they revealed improved disc height and COL2 deposition, as well as inflammation amelioration *in vivo* (Bach et al., 2018*)*, which are hallmarks of tissue repair. More recently, this NC-derived matrix has also been used for other applications. Schmitz and colleagues went a step further by creating an injectable biomaterial based on decellularized NC-derived matrix, which could be used as a vehicle for cells deliver in the IVD (Schmitz et al., 2022).

Interestingly, fetal and young matrices showed increased contraction after repopulation, by appearing more transparent and softer, when compared to the old ones. Although this evaluation was conducted only at macroscopic level, it opened new questions on biomechanical changes, through ageing, which could influence cell behavior after repopulation. As it is known, cells are able to sense surrounding ECMs' mechanical stimuli and convert them into intracellular signals (d'Angelo et al., 2019). Cells can remodel the scaffolds by generating forces, which can ultimately lead to tissue regeneration, adaptation or pathological cascade (Yi et al., 2022). In the IVD context, matrix stiffness can have an important impact on IVD cells mechanobiology, in terms of mRNA expression and matrix

synthesis (Fearing et al., 2018). Gilchrist and colleagues (2011) have previously shown that soft laminin-rich gels (<720 Pa) were able to induce porcine NP cell-cell interaction, cell morphologies and proteoglycans production *in vitro* (Gilchrist et al., 2011). In another work, Navaro *et al* (2015) developed hydrogels (fibrinogen and poloxameric block copolymers) with different shear storage modulus (1 kPa and 2 kPa) in order to investigate the role of ECM's stiffness on proliferation, differentiation and matrix remodeling of NP-derived stem cells. As results, hydrogel with lower shear storage modulus induced higher NP cell proliferation, chondrogenic differentiation and cell attachment, when compared to the 2 kPa ones. Moreover, it was also able to increase *acan* and *sox9* gene expression, as well as GAGs production (Navaro et al., 2015). In the present work, changes in biomechanical properties were already detected in decellularized NPs from different donor ages before repopulation, by rheology. In particular, fetal decellularized matrices showed a softer like-behavior (~75 Pa), when compared to young (~180 Pa) and old ones (~160 Pa). Therefore, we hypothesize that softer fetal decellularized matrices could provide a more favorable 3D microenvironment for cell seeding, thus promoting higher cell survival and adhesion, as well as increasing protein production, when compared to the stiffer old ECM-based scaffolds (prototypical of a degenerated tissue). In order to address this hypothesis, a mechanical characterization at nano- and micro-scale should be performed in repopulated NPs from different donor ages. This could be conducted by nanoindentation or atomic force microscopy.

In Chapter IV, we have addressed the angiogenic potential of decellularized matrices from different aged donors, by performing a chick embryo chorioallantoic membrane (CAM) *in vivo* assay. Specifically, we aimed to understand if younger matrices were able to mimic an anti-angiogenic scenario similar to native and healthy discs. After 3 days of scaffolds implantation in the CAMs, fetal matrices demonstrated an anti-angiogenic potential, by decreasing the number of vessels growing towards the basic fibroblast growth factor 2 ($bFGF_2$)-treated CAMs. More interestingly, the anti-angiogenic properties of fetal scaffolds were also preserved in contact with human immortalized NP (iNP) cells, as reported in the Chapter VI of this thesis. These data delivered the first *in vivo* proof-of-concept of fetal matrices' ability to provide an avascular microenvironment to IVD cells. Bovine NP decellularized matrices may contain pro-/anti-angiogenic factors differentially expressed during ageing. For example, pigment epithelium-derived factor (PEDF), which is an angiogenesis inhibitor, was reported to be upregulated in the matrisome profiling of native fetal NPs (Caldeira et al., 2017). Recently, it was demonstrated that PDEF is able to

suppress blood vessels' growth, through inhibition of vascular endothelial growth factor (VEGF)-R2 (receptor of VEGFA), in retinal endothelial cells (Tombran-Tink & Barnstable, 2003; Zhang et al., 2021). Therefore, higher expression of PEDF could be one of the factors involved in the regulation of the anti-angiogenic properties of fetal decellularized matrices. A part from PEDF, fetal native NPs also showed upregulation of thrombospondin – 1 (TSP-1), another angiogenesis inhibitor (Caldeira et al., 2017). TSP-1 is able to mediate inflammation, cancer and angiogenesis through the interactions with several receptors (Lopez-Dee et al., 2011). Therefore, TSP-1 may be involved in the higher inflammatory score revealed in fetal decellularized matrices after *in vivo* CAM assay (reported in the Chapter VI of this thesis). Nevertheless, although the results from the CAM assay as a preclinical *in vivo* model were promising, angiogenesis should also be investigated in a more suitable animal model for clinical relevance (*e.g.*, mice or rats).

In the Chapter VI, we have analyzed several inflammatory and angiogenic soluble factors in conditioned media derived from decellularized NPs of different aged donors at day 3 of *ex vivo* culture, by using a bovine cytokine array. The rationale behind this work was to provide a first proof-of-concept of the mechanism controlling inflammation and angiogenesis in decellularized matrices, knowing its essential role for the biomaterials' success upon implantation. Herein, we did not detect a significantly increase of inflammatory and pro-angiogenic cytokines in decellularized NPs from different aged donors. Although it seems that decellularized NPs are not pro-inflammatory nor pro-angiogenic, some limitations exist in this work. Firstly, we have conducted the experiments by using two pools of different biological replicates, thus not reaching statistical significance given the high variability of the samples. Moreover, we performed the assay by using samples at day 3 of *ex vivo* culture, after 1 day of culture. Thus, we cannot exclude cytokine removal and dilution of the effect at this time point. Therefore, further studies are needed to understand the factors behind the occurring angiogenic and inflammatory responses.

Overall, this work demonstrated that choosing an adequate tissue donor age is an essential step for the design of suitable biomaterials for tissue-engineering and regenerative medicine applications. We have shown that younger matrices, in particular fetal ones, are more appropriate tissue source to be used as a therapy due to their superior pro-regenerative potential, through increased ECM *de novo* synthesis, tissue remodeling and reduced angiogenesis. Old decellularized matrices revealed to be an interesting *ex vivo* model to investigate molecular cues underlying disc degeneration along aging as well as to screen for new molecules or drugs intended for disc regeneration.

This project has contributed to the field of matrix engineering and regenerative medicine by uncovering essential knowledge on the benefit of using fetal-derived matrices for restoring a healthy tissue microenvironment. The data generated in this work will be of utmost importance for the development of minimally invasive strategies to guide IVD repair *in vivo*.

Our whole vision for future therapeutic approaches focuses on the use of fetal matrices as a minimally invasive strategy to resolve IVD degeneration and LBP. These biomaterials could be administered as particles or processed to form a hydrogel, which could be injected through IVD. However, injection through the annulus fibrosus (AF) can led to tissue damage and consequent secondary degeneration. Thus, these solutions should be injected by adopting a transpedicular approach through the endplates in order to reduce the risk of tissue disruption (Vadalà et al., 2013). This strategy will decrease the risks associated with invasive surgeries, such as infections and secondary degeneration, as well as the days of hospitalization. This therapy could be particularly effective for LBP patient's affected by milder disc degeneration, since fetal matrices could be able to rejuvenate the biochemical signals of endogenous disc cells through ECM proteins production, finally leading to tissue reconstruction. For severe IVD degenerative stages, hydrogel derived from fetal tissue could be combined with MSCs, the most promising cell source used in LBP trials (Atluri et al., 2022; Kumar et al., 2017), to enhance tissue regeneration.

Although further validations are needed, the fetal-based biomaterials, herein developed, could globally revolutionize matrix-based therapies for the regeneration of different tissues (*e.g*., cartilage). For instance, injection of fetal-derived matrices could be used for accelerating tendon or ligaments repair after injury of professional athletes. Moreover, fetal-derived matrices could be also used as adjuvants during chemotherapy to revert degenerative outcomes, caused by these aggressive treatments. Therefore, several fields of study could take advantages of the knowledges herein achieved for the treatment of different pathological conditions, in which endogenous self-repair is impaired.

2. FUTURE PERSPECTIVE

This thesis opened new doors for several projects in our groups, which are currently funded by different national and international sources, including: FETBIO ("Fetal-inspired hierarchical biomaterials for regeneration in a harsh microenvironment: the nucleus of the intervertebral disc"), funded by Fundação para a Ciência e a Tecnologia (FCT - PTDC/BTM-MAT/0438/2020); CLOCKit: "Rewinding the clock: CRISPR-mediated NP cell editing for IVD rejuvenation", funded by ON Foundation, which intend to recapitulate fetal-inspired cues by CRISPR-engineering NP cells; "Characterization of the MSC-derived extracellular matrix", funded by FCT (EXPL/BTM-ORG/0880/2021).

The discoveries of this work represented also the starting point for the establishment of the FETALIX startup, in which I am one of the Co-Founder, which intend to provide the first minimally invasive therapeutic strategy to treat IVD degeneration and solve LBP, through the use of fetal decellularized matrices, herein developed.

In this thesis we were able to develop fetal decellularized NPs, which were fully characterized at structural, biochemical and biomechanical levels, as well as in terms of cytocompatibility and toxicity. But, further studies are needed to translate these biomaterials into clinical applications. A mild sterilization method for decellularized scaffolds should be explored in order to remove any contaminants. Moreover, the presence of specific antigens (*e.g.*, alpha-gal) and endotoxins should be also investigated. These studies will be essential to reduce the risk of host rejection upon implantation, due to an immune or inflammatory response or infections.

In the future, a complex bioreactor system could be designed to decellularize, sterilize and recellularize tissues at the same moment in order to obtain scaffolds in a faster way. Moreover, decellularized ECM could be combined with bioink, fabricated by using a bioprinting-based strategy (Park et al., 2021; Vernengo et al., 2020), in order to improve the topography of these scaffolds for clinical applications.

In this thesis, we have demonstrated the superior capacity of fetal decellularized matrices to induce ECM *de novo* synthesis by seeded NP cells. These discoveries opened new challenges, particularly on dissecting the specific ECM cues, which could guide tissue regeneration. To address this question, a deeper analysis of the human IVD transcriptomic profile will be performed at single cell level.

In this work, we have focused on the pro-regenerative potential of fetal scaffolds at matrix level, without considering the cellular signals, which are essential for guiding tissue repair. In the future NC-derived matrix or secretome could be also explored for IVD regeneration.

Herein, we have addressed cell behavior in the different matrices by using bovine NP cells. In the future, repopulation with other cells, as canine or human (isolated from degenerated IVD) NP cells should be also explored to validate the aforementioned observations by using a cell source derived from a model of disc degeneration. Moreover, the potential of fetal decellularized NPs to induce human MSCs differentiation in NP-like cells should be investigated, envisaging the use of these biomaterials for cell delivery for more severe IVD degeneration.

For future clinical application and market translation, the fetal matrices' therapeutic potential and biocompatibility require *in vivo* validation, by using relevant animal models of IVD degeneration (*e.g.*, chondrodystrophic dogs) (Thompson et al., 2018).

The work developed under the scope of this thesis opened also new avenues for the investigation of COL12 and COL14 reactivation *in vivo*. Indeed, there is no proof of concept of the role of these two proteins in the fetal NPs. One approach could be to knockdown or upregulate both proteins in an *in vivo* animal model and evaluate the outcomes.

Finally, fetal ECM-based scaffolds could be processed to form a hydrogel. The advantage of this approach is the possibility to tune the physical and mechanical composition of the scaffolds, by adopting specific crosslinking, in order to mimic the biomechanical properties of human IVD and resemble a physiological scenario. If ethical concerns regarding prions, safety, fetal origin or variability, an alternative could be to produce CRISPR-tailored fetal-inspired ECM through engineered MSCs.

An intrigued aspect that could be also investigated is the effect of fetal-derived matrices on tissues exposed to chemotherapy or radiotherapy-based treatments to understand if it will be possible to revert the degenerative effects caused by these aggressive therapies, commonly used for cancer.

In conclusion, our future goal is the translation of fetal ECM-based biomaterials into the market of LBP and other pathologies, after the required validations, in order to offer a valid therapy that could be able to reduce patients' disability and pain.

3. REFERENCES

Alini, M., Eisenstein, S. M., Ito, K., Little, C., Kettler, A. A., Masuda, K., Melrose, J., Ralphs, J., Stokes, I., & Wilke, H. J. (2008). Are animal models useful for studying human disc disorders/degeneration? *European Spine Journal*, *17*(1), 2-19. https://doi.org/10.1007/s00586-007-0414-y

Alizadeh, M., Rezakhani, L., Soleimannejad, M., Sharifi, E., Anjomshoa, M., & Alizadeh, A. (2019). Evaluation of vacuum washing in the removal of SDS from decellularized bovine pericardium: method and device description. *Heliyon*, *5*(8), e02253-e02253. https://doi.org/10.1016/j.heliyon.2019.e02253

Antons, J., Marascio, M. G., Aeberhard, P., Weissenberger, G., Hirt-Burri, N., Applegate, L. A., Bourban, P. E., & Pioletti, D. P. (2018). Decellularised tissues obtained by a CO(2)-philic detergent and supercritical CO(2). *Eur Cell Mater*, *36*, 81-95. https://doi.org/10.22203/eCM.v036a07

Antunes, J. C., Pereira, C. L., Teixeira, G. Q., Silva, R. V., Caldeira, J., Grad, S., Gonçalves, R. M., & Barbosa, M. A. (2017). Poly(γ-glutamic acid) and poly(γ-glutamic acid)-based nanocomplexes enhance type II collagen production in intervertebral disc. *J Mater Sci Mater Med*, *28*(1), 6. https://doi.org/10.1007/s10856-016-5787-1

Atluri, S., Murphy, M. B., Dragella, R., Herrera, J., Boachie-Adjei, K., Bhati, S., Manocha, V., Boddu, N., Yerramsetty, P., Syed, Z., Ganjam, M., Jain, D., Syed, Z., Grandhi, N., & Manchikanti, L. (2022). Evaluation of the Effectiveness of Autologous Bone Marrow Mesenchymal Stem Cells in the Treatment of Chronic Low Back Pain Due to Severe Lumbar Spinal Degeneration: A 12-Month, Open-Label, Prospective Controlled Trial. *Pain Physician*, *25*(2), 193-207.

Bach, F. C., Tellegen, A. R., Beukers, M., Miranda-Bedate, A., Teunissen, M., de Jong, W. A. M., de Vries, S. A. H., Creemers, L. B., Benz, K., Meij, B. P., Ito, K., & Tryfonidou, M. A. (2018). Biologic canine and human intervertebral disc repair by notochordal cell-derived matrix: from bench towards bedside. *Oncotarget*, *9*(41), 26507-26526. https://doi.org/10.18632/oncotarget.25476

Butler, C. R., Hynds, R. E., Crowley, C., Gowers, K. H., Partington, L., Hamilton, N. J., Carvalho, C., Platé, M., Samuel, E. R., Burns, A. J., Urbani, L., Birchall, M. A., Lowdell, M. W., De Coppi, P., & Janes, S. M. (2017). Vacuum-assisted decellularization: an accelerated protocol to generate tissue-engineered human tracheal scaffolds. *Biomaterials*, *124*, 95-105. https://doi.org/10.1016/j.biomaterials.2017.02.001

Caldeira, J., Santa, C., Osório, H., Molinos, M., Manadas, B., Gonçalves, R., & Barbosa, M. (2017). Matrisome Profiling During Intervertebral Disc Development And Ageing. *Sci Rep*, *7*(1), 11629. https://doi.org/10.1038/s41598-017-11960-0

Caldeira, J., Sousa, A., Sousa, D. M., & Barros, D. (2018). 2 - Extracellular matrix constitution and function for tissue regeneration and repair. In M. A. Barbosa & M. C. L. Martins (Eds.), *Peptides and Proteins as Biomaterials for Tissue Regeneration and Repair* (pp. 29-72). Woodhead Publishing. https://doi.org/https://doi.org/10.1016/B978-0-08-100803-4.00002-4

Chan, L. K. Y., Leung, V. Y. L., Tam, V., Lu, W. W., Sze, K. Y., & Cheung, K. M. C. (2013). Decellularized bovine intervertebral disc as a natural scaffold for xenogenic cell studies. *Acta Biomaterialia*, *9*(2), 5262-5272. https://doi.org/https://doi.org/10.1016/j.actbio.2012.09.005

Colombier, P., Clouet, J., Hamel, O., Lescaudron, L., & Guicheux, J. (2014). The lumbar intervertebral disc: from embryonic development to degeneration. *Joint Bone Spine*, *81*(2), 125-129. https://doi.org/10.1016/j.jbspin.2013.07.012

Cornelison, R. C., Wellman, S. M., Park, J. H., Porvasnik, S. L., Song, Y. H., Wachs, R. A., & Schmidt, C. E. (2018). Development of an apoptosis-assisted decellularization method for maximal preservation of nerve tissue structure. *Acta Biomaterialia*, *77*, 116-126. https://doi.org/https://doi.org/10.1016/j.actbio.2018.07.009

d'Angelo, M., Benedetti, E., Tupone, M. G., Catanesi, M., Castelli, V., Antonosante, A., & Cimini, A. (2019). The Role of Stiffness in Cell Reprogramming: A Potential Role for Biomaterials in Inducing Tissue Regeneration. *Cells*, *8*(9). https://doi.org/10.3390/cells8091036

de Wit, R. J. J., van Dis, D. J., Bertrand, M. E., Tiemessen, D., Siddiqi, S., Oosterwijk, E., & Verhagen, A. F. T. M. (2023). Scaffold-based tissue engineering: Supercritical carbon dioxide as an alternative method for decellularization and sterilization of dense materials. *Acta Biomaterialia*, *155*, 323-332. https://doi.org/https://doi.org/10.1016/j.actbio.2022.11.028

Dou, Y., Sun, X., Ma, X., Zhao, X., & Yang, Q. (2021). Intervertebral Disk Degeneration: The Microenvironment and Tissue Engineering Strategies [Review]. *Frontiers in Bioengineering and Biotechnology*, *9*. https://doi.org/10.3389/fbioe.2021.592118

Duarte, M. M., Ribeiro, N., Silva, I. V., Dias, J. R., Alves, N. M., & Oliveira, A. L. (2021). Fast decellularization process using supercritical carbon dioxide for trabecular bone. *The Journal of Supercritical Fluids*, *172*, 105194. https://doi.org/https://doi.org/10.1016/j.supflu.2021.105194

Ehnis, T., Dieterich, W., Bauer, M., Lampe, B., & Schuppan, D. (1996). A chondroitin/dermatan sulfate form of CD44 is a receptor for collagen XIV (undulin). *Exp Cell Res*, *229*(2), 388-397. https://doi.org/10.1006/excr.1996.0384

Fearing, B. V., Hernandez, P. A., Setton, L. A., & Chahine, N. O. (2018). Mechanotransduction and cell biomechanics of the intervertebral disc [https://doi.org/10.1002/jsp2.1026]. *JOR Spine*, *1*(3), e1026. https://doi.org/https://doi.org/10.1002/jsp2.1026

Ferreira, J. R., Teixeira, G. Q., Neto, E., Ribeiro-Machado, C., Silva, A. M., Caldeira, J., Leite Pereira, C., Bidarra, S., Maia, A. F., Lamghari, M., Barbosa, M. A., & Gonçalves, R. M. (2021). Il-1β-pre-conditioned mesenchymal stem/stromal cells' secretome modulates the inflammatory response and aggrecan deposition in the intervertebral disc [Article]. *European Cells and Materials*, *41*, 431-453. https://doi.org/10.22203/eCM.v041a28

Friedrich, E. E., Lanier, S. T., Niknam-Bienia, S., Arenas, G. A., Rajendran, D., Wertheim, J. A., & Galiano, R. D. (2018). Residual sodium dodecyl sulfate in decellularized muscle matrices leads to fibroblast activation in vitro and foreign body response in vivo. *J Tissue Eng Regen Med*, *12*(3), e1704-e1715. https://doi.org/10.1002/term.2604

Gilchrist, C. L., Darling, E. M., Chen, J., & Setton, L. A. (2011). Extracellular matrix ligand and stiffness modulate immature nucleus pulposus cell-cell interactions. *PLoS One*, *6*(11), e27170. https://doi.org/10.1371/journal.pone.0027170

Guler, S., Aslan, B., Hosseinian, P., & Aydin, H. M. (2017). Supercritical Carbon Dioxide-Assisted Decellularization of Aorta and Cornea. *Tissue Eng Part C Methods*, *23*(9), 540-547. https://doi.org/10.1089/ten.TEC.2017.0090

Hussey, G. S., Dziki, J. L., & Badylak, S. F. (2018). Extracellular matrix-based materials for regenerative medicine. *Nature Reviews Materials*, *3*(7), 159-173. https://doi.org/10.1038/s41578-018-0023-x

Kumar, H., Ha, D.-H., Lee, E.-J., Park, J. H., Shim, J. H., Ahn, T.-K., Kim, K.-T., Ropper, A. E., Sohn, S., Kim, C.-H., Thakor, D. K., Lee, S.-H., & Han, I.-B. (2017). Safety and tolerability of intradiscal implantation of combined autologous adipose-derived mesenchymal stem cells and hyaluronic acid in patients with chronic discogenic low back pain: 1-year follow-up of a phase I study. *Stem Cell Research & Therapy*, *8*(1), 262. https://doi.org/10.1186/s13287-017-0710-3

Lang, G., Liu, Y., Geries, J., Zhou, Z., Kubosch, D., Südkamp, N., Richards, R. G., Alini, M., Grad, S., & Li, Z. (2018). An intervertebral disc whole organ culture system to investigate proinflammatory and degenerative disc disease condition [https://doi.org/10.1002/term.2636]. *Journal of Tissue Engineering and Regenerative Medicine*, *12*(4), e2051-e2061. https://doi.org/https://doi.org/10.1002/term.2636

Lange, P., Greco, K., Partington, L., Carvalho, C., Oliani, S., Birchall, M. A., Sibbons, P. D., Lowdell, M. W., & Ansari, T. (2017). Pilot study of a novel vacuum-assisted method for decellularization of tracheae for clinical tissue engineering applications. *J Tissue Eng Regen Med*, *11*(3), 800-811. https://doi.org/10.1002/term.1979

Li, Z., Gehlen, Y., Heizmann, F., Grad, S., Alini, M., Richards, R. G., Kubosch, D., Südkamp, N., Izadpanah, K., Kubosch, E. J., & Lang, G. (2020). Preclinical ex-vivo Testing of Anti-inflammatory Drugs in a Bovine Intervertebral Degenerative Disc Model. *Frontiers in Bioengineering and Biotechnology*, *8*, 583-583. https://doi.org/10.3389/fbioe.2020.00583

Lopez-Dee, Z., Pidcock, K., & Gutierrez, L. S. (2011). Thrombospondin-1: multiple paths to inflammation. *Mediators Inflamm*, *2011*, 296069. https://doi.org/10.1155/2011/296069

Ma, K., Chen, S., Li, Z., Deng, X., Huang, D., Xiong, L., & Shao, Z. (2019). Mechanisms of endogenous repair failure during intervertebral disc degeneration. *Osteoarthritis and Cartilage*, *27*(1), 41-48. https://doi.org/https://doi.org/10.1016/j.joca.2018.08.021

Navaro, Y., Bleich-Kimelman, N., Hazanov, L., Mironi-Harpaz, I., Shachaf, Y., Garty, S., Smith, Y., Pelled, G., Gazit, D., Seliktar, D., & Gazit, Z. (2015). Matrix stiffness determines the fate of nucleus pulposus–derived stem cells. *Biomaterials*, *49*, 68-76. https://doi.org/https://doi.org/10.1016/j.biomaterials.2015.01.021

Park, W., Gao, G., & Cho, D.-W. (2021). Tissue-Specific Decellularized Extracellular Matrix Bioinks for Musculoskeletal Tissue Regeneration and Modeling Using 3D Bioprinting Technology. *International Journal of Molecular Sciences*, *22*(15).

Pereira, C. L., Teixeira, G. Q., Ribeiro-Machado, C., Caldeira, J., Costa, M., Figueiredo, F., Fernandes, R., Aguiar, P., Grad, S., Barbosa, M. A., & Gonçalves, R. M. (2016). Mesenchymal Stem/Stromal Cells seeded on cartilaginous endplates promote Intervertebral Disc Regeneration through Extracellular Matrix Remodeling. *Sci Rep*, *6*, 33836. https://doi.org/10.1038/srep33836

Pizzute, T., He, F., Zhang, X.-B., & Pei, M. (2018). Impact of Wnt signals on human intervertebral disc cell regeneration [https://doi.org/10.1002/jor.24115]. *Journal of Orthopaedic Research*, *36*(12), 3196-3207. https://doi.org/https://doi.org/10.1002/jor.24115

Ren, T., Faust, A., Van Der Merwe, Y., Xiao, B., Johnson, S., Kandakatla, A., Gorantla, V. S., Badylak, S. F., Washington, K. M., & Steketee, M. B. (2018). Fetal extracellular matrix nerve wraps locally improve peripheral nerve remodeling after complete transection and direct repair in rat [Article]. *Scientific Reports*, *8*(1), Article 4474. https://doi.org/10.1038/s41598-018-22628-8

Schmitz, T. C., van Doeselaar, M., Tryfonidou, M. A., & Ito, K. (2022). Detergent-Free Decellularization of Notochordal Cell-Derived Matrix Yields a Regenerative, Injectable, and Swellable Biomaterial. *ACS Biomater Sci Eng*, *8*(9), 3912-3923. https://doi.org/10.1021/acsbiomaterials.2c00790

Song, Y. H., Maynes, M. A., Hlavac, N., Visosevic, D., Daramola, K. O., Porvasnik, S. L., & Schmidt, C. E. (2021). Development of novel apoptosis-assisted lung tissue decellularization methods. *Biomater Sci*, *9*(9), 3485-3498. https://doi.org/10.1039/d1bm00032b

Syed, O., Walters, N. J., Day, R. M., Kim, H.-W., & Knowles, J. C. (2014). Evaluation of decellularization protocols for production of tubular small intestine submucosa scaffolds for use in oesophageal tissue engineering. *Acta Biomaterialia*, *10*(12), 5043-5054. https://doi.org/https://doi.org/10.1016/j.actbio.2014.08.024

Teixeira, G. Q., Boldt, A., Nagl, I., Pereira, C. L., Benz, K., Wilke, H. J., Ignatius, A., Barbosa, M. A., Gonçalves, R. M., & Neidlinger-Wilke, C. (2016). A Degenerative/Proinflammatory Intervertebral Disc Organ Culture: An Ex Vivo Model for Anti-inflammatory Drug and Cell Therapy. *Tissue Eng Part C Methods*, *22*(1), 8-19. https://doi.org/10.1089/ten.tec.2015.0195

Tessier, S., & Risbud, M. V. (2021). Understanding embryonic development for cell-based therapies of intervertebral disc degeneration: Toward an effort to treat disc degeneration subphenotypes. *Dev Dyn*, *250*(3), 302-317. https://doi.org/10.1002/dvdy.217

Thompson, K., Moore, S., Tang, S., Wiet, M., & Purmessur, D. (2018). The chondrodystrophic dog: A clinically relevant intermediate-sized animal model for the study of intervertebral disc-associated spinal pain. *JOR Spine*, *1*(1), e1011. https://doi.org/10.1002/jsp2.1011

Tombran-Tink, J., & Barnstable, C. J. (2003). Therapeutic prospects for PEDF: more than a promising angiogenesis inhibitor. *Trends in Molecular Medicine*, *9*(6), 244-250. https://doi.org/https://doi.org/10.1016/S1471-4914(03)00074-1

Urban, J. P. G., & Roberts, S. (2003). Degeneration of the intervertebral disc. *Arthritis research & therapy*, *5*(3), 120-130. https://doi.org/10.1186/ar629

Vadalà, G., Russo, F., Pattappa, G., Schiuma, D., Peroglio, M., Benneker, L. M., Grad, S., Alini, M., & Denaro, V. (2013). The transpedicular approach as an alternative route for intervertebral disc regeneration. *Spine (Phila Pa 1976)*, *38*(6), E319-324. https://doi.org/10.1097/BRS.0b013e318285bc4a

Vernengo, A. J., Grad, S., Eglin, D., Alini, M., & Li, Z. (2020). Bioprinting Tissue Analogues with Decellularized Extracellular Matrix Bioink for Regeneration and Tissue Models of Cartilage and Intervertebral Discs [https://doi.org/10.1002/adfm.201909044]. *Advanced Functional Materials*, *30*(44), 1909044. https://doi.org/https://doi.org/10.1002/adfm.201909044

Wehner, D., Tsarouchas, T. M., Michael, A., Haase, C., Weidinger, G., Reimer, M. M., Becker, T., & Becker, C. G. (2017). Wnt signaling controls pro-regenerative Collagen XII in functional spinal cord regeneration in zebrafish. *Nat Commun*, *8*(1), 126. https://doi.org/10.1038/s41467-017-00143-0

Wu, L.-C., Chiang, C.-J., Liu, Z.-H., Tsuang, Y.-H., Sun, J.-S., & Huang, Y.-Y. (2014). Fabrication and properties of acellular porcine anulus fibrosus for tissue engineering in spine surgery. *Journal of Orthopaedic Surgery and Research*, *9*(1), 118. https://doi.org/10.1186/s13018-014-0118-z

Wu, L.-C., Kuo, Y.-J., Sun, F.-W., Chen, C.-H., Chiang, C.-J., Weng, P.-W., Tsuang, Y.-H., & Huang, Y.-Y. (2017). Optimized decellularization protocol including α-Gal epitope reduction for fabrication of an acellular porcine annulus fibrosus scaffold. *Cell and Tissue Banking*, *18*(3), 383-396. https://doi.org/10.1007/s10561-017-9619-4

Yi, B., Xu, Q., & Liu, W. (2022). An overview of substrate stiffness guided cellular response and its applications in tissue regeneration. *Bioactive Materials*, *15*, 82-102. https://doi.org/https://doi.org/10.1016/j.bioactmat.2021.12.005

Zhang, M., Tombran-Tink, J., Yang, S., Zhang, X., Li, X., & Barnstable, C. J. (2021). PEDF is an endogenous inhibitor of VEGF-R2 angiogenesis signaling in endothelial cells. *Experimental Eye Research*, *213*, 108828. https://doi.org/https://doi.org/10.1016/j.exer.2021.108828

Zhou, X., Wang, J., Huang, X., Fang, W., Tao, Y., Zhao, T., Liang, C., Hua, J., Chen, Q., & Li, F. (2018). Injectable decellularized nucleus pulposus-based cell delivery system for differentiation of adipose-derived stem cells and nucleus pulposus regeneration. *Acta Biomaterialia*, *81*, 115-128. https://doi.org/https://doi.org/10.1016/j.actbio.2018.09.044